

REPUBLIQUE DU CAMEROUN

Paix-Travail-Patrie

UNIVERSITE DE YAOUNDE I

FACULTE DES SCIENCES



REPUBLIC OF CAMEROON

Peace-Work-Fatherland

THE UNIVERSITY OF YAOUNDE I

FACULTY OF SCIENCE

DÉPARTEMENT DE PHYSIQUE
DEPARTMENT OF PHYSICS

ATTESTATION DE CORRECTION DE LA THÈSE DE DOCTORAT/PhD

Nous soussignés, Professeur **TCHAWOUA Clément** et Professeur **DJUIDJE KENMOE Germaine**, respectivement Président et Examineur du jury de la Thèse de Doctorat/PhD de Madame **GANYOU Stéphanie**, Matricule **11W0329**, préparée sous la direction du Professeur **FEWO Serge Ibraïd**, intitulée : « **DYNAMICS OF ION-ACOUSTIC WAVES IN MAGNETIZED PLASMA** », soutenue le **Vendredi, 20 septembre, 2024**, en vue de l'obtention du grade de Docteur/PhD en Physique, Spécialité **Mécanique, Matériaux et Structures**, Option **Mécanique Fondamentale et Systèmes Complexes**, attestons que toutes les corrections demandées par le jury de soutenance ont été effectuées.

En foi de quoi, la présente attestation lui est délivrée pour servir et valoir ce que de droit.

Fait à Yaoundé, le **04 OCT 2024**

Examineur

DJUIDJE KENMOE Germaine

Professeure

Président du jury

TCHAWOUA Clément

Professeur

Le Chef de Département



NDJAKA Jean-Marie Bienvenu

Professeur

REPUBLIQUE DU CAMEROUN

Paix-Travail-Patrie

UNIVERSITE DE YAOUNDE I

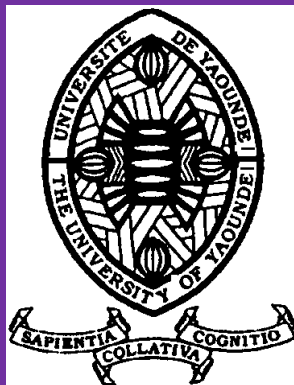
FACULTE DES SCIENCES

CENTRE DE RECHERCHE ET DE
FORMATION DOCTORALE EN
SCIENCES, TECHNOLOGIES ET
GEOSCIENCES

UNITE DE RECHERCHE ET DE
FORMATION DOCTORALE PHYSIQUE
ET APPLICATIONS

B. P : 812 Yaoundé

E-mail : crfd_stg@uy1.uninet.cm



REPUBLIC OF CAMEROON

Peace-Work-Fatherland

THE UNIVERSITY OF YAOUNDE I

FACULTY OF SCIENCE

POSTGRADUATE SCHOOL OF
SCIENCES, TECHNOLOGY AND
GEOSCIENCES

RESEARCH AND POSTGRADUATE
TRAINING UNIT FOR PHYSICS AND
APPLICATIONS

P. O. Box: 812 Yaoundé

E-mail : crfd_stg@uy1.uninet.cm

DYNAMICS OF ION-ACOUSTIC WAVES IN MAGNETIZED PLASMA MEDIA

Thesis

Submitted and defended in fulfillment of the requirements for the degree of
Doctor of Philosophy (Ph.D) in Physics

Speciality : Mechanics, Materials and Structures

Option : Fundamental Mechanics and Complex Systems

By :

GANYOU Stéphanie

Registration number : 11W0329

Master of Science in Physics

Under the supervision of :

FEWO Serge Ibraïd

Associate Professor

University of Yaounde I



Year 2024

DYNAMICS OF ION-ACOUSTIC WAVES IN MAGNETIZED PLASMA MEDIA

Submitted and defended in Fulfillment of the award for the Degree of
Doctor of Philosophy in Physics

Speciality: Mechanics, Materials and Structures

Option: Fundamental Mechanics and Complex Systems

by:

GANYOU Stéphanie

M. Sc. in Physics

Registration Number: **11W0329**

Under the Supervision of:

FEWO Serge Ibraïd

Associate Professor

University of Yaounde I

Faculty of Science

Department of Physics

e-mail address: stephanieganyou@gmail.com

Year: 2024

Contents

Declaration	iv
Dedication	v
Acknowledgements	vi
Citations	ix
List of abbreviations	x
List of figures	xi
List of tables	xv
Abstract	xvi
Résumé	xvii
General introduction	1
0.1 Context of the thesis	1
0.2 Problem statement and objectives of the thesis	5
0.3 Outlines of the thesis	6
Chapter 1 Litterature review	7
1.1 Plasma discovery history and plasma formation	8
1.1.1 Plasma discovery history	8
1.1.2 Plasma formation	9
1.1.3 Multi-photon ionization and plasma generation	10
1.2 Characteristics of plasma	11
1.2.1 Plasma density and degree of ionization	11
1.2.2 Quasi-neutrality in plasma	12

1.2.3	Plasma temperature	12
1.2.4	Plasma frequency	13
1.2.5	Debye length and Debye shielding	14
1.2.6	Plasma parameter	17
1.2.7	Criteria for ionized gas to be a plasma	17
1.2.8	Particle interactions and collective effects	17
1.2.9	Collisions in plasmas	18
1.3	Types of plasmas and Applications	20
1.3.1	Types of plasmas	20
1.3.2	Some applications of plasmas	24
1.4	Electronegative plasma concept	27
1.4.1	Electronegative plasma description	27
1.4.2	The technological interest of electronegative plasmas	28
1.5	Magnetized plasma concept	29
1.6	Magnetized electronegative plasma	29
1.7	Waves in plasma	30
1.7.1	Electromagnetic electron waves	31
1.7.2	Electrostatic waves	31
1.7.3	Ion-acoustic waves	31
1.7.4	Ion-cyclotron waves	32
1.7.5	Nonlinearity and wave structures	33
1.7.6	Summary of elementary plasma waves	34
1.7.7	Solitary waves, soliton and dromions	35
1.8	Theoretical description of plasma phenomena	36
1.9	Fluid description of plasma and basic equations	37
1.9.1	Continuity equation	38
1.9.2	Momentum equation	38
1.9.3	Poisson's equation	39
1.9.4	Closed system of fluid equations	39
1.9.5	Cold plasma model	40
1.9.6	Warm plasma model	40
Chapter 2 Models description and methods		42
2.1	Governing equations in (2+1)-dimensions	42

2.2	The reductive perturbation method and derivation of NLS equation and DS equations	44
2.2.1	The reductive perturbation method	44
2.2.2	Derivation of the nonlinear schrödinger equation	44
2.2.3	Derivation of Davey-Stewartson equations	47
2.3	Analytical methods	51
2.3.1	Linear stability analysis of plane wave solutions in NLS equation . .	52
2.3.2	Linear stability analysis of plane wave solutions in DS equation . .	53
2.3.3	Variational approach	55
2.3.4	The Hirota's bilinear method	58
2.3.5	Construction of one-dromion solutions	62
2.3.6	Construction of two-dromion solutions	62
2.4	Numerical methods	63
2.4.1	Fourth-order Runge-Kutta method	64
2.4.2	Split-step fourier method	65
Chapter 3 Results and discussion		68
3.1	Dynamics of modulated nonlinear IAW packets in magnetized ENP	69
3.1.1	Evolution of wave frequency of IAWs in NLS equation	69
3.1.2	Modulational instability analysis of IAWs in NLS equation	71
3.1.3	Dynamics of IAWs characteristic parameters	75
3.2	Dynamics of propagation of ion-acoustic dromions in a magnetized ENP .	81
3.2.1	Evolution of wave frequency of IAWs in the DS equations	81
3.2.2	Modulational instability analysis of IAWs in the DS system	82
3.2.3	One- and two-dromion solutions of the Davey-Stewartson equations	87
General conclusion		95
Appendix		98
.1	Various coefficients	98
.2	Equations and other coefficients	98
.3	Coefficients of DSEs	99
Bibliography		100

♣ Certification ♣

I the undersigned, **Mrs. GANYOU Stéphanie**, registration number 11W0329, certify that the scientist research work presented in this thesis, entitled **Dynamics of ion-acoustic waves in magnetized plasma media** is the fruit of my proper work in the research and postgraduate training unit for Physics and applications of the University of Yaoundé 1, under the supervision of **Pr. FEWO Serge Ibraïd**. No part of this thesis has been submitted anywhere else for any other degree. This thesis is submitted and defended in fulfillment of the requirements for the award of a **Doctorat/Ph.D degree in Physics**, Speciality: **Mechanics, Materials and Structures**, option: **Fundamental Mechanics and Complex Systems**.

Author

GANYOU Stéphanie

M. Sc. in Physics

PhD student

University of Yaoundé 1

Supervisor

FEWO Serge Ibraïd

Associate Professor

University of Yaoundé 1

♣ Dedication ♣

*My dedication is devoted to
all my family, in ♡ particular: to my par-
ents: my father **Mr. KAMCHE Pierre** and
my sweet mother **Mrs. MIBE Marie**. This
thesis would not be possible without my parents
who have always supported and encouraged
me in my efforts to access ever more
knowledge. "My only trophies
are your smiles."*



♣ Acknowledgements ♣

At the time this thesis is writting, I am animated by the thought of gratitude that I carry towards all those who did not fail to bring their contribution to the edification of this work. For that,

♠ First of all, I thank **Almighty God** for the strength, health, wisdom and comfort that he has always granted me and who, in the perfume of his infinite love for me, having made possible to complete this thesis.

♠ I would like to thank very particularly my supervisor, **Prof. FEWO Serge Ibraïd**, Associate Professor in the Department of Physics at the University of Yaoundé I, who suggested the subject and gave me the opportunity to discover the wonderful world of plasma physics. Through his efforts and the advice he has gave me, he enabled this work to progress in a spirit of friendship. May he find here the expression of my deepest gratitude.

♠ I warmly thank **Prof. NDJAKA Jean-Marie Bienvenu**, Head of Department of Physics at the University of Yaoundé I for his teachings, his trust, his advice and various edifications during all these years.

♠ I sincerely thank **the Honorable Members of the Jury: Prof. TCHAWOUA Clément, Prof. FEWO Serge Ibraïd, Prof. FOTUE Alain Jervé, Prof. KENFACK JIOTSA Aurelien and Prof. DJUIDJE KENMOE Germaine** who have the task of reading and appreciating this document, and also participating in the defense of this thesis. May they find here the expression of my deepest respect.

♠ I warmly thank **Prof. KOFANE Timoléon Crépin**, former Head of Department of Physics at the University of Yaoundé I, **Prof. TABI Conrad Bertrand**, Professors in the Department of Physics and Astronomy of the Bostwana International

University of Science and Technology and **Dr. PANGUETNA Chérif Souléman** for their edifying advice, the team's research work during all these years.

♠ I would also like to thank **all my Committee Members and international Reviewers** for their stimulating questions on this work. Thank you to have agreed to discuss and appreciate the results of this thesis.

♠ It would be very nice to recognize the exchanges and constructive discussions combined with great moments of sharing with all the teachers of the Department of Physics, who ensured my academic training in which I was able to complete this dissertation, in particular **Prof. TCHAWOUA Clément**, **Prof. WOAFO Paul**, **Prof. ENYEGUE A NYAM Françoise**, **Prof. Germain Hubert BENBOLIE**, **Prof. SIEWE SIEWE Martin**, **Prof. DJUIDJE KENMOE Germaine**, **Prof. Jacque HONA**, **Prof. ZEKENG Serge Sylvain**, **Prof. NANA NBENDJO Blaise Roméo**, **Prof. SAIDOU**, **Prof. MBINACK Clément**, **Prof. NDJANDJOCK NOUCK Philippe**, **Prof. BODO Bernard**, **Prof. MVOGO Alain**, and **Pr. SIMO Elie**.

♠ I would like to thank **Prof. BOUETOU BOUETOU Thomas**, **Prof. TCHOMGO FELENOU Emmanuel**, **Prof. BOYOMO Marthe**, **Prof. FANDIO SENDJA Bridinette** and **Dr. TAKEMBO NTAHKIE Clovis** for their daily support and especially for their moral support when I was sometimes tempted to get discouraged by the queries of some reviewers.

♠ I very warmly thank **Mr. NOUBISSI François** for accepting me as his beloved daughter, for the tireless support he has always given me throughout my academic career, even in the most difficult moments of my life during my time at the University, in order to carry out this work. May he find here the expression of my deepest gratitude.

♠ I would especially like to thank **Prof. KEMMEGNE MBOUGUEN Justin Claude** for his support, his prayers, his advice and his encouragement which he never ceased to send on my behalf, without forgetting **Mr. KALASSI Mathias**, **Mr. FOKOU Zacharie**, **Mr. MBUH Edwin** and **Mr. TCHINDA Charles Sisco** for all their supports. May they find here the expression of my deepest gratitude.

♠ I would like to thank my elders and labmates, in particular **Dr. MEGNE TIAM Laure**, **Dr. AMBASSA OTSOBO Jenny Alban**, **Dr. DJAZET Alain**, **Dr. ZANGA Dieudonné**, **Dr. TEMGOUA DJOUTSA Diane Estelle**, **Dr. NGA ONGODO Dieudonné**, **Dr. NGATCHA TANLY Nelly Danielle**, **Dr. FOUEDJI Chenceline**, **Mr. SIGNE Eric Martial**, **Mr. TCHIENKOUA Cétrigue**, **Mrs. NDZIA WANDJI Lina Maureen** and **Mrs. GBOULIE POFOURA Aïcha Sidica** who have always been there to listen to me and find solutions to my various problems, thank you one more time and special thought to the other PhD students of the Lab.

♠ I would also like to thank **all my friends from the Master's promotion** and **all the members of our association of young researchers (G11)** with whom we are used to discussing the progress of our thesis work every first Friday of the month, for the warmth, the joy, the friendship they gave me and the edifying debates every day.

♠ I would particularly like to thank my sisters: **Mrs. YOUNGANG KAMCHE Carine** wife **FEZEU Roger** and **Mrs. MEUDJE KAMCHE Christiane** wife **DEFO Patrice Aimé**, my brothers: **Mr. TCHOUPE KAMCHE Zéphirin**, **Mr. KAMGANG KAMCHE Julio** and **Mr. DASSI KAMGANG Caleb Brayane**, my uncle and his wife **Mr. KENMOGNE Jean Pierre** and **Mrs. MBOUMEGNI Béatrice Sylvie** for all their supports, their prayers, their advice and encouragement which they never ceased to send on my behalf. "My only trophies are your smiles."

♠ I address my warmest thanks to **all my family**, to my primary and secondary school Teachers and to my promotion from the Bilingual Secondary School. May they find here the expression of my most distinguished feelings.

♠ My thanks also go to **all those**, who with this question recurrent, and sometimes very distressing in times of doubt, "when do you support your thesis?", allowed me to always follow my final objective.

♠ My feelings of gratitude and my thanks go out to **everyone** who participated directly or indirectly from near or far in the realization of this work and also to those I inevitably forget, I hope they will forgive me!

♣ Citations ♣

"True Laws of Nature cannot be linear."

Albert Einstein

*"There are endless planes of attention, endless realities and endless mind states.
They're like collections of atoms and protons and neutrons, nuclei. They just go on
forever. They're plasma, they're fluid...they're alive."*

Frederick Lenz

♣ List of abbreviations ♣

ENP: Electronegative plasma;
DS: Davey-Stewartson;
DSEs: Davey-Stewartson Equations;
IAWs: Ion-acoustic waves;
IA: Ion-acoustic;
IASs: Ion-acoustic solitons;
(2+1)D: (2+1)-dimensions;
NLS: Nonlinear Schrödinger;
KdV: Korteweg-de Vries;
MI: Modulational Instability;
PDEs: Partial Differential Equations;
MPI: Multiphoton ionization;
RK4: Fourth-order Runge-Kutta;
SSFM: Split-Step Fourier Method;
FFT: Finite-Fourier-Transform.

♣ List of figures ♣

List of Figures

Figure 1.1	Example of a discharge lamp [120].	8
Figure 1.2	Plasma formation by supplying energy/temperature [121].	9
Figure 1.3	Different phase changes between these states of the matter.	10
Figure 1.4	Debye shielding of charged spheres immersed in a plasma [128].	14
Figure 1.5	Densities and electronic temperatures of the main types of plasmas (the free electrons in a metal can be considered as an electron plasma), https://fr.wikipedia.org/wiki/Physique des plasmas [Consulted on 13/09/23].	21
Figure 1.6	Flame (left panel), trail of shooting stars (middle panel) and Plasma lamp (right panel), https://fr.wikipedia.org/wiki/ état plasma [Consulted on 13/09/23].	22
Figure 1.7	The sun is a ball of plasma (left panel), and the solar wind plasma and magnetosphere (right panel), www.sciencelern.org.nz [Consulted in 13/09/23].	22
Figure 1.8	Plasma lighting, https://fr.wikipedia.org/wiki/état plasma [Consulted on 13/09/23].	23
Figure 1.9	Plasma screen of TV [121].	25
Figure 1.10	Surface treatment (first two panels), materials for plasma spray coating (third panel) and welding-plasma-cutting (last panel) [121].	25
Figure 1.11	Food treatment [121].	26

Figure 1.12	Plasma modification of biomedical surfaces: plasma based Decontamination/Sterilization, direct therapeutic plasma application (left panel) and teeth whitening with Plasma (right panel) [121].	26
Figure 3.1	Plot of the frequency ω against k in panels (a) and (c), and the group velocity v_g versus k in panels (b) and (d) of wave packets for different values of α (upper panels for $\sigma_n = 5$) and σ_n (down panels for $\alpha = 0.1$).	70
Figure 3.2	Panels show P/Q against the carrier wave number k for different values of negative ion to electron density ratio α (a) as in Fig. 3.1 and S versus the carrier wave number k for different values of plasma frequency ω_p (b).	72
Figure 3.3	The stable/unstable regions for fixed values of the system parameters $\alpha = 0.1$, $\sigma_n = 5$ and $\omega_p = 0.2$ is shown by the contour plots of $P/Q = 0$ against the wave frequency ω and the modulation angle θ .	73
Figure 3.4	Plot of the modulational instability growth rate against the modulation wave number K for different values of ω_p and fixed values of α and σ_n : $\alpha = 0.1$ and $\sigma_n = 5$ (see the panel (a)), $\alpha = 0.1$ and $\sigma_n = 10$ (see the panel (b)), $\alpha = 0.3$ and $\sigma_n = 5$ (see the panel (c)) and $\alpha = 0.3$ and $\sigma_n = 10$ (see the panel (d)).	74
Figure 3.5	Plot of the potential function given by Eq. (3.39) versus the (S,Q)-plane for $\alpha = 0.1$, $\sigma_n = 5$ and $\omega_p = 0.2$.	78
Figure 3.6	Evolution of Gaussian parameters: amplitude $C(\tau)$, spatial widths $X(\tau)$, $Y(\tau)$, spatial chirps $a(\tau)$, $b(\tau)$ and phase φ .	79
Figure 3.7	Exact solution (input profile) in left panel, numerical solution (output profile) in right panel and relative error in down panel of modified NLS Eq. (3.1).	80
Figure 3.8	Panel (a) shows the variation of the wave frequency ω versus the wavenumber k , and panel (b) the variation of the group velocity, both under the changing effect of the magnetic field. The electron-to-negative ion temperature ratio σ_n and the negative-ion concentration ratio α take the respective values $\sigma_n = 2.5$ and $\alpha = 0.01$.	82

- Figure 3.9** Panels show the MI growth rate in the (μ_1, μ_2) -plane for a fixed value of $\alpha = 0.2$ and the ion cyclotron frequency taking the values: (a) $\Omega = 0.17$, (b) $\Omega = 0.25$ and (c) $\Omega = 0.3$. The other parameters are: $\sigma_n = 20.5$, $k = 2.4$, $\alpha_1 = 2.5$, $\alpha_2 = 2.5$, $\psi_{10} = 0.06$, and $\psi_{20} = 0.025$ 83
- Figure 3.10** Panels show the growth rate of MI versus the electron-to-negative ion temperature ratio σ_n and the frequency Ω when the negative-ion concentration ratio α takes the respective values (a) $\alpha = 0.01$, (b) $\alpha = 0.05$ and (c) $\alpha = 0.2$, with the other parameter values being: $\sigma_n = 20.5$, $k = 2.4$, $\alpha_1 = 2.5$, $\alpha_2 = 2.5$, $\psi_{10} = 0.06$, and $\psi_{20} = 0.025$ 84
- Figure 3.11** Panels show the growth rate of MI versus the frequency Ω for two sets of the wavenumbers (a) $\mu_1 = \mu_2 = 0.85$ and (b) $\mu_1 = \mu_2 = 0.15$. In each of the panels, the negative-ion concentration ratio α takes increasing values, while the other parameters are fixed as: $\sigma_n = 20.5$, $k = 2.4$, $\alpha_1 = 2.5$, $\alpha_2 = 2.5$, $\psi_{10} = 0.06$, and $\psi_{20} = 0.025$. 85
- Figure 3.12** Panels show the MI growth rate versus the negative-ion concentration ratio α and the frequency Ω when the electron-to-negative ion temperature ratio takes the respective values: $\sigma_n = 12.5$, (b) $\sigma_n = 17$ and (c) $\sigma_n = 21.5$. The other parameter values are: $k = 2.4$, $\alpha_1 = 2.5$, $\alpha_2 = 2.5$, $\psi_{10} = 0.06$, and $\psi_{20} = 0.025$ 86
- Figure 3.13** Panels show the plotted of γ_1 , γ_2 and γ_3 versus k (Eqs. (61b), (61d)) and (61e)) for $\alpha = 0.01$, and $\sigma_n = 5.5$ and different values of Ω 87
- Figure 3.14** Panels show the behaviors of the one-dromion solution with increasing the magnetic field. For (a), the negative ion concentration ratio is fixed as $\alpha = 0.01$, while (b) corresponds to $\alpha = 0.08$, with Ω taking the increasing values 0, 0.01 and 0.2 in each of the panels. The other parameters are $\sigma_n = 5.5$, and $J = K = L = 1$. . 89
- Figure 3.15** Panels show the propagation of one-dromion solutions (3.55) for increasing values of the magnetic field Ω and at different instants τ when $\alpha = 0.01$, $\sigma_n = 5.5$, and $J = K = L = 1$ 90

- Figure 3.16** Panels show elastic collision of the two-dromion solution (3.56) in a moving frame, where panels (aj)_{j=1,2,3,4} display results in the absence of the magnetic field ($\Omega = 0$) and panels (bj)_{j=1,2,3,4} show results in the presence of the magnetic field. In the process, two identical dromions interact and keep their shapes after collision. However, the presence of the magnetic field accelerates such a collision, with the other parameters being $\alpha = 0.01$, $\sigma_n = 20.5$, and $A = B = C = D = E = F = G = H = I = 1$ 91
- Figure 3.17** Panels show elastic collision of two dromions with energy exchange both in absence (panels (aj)_{j=1,2,3,4}) and in presence (panels (bj)_{j=1,2,3,4}) of the magnetic field. The colliding objects involve two dromions of different amplitudes which, after collision, give rise to entities with equal amplitudes. The parameters are $\alpha = 0.01$, $\sigma_n = 20.5$, and $A = B = C = D = E = F = G = H = I = 1$. 92
- Figure 3.18** Panels show inelastic collision of two dromions both in absence (panels (aj)_{j=1,2,3,4}) and in presence (panels (bj)_{j=1,2,3,4}) of the magnetic field. In both cases, the dromions after collision combine and give rise to one soliton, but the presence of the magnetic field accelerates such a process. The parameters are $\alpha = 0.01$, $\sigma_n = 20.5$, and $A = B = C = D = E = F = G = H = I = 1$ 93

♣ List of tables ♣

List of Tables

Table 1.1	The table shows the number density, the electron temperature, the magnetic field and the Debye length of some natural and artificial plasmas [129].	16
Table 1.2	Summary of elementary plasma waves, https://en.wikipedia.org/wiki/Waves in plasmas [Consulted on 13/09/23].	34

♣ Abstract ♣

In this thesis, we study theoretically and numerically the dynamics of propagation of (2+1)-dimensional ion-acoustic waves in magnetized electronegative plasma made of a significant number of negative ions, with electrons both in Boltzmann distribution and cold mobile positive ions, under the influence of the external magnetic field. For this purpose, from the hydrodynamic equations of the two-dimensional magnetized electronegative plasma, the dynamics of the system is reduced via the standard reductive perturbation method on the one hand, to the nonlinear Schrödinger (NLS) equation and on the other hand, to the Davey-Stewartson (DS) equations. Through the linear stability analysis of plane waves, an expression of the modulational instability growth rate is derived to analyse the areas of the emergence of solitary waves. The existence of ion-acoustic waves in the both models is confirmed. In the case of the NLS equation and in order to describe the main characteristics of ion-acoustic waves, the variational method is performed involving trial function solution of this equation and the exact (input profile) and numerical (output profile) solutions are obtained and discussed. In the case of the DS equations, one-dromion and two-dromion solutions are investigated analytically using the Hirota's bilinear method, and numerically. The impact of the magnetic field is discussed in that context, and particular attention is given to dromion interactions under different scenarios. We noted a slowing effect on the propagation of the dromion solutions in the presence of the external magnetic field. Elastic (inelastic) collision of two-dromion solutions is observed during their evolution, with an acceleration of the process in the presence of external the magnetic field.

Keywords: Magnetized electronegative plasma; Nonlinear Schrödinger equation; Davey-Stewartson equations; Modulational instability; Variational approach; Ion-acoustic waves; Dromions like solutions.

♣ Résumé ♣

Dans cette thèse, nous étudions théoriquement et numériquement la dynamique de propagation des ondes acoustiques ioniques à $(2+1)$ dimensions dans un plasma électronégatif magnétisé constitué d'un nombre important d'ions négatifs avec des électrons, à la fois dans une distribution de Boltzmann et des ions positifs froids mobiles, soumis à l'influence du champ magnétique externe. A cet effet, à partir des équations hydrodynamiques du plasma électronégatif magnétisé bidimensionnel, la dynamique du système est réduite via la méthode de perturbation réductrice standard d'une part, à l'équation de Schrödinger non linéaire et d'autre part, aux équations de Davey-Stewartson (DS). Grâce à l'analyse de la stabilité linéaire des ondes planes, une expression du gain d'instabilité de modulation est dérivée pour analyser les zones d'émergence des ondes solitaires. L'existence d'ondes acoustiques ioniques dans les deux modèles est confirmée. Dans le cas du plasma modélisé par l'équation de NLS et afin de décrire les principales caractéristiques des ondes acoustiques ioniques, la méthode variationnelle est effectuée impliquant une solution de fonction d'essai de cette équation et les solutions exactes (profil d'entrée) et numériques (profil de sortie) sont obtenues et discutées. Dans le cas du plasma modélisé par les équations de DS, les solutions à un et deux dromions sont obtenues et discutées analytiquement en utilisant la méthode bilinéaire d'Hirota, et numériquement. L'impact du champ magnétique est discuté dans ce contexte, et une attention particulière est accordée aux interactions des dromions dans différents scénarios. Nous avons noté un effet ralentissant sur la propagation des solutions dromions en présence du champ magnétique externe. Une collision élastique (inélastique) des solutions à deux dromions est observée au cours de leur évolution, avec une accélération du processus en présence du champ magnétique.

Mots clés: Plasma électronégatif magnétisé; Equation de Schrödinger non linéaire; Equations de Davey-Stewartson; Instabilité modulationnelle; Approche variationnelle; Ondes acoustiques ioniques; Solutions de type dromions.

♣ General introduction ♣

What is a plasma? Plasma is the fourth state of the matter, just like solid, liquid and gaseous states. It is usually composed of charged particles (negative ions, positive ions and electrons) and neutral particles (atoms and molecules). In the presence of a significant number of negative ions, it is qualified as electronegative plasma (ENP). The presence of negative ions in a plasma modifies its basic nature and importantly affects wave propagation of various kinds as well as their characteristics. The charge neutrality condition gets modified in that context, leading to the increase in the negative ion density, while the number density of electrons decreases. This means that the shielding effect produced by the electrons decreases and the behavior of the plasma consequently changes. The electronegative plasma, in the presence of the external magnetic field is so-called magnetized electronegative plasma. Moreover, the presence of the external magnetic field can be used to control the directions, the velocity and the electrical properties of the plasma and improve the performance of these processes by confining the plasma and increasing the reaction rate. Plasma, in physics, not to be confused with blood plasma, is an electrically conducting medium and produced when the atoms in gas become ionized. On the other hand, the blood plasma is the largest part of our blood which carries the blood components throughout the body.

0.1 Context of the thesis

During recent years, the effect of charged particles (electrons, positive or negative ions) on the plasma properties such as quantum plasmas [1–6], dust plasmas [7–14], pair-ion plasmas [15–19], electronegative plasmas [20–23], magnetized electronegative plasmas [24–35], just name to a few, has long been the subject of significant interest. The solar system is made up of planets surrounded by plasma with various characteristics (electron density, temperature, collision frequency...). By supplying energy to a neutral gas, one

can cause a formation of charged particles (electrons, negative ions, positive ions) which, with the non-ionized atoms or the molecules of the gas, become the components of the generated plasma. Plasma is so-called an ionized gas. The term plasma was first officially introduced in Physics by Irving Langmuir in 1928 [36] to describe the ionized gas by its behavior in discharge tubes. Thus, following this discovery, several scientific researchers became interested in the study of Plasma physics. The way of energy is transferred depends not only on the method of production of plasma, but also on its physical properties and potential applications, both in the laboratory and in technology. On the scale of the Universe, plasma represents up to 99% of the available matter (Research shows that plasma constitutes 99% of the visible universe. We belong to the rest 1% of the matter on earth which is something different from plasma) [37, 38]. Amongst its characteristics, a plasma displays high sensitivity to electric and magnetic fields. Many scientists are interested in studying plasma because of their temperature, density and the types of particles they contain which are its main characteristics.

Plasmas are considered as one of the four states of matter and they are said to be electronegative plasmas (ENPs) [39–43] in the presence of a significant amount of negative ions. The latter nowadays has become a fascinating topic because of fundamental scientific interest, and it is observed in astrophysical objects (Earth’s ionosphere [44, 45]), (D-region [46–48] and F-region [49]), Solar wind magnetosphere [50, 51], in industries [52] and laboratory experiment [53]. However, Plasmas, which are nonlinear and dispersive media, have vast opportunities to observe different nonlinear wave phenomena such as ion acoustic solitons (IASs), shock waves and different kinds of instabilities. Due to the suitable balance between nonlinearity and dispersion, ion acoustic waves (IAWs), and solitons in general, can spread over long distances, keeping intact their characteristics and shape. Various applications in plasma science and industry [54, 55], and the proof of its existence in astrophysics, space, and laboratory experiments make ENPs a subject of growing interest as witnessed by recent contributions both in one-dimensional and multidimensional contexts [56–62]. In some previous works, the study of negative ions including charge evolution in dust plasmas and ion-acoustics (IA) waves were investigated [46, 63, 64]. The structure of electronegative plasmas sheath without magnetic field [20–23] and with magnetic field [24] are investigated. For ion-acoustic waves in electronegative plasma in the presence of the magnetic field, the solitary wave which is described by the well-known nonlinear Schrödinger equation can propagate. The study of other aspects and characteristics of such plasmas waves, related to their response to external magnetic fields

using the hydrodynamic equations, in one or more dimensions [21–23] can be reduced by introducing the reductive perturbation approximation to nonlinear Schrödinger (NLS) equation, Davey-stewartson (DS) equations, just to name a few, modelling the dynamics of propagation of IAWs in magnetized electronegative plasma. An analytical approach such as the variational method can be applied to the NLS equation in order to study the dynamics of the relevant parameters of IAWs in plasma medium. This method is well known in classical mechanics and can be used in various contexts. To remind, in nonlinear optics in general and the propagation of pulses in optical fibers in particular, it was applied for the first time in 1983 by Anderson [65]. The basic physical assumption of this approach is based on the fact that a propagating pulse retains its initial shape or profile while only its characteristics such amplitude, width, chirp and phase can change continuously according to the propagation distance.

Over the past twenty years, solitonic structures have been investigated in nonlinear physical systems and their importance has been discussed in a broad range of contexts that include non-exhaustively optic communication [66–71], Biophysics [72–75], Bose-Einstein condensates [76–78] and Plasma physics [79, 80]. From the seminal work of Washimi and Taniuti [81], who first derived the KdV equation for ion-acoustic waves in the plasmas, soliton theory has been a center of interest for the Plasma physics community with a particular interest in nonlinear phenomena related to structures, instabilities, wave interaction, wave-particle interaction, and methodology related to plasma nonlinear oscillations. Resulting from the suitable balance between nonlinear and dispersive effects, ion-acoustic waves (IAWs), and soliton in general, can spread over long distances, keeping intact their characteristics and shape. One of the direct mechanisms responsible for the formation of solitonic structures in nonlinear media is the modulational instability (MI). The latter occurs when a constant wave background becomes unstable and induces sinusoidal modulations under the competitive contribution of nonlinear and dispersive effects. The result is a self-organization of the system that leads to the emergence of nonlinear structures and solitons. Due to its importance in stable wave propagation, the MI of different waves modes in plasma systems has gained a great attention. Recently, the MI of IAWs in electronegative plasma and other types of plasma has been investigated in some previous works [1, 22, 82–87].

Various applications in plasma science and industry [43, 55, 88, 89], and the proof of its existence in Astrophysics, space, and laboratory experiments make ENPs a subject of growing interest, as witnessed by recent contributions both in one-dimensional and

multidimensional contexts. ENPs have been generated in the laboratory by many different methods [53, 90, 91], which corroborates their presence in many space observations, which include $(\text{H}^+ - \text{H}^-)$ and $(\text{H}^+ - \text{O}_2^-)$ and in the D- and F-regions of the Earth's ionosphere [92, 93]. Moreover, the dynamics and head-on collisions of IAWs in $\text{Ar}^+ - \text{F}^-$ plasmas have been reported experimentally [94], while Ichiki et al. [90] addressed the propagation features of IAWs in $\text{Ar}^+ - \text{SF}_6^-$ plasma. Theoretically, based on such experimental observations, Mamun et al. [95] have regarded the existence of IA and DIA waves in an ENP constituted by Boltzmann negative ions, Boltzmann electrons, and cold mobile positive ions. It was also highlighted recently by Tabi and co-workers that the negative ion concentration ratio and the electron-to-negative ion temperature ratio importantly affect the modulational instability (MI) both in one-, two- and three-dimensional contexts with (without) the presence of the external magnetic field [21–25, 96]. In addition to the above, the structure of the electronegative plasmas sheath without a magnetic field was investigated in Refs. [20, 21, 23] and with magnetic field in Ref. [24]. The study of other aspects and characteristics of such plasmas waves, related to their response to external magnetic fields [63, 64, 97] in the vicinity of the Korteweg-de Vries (KdV) equations are obtained from the reductive perturbation approximation. In the context of the present work, we show that when two- and higher dimensions are considered, magnetized plasma can asymptotically be described by the Davey-Stewartson equations (DSEs). It is, however, important to precise that DSEs are nonlinear partial differential equations, as the Riemann wave system [98], the Novikov-Veselov system [99], the chemotaxis models [100], just to name a few, that were first introduced in fluid dynamics in order to understand the evolution of three-dimensional wave packets in water of finite depth [101]. Since then, they have found application in many areas of Physics, most notably in nonlinear optics [102] as well as related fields such as Bose-Einstein condensates [103] and electromagnetic waves in ferromagnets [104]. A surprising and interesting property of the DSEs is that they are among the few multidimensional systems whose inverse scattering transform is well known [105, 106], and one can actually get a broad range of exact solutions among which are rogue waves [107–109], Langmuir waves [110–112] and dromions [21, 113, 114]. Dromions, defined by an exact and nonlinear solution of any of a large class of two-dimensional partial differential equations, were first time investigated theoretically by Boiti et al. [115]. A particular and important characteristic of dromion solutions is that they are localized wave packets in various physical systems such as plasma physics, fluid dynamics and nonlinear optics [116] and the interactions of dromions for the

(2+1)-dimensional equations may be elastic or inelastic [117–119]. On this basis, important additional features, compared to the NLS equation, may take place and picture very rich behaviors of the multi-dimensional MI activation and the resulting plasma modes, especially when system parameters are suitably chosen. One feature of the present work is to pay an attention to a comprehensive analysis of MI and additionally proposes exact solutions to the DS equations, with the use of the Hirota’s bilinear method [113], and their response to changing system parameters such as the electron-to-negative ion temperature ratio, the negative ion concentration ratio and, more importantly, the magnetic field.

0.2 Problem statement and objectives of the thesis

A limited number of contributions have been devoted the unmagnetized electronegative plasmas made of the electrons, cold positive ions and significant number of negative ions in one and more dimensions [21–23]. In the present thesis, we extend the results of these previous model of unmagnetized electronegative plasma studied by Panguetna et al. [21] to include the external magnetic field. This electronegative plasma model in the presence of the external magnetic field is so-called magnetized electronegative plasma. We are interested by the dynamics of propagation of ion-acoustic waves in electronegative plasma in the presence of external magnetic field, because magnetized plasmas play a very important role in the study of plasma physics. Indeed, the introduction of a magnetic field considerably enriches the physical phenomena that can be generated in plasmas. One of our interests in magnetized plasma has concerned the anisotropic characteristic of plasma in the presence of magnetic field and the properties of waves which depend on the direction of wave vector relative to the magnetic field vector. Moreover, the presence of the external magnetic field can be used to control the directions, the velocity and the electrical properties of the plasma and improve the performance of these processes by confining the plasma and increasing the reaction rate.

The main objective of this present thesis is to analyze the impact of the physical parameters of the system on the activation of modulational instability and on the emergence and propagation of the ion-acoustic waves in the magnetized electronegative plasma. More precisely in our contribution, several specific objectives of the research presented in this thesis are:

- The derivation of the two plasma models from the system consisting of continuity

equation, momentum equation and Poisson's equation by the using of the reductive perturbation method, method, namely, the nonlinear Schrödinger equation and the coupled Davey-stewartson equations.

- The analysis of the generation of the ion-acoustic waves through the models of study using the linear stability analysis.
- The study of the evolution of the relevant parameters of IAWs propagating through the models using the variational approach in NLS equation.
- The obtention of the exact and nonlinear dromion solutions using the bilinear Hirota's method in DS equations, and the study of their interactions.

0.3 Outlines of the thesis

To carry out this thesis, the dissertation is organized as follows

Chapter I is devoted to the literature review on the generalities related to plasma theory. The following the concepts will therefore be addressed: history of plasmas, type of plasmas and some of their useful properties and characteristics, ENPs and magnetized ENPs. Finally, we present the plasmas fluid description that will be the starting-point for studying plasmas dynamics.

Chapter II consists of presenting the models description of the governing equations for the propagation of ion-acoustic waves along the external magnetic field in an electronegative plasma and the method used along the thesis. Here, we present some analytical and numerical methods used to obtain our results.

Chapter III presents the main results and discussion of this thesis. These results concern the dynamics of modulated nonlinear ion-acoustic wave packets and the dynamics of ion-acoustic dromions, both in magnetized electronegative plasma.

We end the present thesis with a general conclusion where we summarize the main results obtained, and give some outlook related to our future investigations.

Literature review

Introduction

Ionized gases are gases made of neutral particles (atoms, molecules) and charged particles (electrons, ions). When the proportion of charged particles is large, it is called plasma. A plasma is therefore a highly ionized or totally ionized gas. We can also say that an ionized gas is the union of a neutral gas and a plasma. Plasma is often described as a state of matter (fourth state of matter), just like the solid state, the liquid state or the gaseous state, although there is no abrupt transition from one of these states to the plasma or vice versa. Plasma is only visible on earth at very high temperatures, when the energy is such that it succeeds in tearing electrons from atoms. We then observe what it is conventionally called a sort of "soup" of extremely active electrons in which the nuclei of atoms "bathe". The nature and composition of plasma allow it to exhibit complex and interesting behaviors. Research shows that plasma constitutes 99% of the visible Universe. We belong to the remaining 1% of the matter on earth which is something different from plasma [38]. Plasmas are found in and around the earth, in lightning channels of the ionosphere, in the aurora, and the earth's magnetosphere. Plasmas are found in the solar wind, in the magnetosphere, and in comets. Around Jupiter and Saturn, we have plasmas in the form of gigantic plasma toroids. The sun and the other stars are nothing but enormous plasma balls. Not only the stars but also the nebula within the galaxies is also composed of plasma and so on. The analysis of plasma properties does not only help to explain some natural phenomena, but also to set devices and some industrial processes. In this chapter, we stand out the literature review on plasmas. Some useful characteristics of plasma like Debye length, temperature, and so on, are presented. Space plasma, plasma production and applications are also introduced here. Finally, we present the plasma fluid models with emphasis in magnetized ENPs.

1.1 Plasma discovery history and plasma formation

1.1.1 Plasma discovery history

The word plasma comes from Greek $\piλάσμα$, meaning something molded or fashioned [37], and describes the collective behavior of the ionized atomic nuclei and the electrons within the surrounding region of the plasma. The term plasma was first used in physics by the American physicist Irving Langmuir in 1928 [36], when he observed the behavior of ionized gas in gas discharge tubes. The oscillations of all the ions observed in these tubes were reminiscent of the oscillations that can be seen in a gelatinous medium (plasma means gelatinous matter in Greek). Except near the electrodes, where there are sheaths containing very few electrons, the ionized gas contains ions and electrons in about equal numbers so that the resultant space charge is very small. We shall use the name plasma to describe this region containing balanced charges of ions and electrons [36]. The development of plasma physics was made following these first discoveries. Originally, a plasma designated a globally neutral ionized gas, then this definition was extended to partially ionized gases whose behavior differs from that of a neutral gas. Today, we talk about plasma when the matter we observe a large number of particles of different natures which can interact with each other and with the environment: it is a soup of electrons, cations, anions, atoms neutrals.... An example of a discharge tube is shown in Figure 1.1.



Figure 1.1: Example of a discharge lamp [120].

1.1.2 Plasma formation

Under the usual conditions, the atoms are in neutral, atomic or molecular form. In the rest of the Universe, however, this "fourth" state of matter is the normal state. To create a plasma from a neutral gas, energy must be supplied to tear one or more electrons from each atom. It is therefore necessary that a sufficient energy is supplied to the atoms so that they are partially, or even totally ionized. The transition from one state to another being achieved by a certain supply of energy ΔE (temperature) as indicated below $Solid \xrightarrow{\Delta E} Liquid \xrightarrow{\Delta E} Gas \xrightarrow{\Delta E} Plasma$ in Fig. 1.2

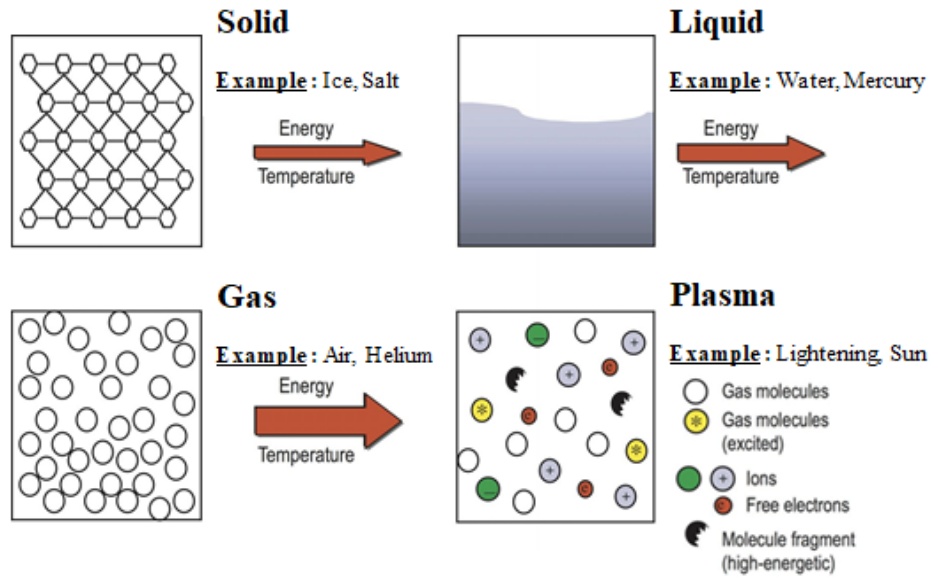


Figure 1.2: Plasma formation by supplying energy/temperature [121].

The different phase changes between these states of the matter are as follows (see Fig. 1.3):

- Freezing: Change of a substance from liquid phase to solid phase;
- Melting: Change from solid phase to liquid phase;
- Vaporization: Change from liquid phase to gaseous phase;
- Condensation: Change from gas phase to liquid phase;
- Sublimation: Change from solid phase to a gas phase without becoming a liquid;
- Deposition: Change from gas phase to solid phase without becoming a liquid;
- Ionization: Change from a gaseous phase to plasma (ionized particles);

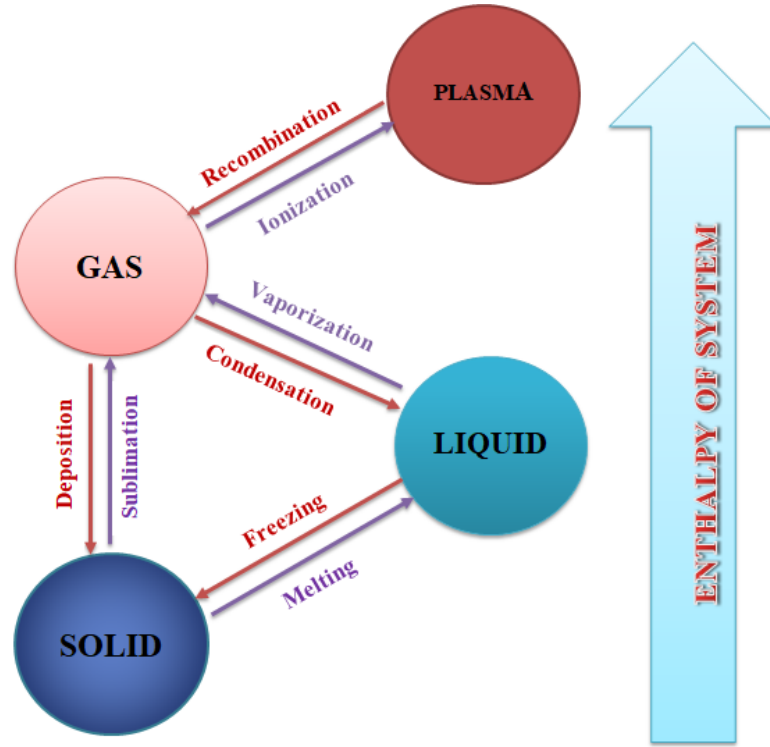


Figure 1.3: Different phase changes between these states of the matter.

- Recombination: Change from plasma to gas.

The enthalpy is defined by the measurement of energy in a thermodynamic system. The physical quantity of enthalpy is equal to the total content of heat of a system, and equivalent to the system's internal energy plus the the product of pressure and volume. A gaseous medium does not allow the conduction of electricity. When this medium is subjected to a weak electric field, a pure gas is considered as a perfect insulator, because it contains no free charged particles (electrons or positive ions). Free electrons and positive ions can appear if the gas is subjected to a strong electric field or to sufficiently high temperatures, if it is bombarded with particles or if it is subjected to a very intense electromagnetic field. When the ionization is significant enough for the number of electrons per unit volume to be comparable to that of neutral molecules, the gas then becomes a highly conductive fluid called plasma.

1.1.3 Multi-photon ionization and plasma generation

For laser intensities ranging from 10^{13} to 10^{14} W/cm^2 , higher order nonlinear processes occur, in particular multiphoton ionization (MPI). At 800 nm, 8 to 10 photons are needed to ionize the nitrogen and oxygen molecules and produce a plasma [122]. Ioniza-

tion by tunnel effect can also occur thanks to the very large electric fields carried by the laser pulse. However, according to Keldysh's theory [123], multi-photon ionization dominates for intensities less than or equal to 10^{14} W/cm^2 . Taken separately, beam collapse due to Kerr self-focusing, like plasma-induced defocusing, should prohibit any long-range propagation of high-power laser pulses through air. However, these two processes can compensate each other and give rise to a self-guided, quasi-solitonic propagation [124]. The laser beam first self-focuses by the Kerr effect. Then, when the intensity is high enough, a plasma is generated by MPI, which defocuses the beam.

1.2 Characteristics of plasma

To characterize a plasma, it is necessary to take into account the number of species present and their different charge states, and study the evolution of the density, the electronic temperature and the distribution function in space and in speed. If the recombination processes between electrons and ions do not balance the ionization process, the plasma is said to be out of thermodynamic equilibrium. The complete study of all the phenomena appearing in a plasma is currently impossible, resulting in an initial simplification necessary for the distinction and classification of plasmas. Faced with this classification difficulty, plasmas are characterized based on their degree of ionization, their density and their electronic temperature. Amongst its characteristics, a plasma displays high sensitivity to electric and magnetic fields. Many scientists are interested in studying plasma because of their temperature, density and the types of particles they contain which are its main characteristics.

1.2.1 Plasma density and degree of ionization

Degree of ionization is the number of electrons, a neutral atom has lost in an ionizing physical process, such as radiation, shock, or collision. The degree of ionization of the plasma is defined by:

$$\alpha = \frac{n_e}{n_e + n_0}, \quad (1.1)$$

where n_e is the density of electrons and n_0 the density of neutral particles. α is included between 0 and 1, which makes it possible to define three types of ionized gases:

If $\alpha \ll 1$, the plasma is said to be weakly ionized.

If $\alpha < 1$, the plasma is said to be partially ionized. Movements are governed by an

external electromagnetic field.

If $\alpha = 1$, the plasma is said to be completely ionized. Movements are dominated by collective interactions between particles (far Coulomb interactions).

1.2.2 Quasi-neutrality in plasma

Quasi-neutrality criterion indicates that a plasma is globally electrically neutral, that is to say that there are as many positive as negative charges. When no external disturbance like an electron or ion is present, a plasma is macroscopically neutral. This means that under equilibrium conditions, with no external forces, in a volume of the plasma sufficiently large to contain a large number of particles and yet sufficiently small compared to the characteristic lengths for variation of macroscopic parameters such as density and temperature, the net resulting electric charge in a plasma is zero. Therefore, the equilibrium charge neutrality condition in the case of three species plasma is given by

$$q_i n_{i0} + q_n n_{n0} - e n_{e0} = 0, \quad (1.2)$$

where n_{i0} , n_{n0} and n_{e0} are respectively, the unperturbed number densities of positive ions, negative ions and electrons. $q_i = Z_i e$ is the positive ions charge, $q_n = -Z_n e$ is the negative ions charge and e is the magnitude of the electron charge. Quasi-neutrality is notably the result of the conservation of the electric charge during the ionization process. If a local potential is imposed in the plasma, the opposite charged particles organize in order to confine the electric field from leaking in to the plasma.

1.2.3 Plasma temperature

Plasma is a collection of many species with range of velocities in three dimensional phase-space. When the density of particles in a velocity space is plotted against the velocity ranging from $-\infty$ to $+\infty$, we get a peak at the centre which falls away from the centre as described by a Maxwellian distribution [125]. The full width at half maximum of the distribution determines the temperature of the species and is associated with the mean velocity of the particles. The Maxwellian distribution of electrons is given by

$$f(v) = n \left(\frac{m}{2\pi kT} \right)^{3/2} \exp \left(-\frac{mv^2}{2kT} \right). \quad (1.3)$$

In the above expression, m denotes mass of electron and T denotes the temperature of the electron. The distribution function $f(v)$ describes the number of particles (dn) in a given

velocity interval, $dn = f(v)dv$. This can be expressed in terms of energy and the electron energy distribution function, $f(E)$ is obtained from the velocity distribution function as

$$f(E) = n \left(\frac{4E}{\pi} \right)^{1/2} (kT)^{-3/2} \exp \left(-\frac{E}{kT} \right). \quad (1.4)$$

One can obtain the average particle velocity, \bar{v} from the velocity distribution function as

$$\bar{v} = \left(\frac{8kT}{\pi m} \right)^{1/2}. \quad (1.5)$$

T_e , T_i , T_- are generally used to denote the temperature of electrons, positive ions and negative ions. If plasma species fulfil the condition $T_g = T_i = T_e = T_{ex} = T_d = T_r$ where T_g , T_i , T_e , T_{ex} , T_d and T_r denote respectively to gas temperature, ion temperature, electron temperature, excitation temperature, dissociation temperature, and radiation temperature, then the plasma is said to be in thermal equilibrium. Complete thermal equilibrium is very difficult to observe, however, under certain laboratory conditions local thermal equilibrium can be achieved. If the ion temperature and gas temperature is comparable with the electron temperature, the plasma is said to be in local thermal equilibrium. Typically for low pressure plasmas, $T_e \gg T_i \approx T_g$ and therefore, the plasma is said to be in non-thermal equilibrium.

1.2.4 Plasma frequency

Plasma frequency is a cut-off pulse defined as the minimum value below which the wave can not propagate in the plasma. However when the electrons in a quasineutral plasma (the equilibrium of the plasma) are perturbed from their equilibrium positions, an electric field will be built in such a direction such that the resulting internal space charge fields give rise to collective particle motions that tend to restore the original charge neutrality. As the ions are massive compared to the electrons, they form a uniform background. Due to inertia, the electrons will overshoot and oscillate about their equilibrium positions with a characteristic frequency, which is known as plasma frequency. Since these collective oscillations are high-frequency oscillations, the ions, because of their heavy mass, are, to a certain extent, unable to follow the motion of the electrons. On solving the basic fluid equations for a plasma with singly charged ions, the electron-plasma frequency ω_p is [126]

$$\omega_p = \sqrt{\frac{ne^2}{\varepsilon_0 m_e}}, \quad (1.6)$$

where m_e stands for the mass of an electron. For the properties of the plasma to be determined by electromagnetic rather than hydrodynamic collision, the plasma frequency must be large compared to the ordinary collision frequency.

1.2.5 Debye length and Debye shielding

One of the most important property of a plasma is the shielding of every charge in the plasma by a cloud of opposite charged particles and it is called the Debye Shielding. The Debye length is an important physical parameter for the description of a plasma [127]. It provides a measure of the distance over which the influence of the electric field of an individual charged particle is felt by the other charged particles inside the plasma. The charged particles arrange themselves in such a way as to effectively shield any electrostatic fields within a distance of the order of the Debye length. This shielding of electrostatic fields is a consequence of the collective effects of the plasma particles. A Debye sphere is a volume whose radius is the Debye length, in which there is a sphere of influence, and outside of which charges are screened. In most types of plasma, quasi-neutrality is not just an ideal equilibrium state, it is a state that the plasma actively tries to achieve by readjusting the local charge distribution in response to a disturbance. A fundamental characteristic of plasma behavior is its ability to shield electrical potentials applied to it. Suppose we try to create by a hypothetical experiment an electric field inside a

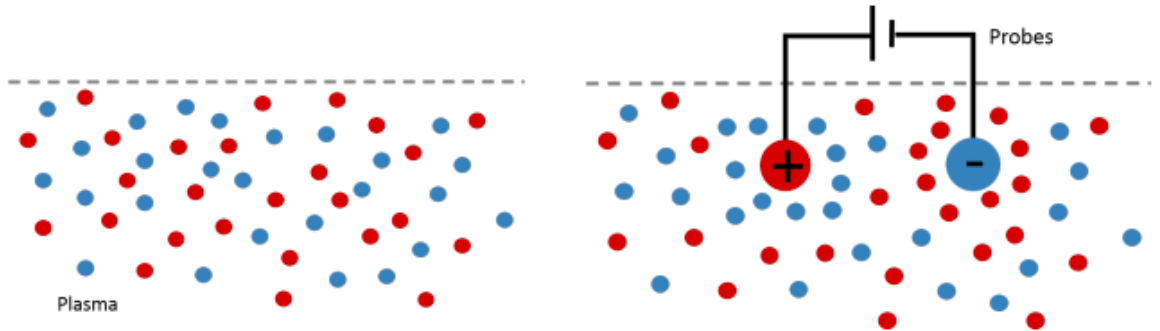


Figure 1.4: Debye shielding of charged spheres immersed in a plasma [128].

plasma by inserting two charged balls connected to a battery [37, 128]. After a while, as materialized in Fig. 1.4 the balls will attract plasma particles of opposite charge, and almost immediately a cloud of ions will surround the negative ball and a cloud of electrons will surround the positive ball. It turns out that, the potential $\phi(r)$ of this ball after such a readjustment has taken place, can be obtained from the solution of Poisson's equation.

$$\nabla^2 \phi = -\frac{e}{\varepsilon_0}(n_i - n_e). \quad (1.7)$$

Assuming Boltzmann distribution for the electrons ($n_e = n_0 \exp(e\phi/kT_e)$) and for a small change in the sheath potential ($e\phi \ll kT_e$), such that the positive ion density is fixed ($n_i = n_0$), the equation (1.7) after Taylor's expansion of exponent term and neglecting all the higher order terms of ϕ gives

$$\frac{d^2 \phi}{dx^2} = \frac{e^2 n_0}{\varepsilon_0 k T_e} \phi, \quad (1.8)$$

where n_0 is the plasma density far away from the charged conductor at potential ϕ_0 and ϕ is the potential at a distance x from the conductor. The solution to this equation can be written as

$$\phi = \phi_0 \exp\left(-\frac{|x|}{\lambda_D}\right), \quad (1.9)$$

where the Debye length is defined as

$$\lambda_D = \left(\frac{\varepsilon_0 k T_e}{e^2 n_e}\right)^{1/2}. \quad (1.10)$$

Thus quasineutrality, which is the basic criterion for an ionized gas to be plasma, will exist if the dimensions of the system are large compare to the Debye length. Also for Debye shielding to be statistically valid there must be a large number of particles N_D in a Debye sphere. As mentioned before, the Debye length can also be regarded as a measure of the distance over which fluctuating electric potentials may appear in a plasma, corresponding to a conversion of the thermal particle kinetic energy into electrostatic potential energy. When a boundary surface is introduced in a plasma, the perturbation produced extends only up to a distance of the order of λ_D from the surface. In the neighborhood of any surface inside the plasma there is a layer of width of the order of λ_D , known as the plasma sheath, inside which the condition of macroscopic electrical neutrality may not be satisfied. Beyond the plasma sheath region there is the plasma region, where macroscopic neutrality is maintained. Generally, λ_D is very small. For example, in a gas discharge, where typical values for T and n_e are around $10^4 K$ and $10^{16} m^{-3}$, respectively, we have $\lambda_D = 10^{-4} m$. For the Earth's ionosphere, typical values can be taken as $n_e = 10^{12} m^{-3}$ and $T = 10^3 K$, yielding $\lambda_D = 10^{-4} m$. In the interstellar plasma, on the other hand, the Debye length can be several meters long as we can see in table 1.1.

Plasma	Electron density (m^3)	Electron temperature (K)	Magnetic field (T)	Debye length (m)
Gas discharge	10^{16}	10^4	-	10^{-4}
Tokamak	10^{20}	10^8	10	10^{-4}
Ionosphere	10^{12}	10^3	10^{-5}	10^{-3}
Magnetosphere	10^7	10^7	10^{-8}	10^2
Solar core	10^{32}	10^7	-	10^{-11}
Solar wind	10^6	10^5	10^{-9}	10
Interstellar medium	10^5	10^4	10^{-10}	10
Intergalactic medium	1	10^6	-	10^5

Table 1.1: The table shows the number density, the electron temperature, the magnetic field and the Debye length of some natural and artificial plasmas [129].

It is convenient to define a Debye sphere as a sphere inside the plasma of radius equal to λ_D . Any electrostatic field originated outside a Debye sphere is effectively screened by the charged particles and do not contribute significantly to the electric field existing at its center. Consequently, each charge in the plasma interacts collectively only with the charges that lie inside its Debye sphere, its effect on the other charges being effectively negligible. The number of electrons N_D , inside a Debye sphere, is given by

$$N_D = \frac{4}{3}\pi\lambda_D^3 n_e = \frac{4}{3}\pi \left(\frac{\epsilon_0 kT}{n_e^{1/3} e^2} \right)^{3/2}. \quad (1.11)$$

The Debye shielding effect is a characteristic of all plasmas, although it does not occur in every medium that contains charged particles. A necessary and obvious requirement for the existence of a plasma is that the physical dimensions of the system be large compared to λ_D . Otherwise there is just not sufficient space for the collective shielding effect to take place, and the collection of charged particles will not exhibit plasma behavior. If L is a characteristic dimension of the plasma, a first criterion for the definition of a plasma is therefore

$$L \gg \lambda_D. \quad (1.12)$$

Since the shielding effect is the result of the collective particle behavior inside a Debye sphere, it is also necessary that the number of electrons inside a Debye sphere be very large. A second criterion for the definition of a plasma is therefore

$$n_e \lambda_D^3 \gg 1 \implies N_D \gg 1. \quad (1.13)$$

This means that the average distance between electrons, which is roughly given by $n_e^{-1/3}$, must be very small compared to λ_D .

1.2.6 Plasma parameter

Plasma parameter is the quantity defined by

$$g = \frac{1}{n_e \lambda_D^3}, \quad (1.14)$$

and the condition $g \ll 1$ is called the plasma approximation [128]. This parameter is also a measure of the ratio of the mean interparticle potential energy to the mean plasma kinetic energy. Note that the macroscopic neutrality is sometimes considered as a third criterion for the existence of a plasma.

1.2.7 Criteria for ionized gas to be a plasma

We have given two conditions that an ionized gas must satisfy to be called a plasma. A third condition has to do with collisions. Plasma oscillation is an example of collective response of plasma particles. In case of weakly ionized gases plasma particles may make frequent collisions with neutral atoms and then the notion of collective response fails. So for an ionized gas to be a plasma, the period of typical plasma oscillation must be much smaller than the mean time (τ) between collisions with neutral atoms. So we require [37, 38, 130]

$$w_p \tau > 1, \quad (1.15)$$

where w_p is the frequency of typical plasma oscillation. Finally, the three conditions a plasma must satisfy are therefore:

$$L \gg \lambda_D, \quad N_D \gg 1, \quad w_p \tau > 1. \quad (1.16)$$

1.2.8 Particle interactions and collective effects

The properties of a plasma are markedly dependent upon the particle interactions. The existence of collective effects is one of the basic features that distinguish the behavior of plasmas from that of ordinary fluids and solids. Due to the long range of electromagnetic forces, each charged particle in the plasma interacts simultaneously with a considerable number of other charged particles, resulting in important collective effects that are responsible for the wealth of physical phenomena that take place in a plasma [37]. The particle

dynamics in a plasma is governed by the internal fields due to the nature and motion of the particles themselves, and by externally applied fields. The basic particle interactions are electromagnetic in character. Quantum effects are negligible, except for some cases of close collisions. In a plasma, we must distinguish between charge-charge and charge-neutral interactions. A charged particle is surrounded by an electric field and interacts with the other charged particles according to the coulomb force law, with its dependence on the inverse of the square of the separation distance. Furthermore, a magnetic field is associated with a moving charged particle, which also produces a force on other moving charges. The charged and neutral particles interact through electric polarization fields produced by distortion of the neutral particle's electronic cloud during a close passage of the charged particle. The field associated with neutral particles involves short-range forces, such that their interaction is effective only for interatomic distances sufficiently small to perturb the orbital electrons. It is appreciable when the distance between the centers of the interacting particles is of the order of their diameter, but nearly zero when they are farther apart. Its characteristics can be adequately described only by quantum-mechanical considerations. In many cases this interaction involves permanent or induced electric dipole moments. A distinction can be made between weakly ionized and strongly ionized plasmas in terms of the nature of the particle interactions. In a weakly ionized plasma the charge-neutral interactions dominate over the multiple coulomb interactions. When the degree of ionization is such that the multiple coulomb interactions become dominant, the plasma is considered strongly ionized. As the degree of ionization increases, the coulomb interactions become increasingly important so that in a fully ionized plasma all particles are subjected to the multiple coulomb interactions.

1.2.9 Collisions in plasmas

Collisions between charged particles in a plasma differ fundamentally from those between molecules in a neutral gas because of the long-range character of the Coulomb force. In fact, binary collision processes can only be defined for weakly coupled plasmas. However, that binary collisions in weakly coupled plasmas are still modified by collective effects. Nevertheless, for large Λ , where Λ is the typical number of particles contained in a Debye sphere, we can speak of binary collisions, and therefore of a collision frequency, denoted by $\nu_{ss'}$ [126]. Here, $\nu_{ss'}$ measures the rate at which particles of species s are scattered by those of species s' . When specifying only a single subscript, one is generally

referring to the total collision rate for that specie, including impacts with all other species. Very roughly,

$$\nu_s \simeq \sum_{s'} \nu_{ss'}. \quad (1.17)$$

The species designations are generally important. For instance, the relatively small electron mass implies that for unit ionic charge and comparable species temperatures, we have

$$\nu_e \sim \left(\frac{m_i}{m_e} \right)^{1/2} \nu_i. \quad (1.18)$$

Furthermore, the collision frequency ν measures the frequency with which a particle trajectory undergoes a major angular change due to Coulomb interactions with other particles. Coulomb collisions are, in fact, predominately small-angle scattering events, so the collision frequency is not the inverse of the typical time between collisions. Instead, it is the inverse of the typical time needed for enough collisions to occur that the particle trajectory is deviated through 90° . For this reason, the collision frequency is sometimes termed the 90° -*scattering rate*. It is conventional to define the mean-free-path

$$\lambda_{\text{mfp}} \equiv v_t / \nu. \quad (1.19)$$

Clearly, the mean-free-path measures the typical distance a particle travels between collisions (i.e., scattering events). A collision-dominated, or collisional plasma is one in which

$$\lambda_{\text{mfp}} \ll L, \quad (1.20)$$

where L is the observation length-scale. The opposite limit of large mean-free-path is said to correspond to a collisionless plasma. Collisions greatly simplify plasma behaviors by driving the system towards statistical equilibrium, characterized by Maxwell-Boltzmann distribution functions. Furthermore, short mean-free-paths generally ensure that plasma transport is local (i.e., diffusive) in nature, which is a considerable simplification. The typical magnitude of the collision frequency is

$$\nu \sim \frac{\ln \Lambda}{\Lambda} \omega_p. \quad (1.21)$$

Note that $\nu \ll \omega_p$ in a weakly coupled plasma. It follows that collisions do not seriously interfere with plasma oscillations in such systems. On the other hand, in a strongly coupled plasma, $\nu \gg \omega_p$, which suggests that collisions effectively prevent plasma oscillations

in such systems. This accords well with our basic picture of a strongly coupled plasma as a system dominated by Coulomb interactions which does not exhibit conventional plasma dynamics. It follows that

$$\nu \sim \frac{e^4 \ln \Lambda}{4\pi\epsilon_0^2 m^{1/2}} \cdot \frac{n}{T^{3/2}}. \quad (1.22)$$

Thus, diffuse, high temperature plasmas tend to be collisionless, whereas dense, low temperature plasmas are more likely to be collisional. Note that while the collisions are crucial to the confinement and dynamics (e.g., sound waves) of neutral gases, they play a far less important role in plasmas. In fact, in many plasmas the magnetic field effectively plays the role that collisions play in a neutral gas. In such plasmas, charged particles are constrained from moving perpendicular to the field by their small Larmor orbits, rather than by collisions. Confinement along the field-lines is more difficult to achieve, unless the field-lines form closed loops or closed surfaces. Thus, it makes sense to talk about a collisionless plasma, whereas it makes little sense to talk about a collisionless neutral gas. Note that many plasmas are collisionless to a very good approximation, especially those encountered in astrophysics and space plasma physics contexts.

1.3 Types of plasmas and Applications

1.3.1 Types of plasmas

The creation of a plasma requires a significant input of energy. This can be done by heating, by bombardment with a very intense laser beam or even by electric discharge in a gas subjected to a very high potential difference (in devices known as discharge tubes). Two types of plasma are traditionally distinguished: **cold plasmas**, also called **non-thermal plasmas** whose temperature remains below $10^5 K$ (the electrons have acquired enough energy to carry out reactions by collision with other species) and **hot plasmas**, even **thermal plasmas** for which the temperature exceeds $10^6 K$ (the electrons, but also the ions are energetic enough to influence the behavior of the plasma).

In the following figure (Fig. 1.5), the logarithmic scales show the extent of the ranges of parameters that are encountered in nature and in laboratory plasmas. Plasmas are extremely widespread in the Universe since they represent more than 99% of the available matter [37]. However, they pass almost unnoticed in our immediate environment, given their conditions of appearance very far from the temperature and pressure conditions of the Earth's atmosphere. Examples of plasmas in nature are numerous, we can cite:

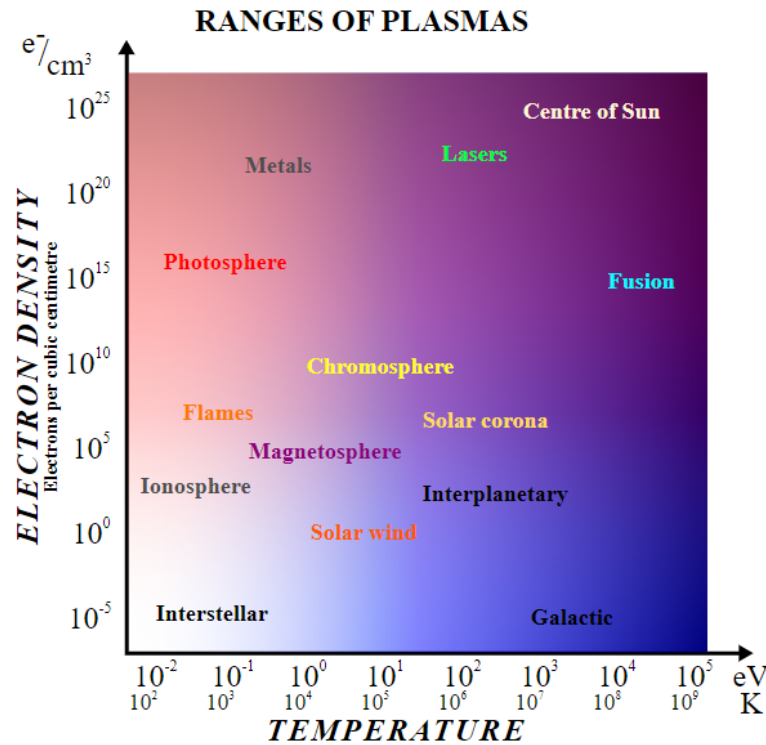


Figure 1.5: Densities and electronic temperatures of the main types of plasmas (the free electrons in a metal can be considered as an electron plasma), [https://fr.wikipedia.org/wiki/Physique des plasmas](https://fr.wikipedia.org/wiki/Physique_des_plasmas) [Consulted on 13/09/23].

- Earth's magnetosphere and ionosphere.
- The core of stars, an example of hot and very dense plasma.
- Neon tubes and the phenomenon of lightning (electric discharges).
- Flames (The query of whether the flames are true plasmas is not settled: if the gas present in the flame is luminous, it is basically because of the temperature due to the exothermic combustion reactions (this gas behaves approximately like a black body) and is only very partially ionized.)

Thus, we can distinguish between natural plasmas and artificial plasmas (created by man):

■ **Natural plasmas:** Earth's natural plasma, Space and astrophysical plasmas:

- Flames;
- Lightning;
- The ionosphere;



Figure 1.6: Flame (left panel), trail of shooting stars (middle panel) and Plasma lamp (right panel), [https://fr.wikipedia.org/wiki/ état plasma](https://fr.wikipedia.org/wiki/état_plasma) [Consulted on 13/09/23].

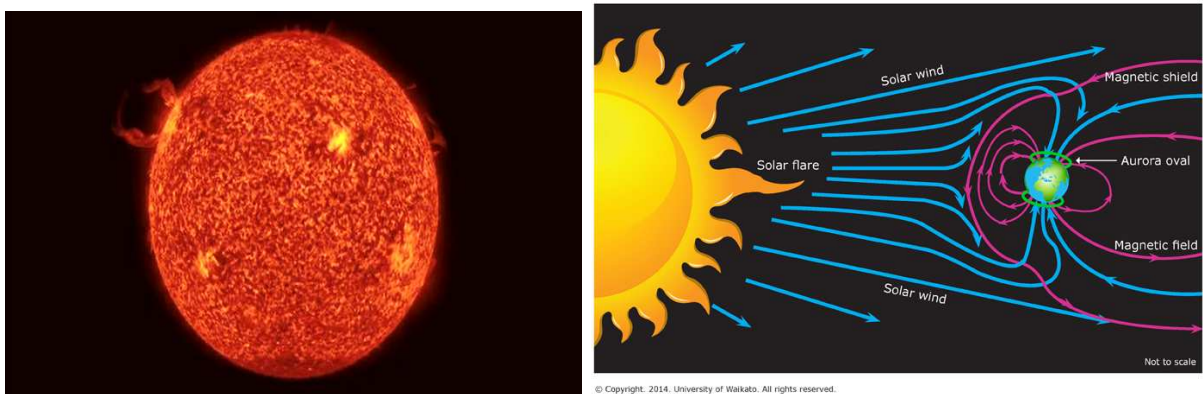


Figure 1.7: The sun is a ball of plasma (left panel), and the solar wind plasma and magnetosphere (right panel), www.sciencelern.org.nz [Consulted in 13/09/23].

- Sun
- The solar wind;
- Stars, gaseous nebulae, quasar, pulsar;
- The aurora borealis;
- The tail of comets;
- the trail of shooting stars;

The panels of figure 1.6 show three examples of plasma, namely flame in the left panel, the trail of shooting stars in the middle panel and plasma lamp in the right panel. Also, the sun (Fig. 1.7), as well as most stars, is made of plasma. Due to the very high temperatures found within the sun, these elements exist not in the gaseous state but as plasma. The sun emits a vast amounts of energy due to the thermonuclear fusion reactions

occurring within the core that convert hydrogen nuclei into helium nuclei. The energy output from this reaction has been estimated to $3.86 \times 10^{23} \text{ kJ}$ per second. Otherwise, the outer atmosphere of the Sun is known as the corona. Temperatures within this region are extremely high, giving some of the charged particles present sufficient energy to escape from the strong gravitational pull of the Sun. This stream of charged particles emanating from the Sun in all directions at speeds of about 400 km/s is called the solar wind Fig. 1.7. It is a rapidly moving plasma that pushes out the edge of the solar system. The solar wind is not uniform. Although it is always directed away from the sun, its intensity and speed are dependent on the activity of the sun. For example, major solar eruptions known as coronal mass ejections (CMEs) can increase the plasma density and speed of the solar wind. This can impact on the Earth's magnetic field, causing increased auroral activity and, in extreme cases, geomagnetic storms that can disrupt communication systems and cause power surges on electrical transmission grids.

■ **Artificial created plasmas:** industrial plasmas or laboratory plasmas:

- Plasma screens (televisions, monitors);
- Plasma discharges (as in a high-voltage circuit breaker), or discharge tube (lamps, screens, cutting torch, X-ray production), see Fig. 1.8;

Plasma lighting



Figure 1.8: Plasma lighting, https://fr.wikipedia.org/wiki/état_plasma [Consulted on 13/09/23].

- Plasmas processing for deposition, etching, surface modification or doping by ion implantation;
- Plasma propulsion;
- Nuclear fusion (see also Tokamak, Stellarator and Z-pinch);

- and many other applications which are still only laboratory experiments or prototypes (radar, combustion improvement, waste treatment, sterilization, etc.).

The panels of Fig. 1.8 show the examples of Plasma discharges (as in a high-voltage circuit breaker) and discharge tube (lamps) produced in laboratory. Most artificial plasmas are generated by the application of electric and/or magnetic fields through a gas. Plasma generated in a laboratory setting and for industrial use can be generally categorized by: the type of power source used to generate the plasma DC, AC (typically with radio frequency (RF)) and microwave, the pressure they operate at vacuum pressure ($< 10\text{mTorr}$ or 1Pa), moderate pressure ($\approx 1\text{Torr}$ or 100Pa), atmospheric pressure (760Torr or 100kPa), the degree of ionization within the plasma fully, partially, or weakly ionized, the temperature relationships within the plasma-thermal plasma ($T_e = T_i = T_{\text{gas}}$), non-thermal or "cold" plasma ($T_e \gg T_i = T_{\text{gas}}$), the electrode configuration used to generate the plasma and the magnetization of the particles within the plasma-magnetized (both ion and electrons are trapped in Larmor orbits by the magnetic field), partially magnetized (the electrons but not the ions are trapped by the magnetic field), non-magnetized (the magnetic field is too weak to trap the particles in orbits but may generate Lorentz forces)

1.3.2 Some applications of plasmas

The applications of plasma physics (even in the presence of the external magnetic field) are very diverse and in full development, in fields as varied as:

Thermonuclear fusion: by producing a plasma of very high density and with very high temperature, physicists hope to initiate nuclear fusion reactions and thus create a considerable energy generator. The most exciting application of plasmas is the production of power from thermonuclear fusion. Nuclear fusion is the process of recombining nuclei to form different nuclei and release vast amounts of energy. This is the process that powers the sun. The presence of an external magnetic field can be used to control the direction and velocity of the plasma, improving the efficiency of the propulsion system.

Plasma-based electronics: the use of cold plasmas makes it possible to produce electronic circuits integrated, for example in the plasma screens of some televisions, see Fig. 1.9. It can be used in plasma-based electronics for displays, lighting, and energy generation. Plasma is also being used in many high technology industries. It is used in making many microelectronic or electronic devices such as semiconductors. It can help make features on chips for computers. Plasma is also used in making transmitters for microwaves

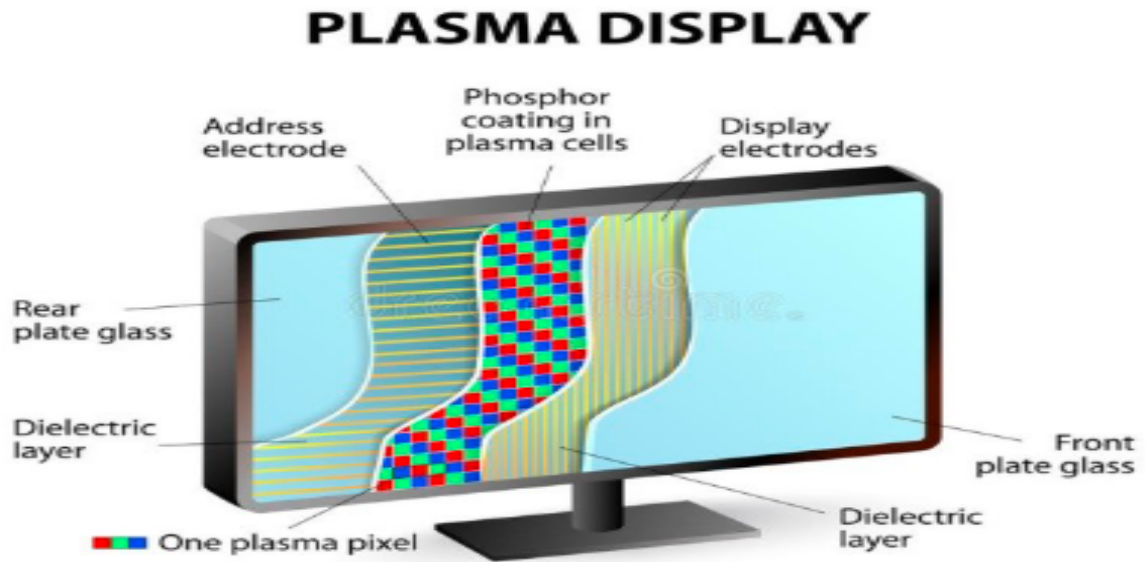


Figure 1.9: Plasma screen of TV [121].

or high temperature films. It can even be used in work with minerals such as diamond, and in extracting economically valuable metals from rock. The presence of an external magnetic field can be used to control the electrical properties of the plasma, allowing for more efficient and flexible electronic devices.

Materials processing: plasma etching and deposition in semiconductor technology are a very important related enterprise.

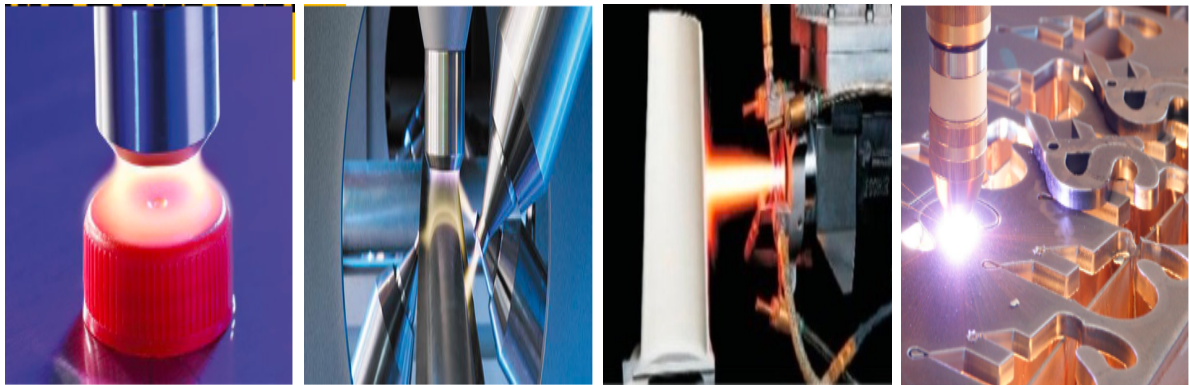


Figure 1.10: Surface treatment (first two panels), materials for plasma spray coating (third panel) and welding-plasma-cutting (last panel) [121].

Plasmas used for these purposes are sometimes called process plasmas. Plasmas are used to destroy, transform (modify, see Fig. 1.10), analyze, weld, create, ...matter. For example, plastic fibers can be plasma treated to become waterproof. A whole field of plasma chemistry exists where the chemical processes that can be accessed through highly excited atomic states are exploited, see Fig. 1.11. The presence of an external magnetic field can

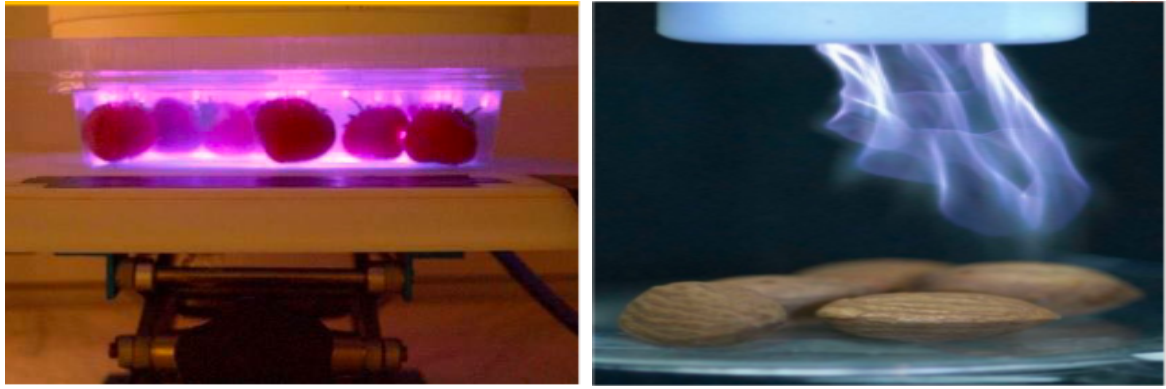


Figure 1.11: Food treatment [121].

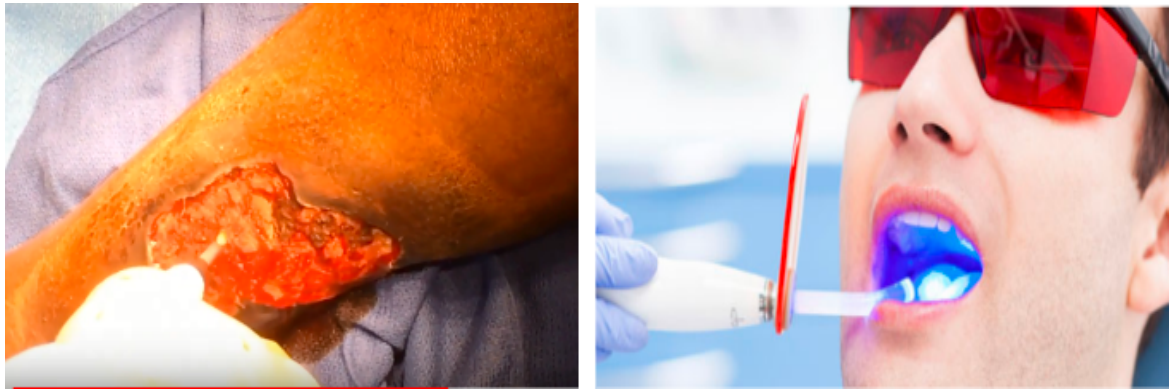


Figure 1.12: Plasma modification of biomedical surfaces: plasma based Decontamination/Sterilization, direct therapeutic plasma application (left panel) and teeth whitening with Plasma (right panel) [121].

improve the performance of these processes by confining the plasma and increasing the reaction rate.

Plasma medicine: plasmas have been shown to have antimicrobial properties and can be used in medical applications such as wound healing and sterilization. It is an emerging field that combines plasma physics, life sciences and clinical medicine. It is being studied in disinfection, healing, and cancer [131]. It uses ionized gas (physical plasma) for medical uses or dental applications [132], see the right panel of Fig. 1.12. Generally, the plasma sources used for plasma medicine are generally low temperature plasmas, and they generate ions, chemically reactive atoms and molecules, and UV-photons. the use of cold plasmas at atmospheric pressure for biomedical applications is a young and promising field of research in which active species (molecular or ionic) are generated in plasmas to treat biological tissues, making it possible in particular to carry out local treatment. The plasma sources developed generally take the form of plasma jets, micro discharges or dielectric barrier discharges and the applications studied concern the sterilization of

plates (like subjecting human body or internal organs to plasma treatment for medical purposes, see the left panel of Fig 1.12), tissue regeneration or even the treatment of cancer cells (apoptosis induced by plasma treatment). Currently, most Most of the research is in vitro and in animal models. This possibility is being heavily investigated by research groups worldwide under the highly-interdisciplinary research field called plasma medicine. The presence of an external magnetic field can enhance the effectiveness of the plasma on targeted areas.

1.4 Electronegative plasma concept

Electronegative plasmas can be defined as those formed in electron attaching gases and having such a density of negative ions that they must be taken into account. By contrast the properties of conventional electropositive plasmas owe much to the large mass difference between the positive and negative charge carriers.

1.4.1 Electronegative plasma description

Considered as one of the four states of matter, just like solids, liquids, and gas, plasmas are composed of positive ions in addition to negative ions and electrons, and, when a significant amount of negative ions is involved, they are known as electronegative plasma (ENP). The self-consistent electric field acting in a plasma retards the most mobile charged particles, which usually leads to a Boltzmann distribution of electrons. If negative ions cross the discharge volume several times during their lifetime in the volume processes, these particles also obey the Boltzmann distribution. It is demonstrated that this condition is usually satisfied when the characteristic time of electron attachment is small as compared to the time of ambipolar diffusion of the negative ions (ion diffusion at an electron temperature). In the opposite case, the profiles of electrons and negative ions are similar. An assumption that is frequently made in plasma physics is that when the plasma is contained in a potential well that confines the negative particles, it accelerates the positive ones so that the fluxes of particles of opposite sign are equal throughout the volume all the way to the boundary wall. In the absence of negative ions, this gives rise to the concept of ambipolar diffusion at higher pressure [133]. In situations where there are a significant number of negative ions and the plasma is essentially collisionless, it is

permissible to set

$$n_e = n_{e0} \exp(\phi), \quad (1.23)$$

where n_e is the electron density, n_{e0} the unperturbed density of electron and $\phi = \frac{eV}{kT_e}$ (where V is the electrostatic potential and T_e the electron temperature) measured relative to the potential at the center (k is Boltzmann's constant and e the electronic charge) and to set

$$n_n = n_{n0} \exp(\sigma_n \phi), \quad (1.24)$$

where n_n is the negative ion density and $\sigma_n = T_e/T_n$ (where T_n is the negative-ion temperature). This follows from their respective equations of motion to the walls under the potential gradient.

1.4.2 The technological interest of electronegative plasmas

Electronegative plasmas have been used for decades in fundamental plasma physics studies and for various applications, including etching for micro-electronics, thermonuclear fusion and more recently, spacecraft propulsion [134, 135]. These plasmas can be formed using many different types of electrical discharges powered by the electronegative gases (such as H_2 , O_2 , CF_4 , SF_6 , Cl_2 , I_2) [135, 136]. For example Cl_2 based discharges are found to be a good source of etchant for platinum and aluminium [137]. The active chlorine atoms are produced in the plasma by electron impact dissociation of chlorine molecule according to the reaction $2e^- + Cl_2 \rightarrow 2Cl^-$. Along with the formation of reactive species the electronegative gases also produces negative ions mainly through dissociative attachment. The role of negative ions in plasmas is important as their presence in the discharge can modify the Bohm speed that affects the positive ion flux at the substrate. With an abundance of negative ions, the electron population may reduce significantly in the plasma. On the other hand, the effective temperature of the plasma may increase as low energy electrons are lost via attachments with neutrals to form negative ions. The discharge impedance also increases with the increase of negative ions. Very electronegative, or ion-ion (also called pair-ion), plasmas where the ratio between the negative ion and electron densities (referred to as the electronegativity) reaches values of a few thousand or more, have potential use in the majority of the above-mentioned applications because of the reduced impact of electrons on wall sheath formation, and similar responses of the plasma to positive or negative voltage biases.

1.5 Magnetized plasma concept

A plasma in which the magnetic field is strong enough to influence the movement of the charged particles is called magnetized plasmas. A general quantitative criterion is that an average particle completes at least one gyration around the magnetic field before it collides (i.e. $\omega_{ce}/\nu_{coll} \geq 1$ [38], where ω_{ce} is the electron gyrofrequency and ν_{coll} is the electron collision rate). It is often the case that the electrons are magnetized while the ions are not. Magnetized plasmas are anisotropic, meaning their properties in the direction parallel to the magnetic field differ from those perpendicular to them. While the electric field in plasmas is usually small due to its high conductivity, the electric field associated with a plasma moving in a magnetic field is given by $\mathbf{E} = -\mathbf{v} \times \mathbf{B}$ (where \mathbf{E} is the electric field, \mathbf{v} is the speed, and \mathbf{B} is the magnetic field) and is not affected by the Debye shield.

Lorentz Force: The amalgamation of the electric force and magnetic force on a point charge produces electromagnetic force, which is also known as Lorentz force. It happens because of the electromagnetic field. The equation of motion is

$$m \frac{d\mathbf{v}}{dt} = \mathbf{F} = q(\mathbf{E} + \mathbf{v} \times \mathbf{B}), \quad (1.25)$$

where m and q are the charge of the particle and particle mass, respectively.

Gyrofrequency and Gyroradius: Let us consider that particle is moving in a homogeneous and stationary magnetic field which is working along the z-axis. Let $\mathbf{E} = 0$ and $\mathbf{B} = (0, 0, B_z)$. From 1.25, we obtain

$$\omega_c = \frac{|q|B_z}{m}, \quad (1.26)$$

which is known as cyclotron frequency or gyrofrequency and it is always positive.

1.6 Magnetized electronegative plasma

The electronegative plasma (referring to a type of plasma that has a significant presence of negative ions) with the presence of the external magnetic field is so-called magnetized electronegative plasma. This plasma is made of negative ions, electrons, cold mobile positive ions and the external magnetic field. The practical existence of the model is characterized by its potential to enhance several applications across various fields such as plasma etching, surface treatment, ion implantation, and fabrication of semiconductor

devices [138–140]. Moreover, the presence of the external magnetic field can be used to control the directions, the velocity and the electrical properties of the plasma and improve the performance of these processes by confining the plasma and increasing the reaction rate.

1.7 Waves in plasma

In a plasma, the existence of the electric charges which constitute it, cannot be considered independently of the electric and magnetic fields which reign within it. One of the characteristics of this domain is the need to treat on an equal footing the dynamics of particles and those of fields. In order to group plasmas into different classes, certain parameters must be defined characteristics of the behavior of particles in a plasma subjected to electromagnetic fields: ionization degree, plasma frequency, temperature, density of plasma particles. Waves in plasmas can be classified as electromagnetic or electrostatic according to whether or not there is an oscillating magnetic field. Applying Faraday's law of induction to plane waves, we find $\omega \mathbf{B} = \mathbf{k} \times \mathbf{E}$ equation implying that an electrostatic wave must be purely longitudinal. An electromagnetic wave, in contrast, must have a transverse component, but may also be partially longitudinal [141, 142]. It is well known that plasma is a dispersive media. Again from the study of plasma oscillation it is obvious that plasma waves can propagate in a dispersive media. So in plasma medium, plasma particles and waves can coexist and they can interact with each other and the oscillation can occur. It is also used in the communication technology. As the information between the human beings is exchanged by the radio waves, so plasma has great applications in this field. Waves are also important for large-scale processes in nature. These waves helped in the propagation of light from sun to earth. The light waves present in the solar radiation heat the earth, but effect of this heating is balanced by cooling due to emission of long wavelength thermal wave radiation from the earth. Plasma waves are accelerating the ionized particles to speeds above the escape velocity. In space plasma, the study of plasma is dealing with the reorganization of basic properties of the plasma like effect of magnetic field and density etc. It also involves the measurement of the characteristic frequencies of the plasma to understand these basic properties. Strong interactions can occur between these plasma waves because the charged in plasma respond to static and oscillatory electromagnetic fields. These strong interactions are often referred as instabilities. Langmuir waves named after the scientist Irving Langmuir are an example

of these plasma oscillations. These are the rapid oscillations of the electron density in conducting media such as plasmas or metals. These plasma waves and instabilities are sometimes important to study the energy evolution and flux of plasma in its magnetized phase. These are also beneficial to predict the state of plasma and can also apply to other plasma related phenomenon.

1.7.1 Electromagnetic electron waves

In plasma physics, an electromagnetic electron wave is a wave in a plasma which has a magnetic field component and electrons are the main particles that oscillate. In an unmagnetized plasma, an electromagnetic electron wave is simply a light wave modified by the plasma. In a magnetized plasma, there are two modes perpendicular to the field, the O and X modes (ordinary and extraordinary modes), and two modes parallel to the field, the R and L waves (right-hand circularly polar wave and left-hand circularly polar wave). These are transverse in nature. In these waves the electric and magnetic field vectors are perpendicular to each other and also perpendicular to the direction of propagation of wave.

1.7.2 Electrostatic waves

Electrostatic waves are longitudinal waves produced in plasma. They occur due to local perturbations of the electric neutrality, which accelerate charged particles in the plasma's neighbourhood, resulting in charge oscillations. These plasma oscillations can be produced by a local pulse [143] due to a probe or a grid launcher excitation [144, 145]. Electrostatic waves are longitudinal and have no electric field component perpendicular to the direction of propagation ($\mathbf{k} \times \mathbf{E} = \omega = 0$). Since, \mathbf{k} is in direction of propagation, \mathbf{E} and \mathbf{k} are parallel. Thus, the magnetic field of the wave is zero.

1.7.3 Ion-acoustic waves

In plasma physics, an ion acoustic wave is one type of longitudinal oscillation of the ions and electrons in a plasma, much like acoustic waves traveling in neutral gas. However, because the waves propagate through positively charged ions, ion acoustic waves can interact with their electromagnetic fields, as well as simple collisions. In plasmas, ion acoustic waves are frequently referred to as acoustic waves or even just sound waves. These waves can propagate through collisionless medium while sound waves do not do the same.

This is the main difference between these two types of waves. A second difference is that plasma also contains electrons which have their effect on the wave dispersion equation. Electrons are very mobile due to their small size and mass so they quickly follow the ion motion trying to maintain the charge neutrality in the medium. Motion of these electrons is due to a small electric field that are generated by the plasma as a result of variations in the local ion density. Ion acoustic wave is the low frequency plasma wave. Here, the electron and ion fluids must be considered together. According to [144], the ordinary acoustic waves and ion acoustic waves can differentiate on the basis of the electric field induced by a slight charge separation. The electron component of the ion acoustic wave tends to propagate faster than the ion component. The electric field retards the electron motion, forcing the two species to propagate together. They commonly govern the evolution of number density, for instance due to pressure gradients, on time scales longer than the frequency corresponding to the relevant length scale. Ion acoustic waves can occur in an unmagnetized plasma or in a magnetized plasma parallel to the magnetic field. For a single ion species plasma and in the long wavelength limit, the waves are dispersionless ($\omega = v_s k$) with a speed given by

$$v_s = \sqrt{\frac{\gamma_e Z k_B T_e + \gamma_i k_B T_i}{m}}, \quad (1.27)$$

where k_B is Boltzmann's constant, M is the mass of the ion, Z is its charge, T_e is the temperature of the electrons and T_i is the temperature of the ions. Normally γ_e is taken to be unity, on the grounds that the thermal conductivity of electrons is large enough to keep them isothermal on the time scale of ion acoustic waves, and γ_i is taken to be 3, corresponding to one-dimensional motion. In collisionless plasmas, the electrons are often much hotter than the ions, in which case the second term in the numerator can be ignored.

1.7.4 Ion-cyclotron waves

An electrostatic ion cyclotron wave, in plasma physics, is a longitudinal oscillation of the ions (and electrons) in a magnetized plasma, propagating nearly (but not exactly) perpendicular to the magnetic field. The angle (in radians) between the direction of propagation and the direction perpendicular to the magnetic field must be greater than about the square root of the mass ratio $\sqrt{\frac{m_e}{m_i}}$, in order that the electrons can move along the field lines from crest to trough to satisfy the Boltzmann relation. The dispersion

relation is

$$\omega^2 = \Omega_c^2 + k^2 v_s^2, \quad (1.28)$$

where Ω_c is the ion cyclotron frequency and v_s is the ion sound speed. This relation is the result of restoring forces due to the Lorentz force (case of the upper hybrid oscillation i.e when the magnetic field is perpendicular to the wave vectors), the electrostatic force (T_e term in v_s), and the ion pressure (T_i term in v_s).

1.7.5 Nonlinearity and wave structures

Nonlinear science is believed by many to be the most deeply important frontier for understanding nature since they are of great importance in the physical world. Nonlinear waves are present in a large quantity around us. These involve the disasters like tidal waves, explosions and sonic blasts. These problems are occurring due to the disturbances in our natural environment as well as with human activities. Due to which they respond beyond their linear regions or limits. In spite of these disadvantages, they are very popular in many phenomena of physics. They have many applications in different regions of physics like these waves are responsible for describing the plasma behaviour and also help in energy transport in biological molecules. Nonlinear waves are also used in art technology, communication technology and femtosecond pulsed lasers. Nonlinearities can not be ignored, when the amplitudes of the waves are sufficiently large. There are many factors due to which the nonlinearities come into play. These nonlinearities come from the harmonic generation involving fluid advection, the nonlinear Lorentz force, trapping of particles in the wave potential, ponderomotive force and so on. Moreover, the nonlinearity in plasmas contributes to the localization of waves, involving the different and nonlinear coherent structures, such as the solitary structures, the shock waves, the vortices, double layers, etc. Study of these structures is very important from both theoretical and experimental points of view. The nonlinear structures take away the plasma from the thermodynamic equilibrium. These structures are either impulsively produced in laboratory and space plasmas because of free energy sources or superficially launched in laboratory plasmas under controlled conditions.

1.7.6 Summary of elementary plasma waves

The various plasma wave modes can be classified as electromagnetic or electrostatic according to whether they propagate in an unmagnetized plasma or parallel, perpendicular, or oblique to the stationary magnetic field. Finally, for perpendicular electromagnetic electron waves, the perturbed electric field can be parallel or perpendicular to the stationary magnetic field. Due to its electrical conductivity, a plasma couples to electric and magnetic fields. The following table 1.2 presents the different types of plasma oscillations. EM character denote de the electrostatic and electromagnetic characters and the subscript 0 denotes the static part of the electric or magnetic field, and the subscript 1 denotes the oscillating part.

EM character	oscillating species	conditions	name
electrostatic	electrons	$\mathbf{B}_0 = \mathbf{0}$ or $\mathbf{k} \parallel \mathbf{B}_0$	plasma oscillation (Langmuir wave)
\sim	\sim	$\mathbf{k} \perp \mathbf{B}_0$	upper hybrid oscillation
\sim	ions	$\mathbf{B}_0 = \mathbf{0}$ or $\mathbf{k} \parallel \mathbf{B}_0$	ion acoustic wave
\sim	\sim	$\mathbf{k} \perp \mathbf{B}_0$ (nearly)	electrostatic ion cyclotron wave
\sim	\sim	$\mathbf{k} \perp \mathbf{B}_0$ (exactly)	lower hybrid oscillation
electromagnetic	electrons	$\mathbf{B}_0 = \mathbf{0}$	light wave
\sim	\sim	$\mathbf{k} \perp \mathbf{B}_0, \mathbf{E}_1 \parallel \mathbf{B}_0$	ordinary (O) wave
\sim	\sim	$\mathbf{k} \perp \mathbf{B}_0, \mathbf{E}_1 \perp \mathbf{B}_0$	extraordinary (X) wave
\sim	\sim	$\mathbf{k} \parallel \mathbf{B}_0$	right-hand (R) circularly polar wave (whistler mode)
\sim	\sim	$\mathbf{k} \parallel \mathbf{B}_0$	left-hand (L) circularly polar wave
\sim	ions	$\mathbf{B}_0 = \mathbf{0}$	none
\sim	\sim	$\mathbf{k} \parallel \mathbf{B}_0$	Alfvén wave
\sim	\sim	$\mathbf{k} \perp \mathbf{B}_0$	magnetosonic wave

Table 1.2: Summary of elementary plasma waves, [https://en.wikipedia.org/wiki/Waves in plasmas](https://en.wikipedia.org/wiki/Waves_in_plasmas) [Consulted on 13/09/23].

1.7.7 Solitary waves, soliton and dromions

Much type of nonlinear waves is seen in the space plasmas. A solitary wave is a hump or dip shaped nonlinear wave of permanent profile. It is formed due to the balance between nonlinearity and the dispersion, where these latter cancel the effect of each other and balance one another. The same has been done only in the case when the effect of dissipation is negligible compared to those of the effects of nonlinearity and dispersion. While when the dissipative effect is greater than or comparable to the dispersive effect then these shock structures are encountered. Solitons are a specific type of solitary waves with the remarkable feature that, when two (or more) of them collide, they do not scatter but emerge with the same shape and velocity. The word soliton was coined by Zabusky and Kruskal [146] to emphasize that a soliton is a localized entity which may keep its identity after an interaction. In the absence of nonlinearity, dispersion can destroy a solitary wave as the various components of the wave propagate at different velocities. Introducing nonlinearity without dispersion again rules out the possibility of solitary waves because the pulse energy is continuously injected into high frequency modes. But with both dispersion and nonlinearity, solitary waves can again form. The history of solitons is an interesting one [147], with solitons first being seen as water waves in canals in England [148]. By studying the nature of waves, Russell claimed that the propagation of isolated wave was a consequence of the property of the medium rather than the circumstances of the wave generation. Since then, it took rather a long time to establish that some special nonlinear wave equations admit solutions consisting of isolated wave that can propagate and undergo collisions without losing their respective identities. The first theoretical work describing solitons was done by Rayleigh in 1879, and in 1895, Korteweg and de Vries [149] found the first equation describing a solitary wave [149] (the KdV equation). Special solution of the KdV equation leads to the solitary wave. It means that the soliton wave becomes an important tool in the mathematical examination of KdV equation. The concept of soliton has had a significant effect and consequences in various branches of mathematics, physics, and engineering. This becomes possible only after the discovery of the inverse scattering transform [150]. This discovery contributes to exact solutions of nonlinear partial differential equations. In the last stage of the 20th century, soliton theory made its impact in industry also. When the term soliton is mentioned in the history of science, numerical simulations played an important role. Along with the inverse scattering transform, numerical simulations have been powerful tools to reveal the

mysterious characteristics of solitons. Zabusky and Kruskal [146] investigated a numerical study of KdV equation. They observed that a single solitary wave behaves like a particle in its interaction with another one. They also observed that under certain conditions any initial pulse can break up into a number of solitons which can move in plasma with different phase velocities. Also the solitons interact with each other and after the interaction they emerge out without any change in their shape and velocity. Some important nonlinear equations which give rise to solitary waves in plasma are KdV equation, modified KdV equation, Gardner equation, nonlinear Schrodinger equation etc. Moreover, it exists another exact and localized solutions of nonlinear PDEs, namely dromions. By definition, dromions are exact and nonlinear localized solutions of any of a large class of two-dimensional partial differential equations, and were first time investigated theoretically by Boiti et al. [115]. The basic concept behind the dromions is the existence of ghost solitons which are not physical themselves, but whose interaction creates a physical local effect. A particular and important characteristic of dromion solutions is that they are localized wave packets in various physical systems such as plasma physics, fluid dynamics and nonlinear optics [116] and the interactions of two dromions for the (2+1)-dimensional equations may be elastic or inelastic [117–119]. Hietarinta et Hirota constructed dromion solutions by the bilinear method, which yields more general solutions than those obtained by any other method, Blacklund and Darboux transformation method for example

1.8 Theoretical description of plasma phenomena

For the theoretical description of plasma phenomena, there are basically four principal approaches with several different choices of approximations, each of which applies to different circumstances. One useful approximation, known as particle orbit theory, consists in studying the motion of each charged particle in the presence of specified electric and magnetic fields. This approach is not really plasma theory, but rather the dynamics of a charged particle in given fields. Nevertheless it is important, since it provides some physical insight for a better understanding of the dynamic processes in plasmas. It has proven to be useful for predicting the behavior of very low density plasmas, which is determined primarily by the interaction of the particles with external fields. This is the case, for example, of the highly rarefied plasmas of the Van Allen radiation belts and the solar corona, as well as of cosmic rays, high energy accelerators, and cathode ray tubes. Since a plasma consists of a very large number of interacting particles, in order to provide

a macroscopic description of plasma phenomena it is appropriate to adopt a statistical approach. This implies a great reduction in the amount of information to be handled. In the kinetic theory statistical description it is necessary to know only the distribution function for the system of particles under consideration. The problem consists in solving the appropriate kinetic equations that govern the evolution of the distribution function in phase space. One example of differential kinetic equation is the Vlasov equation, in which the interaction between the charged particles is described by smeared out internal electromagnetic fields consistent with the distributions of electric charge density and current density inside the plasma, and the effects of short-range correlations (close collisions) are neglected. When collisions between the plasma particles are very frequent, so that each species is able to maintain a local equilibrium distribution function, then each species can be treated as a fluid described by a local density, local macroscopic velocity and local temperature. In this case the plasma is treated as a mixture of two or more interpenetrating fluids. This theory is called two-fluid or many-fluid theory, depending on the number of different species considered. In addition to the usual electrodynamic equations, there is a set of hydrodynamic equations expressing conservation of mass, of momentum, and of energy for each particle species in the plasma. Another approach consists in treating the whole plasma as a single conducting fluid using lumped macroscopic variables and their corresponding hydrodynamic conservation equations. This theory is usually referred to as the one-fluid theory. An appropriately simplified form of this theory, applicable to the study of very low frequency phenomena in highly conducting fluids immersed in magnetic fields, is usually referred to as the magnetohydrodynamic (MHD) approximation.

1.9 Fluid description of plasma and basic equations

Plasma can be considered as a fluid with several components. The various components of plasma are the electrons, the different species of ions, and possibly the neutrals. Practically, it is impossible to predict the behaviour of plasma because of the complicated trajectory of each of these particles [130]. Fortunately, majority of plasma phenomena observed in laboratory can be explain by a fluid model. Here, identity of the individual specie is neglected and only the motion of fluid particles is considered as in fluid mechanics. In the fluid approximation, it is assumed that each plasma particles is able to maintain a local equilibrium, as for example $n_i = n_e = n$ for a plasma comprising two components: electrons (density n_e), ions (density n_i).

1.9.1 Continuity equation

The continuity equation expresses the conservation of the number of particles. In fact, the motion of a fluid is described by a vector velocity field $\mathbf{v}_s(\mathbf{r})$, the mean velocity of all the individual particles which make up the fluid at \mathbf{r} . In addition, the particle density $n(\mathbf{r})$ is required. We are here discussing the motion of fluid of a s type of particle of mass m_s and charge q_s , so the charge and mass density are $q_s n_s$ and $m_s n_s$, respectively. The conservation equation of a one type particle thus reads:

$$\frac{\partial n_s}{\partial t} + \nabla \cdot (n_s \mathbf{v}_s) = 0. \quad (1.29)$$

1.9.2 Momentum equation

The momentum equation brings out the conservation of the quantity of motion of particles. In fact, Several forces generally interact in plasmas, but three of these forces strongly determine their behavior. It is the Lorentz force, the pressure gradient force and the collision effects. Unlike neutral fluids where the dominant external force is gravity, the force to be taken into account for plasmas is the electromagnetic force defined by:

$$\mathbf{F}_s = q_s(\mathbf{E} + \mathbf{v}_s \times \mathbf{B}), \quad (1.30)$$

where q_s and \mathbf{v}_s are the charge and velocity of the particle s , respectively. \mathbf{E} and \mathbf{B} are the electric and magnetic fields, respectively. As a plasma component can exchange momentum with the other components k of the plasma during collisions, it is appropriate to add a frictional force (elastic collision case) which is generally written in the form:

$$\mathbf{F}_c = -m_s \sum_{k \neq s} \nu_{sk} (\mathbf{v}_s - \mathbf{v}_k), \quad (1.31)$$

where m_s is the mass of the particle s , \mathbf{v}_k is the velocity of the particle k and ν_{sk} denote to the collision frequency between species s and species k . On the other hand, the viscosity contributions are generally negligible for electrons and ions (but not always for neutrals) so that

$$\mathbf{F}_p = -\nabla p_s = -\nabla (n_s k_B T_s). \quad (1.32)$$

Here, k_B is the Boltzmann constant, m_s and T_s are the mass and velocity of the particle s . For the cold plasmas approximation, $T_s = 0$ and then $p_s = 0$. This means that the effects due to thermal motion of plasma particles are neglected. For the isothermal

approximation, $\frac{p_s}{n_s} = cst$. For the adiabatic approximation, $\frac{p_s}{n_s^\gamma} = cst$, with $\gamma = \frac{C_p}{C_v}$ the ratio of specific heats at constant pressure and at constant volume.

Thus, we can immediately generalize using Eqs. (1.30), (1.31) and (1.32) the momentum equation for species k to

$$m_s n_s \frac{d\mathbf{v}_s}{dt} = m_s n_s \left[\frac{\partial \mathbf{v}_s}{\partial t} + \mathbf{v}_s \cdot \nabla \mathbf{v}_s \right] = q_s n_s (\mathbf{E} + \mathbf{v}_s \times \mathbf{B}) - \nabla (n_s k_B T_s) - m_s n_s \sum_{k \neq s} \nu_{sk} (\mathbf{v}_s - \mathbf{v}_k). \quad (1.33)$$

1.9.3 Poisson's equation

The Poisson's equation expresses the conservation of the electric charges in the plasma. It makes it possible to express the link between the spatiale distribution of charge and the electrical field. The electric field that exist in this plasma may obey Maxwell-Gauss equations

$$\nabla \cdot \mathbf{E} = \frac{\rho_s}{\varepsilon_0}, \quad (1.34)$$

where $\mathbf{E} = -\nabla \phi$, with ϕ is the electric potential and $\rho = \sum_s q_s n_s$ and the Eq. 1.34 leads to the following Poisson's equation

$$\nabla^2 \phi = -\frac{1}{\varepsilon_0} \sum_s q_s n_s, \quad (1.35)$$

For example, let's consider a three-component ENP made by of positive ions, negative ions and electrons. The quasi-neutrality condition of charche at is given by

$$Z_+ n_{+0} = Z_- n_{-0} + n_{e0}, \quad (1.36)$$

where Z_- and Z_+ are, respectively, the atomic numbers of negative and positive species, n_{+0} , n_{-0} and n_{e0} are the number densities of positive and negative species and electrons, respectively at equilibrium. Finally, the equation 1.35 leads to

$$\Delta \phi = -\frac{e}{\varepsilon_0} (Z_+ n_+ - Z_- n_- - n_e). \quad (1.37)$$

Here, e is the magnitude of the electron charge.

1.9.4 Closed system of fluid equations

The continuity equation (1.29) relates two macroscopic variables, namely number density n and flow velocity \mathbf{v}_s . To determine these two variables, we need two independent

macroscopic transport equations. The momentum conservation equation or the equation of motion (1.33) relates \mathbf{v}_s , n_s and pressure p_s (the variables \mathbf{E} and \mathbf{B} being provided by Maxwell's equations). Therefore, the two transport equations (1.29) and (1.33) relate three independent variables. We may go to the next higher order transport equation, namely the Poisson's equation or the energy conservation equation (1.35). But it is found to relate four variables, \mathbf{v}_s , n_s , p_s and heat flow. Then one gets three independent equations for four variables. Thus, we find that transport equations do not form a closed set in the sense that number of equations is not sufficient to determine all the variables that appear in them. Thus one needs to introduce some simplifying assumptions. In order to get a complete set of fluid equations generally there are two widely used approximations the so-called cold and warm plasma models.

1.9.5 Cold plasma model

The cold plasma model uses only the continuity equation and the equation of motion. The effects due to thermal motion of plasma particles are neglected and the force due to pressure gradient term is taken equal to zero. This cold plasma model has been successfully applied, for example, in the investigation of wave propagation in plasma with phase velocities much larger than the thermal velocity of the particles.

1.9.6 Warm plasma model

In warm (hot) plasma model the heat flux term that appears in the energy transport equation is taken to be zero. This means that the processes occurring in plasma are such that there is no heat flow. This approximation is also called adiabatic approximation. In addition neglecting the effects of viscosity and energy transfer due to collision it can be shown that the energy equation reduces to the following adiabatic equation of state relating pressure to density:

$$p\rho m^\gamma = C, \quad (1.38)$$

where C is a constant, ρm is the mass density and $\gamma = C_P/C_V$ is the ratio of specific heats at constant pressure and at constant volume. The parameter γ is related to the number of degrees of freedom f of a gas by the relation

$$\gamma = 1 + \frac{1}{f}. \quad (1.39)$$

The equation of continuity, equation of motion and the adiabatic equation of state Eq. (1.38) form a closed set of equations. Compared to cold plasma model the warm plasma model gives a more precise description of various plasma phenomena.

Conclusion

This chapter was devoted to the litterature review and has provided an overview of the generalities and the dynamics on some theoretical aspects of plasmas and magnetized electronegative plasma. We have also presented the historical background on plasmas and highlighted some properties and characteristics of plasma which will be useful in this work. Finally, we have presented, in a succinct but detailed way, the fluid description of plasma that will be the starting-point for studying the dynamics of plasmas. We intend to use this fluid model in the next chapter to present different methods that we use in this work in the particular case of cold magnetized ENPs.

Models description and methods

Introduction

The present chapter is devoted to the models description of the governing equations for the propagation of ion-acoustic waves along the external magnetic field in an electronegative plasma and the methods used along the thesis. Theoretical methods concerning both analytical and numerical methods are presented: the reductive perturbation method used to derive NLS equation and DS equations, the linear stability analysis for planar wave to derive the modulational instability growth rate, the Hirota's bilinear method to derive one- and two-dromion solutions, the fourth-order Runge- Kutta (RK4) method and the Split-Step Fourier method for numerical resolution.

2.1 Governing equations in (2+1)-dimensions

In this section, we present the (2+1)-dimensional mathematical model for the propagation of positive ion-acoustic waves along the external magnetic field $\mathbf{B} = B_0 \mathbf{z}$ in an electronegative plasma. For that, we use a plasma system composed of electrons and negative ions, both in Boltzmann distribution, in addition to cold mobile positive ions [151, 152]. In plasma systems, the charge neutrality condition ($Z_p n_p = Z_n n_n + n_e$), is modified by the presence of negative ions, with n_e , n_p , and n_n the electron, positive, and negative ions densities, respectively. Z_p and Z_n are the charge number of positive and negative ions. Let's consider the following fluid continuity, momentum and Poisson's equations for the positive ions:

$$\frac{\partial n_p}{\partial t} + \nabla \cdot (n_p \mathbf{v}_p) = 0, \quad (2.1)$$

$$\frac{\partial \mathbf{v}_p}{\partial t} + (\mathbf{v}_p \cdot \nabla) \mathbf{v}_p = -\frac{q_p}{m_p} \nabla \Phi + \frac{q_p}{m_p} (\mathbf{v}_p \times \mathbf{B}), \quad (2.2)$$

$$\nabla^2 \Phi = -4\pi e(Z_p n_p - Z_n n_n - n_e). \quad (2.3)$$

Here, $n_e = n_{e0} e^{\frac{e\Phi}{k_B T_e}}$, $n_p = n_{p0} e^{\sigma_n \frac{e\Phi}{k_B T_e}}$, with the electron-to-negative ion temperature ratio $\sigma_n = \frac{T_e}{T_n}$, the positive ions charge $q_p = +Z_p e$ of mass m_p , the negative ions charge $q_n = -Z_n e$ of mass m_n and the electrons charge $q_e = -e$, mass m_e . \mathbf{v}_p , q_p , m_p and $\mathbf{E} = -\nabla \Phi$ are the positive ion mean velocity, ion charges, ion mass and the electric field derived from the electrostatic potential Φ , respectively. We also assume that in plane (x, z) , $\nabla = (\frac{\partial}{\partial x}, 0, \frac{\partial}{\partial z})$ and the normalized ion continuity, momentum and Poisson's equations take the form of a system of (scalar) equations:

$$\frac{\partial n}{\partial t} + \frac{\partial(nv_x)}{\partial x} + \frac{\partial(nv_z)}{\partial z} = 0, \quad (2.4)$$

$$\frac{\partial v_x}{\partial t} + (v_x \frac{\partial}{\partial x} + v_z \frac{\partial}{\partial z})v_x = -\frac{\partial \phi}{\partial x} + \omega_p v_y, \quad (2.5a)$$

$$\frac{\partial v_y}{\partial t} + (v_x \frac{\partial}{\partial x} + v_z \frac{\partial}{\partial z})v_y = -\omega_p v_x, \quad (2.5b)$$

$$\frac{\partial v_z}{\partial t} + (v_x \frac{\partial}{\partial x} + v_z \frac{\partial}{\partial z})v_z = -\frac{\partial \phi}{\partial z}, \quad (2.5c)$$

$$\frac{\partial^2 \phi}{\partial x^2} + \frac{\partial^2 \phi}{\partial z^2} = 1 + c_1 \phi + c_2 \phi^2 + c_3 \phi^3 - n, \quad (2.6)$$

where $n = \frac{n_p}{n_{p0}}$ is the normalized number-density of positive ions, with charge neutrality condition at equilibrium defined by $Z_p n_{p0} = Z_n n_{n0} + n_{e0}$, $\mathbf{v} = (v_x, v_y, v_z) = \frac{\mathbf{v}_p}{C_s}$ is the normalized velocity of positive ions, with $C_s = (\frac{Z_p k_B T_e}{m_i})^{\frac{1}{2}}$ the characteristic speed scale used for velocity normalization, $\phi = \frac{e\Phi}{k_B T_e}$. The space (x, z) and time (t) variables are normalized by the Debye length $\lambda_{De} = (\frac{k_B T_e}{4\pi Z_p n_{p0} e^2})^{\frac{1}{2}}$, $\omega_p = \frac{\omega_i}{w_{pi}}$ is the normalized parameter of ion cyclotron and ion plasma frequency ratio, with $w_{pi} = (\frac{4\pi n_{p0} Z_p^2 e^2}{m_i})^{\frac{1}{2}}$ and $\omega_i = \frac{eB_0}{m_i c}$. The constants $c_1 = \mu_e + \mu_n \sigma_n$, $c_2 = \frac{\mu_e + \mu_n \sigma_n^2}{2}$ and $c_3 = \frac{\mu_e + \mu_n \sigma_n^3}{6}$ are obtained by using the power series expansion of the exponential factor around zero in n_p and n_e . Here, $\mu_e = \frac{n_{e0}}{Z_p n_{p0}} = \frac{1}{1+\alpha}$, $\mu_n = \frac{Z_n n_{n0}}{Z_p n_{p0}} = \frac{\alpha}{1+\alpha}$ which assumes the neutrality condition of the electronegative plasma: $\mu_e + \mu_n = 1$, where $\alpha = \frac{Z_n n_{n0}}{n_{e0}}$ being the density ratio of negative ion to electron (negative ion-to-electron density ratio).

2.2 The reductive perturbation method and derivation of NLS equation and DS equations

2.2.1 The reductive perturbation method

The reductive perturbation method is a very powerful way of deriving simplified models describing nonlinear wave propagation and interaction. It is considered as a method that reduces a set of nonlinear (PDEs) to a single solvable nonlinear evolution equation. Starting from fluid equations (hydrodynamic equations), the evolution equation is obtained in two steps or more. In the first step, the original coordinates x or/and (y, z) and t are transformed to new stretched coordinates ξ or/and (η, ζ) and τ (say) depending on the nature of the problem. Then, the perturbation parameter ε is introduced which has a connection with the wavenumber (and hence, with the frequency and the dispersion relation). In the second step, the same ε is used as a perturbation parameter where the dependent variables are expanded as a power series of ε in the neighbourhood of the equilibrium point. The perturbation of the parameters is considered at a near-equilibrium point not for finding the solution but for obtaining an evolution equation. It can be applied to various systems that include dissipation/dispersion or both. It shows that for long waves, the set of equations can be reduced to Burgers' equation or the KdV equation, for a system with dissipation or dispersion, respectively and if we consider the propagation of a modulated wave of small amplitude, then the evolution equation would be a NLSE equation or DS equations [38, 153].

2.2.2 Derivation of the nonlinear schrödinger equation

In order to investigate the dynamics of propagation of positive IAWs and derive the nonlinear Schrödinger (NLS) equation, we employ the standard reductive perturbation expansion. The stretched coordinates in space and time may be introduced as [21, 153]:

$$\xi = \varepsilon x, \quad \eta = \varepsilon(z - v_g t), \quad \tau = \varepsilon^2 t, \quad (2.7)$$

where v_g is the group velocity that will be found later by the solvability condition of equations (2.4)-(2.5c). ε is a small expansion parameter ($0 < \varepsilon \ll 1$) that measures the strength of nonlinearity [3, 86, 154–156]. The condition about ε implies that the plasma dimension must be much larger than the Debye length, which is satisfied in most cases

of interest [157]. The dependent physical variables around their equilibrium values are expanded as follows [52, 158]:

$$\begin{pmatrix} n \\ v_x \\ v_y \\ v_z \\ \phi \end{pmatrix} = \begin{pmatrix} 1 \\ 0 \\ 0 \\ 0 \\ 0 \end{pmatrix} + \sum_{p=1}^{+\infty} \varepsilon^p \sum_{l=-\infty}^{+\infty} \begin{pmatrix} n_l^{(p)}(\xi, \eta, \tau) \\ v_{xl}^{(p)}(\xi, \eta, \tau) \\ v_{yl}^{(p)}(\xi, \eta, \tau) \\ v_{zl}^{(p)}(\xi, \eta, \tau) \\ \phi_l^{(p)}(\xi, \eta, \tau) \end{pmatrix} A^l(z, t). \quad (2.8)$$

We note that the above series include $A^l(z, t) = e^{il(kz - \omega t)}$, up to order p . These are generated by the nonlinear terms, which means that the corresponding coefficients are of maximum order ε^p . The state variables n , v_{xl} , v_{yl} , v_{zl} and ϕ must satisfy the following condition $(n_l^{(p)})^* = n_{-l}^{(p)}$, $(v_{xl}^{(p)})^* = v_{x-l}^{(p)}$, $(v_{yl}^{(p)})^* = v_{y-l}^{(p)}$, $(v_{zl}^{(p)})^* = v_{z-l}^{(p)}$, $(\phi_l^{(p)})^* = \phi_{-l}^{(p)}$, respectively. The asterisk (*) denotes the complex conjugate. Substituting the trial solutions (2.8) into Eqs. (2.4)-(2.6), and equating the quantities with equal power of ε , we obtain several coupled equations in different orders of ε .

At the first harmonic of perturbation (ε^1), we obtain the following relations:

For $l = 0$, we obtain

$$n_0^{(1)} = v_{x0}^{(1)} = v_{y0}^{(1)} = v_{z0}^{(1)} = \phi_0^{(1)} = 0. \quad (2.9)$$

For $l = 1$, we find

$$\begin{cases} n_1^{(1)} = \frac{k^2}{w^2} \phi_1^{(1)} \\ v_{x1}^{(1)} = v_{y1}^{(1)} = 0 \\ v_{z1}^{(1)} = \frac{k}{w} \phi_1^{(1)}, \end{cases} \quad (2.10)$$

under the condition that the dispersion relation

$$\omega^2 = \frac{k^2}{k^2 + c_1}, \quad (2.11)$$

is verified, leading to the first harmonic of perturbation.

At the second harmonic of perturbation (ε^2), we obtain the following relations:

For $l = 0$,

$$\begin{cases} v_{x0}^{(2)} = v_{y0}^{(2)} = 0, \\ n_0^{(2)} - c_1 \phi_0^{(2)} = 2c_2 |\phi_1^{(1)}|^2. \end{cases} \quad (2.12)$$

For $l = 1$,

$$\begin{cases} n_1^{(2)} = (k^2 + c_1) \phi_1^{(2)} - 2ik \frac{\partial \phi_1^{(1)}}{\partial \eta}, \\ v_{x1}^{(2)} = -\frac{i\omega}{\omega^2 - \omega_p^2} \frac{\partial \phi_1^{(1)}}{\partial \xi}, \\ v_{y1}^{(2)} = -\frac{\omega_p}{\omega^2 - \omega_p^2} \frac{\partial \phi_1^{(1)}}{\partial \xi}, \\ v_{z1}^{(2)} = \frac{k}{\omega} \phi_1^{(2)} + \frac{i}{\omega} (v_g \frac{k}{\omega} - 1) \frac{\partial \phi_1^{(1)}}{\partial \eta}. \end{cases} \quad (2.13)$$

The group velocity is

$$v_g = c_1 \frac{\omega^3}{k^3}. \quad (2.14)$$

For $l = 2$,

$$\begin{cases} n_2^{(2)} = \alpha_n \left(\phi_1^{(1)} \right)^2, \\ v_{x2}^{(2)} = v_{y2}^{(2)} = 0, \\ v_{z2}^{(2)} = \alpha_{v_z} \left(\phi_1^{(1)} \right)^2, \\ \phi_2^{(2)} = \alpha_\phi \left(\phi_1^{(1)} \right)^2. \end{cases} \quad (2.15)$$

with $\alpha_\phi = \frac{k^2}{2\omega^4} - \frac{c_2^2}{3k^2}$, $\alpha_n = (4k^2 + c_1) \alpha_\phi + c_2$, $\alpha_{v_z} = \frac{\omega}{k} (\alpha_n - (k^2 + c_1)^2)$.

In the case of the third-order of perturbation (ε^3), we obtain

For $l = 0$

$$\begin{cases} -v_g n_0^{(2)} + v_{z0}^{(2)} = -\frac{2k^3}{\omega^3} |\phi_1^{(1)}|^2, \\ -v_g v_{z0}^{(2)} + \phi_0^{(2)} = -\frac{k^2}{\omega^2} |\phi_1^{(1)}|^2. \end{cases} \quad (2.16)$$

Using the last relation of Eq. (2.12) from the order (ε^2 , $l = 0$) and the Eq. (2.16), we obtain

$$\begin{cases} n_0^{(2)} = \beta_n |\phi_1^{(1)}|^2, \\ v_{z0}^{(2)} = \beta_{v_z} |\phi_1^{(1)}|^2, \\ \phi_0^{(2)} = \alpha_\phi |\phi_1^{(1)}|^2. \end{cases} \quad (2.17)$$

with $\beta_\phi = \frac{2v_g^2 c_2 - (k^2 + 3c_1)}{1 - c_1 v_g^2}$, $\beta_n = c_1 \beta_\phi + 2c_2$, $\beta_{v_z} = v_g \beta_n - \frac{2\omega}{k} (k^2 + c_1)^2$.

For $l = 1$, we find the following equation

$$i \frac{\partial \phi_1^{(1)}}{\partial \tau} + P \frac{\partial^2 \phi_1^{(1)}}{\partial \eta^2} + Q |\phi_1^{(1)}|^2 \phi_1^{(1)} - S \frac{\partial^2 \phi_1^{(1)}}{\partial \xi^2} = 0, \quad (2.18)$$

where

$$\begin{aligned} P &= \frac{1}{2} \frac{\partial^2 \omega}{\partial k^2} = -\frac{3c_1}{2} \frac{\omega^5}{k^4} = -\frac{3\omega^3}{2k^2} (1 - \omega^2), \\ Q &= -k (\alpha_{v_z} + \beta_{v_z}) - \frac{\omega}{2} (\alpha_n + \beta_n) + \frac{\omega^3}{k^2} \left(c_2 (\alpha_\phi + \beta_\phi) + \frac{3}{2} c_3 \right), \\ S &= \frac{\omega^3}{2k^2} \frac{1 + \omega_p^2 - \omega^2}{\omega_p^2 - \omega^2}. \end{aligned} \quad (2.19)$$

Introducing the notation $\psi = \phi_1^{(1)}$, the equation (2.18) become:

$$i \frac{\partial \psi}{\partial \tau} + P \frac{\partial^2 \psi}{\partial \eta^2} + Q |\psi|^2 \psi - S \frac{\partial^2 \psi}{\partial \xi^2} = 0. \quad (2.20)$$

This partial differential equation (2.20) for a complex field (wave-amplitude ψ) is well-known as the (2+1)-dimensional nonlinear Schrödinger equation, with P , Q and S the longitudinal dispersive coefficient, cubic nonlinear coefficient and the transverse dispersive coefficient depending on the external magnetic field, respectively. It describes the amplitude modulation of the electronegative plasma amplitude ψ of positive ion acoustic wave packets in the external magnetic field. We note that the coefficients of the obtained NLS equation depend on the system parameters specially, not only on the electronegative parameters such as the negative ion concentration ratio and the electron-to-negative ion temperature ratio (α and σ_n , respectively), but also on the magnetic field (ω_p).

2.2.3 Derivation of Davey-Stewartson equations

In the absence of the magnetic field, the model has been extensively used in one, two, and three dimensions to study the emergence of rogue waves, solitons, dromions and their link to the MI phenomenon [21–23, 140]. However, in the presence of a magnetic field, we consider the same (2+1)-dimensional fluid continuity, momentum and Poisson's equations for the positive ions as presented in the previous section (2.1). For that, we just change the velocity v to u and obtain the following equations:

$$\frac{\partial n_p}{\partial t} + \nabla \cdot (n_p \mathbf{u}_p) = 0, \quad (2.21a)$$

$$\frac{\partial \mathbf{u}_p}{\partial t} + (\mathbf{u}_p \cdot \nabla) \mathbf{u}_p = -\frac{q_p}{m_p} \nabla \Phi + \frac{q_p}{m_p} (\mathbf{u}_p \times \mathbf{B}), \quad (2.21b)$$

where \mathbf{u}_p , q_p , m_p , $\mathbf{E} = -\nabla \Phi$ and $\mathbf{B} = (0, 0, B)$ are the positive ion mean velocity, ion charges, ion mass, the electric field derived from the electrostatic potential Φ and external magnetic field, respectively. Variations of the electrostatic potential Φ are described by the Poisson's equation:

$$\nabla^2 \Phi = -4\pi e (Z_p n_p - Z_n n_n - n_e), \quad (2.22)$$

where, $n_e = n_{e0} e^{\frac{e\Phi}{k_B T_e}}$, $n_n = n_{n0} e^{\sigma_n \frac{e\Phi}{k_B T_e}}$, with the electron-to-negative ion temperature ratio $\sigma_n = \frac{T_e}{T_n}$, the positive ions charge $q_p = +Z_p e$ of mass m_p , the negative ions charge

$q_n = -Z_n e$ of mass m_n and the electrons charge $q_e = -e$, mass m_e . We consider for simplicity by introducing the Nabla ($\vec{\nabla}$) operator as $\vec{\nabla} = \frac{\partial}{\partial x} \vec{e}_x + \frac{\partial}{\partial z} \vec{e}_z$, indicating that the waves propagate in the (x, z) -plane and the normalized ion continuity, momentum and Poisson's equations take the form of the following system of scalar equations:

$$\frac{\partial n}{\partial t} + \frac{\partial(nu_x)}{\partial x} + \frac{\partial(nu_z)}{\partial z} = 0, \quad (2.23a)$$

$$\frac{\partial u_x}{\partial t} + \left(u_x \frac{\partial}{\partial x} + u_z \frac{\partial}{\partial z} \right) u_x = -\frac{\partial \phi}{\partial x} + \Omega u_y, \quad (2.23b)$$

$$\frac{\partial u_y}{\partial t} + \left(u_x \frac{\partial}{\partial x} + u_z \frac{\partial}{\partial z} \right) u_y = -\Omega u_x, \quad (2.23c)$$

$$\frac{\partial u_z}{\partial t} + \left(u_x \frac{\partial}{\partial x} + u_z \frac{\partial}{\partial z} \right) u_z = -\frac{\partial \phi}{\partial z}, \quad (2.23d)$$

$$\frac{\partial^2 \phi}{\partial x^2} + \frac{\partial^2 \phi}{\partial z^2} = 1 + a_1 \phi + a_2 \phi^2 + a_3 \phi^3 - n, \quad (2.23e)$$

where $n = \frac{n_p}{n_{p0}}$ is the normalized number-density of positive ions, with charge neutrality condition at equilibrium defined by $Z_p n_{p0} = Z_n n_{n0} + n_{e0}$, $\mathbf{u} = (u_x, u_y, u_z) = \frac{\mathbf{u}_p}{C_s}$ is the normalized velocity of positive ions, with $C_s = \sqrt{\frac{Z_p k_B T_e}{m_i}}$ the characteristic speed scale used for velocity normalization, $\phi = \frac{e\Phi}{k_B T_e}$. The space (x, z) and time (t) variables are normalized by the Debye length $\lambda_{De} = \sqrt{\frac{k_B T_e}{4\pi Z_p n_{p0} e^2}}$, $\Omega = \frac{\Omega_i}{w_{pi}}$ is the normalized parameter of ion cyclotron and ion plasma frequency ratio, with $w_{pi} = \sqrt{\frac{4\pi n_{p0} Z_p^2 e^2}{m_i}}$ and $\Omega_i = \frac{eB}{m_i c}$. The constants $a_1 = \mu_e + \mu_n \sigma_n$, $a_2 = \frac{\mu_e + \mu_n \sigma_n^2}{2}$ and $a_3 = \frac{\mu_e + \mu_n \sigma_n^3}{6}$ are obtained after the power series expansion of the exponential factor around zero in n_p and n_e . Here, $\mu_e = \frac{n_{e0}}{Z_p n_{p0}} = \frac{1}{1+\alpha}$, and $\mu_n = \frac{Z_n n_{n0}}{Z_p n_{p0}} = \frac{\alpha}{1+\alpha}$ which assumes the neutrality condition of the plasma $\mu_e + \mu_n = 1$, with $\alpha = \frac{Z_n n_{n0}}{n_{e0}}$ being the negative-ion concentration ratio.

The standard reductive perturbation expansion will be implemented in order to find the DS equations that govern the propagation of IAWs in the proposed plasma system. To start, we introduce the stretched variables in space and time

$$\xi = \varepsilon(x - v_{gx}t), \quad \eta = \varepsilon(z - v_{gz}t), \quad \tau = \varepsilon^2 t, \quad (2.24)$$

where v_{gx} and v_{gz} are the group velocities in x and z directions, respectively that will be found later using the solvability condition of Eqs. (2.23a)-(2.23d). ε is a small expansion

parameter ($0 < \varepsilon \ll 1$) that measures the strength of nonlinearity. The dependent physical variables around their equilibrium values are expanded via the trial solutions

$$\begin{pmatrix} n(x, z, t) \\ u_x(x, z, t) \\ u_y(x, z, t) \\ u_z(x, z, t) \\ \phi(x, z, t) \end{pmatrix} = \begin{pmatrix} 1 \\ 0 \\ 0 \\ 0 \\ 0 \end{pmatrix} + \sum_{p=1}^{+\infty} \varepsilon^p \sum_{l=-\infty}^{+\infty} \begin{pmatrix} n_l^{(p)}(\xi, \eta, \tau) \\ u_{xl}^{(p)}(\xi, \eta, \tau) \\ u_{yl}^{(p)}(\xi, \eta, \tau) \\ u_{zl}^{(p)}(\xi, \eta, \tau) \\ \phi_l^{(p)}(\xi, \eta, \tau) \end{pmatrix} A^l(x, z, t), \quad (2.25)$$

which includes all overtones $A^l(x, z, t) = e^{il(k_x x + k_z z - \omega t)}$ up to order p , and generated by the nonlinear terms. Here, ω is the wave frequency, k_x and k_z are the wave numbers in x and z directions, such that $k^2 = k_x^2 + k_z^2$. In other words, the corresponding coefficients of such overtones are of maximum order ε^p . Moreover, the relations $(n_l^{(p)})^* = n_{-l}^{(p)}$, $(u_{xl}^{(p)})^* = u_{x-l}^{(p)}$, $(u_{yl}^{(p)})^* = u_{y-l}^{(p)}$, $(u_{zl}^{(p)})^* = u_{z-l}^{(p)}$, $(\phi_l^{(p)})^* = \phi_{-l}^{(p)}$ should be satisfied because of reality condition of the physical variables, with the asterisk (*) denoting the complex conjugate. After substituting the trial solution (2.25) into Eqs. (2.23a)-(2.23e) and equating the quantities with equal power of ε , we obtain several coupled equations in different orders of ε that leads, after a few calculations to the investigated DS equations. In doing so, the first harmonic of perturbation (ε^1), we obtain $n_0^{(1)} = u_{x0}^{(1)} = u_{y0}^{(1)} = u_{z0}^{(1)} = \phi_0^{(1)} = 0$ for $l = 0$ and $u_{x1}^{(1)} = \frac{\beta}{k_x \omega (k^2 + a_1)} n_1^{(1)}$, $u_{y1}^{(1)} = -\frac{i\Omega\beta}{k_x \omega^2 (k^2 + a_1)} n_1^{(1)}$, $u_{z1}^{(1)} = \frac{k_z}{\omega (k^2 + a_1)} n_1^{(1)}$, $\phi_1^{(1)} = \frac{1}{k^2 + a_1} n_1^{(1)}$, for $l = 1$, under the condition that the linear dispersion relation

$$\omega^4 - \left(\frac{k^2}{k^2 + a_1} + \Omega^2 \right) \omega^2 + \frac{\Omega^2 k_z^2}{k^2 + a_1} = 0, \quad (2.26)$$

be verified, leading to the first harmonic of perturbation. The solution of the quadratic equation in ω^2 (Eq. (2.26)) is given by

$$\omega^2 = \frac{1}{2} \left(\frac{k^2}{k^2 + a_1} + \Omega^2 \pm \sqrt{\left(\frac{k^2}{k^2 + a_1} + \Omega^2 \right)^2 - \frac{4k_z^2 \Omega^2}{k^2 + a_1}} \right). \quad (2.27)$$

We note that for the case of pure perpendicular propagation and strong magnetic field ($k_z = 0$), we obtain the following dispersion relation

$$\omega^2 - \Omega^2 = \frac{k^2}{k^2 + a_1}. \quad (2.28)$$

Along the same line, the second harmonic of perturbation (ε^2) admit the relations $u_{x0}^{(2)} = -\frac{2\beta}{k_x \omega (k^2 + a_1)} |n_1^{(1)}|^2$, $u_{y0}^{(2)} = 0$, and $n_0^{(2)} = a_1 \phi_0^{(2)} + \frac{2a_2}{(k^2 + a_1)^2} |n_1^{(1)}|^2$ for $l = 0$, while for $l = 1$, solutions are obtained as $n_1^{(2)} = (k^2 + a_1) \phi_1^{(2)} - \frac{2ik}{k^2 + a_1} \frac{\partial n_1^{(1)}}{\partial \xi} - \frac{2ik}{k^2 + a_1} \frac{\partial n_1^{(1)}}{\partial \eta}$, $u_{x1}^{(2)} =$

$u_{x\phi}\phi_1^{(2)} + iu_{x\xi}\frac{\partial n_1^{(1)}}{\partial \xi} + iu_{x\eta}\frac{\partial n_1^{(1)}}{\partial \eta}$, $u_{y1}^{(2)} = iu_{y\phi}\phi_1^{(2)} + u_{y\xi}\frac{\partial n_1^{(1)}}{\partial \xi} + u_{y\eta}\frac{\partial n_1^{(1)}}{\partial \eta}$, and $u_{z1}^{(2)} = u_{z\phi}\phi_1^{(2)} + iu_{z\xi}\frac{\partial n_1^{(1)}}{\partial \xi} + iu_{z\eta}\frac{\partial n_1^{(1)}}{\partial \eta}$, under the solvability condition

$$v_{gx} = \frac{k_x\omega \left(\frac{\beta_1(\omega^2 - \Omega^2)}{k_x^2} + \omega^2 - 2\omega^2(\omega^2 - \Omega^2) \right)}{2(\omega^4(k^2 + a_1) - k_z^2\Omega)}, \quad v_{gz} = \frac{k_z\omega (\omega^2 - \Omega^2 - \omega^2(\omega^2 - \Omega^2))}{(\omega^4(k^2 + a_1) - k_z^2\Omega)}, \quad (2.29)$$

that gives the group velocities, with $v_g^2 = v_{gx}^2 + v_{gz}^2$. Still at order ε^2 , the following solutions are obtained for $l = 2$: $n_2^{(2)} = \alpha_n \left(n_1^{(1)} \right)^2$, $u_{x2}^{(2)} = \alpha_{u_x} \left(n_1^{(1)} \right)^2$, $u_{y2}^{(2)} = i\alpha_{u_y} \left(n_1^{(1)} \right)^2$, $u_{z2}^{(2)} = \alpha_{u_z} \left(n_1^{(1)} \right)^2$, $\phi_2^{(2)} = \alpha_\phi \left(n_1^{(1)} \right)^2$.

For its part, the third-order (ε^3) reduced equations for $l = 0$ are obtained as set of couple equations in appendix (Eq. (59)), which after some algebra lead to the following equation verified by the potential $\phi_0^{(2)}$

$$\delta_1 \frac{\partial^2 \phi_0^{(2)}}{\partial \xi^2} + \delta_{\xi\eta} \frac{\partial^2 \phi_0^{(2)}}{\partial \xi \partial \eta} + \delta_\eta \frac{\partial^2 \phi_0^{(2)}}{\partial \eta^2} + \delta_2 \frac{\partial^2 |n_1^{(1)}|^2}{\partial \xi^2} + \delta_{23} \frac{\partial^2 |n_1^{(1)}|^2}{\partial \xi \partial \eta} + \delta_3 \frac{\partial^2 |n_1^{(1)}|^2}{\partial \eta^2} = 0. \quad (2.30)$$

Here, the coefficients δ_1 , δ_η and $\delta_{\xi\eta}$ are decided by the first harmonic dynamical field and δ_2 , δ_3 and δ_{23} are decided by the zeroth harmonic static field of the plasmas. Finally, the various expressions derived in the above calculations are considered into the ($l = 1$)–component of the third-order part of the equations, leading to the amplitude equation

$$i \frac{\partial n_1^{(1)}}{\partial \tau} + \gamma_1 \frac{\partial^2 n_1^{(1)}}{\partial \xi^2} + \gamma_{12} \frac{\partial^2 n_1^{(1)}}{\partial \xi \partial \eta} + \gamma_2 \frac{\partial^2 n_1^{(1)}}{\partial \eta^2} + \left(\gamma_3 |n_1^{(1)}|^2 + \gamma_4 \phi_0^{(2)} - k_z u_{z0}^{(2)} \right) n_1^{(1)} = 0. \quad (2.31)$$

We recall that all the different coefficients of equations (2.30) and (2.31) are given in appendix (Eqs. (60) and (61)). The terms with coefficients γ_1 , γ_2 appear due to wave group dispersion and the (2+1)D evolution of the IAWs, these with γ_{12} is due to the oblique modulation. The cubic nonlinearity (Kerr) γ_3 is due to the carrier wave self-interaction originating from the zeroth harmonic modes (or slow modes), and the nonlocal nonlinear (quadratic) one γ_4 appears due to the coupling between the dynamical field associated with the first harmonic (with a cascaded effect from the second harmonic) and a static field generated due to the mean motion (zeroth harmonic) in plasmas. Further adopting the notation $\psi_1 = n_1^{(1)}$ and $\psi_2 = \phi_0^{(2)}$, $k_z = 0$, $v_{gz} = 0$ for case of pure perpendicular, the

set of Eqs. (2.30) and (2.31) reads

$$\begin{aligned} i\frac{\partial\psi_1}{\partial\tau} + \gamma_1\frac{\partial^2\psi_1}{\partial\xi^2} + \gamma_2\frac{\partial^2\psi_1}{\partial\eta^2} + (\gamma_3|\psi_1|^2 + \gamma_4\psi_2)\psi_1 &= 0, \\ \delta_1\frac{\partial^2\psi_2}{\partial\xi^2} + \frac{\partial^2\psi_2}{\partial\eta^2} + \delta_2\frac{\partial^2|\psi_1|^2}{\partial\xi^2} + \delta_3\frac{\partial^2|\psi_1|^2}{\partial\eta^2} &= 0, \end{aligned} \quad (2.32)$$

which is known as the DS equations [101] that couples a complex field, for the wave-amplitude ψ_1 , and a real field, for a mean-flow ψ_2 . Seminally, the DS equations was derived to describe nonlinear evolution of (2+1)-dimensional waves packets in water of finite depth [101]. It has thereafter found applications in diverse areas of physics, including nonlinear-optics [102] as well as related fields such as the study of matter waves in Bose-Einstein condensates [103] and the study of the propagation of electromagnetic waves in ferromagnets [104]. Moreover, in the context of nonlinear propagation of gravity-capillary surface waves under tension, a rigorous derivation of the DS equations was proposed in Ref. [159]. Without being exhaustive, we may also point out various contributions devoted to multi-dimensional classical plasma systems in Refs. [160–163]. Specifically, DSEs were shown in Ref. [160] to arise in multi-dimensional plasmas under the assumption that ion waves were parallel to the magnetic field. More recently, Panguetna et al [21, 96] derived the DS equations both in two- and three dimensions and used then to establish the strong relationship between MI and dromion solutions, even during collision. In the context of the present thesis, one should notice that the different coefficients for Eq. (2.32) depend on the system parameters. This renders easier the evolution of the contribution of both nonlinear and dispersive effects to the emergence of nonlinear waves.

2.3 Analytical methods

It is well known that the NLS equation and DS equation are a nonlinear PDEs that could not be solved, at least not exactly. However, in order to study the dynamics of such system, various technics (include analytical, and numerical) have been developed. The variational method [65, 164, 165], the Hirota's bilinear method [113, 166] have been investigated and some special types of exact and localized solutions for these have also been obtained by means of different approaches. The direct way to emerge solitons and localized structures from nonlinear systems is through the activation of modulational instability [1, 82].

2.3.1 Linear stability analysis of plane wave solutions in NLS equation

One of the direct mechanisms responsible for the formation of solitons in nonlinear media is modulational instability. The latter occurs when a constant wave background becomes unstable and induces sinusoidal modulations under the competitive contribution of nonlinear and dispersive effects. Otherwise, under such effects, a plane wave solution breaks up into trains of solitonic objects. Nonlinear evolution equations admit plane wave solutions that may be stable or unstable, depending on the system parameters.

Let's consider the following NLS equation in plasma system [18, 167]

$$i\frac{\partial\phi}{\partial\tau} + P\frac{\partial^2\phi}{\partial\zeta^2} + Q|\phi|^2\phi - R\left(\frac{\partial^2\phi}{\partial\xi^2} + \frac{\partial^2\phi}{\partial\eta^2}\right) = 0. \quad (2.33)$$

To study the modulation instability of waves in Eq. (2.33), we first consider the development of small modulation $\delta\phi$ according to

$$\phi = [\phi_0 + \delta\phi(K_\xi\xi + K_\eta\eta + K_\zeta\zeta - \Omega\tau)]e^{(-i\Delta\tau)}, \quad (2.34)$$

where the constant ψ_0 is the amplitude of the carrier wave. Substituting Eq. (2.34) into Eq. (2.33), collecting and linearizing terms in the first order, we obtain $\Delta = -Q|\phi_0|^2$, and

$$i\frac{\partial\delta\phi}{\partial\tau} + P\frac{\partial^2\delta\phi}{\partial\eta^2} + Q|\phi_0|^2(\delta\phi + \delta\phi^*) - R\left(\frac{\partial^2\phi}{\partial\xi^2} + \frac{\partial^2\phi}{\partial\eta^2}\right) = 0, \quad (2.35)$$

with $\delta\phi^*$, the complex conjugate of $\delta\phi$.

Introducing $\delta\psi = U + iV$, with $(U, V) = (U_0, V_0)e^{i(K_\xi\xi + K_\eta\eta + K_\zeta\zeta - \Omega\tau)} + c.c$ in Eq. (2.33), where $(K_\xi\xi + K_\eta\eta + K_\zeta\zeta - \Omega\tau)u$ is the modulation phase with Ω the frequency of the modulation and K_ξ , K_η and K_ζ the modulation wave numbers in x , y and z directions, respectively, and separating the real and imaginary parts, we obtain the coupled equations as follows:

$$\begin{aligned} i\Omega V_0 + [2Q|\phi_0|^2 + R(K_\xi^2 + K_\eta^2) - PK_\zeta^2]U_0 &= 0, \\ i\Omega U_0 + [-R(K_\xi^2 + K_\eta^2) + PK_\zeta^2]V_0 &= 0. \end{aligned} \quad (2.36)$$

From Eq. (2.36), we obtain the following nonlinear dispersion relation for the amplitude modulation of the ion acoustic waves modes:

$$\Omega^2 = [PK_\zeta^2 - R(K_\xi^2 + K_\eta^2)]^2 \left[1 - \frac{2Q|\phi_0|^2}{PK_\zeta^2 - R(K_\xi^2 + K_\eta^2)} \right]. \quad (2.37)$$

The MI will be set in if the following condition is satisfied:

$$\frac{2Q|\phi_0|^2}{PK_\xi^2 - R(K_\xi^2 + K_\eta^2)} > 1. \quad (2.38)$$

Letting $K^2 = K_\xi^2 + K_\eta^2 + K_\zeta^2$, the modulation wave number and $\alpha_\theta = \frac{K_\zeta}{\sqrt{K_\xi^2 + K_\eta^2}}$ the parameter related to the modulational obliqueness θ ($\theta = \arctan(\alpha_\theta)$) and the nonlinear dispersion relation Eq. (2.37) reduces to

$$\Omega^2 = K^4 \left(\frac{P\alpha_\theta^2 - R}{1 + \alpha_\theta^2} \right)^2 \left[1 - \frac{2|\phi_0|^2(1 + \alpha_\theta^2)}{K^2} \frac{Q/P}{\alpha_\theta^2 - R/P} \right]. \quad (2.39)$$

From Eq. (2.39), we find that there exists a critical wave number K_c such that

$$K_c^2 = 2|\phi_0|^2(1 + \alpha_\theta^2) \frac{Q/P}{\alpha_\theta^2 - R/P} > K^2, \quad (2.40)$$

and the instability growth rate Γ ($\Omega = i\Gamma$) is given by

$$\Gamma = K^2 \left(\frac{P\alpha_\theta^2 - R}{1 + \alpha_\theta^2} \right) \left[\frac{K_c^2}{K^2} - 1 \right]^{1/2}. \quad (2.41)$$

From Eq. (2.37), the maximum growth rate $\Gamma_{max} = \text{Im}(\Omega)_{max}$ can be obtained as $\Gamma_{max} = Q|\psi_0|^2$ provided $Q|\phi_0|^2 = PK_\xi^2 - R(K_\xi^2 + K_\eta^2)$ is satisfied.

The MI may be observed if one of the following two conditions is verified

$$QP > 0, \quad \alpha_\theta^2 > R/P, \quad (2.42)$$

or

$$QP < 0, \quad \alpha_\theta^2 < R/P. \quad (2.43)$$

The critical value of θ is $\theta_c = \arctan(R/P)^{1/2}$ resulting from Eq. (2.42) and Eq. (2.43) such that the MI occurs when either $PQ > 0$ and $\theta > \theta_c$ or $PQ < 0$ and $\theta < \theta_c$ holds and also indicate that $\omega > \omega_p$ and $\omega < \omega_p$, respectively.

2.3.2 Linear stability analysis of plane wave solutions in DS equation

In this subsection, we consider the modulational instability of a plane wave solutions of the DS system [21, 168, 169]

$$\beta_1 \frac{\partial^2 Q}{\partial \xi^2} + \beta_2 \frac{\partial^2 Q}{\partial \eta^2} = \beta_3 \frac{\partial^2 |A|^2}{\partial \xi^2} - \beta_4 \frac{\partial^2 |A|^2}{\partial \eta^2} = 0, \quad (2.44a)$$

$$i\frac{\partial A}{\partial \tau} + \alpha_1 \frac{\partial^2 A}{\partial \xi^2} + \alpha_2 \frac{\partial^2 F}{\partial \eta^2} + \alpha_3 |A|^2 A + \alpha_4 Q A = 0. \quad (2.44b)$$

The plane wave solution is given by

$$A = A_0 e^{i(p_1 \xi + p_2 \eta - \Omega \tau + \theta)}, \quad Q = Q_0, \quad (2.45)$$

where A_0 , Q_0 , p_1 , p_2 and θ are real constants. Indubitably, such plane wave solutions will propagate in the system if the condition

$$\Omega = \alpha_1 p_1^2 + \alpha_2 p_2^2 - \alpha_3 A_0^2 - \alpha_4 Q_0, \quad (2.46)$$

is satisfied. Here, Ω obtained by substituting Eq. (2.45) in the DS system, is so-called linear dispersion relation or unperturbed dispersion relation. To further proceed, we study the stability of the plane wave solution by introducing small perturbations so that

$$A = (A_0 + A') e^{i(p_1 \xi + p_2 \eta - \Omega \tau + \theta = \theta')}, \quad Q = Q_0 + Q', \quad (2.47)$$

where the small perturbations A' , Q' and θ' are taken to be

$$\begin{pmatrix} A' \\ \theta' \\ Q' \end{pmatrix} = \begin{pmatrix} \Delta A \\ \Delta \theta \\ \Delta Q \end{pmatrix} \text{Re} \left(e^{i(\mu_1 \xi + \mu_2 \eta - \nu \tau)} \right), \quad (2.48)$$

with ΔA , $\Delta \theta$, ΔQ , μ_1 , μ_2 being real constants. Inserting Eqs. (2.47) and 2.48 into (2.44) and making use of the dispersion relation (2.46), we obtain a homogeneous system in ΔA , $\Delta \theta$ and ΔQ , which admits non-trivial solutions if its determinant is non-zero. This leads to the following nonlinear dispersion relation:

$$(\nu - 2\alpha_1 \mu_1 p_1 - 2\alpha_2 \mu_2 p_2)^2 = (\mu_1^2 \alpha_1 + \mu_2^2 \alpha_2) \left(\mu_1^2 \alpha_1 + \mu_2^2 \alpha_2 - 2\alpha_3 A_0^2 + 2A_0^2 \alpha_4 \frac{\mu_1^2 \beta_2 + \mu_2^2 \beta_3}{\mu_2^2 - \mu_1^2 \beta_1} \right). \quad (2.49)$$

If the right hand side of Eq. (2.49) is negative, ν should have an imaginary part, and then the solution (2.45) becomes unstable under the modulation (2.47). Hence the stability condition is given by

$$(\mu_1^2 \alpha_1 + \mu_2^2 \alpha_2) \left(\mu_1^2 \alpha_1 + \mu_2^2 \alpha_2 - 2\alpha_3 A_0^2 + 2A_0^2 \alpha_4 \frac{\mu_1^2 \beta_2 + \mu_2^2 \beta_3}{\mu_2^2 - \mu_1^2 \beta_1} \right) > 0. \quad (2.50)$$

Obviously, the stability/instability condition of the plane wave only depends on the terms $\left(1 - 2A_0^2 \frac{\alpha_3(\beta_1 \mu_1^2 + \mu_2^2) - \alpha_4(\beta_2 \mu_1^2 + \beta_3 \mu_2^2)}{(\alpha_1 \mu_1^2 + \alpha_2 \mu_2^2)(\mu_2^2 - \mu_1^2 \beta_1)} \right)$, which also fixes the threshold amplitude above which the plane wave is expected to break up into solitary structures, i.e.,

$$A_{0,cr}^2 = \frac{(\alpha_1 \mu_1^2 + \alpha_2 \mu_2^2)(\beta_1 \mu_1^2 + \mu_2^2)}{2\alpha_3(\mu_2^2 - \mu_1^2 \beta_1) - 2\alpha_4(\beta_2 \mu_1^2 + \beta_3 \mu_2^2)}. \quad (2.51)$$

For the above, one can deduce the MI growth rate $\Gamma = \sqrt{-\nu_1^2}$, with $\nu_1 = \nu - 2\alpha_1\mu_1p_1 - 2\alpha_2\mu_2p_2$

2.3.3 Variational approach

A variational approach is the method used to describe the main characteristics of pulse evolution involving the trial functions. This method is well known in classical mechanics and used in various contexts. Speaking of nonlinear optics in general, and particularly of the propagation of a pulse in optical fibers, it was applied for the first time in 1983 by D. Anderson [65]. The basic physical assumption (the main advantage) of this approach rests on the fact that a propagating wave retains its initial shape or profile while only its characteristics such as amplitude, width, chirp, and phase change continuously according to the propagation distance. The most important single parameters characterizing the pulse evolution are the first three characteristics.

2.3.3.1 Mathematical description of this approach

in this subsection, we use the standard variational approach [65, 164, 165] for the analysis of the following NLS equation [65]

$$i\frac{\partial\psi}{\partial x} = \alpha\frac{\partial^2\psi}{\partial\tau^2} + \kappa|\psi|^2\psi. \quad (2.52)$$

Mathematically, this variational approach makes use of the Lagrangian density L defined by:

$$L = L\left(\psi, \psi^*, \frac{\partial\psi}{\partial x}, \frac{\partial\psi^*}{\partial x}, \frac{\partial\psi}{\partial\tau}, \frac{\partial\psi^*}{\partial\tau}\right). \quad (2.53)$$

Here, ψ , ψ^* , $\frac{\partial\psi}{\partial x}$, $\frac{\partial\psi^*}{\partial x}$, $\frac{\partial\psi}{\partial\tau}$ and $\frac{\partial\psi^*}{\partial\tau}$ are the generalized coordinates and the principle of least action applied to this functional Lagrangian is written in the following form:

$$\delta \iint L\left(\psi, \psi^*, \frac{\partial\psi}{\partial x}, \frac{\partial\psi^*}{\partial x}, \frac{\partial\psi}{\partial\tau}, \frac{\partial\psi^*}{\partial\tau}\right) dx d\tau = 0. \quad (2.54)$$

Let's consider the following Euler-Lagrange equation $\frac{\delta L}{\delta\psi^*} = 0 \Leftrightarrow$:

$$\frac{\partial}{\partial x}\left(\frac{\partial L}{\partial\psi_x^*}\right) + \frac{\partial}{\partial\tau}\left(\frac{\partial L}{\partial\psi_\tau^*}\right) - \frac{\partial L}{\partial\psi^*} = 0, \quad (2.55)$$

where the first two terms designate respectively the acceleration along the direction of propagation x and the temporal coordinate τ , and the last term represents the gradient

of the potential along the coordinate τ . This last equation is equivalent to Eq. (2.52). Using Eq. (2.55), we find the following Lagrangian density of Eq. (2.52)

$$L = \frac{i}{2} \left(\psi \frac{\partial \psi^*}{\partial x} - \psi^* \frac{\partial \psi}{\partial x} \right) - \alpha \left| \frac{\partial \psi}{\partial \tau} \right|^2 + \frac{\kappa}{2} |\psi|^4. \quad (2.56)$$

We now proceed by assuming a trial function solution of Eq. (2.52) of the form

$$\psi(x, \tau) = A(x) e^{-\frac{\tau^2}{2a^2(x)} + ib(x)\tau^2}, \quad (2.57)$$

where $A(x)$ is the complex amplitude, $a(x)$ the temporal width, and $2b(x)\tau$ the frequency chirp of the carrier wave.

Inserting the trial solution Eq. (2.57) into Eq. (2.56), we obtain the following reduced Lagrangian

$$\langle L \rangle = \int_{-\infty}^{+\infty} L d\tau = \frac{\sqrt{\pi}}{2} \left[ia \left(A \frac{\partial A^*}{\partial x} - A^* \frac{\partial A}{\partial x} \right) + |A|^2 a^3 \frac{\partial b}{\partial x} - \alpha a^3 |A|^2 \left(\frac{1}{a^4} + 4b^2 \right) + \frac{1}{\sqrt{2}} \kappa a |\psi|^4 \right], \quad (2.58)$$

with $\delta \int \langle L \rangle dx = 0$.

2.3.3.2 Variational equations for Gaussian parameters

Now, we can find the variation of $\langle L \rangle$ with respect to the various characteristic of Gaussian parameters of the carrier wave $A(\tau)$, $a(x)$ and $b(x)$. Using the Euler-Lagrange equations for each parameter, we obtain progressively:

$$\begin{aligned} \frac{\delta \langle L \rangle}{\delta A^*} &= \frac{\partial}{\partial x} \left(\frac{\partial \langle L \rangle}{\partial A_x^*} \right) - \frac{\partial \langle L \rangle}{\partial A^*} = 0 \Leftrightarrow \\ \frac{\partial}{\partial x} (iaA) &= -ia \frac{\partial A}{\partial x} + Aa^3 \frac{\partial b}{\partial x} - \alpha a^3 A \left(\frac{1}{a^4} + 4b^2 \right) + \sqrt{2} \kappa a |A|^2 A, \end{aligned} \quad (2.59a)$$

$$\begin{aligned} \frac{\delta \langle L \rangle}{\delta A} &= \frac{\partial}{\partial x} \left(\frac{\partial \langle L \rangle}{\partial A_x} \right) - \frac{\partial \langle L \rangle}{\partial A} = 0 \Leftrightarrow \\ \frac{\partial}{\partial x} (-iaA^*) &= ia \frac{\partial A^*}{\partial x} + A^* a^3 \frac{\partial b}{\partial x} - \alpha a^3 A^* \left(\frac{1}{a^4} + 4b^2 \right) + \sqrt{2} \kappa a |A|^2 A^*, \end{aligned} \quad (2.59b)$$

$$\frac{\delta \langle L \rangle}{\delta b} = \frac{\partial}{\partial x} \left(\frac{\partial \langle L \rangle}{\partial b_x} \right) - \frac{\partial \langle L \rangle}{\partial b} = 0 \Leftrightarrow \frac{\partial}{\partial x} (a^3 |A|^2) = -8\alpha b a^3 |A|^2, \quad (2.59c)$$

$$\begin{aligned} \frac{\delta \langle L \rangle}{\delta a} &= \frac{\partial}{\partial x} \left(\frac{\partial \langle L \rangle}{\partial a_x} \right) - \frac{\partial \langle L \rangle}{\partial a} = 0 \Leftrightarrow \\ i \left(A \frac{\partial A^*}{\partial x} - A^* \frac{\partial A}{\partial x} \right) &+ 3a^2 |A|^2 \frac{\partial b}{\partial x} - 12\alpha a^2 |A|^2 + \frac{\alpha |A|^2}{a^2} + \frac{1}{\sqrt{2}} \kappa |A|^4 = 0. \end{aligned} \quad (2.59d)$$

2.3.3.3 Determination of the equations governing the dynamics of test function parameters and the potential

Multiplying the Eqs. (2.59a) and (2.59b) by $A^*(x)$ and $A(x)$, respectively, we obtain the following equations:

$$A^* \frac{\partial}{\partial x}(iaA) = -iaA^* \frac{\partial A}{\partial x} + |A|^2 a^3 \frac{\partial b}{\partial x} - \alpha a^3 |A|^2 \left(\frac{1}{a^4} + 4b^2 \right) + \sqrt{2\kappa} a |A|^4, \quad (2.60a)$$

$$A \frac{\partial}{\partial x}(-iaA^*) = iaA \frac{\partial A^*}{\partial x} + |A|^2 a^3 \frac{\partial b}{\partial x} - \alpha a^3 |A|^2 \left(\frac{1}{a^4} + 4b^2 \right) + \sqrt{2\kappa} a |A|^4 A. \quad (2.60b)$$

By subtracting and adding the Eqs. (2.60a) and (2.60b), respectively, we obtain the following equations:

$$A \frac{\delta \langle L \rangle}{\delta A} - A^* \frac{\delta \langle L \rangle}{\delta A^*} = 0 \Leftrightarrow \frac{d}{dx} (|A|^2 a) = 0, \quad (2.61a)$$

$$i \left(A^* \frac{\partial A}{\partial x} - A \frac{\partial A^*}{\partial x} \right) = |A|^2 \left[a^2 \frac{\partial b}{\partial x} - \alpha a^2 \left(\frac{1}{a^4} + 4b^2 \right) + \sqrt{2\kappa} |A|^2 \right]. \quad (2.61b)$$

Equation (2.61a) implies a constant of motion, which express the fact that the energy of wave does not change:

$$|A|^2 a = \text{const} = E_0 = |A_0|^2 a_0, \quad (2.62)$$

where $a_0 = a(0)$ and $A_0 = A(0)$ at $x = 0$, with E_0 the conserved quantity related to the wave energy. This result (Eq. (2.62)) could also have been obtained from the well-known invariant of the NLS equation:

$$\int_{-\infty}^{+\infty} |\psi(x, \tau)|^2 d\tau = \text{const}. \quad (2.63)$$

From Eq. (2.59d) and (2.59c), using the fact that $|A|^2 a$ is constant, we obtain:

$$\frac{da}{dx} = -4\alpha ab \quad (2.64)$$

By comparing Eqs. (2.59d) and (2.61b), we obtain:

$$\frac{db}{dx} = 4ab^2 + \frac{\alpha}{X^4} - \frac{\kappa |A|^2}{2\sqrt{2}a^2} = 4ab^2 + \frac{\alpha}{X^4} - \frac{\kappa E_0}{2\sqrt{2}a^3}. \quad (2.65)$$

By deriving Eq. (2.64) and using Eq. (2.65), we obtain:

$$\frac{d^2 a}{dx^2} = \frac{4\alpha^2}{Xa^3} - \frac{\sqrt{2\kappa} |A|^2}{a} = \frac{4\alpha^2}{Xa^3} - \frac{\sqrt{2\kappa} E_0}{a^2}. \quad (2.66)$$

Considering the complexe amplitude $A(x)$, as follows: $A(x) = |A(x)|e^{i\phi(x)}$ and $A^*(x) = |A(x)|e^{(-i\phi(x))}$ its complexe conjugate, we have:

$$\frac{dA}{dx} = \left(\frac{d|A|}{dx} + i|A|\frac{d\phi}{dx} \right) e^{i\phi}, \quad \frac{dA^*}{dx} = \left(\frac{d|A|}{dx} - i|A|\frac{d\phi}{dx} \right) e^{-i\phi}. \quad (2.67)$$

By inserting Eq. (2.67) into Eq. (2.61b) and using Eq. (2.65), we obtain:

$$\frac{d\phi}{dx} = \frac{\alpha}{a^2} - \frac{5\sqrt{2}\kappa|A|^2}{8} = \frac{\alpha}{a^2} - \frac{5\sqrt{2}\kappa E_0}{8a}. \quad (2.68)$$

Equations (2.62), (2.64), (2.65) and (2.68) lead to the following system:

$$\begin{cases} |A|^2 a = E_0 = |a_0|^2 a_0, \\ \frac{d^2 a}{dx^2} = \frac{4\alpha^2}{Xa^3} - \frac{\sqrt{2}\kappa|A|^2}{a} = \frac{4\alpha^2}{Xa^3} - \frac{\sqrt{2}\kappa E_0}{a^2}, \\ \frac{db}{dx} = 4\alpha b^2 + \frac{\alpha}{X^4} - \frac{\kappa|A|^2}{2\sqrt{2}a^2} = 4\alpha b^2 + \frac{\alpha}{X^4} - \frac{\kappa E_0}{2\sqrt{2}a^3}, \\ \frac{d\phi}{dx} = \frac{\alpha}{a^2} - \frac{5\sqrt{2}\kappa|A|^2}{8} = \frac{\alpha}{a^2} - \frac{5\sqrt{2}\kappa E_0}{8a}, \end{cases} \quad (2.69)$$

where $E_0 = \int_{-\infty}^{+\infty} |\psi|^2 d\tau = |A|^2 a = |A_0|^2 a_0$ is the constant linked to the energy of the wave, with $A_0 = A(0)$, $a_0 = a(0)$. The differential equations of the set of Eq. (2.69) represent the dynamic equations of the amplitude, widths, shirps and phase of the ion acoustic waves in electronegative plasma in the presence the external magnetic field. The associated potential of this system can be expressed as

$$V(a) = -\frac{1}{2} \left(\frac{da}{dx} \right)^2. \quad (2.70)$$

Inserting the third relation of Eq. (2.69) into Eq. (2.70), using the normalized variables $y(x) = a(x)/a_0$, we finally obtain the following scalar potential of the system

$$V(a) = \frac{2\alpha}{a^2} - \frac{\sqrt{2}\alpha\kappa E_0}{a} + const \implies V(y) = \frac{\mu}{y^2} - \frac{\nu}{y} + K, \quad (2.71)$$

describing the motion of particles in the potential well, where the constants μ and ν are defined as follows $\mu = \frac{2\alpha}{a_0^4}$, $\nu = -\frac{\sqrt{2}\alpha\kappa E_0}{a_0^3}$ and $K = \frac{const}{a_0^2}$. Assuming that $[\frac{da}{dx}]_{x=0} = 0$ and $a(0) = a_0$, we obtain $K = -(\mu + \nu)$.

2.3.4 The Hirota's bilinear method

The Hirota's bilineaire method was introduced for the first time by Hirota [?] to construct multisoliton solutions of integrable nonlinear evolution equations. The idea was to make a transformation into new variables, so that in these new variables multisoliton

solutions appear in a particularly simple form. The method is an algebraic one, based on the bilinear form of the nonlinear equation, used to solve nonlinear partial differential equations (PDEs). The main feature of the method is the derivation of multi-soliton solutions of some physical systems [?, ?, ?, ?]. Research on exact solutions for nonlinear evolution equations has attracted a lot of interest during the last decades. In this regard, a collection of analytical methods for investigating exact solutions to nonlinear partial differential equations (PDEs) have been proposed, amongst which are the inverse scattering method [170], the Backlund and Darboux transformation method [171], the Hirota bilinear method [113, 166], pseudo-spectral method [172], the hyperbolic function method [173, 174], the homogeneous balance method and formal variable separation method [175–177], the generalized Riccati equation method [178] unified algebraic method and varied Jacobi elliptic function methods [179, 180]. Interestingly, the Hirota bilinear method [113, 166] has been used to construct dromions-like solutions to a system of equations similar to the DS system. We should indicate that there exist types I and II DS equations depending on the sign of their coefficients [181, 182]. However, from the results of Sec. 2.3.2, one may obtain the two types of systems. It has been shown that the system of Eq. (2.32) may display DS-I behaviors if the conditions $\gamma_1/\gamma_2 > 0$ and $\gamma_3 > 0$ are satisfied [183, 184].

Let consider the following Davey-Stewartson equations [21], similar to [160]

$$i \frac{\partial F}{\partial \tau} + \gamma_1 \frac{\partial^2 F}{\partial \xi^2} + \gamma_2 \frac{\partial^2 F}{\partial \eta^2} + (\gamma_3 |F|^2 + \gamma_4 G) F = 0, \quad (2.72a)$$

$$\delta_1 \frac{\partial^2 G}{\partial \xi^2} - \frac{\partial^2 G}{\partial \eta^2} - \delta_2 \frac{\partial^2 |F|^2}{\partial \xi^2} - \delta_3 \frac{\partial^2 |F|^2}{\partial \eta^2} = 0. \quad (2.72b)$$

We used the Hirota's bilinear method to obtain one- and two-dromion solutions for this DS system of equations. Such solutions are investigated by first studying their domain of existence. Therefore, we first rescale dependent and independent variables as follows:

$$\xi' = \frac{1}{(\delta_1 \gamma_3 - \delta_2 \gamma_4)^{1/2}} \xi, \quad \eta' = \frac{1}{(\delta_3 \gamma_4 - \gamma_3)^{1/2}} \eta, \quad Q = \gamma_3 |F|^2 + \gamma_4 G. \quad (2.73)$$

We also introduce the following new independent variables through a coordinate axis rotation by 45°:

$$X = \frac{1}{\sqrt{2}}(\xi' + \eta'), \quad Y = \frac{1}{\sqrt{2}}(\xi' - \eta'). \quad (2.74)$$

Substituting the relations (2.73) and (2.74) into Eqs. (2.72), we obtain the following set of equations

$$iF_\tau + a(F_{XX} + F_{YY}) + bF_{XY} + FQ = 0, \quad (2.75a)$$

$$a'(Q_{XX} + Q_{YY}) + b'Q_{XY} = 2(|F|^2)_{XY}, \quad (2.75b)$$

where a , b , a' and b' are constants given by,

$$\begin{aligned} a &= \frac{1}{2} \left(\frac{\gamma_1}{\delta_1\gamma_3 - \delta_2\gamma_4} + \frac{\gamma_2}{\delta_3\gamma_4 - \gamma_3} \right), & b &= \frac{1}{2} \left(\frac{\gamma_1}{\delta_1\gamma_3 - \delta_2\gamma_4} - \frac{\gamma_2}{\delta_3\gamma_4 - \gamma_3} \right), \\ a' &= \frac{1}{2} \left(\frac{\delta_1}{\delta_1\gamma_3 - \delta_2\gamma_4} - \frac{1}{\delta_3\gamma_4 - \gamma_3} \right), & b' &= \frac{1}{2} \left(\frac{\delta_1}{\delta_1\gamma_3 - \delta_2\gamma_4} + \frac{1}{\delta_3\gamma_4 - \gamma_3} \right). \end{aligned} \quad (2.76)$$

Solutions for system (2.75) are investigated by introducing the new dependent variable transformations f (real) and g (complex) so that

$$F = \left(\frac{g}{f} \right), \quad \text{and} \quad Q = c(\ln f)_{XY}. \quad (2.77)$$

This leads with the D-operators to the bilinear form

$$(iD_\tau + a(D_{XX} + D_{YY}))(g \cdot f) = 0, \quad (2.78a)$$

$$D_{XY}f \cdot f = mg \cdot g^*, \quad (2.78b)$$

where D is an operator defined by

$$D_x^n g \cdot f = (\partial_{x_1} - \partial_{x_2})^n g(x_1) f(x_2) \big|_{x_2=x_1=x}, \quad (2.79a)$$

$$D_t^m D_x^n g \cdot f = (\partial_{t_1} - \partial_{t_2})^m (\partial_{x_1} - \partial_{x_2})^n g(x_1) f(x_2) \big|_{t_2=t_1=t, x_2=x_1=x}, \quad (2.79b)$$

which is known as the Hirota bilinear operators and also called Hirota derivatives, with $m, n = 0, 1, 2, 3, \dots$. For example

$$\begin{aligned} D_t g \cdot f &= g_t f - g f_t, \\ D_x g \cdot f &= g_x f - g f_x, \\ D_t D_x g \cdot f &= g_{tx} f - g_t f_x - g_x f_t + g f_{tx}, \\ D_x^2 g \cdot f &= g_{xx} f - 2g_x f_x + g f_{xx}, \\ D_x^2 f \cdot f &= 2f_{xx} f - 2f_x^2. \end{aligned} \quad (2.80)$$

We further expand the new variables F and G in the power series of small arbitrary parameter δ as

$$\begin{aligned} g &= \delta g_1 + \delta^3 g_3 + \dots, \\ f &= 1 + \delta^2 f_2 + \delta^4 f_4 + \dots, \end{aligned} \quad (2.81)$$

in order to obtain the dromion-like solutions [21, 183]. The new variables f and g in Eq. (2.81) are introduced into (2.78) to find g_1 , g_3 , f_2 and f_4 by collecting the terms with same power in δ :

$$\delta : (iD_\tau + a(D_{XX} + D_{YY}))g_1 \cdot 1 = 0, \quad (2.82a)$$

$$\delta^2 : D_{XY}(1 \cdot f_2 + f_2 \cdot 1) = mg_1 \cdot g_1^*, \quad (2.82b)$$

$$\delta^3 : (iD_\tau + a(D_{XX} + D_{YY}))(g_1 \cdot f_2 + g_3 \cdot 1) = 0, \quad (2.82c)$$

$$\delta^4 : D_{XY}(f_2 \cdot f_2 + 1 \cdot f_4 + f_4 \cdot 1) = m(g_1 \cdot g_3^* + g_3 \cdot g_1^*), \quad (2.82d)$$

and so on. Now, solving (2.82a) to generate the line solitons, g_1 to be in the form

$$g_1 = \sum_{j=1}^N \exp \eta_j, \quad \eta_j = p_j X + q_j Y + ia(p_j^2 + q_j^2)\tau + \eta_{0j}, \quad (2.83)$$

with p_j , q_j , and η_{0j} being the complex constants. To construct the one soliton solution, we take $N = 1$ in (2.83) and so we have

$$g_1 = \exp \eta_1 \quad \eta_1 = p_1 X + q_1 Y + ia(p_1^2 + q_1^2)\tau + \eta_{01}. \quad (2.84)$$

Substituting (2.84) in (2.82b), we obtain

$$f_2 = \exp(\eta_1 + \eta_1^* + 2\beta), \quad \exp 2\beta = \frac{1}{p_{1R}q_{1R}}, \quad (2.85)$$

where p_{1R}, q_{1R} being the real part of p_1 , q_1 , respectively. Using g_1 and f_2 from Eqs. (2.82a) and (2.82b) into Eqs. (2.82c) and (2.82d), one can show that $g_{(j)} = 0$ for $j \geq 3$ and $f_{(j)} = 0$ for $j \geq 4$, respectively. Now, substituting (2.84) and (2.85) in (2.77), the physical quantities F and G take the following form

$$F = \sqrt{\frac{cp_{1R}q_{1R}}{2}} \operatorname{sech}(\eta_{1R} + \beta) \exp(i\eta_{1I}), \quad (2.86a)$$

$$Q = 2cq_{1R}^2 \text{sech}^2(\eta_{1R} + \beta), \quad (2.86b)$$

where η_{1I} is the imaginary part of η_1 . This treatment can be extended to generate N-line soliton solutions as well.

2.3.5 Construction of one-dromion solutions

To construct one-dromion solution, we use the ansatz [182, 185–187]

$$\begin{aligned} f_{1D} &= 1 + J \exp(\eta_1 + \eta_1^*) + K \exp(\eta_2 + \eta_2^*) + L \exp(\eta_1 + \eta_1^* + \eta_2 + \eta_2^*), \\ \eta_1 &= pX + iap^2\tau + \eta_{01}, \quad \eta_2 = qY + iaq^2\tau + \eta_{02}, \end{aligned} \quad (2.87)$$

where J , K and L are real constants, $p = p_1$ and $q = q_1$. Substituting Eq. (2.87) into (2.82b), we obtain

$$g_{1D} = \rho \exp(\eta_1 + \eta_2), \quad |\rho|^2 = 2L(p + p^*)(q + q^*) = 8Lp_Rq_R. \quad (2.88)$$

The generalized form of one-dromion solution is obtained as

$$\begin{aligned} F_{1D} &= \frac{g_{1D}}{f_{1D}} = \frac{\rho \exp(\eta_1 + \eta_2)}{\left\{ 1 + J \exp(\eta_1 + \eta_1^*) + K \exp(\eta_2 + \eta_2^*) + L \exp(\eta_1 + \eta_1^* + \eta_2 + \eta_2^*) \right\}}, \\ \eta_1 &= pX + iap^2\tau + \eta_{01}, \quad \eta_2 = qY + iaq^2\tau + \eta_{02}. \end{aligned} \quad (2.89)$$

Similar solutions have already been reported in the work of Panguetna et al. [21] as the excitation of ion-acoustic waves in unmagnetized electronegative plasmas.

2.3.6 Construction of two-dromion solutions

Moreover, one can proceed in a similar way and construct multidromion solutions. For example, to generate two-dromion, we take the ansatz [21, 187]:

$$\begin{aligned} f_{2D} &= 1 + A \exp(\eta_1 + \eta_1^*) + B \exp(\eta_2 + \eta_2^*) + C \exp(\eta_3 + \eta_3^*) \\ &+ D[\exp(\eta_1 + \eta_2^*) + \exp(\eta_2 + \eta_1^*)] \\ &+ E[\exp(\eta_1 + \eta_2^* + \eta_3 + \eta_3^*) + \exp(\eta_2 + \eta_1^* + \eta_3 + \eta_3^*)] \\ &+ F \exp(\eta_1 + \eta_1^* + \eta_2 + \eta_2^*) + G \exp(\eta_2 + \eta_2^* + \eta_3 + \eta_3^*) \\ &+ H \exp(\eta_1 + \eta_1^* + \eta_3 + \eta_3^*) + I \exp(\eta_1 + \eta_1^* + \eta_2 + \eta_2^* + \eta_3 + \eta_3^*), \end{aligned} \quad (2.90a)$$

$$\eta_1 = p_1 X + iap_1^2 \tau + \eta_{01}, \quad \eta_2 = p_2 X + iap_2^2 \tau + \eta_{02}, \quad \eta_3 = q_1 Y + iaq_1^2 \tau + \eta_{03}, \quad (2.90b)$$

where A, B, C, D, E, F, G, H and I are real, positive constants. Now, substituting (2.90a) with (2.90b) in (2.78b) and choosing $p_{2I} = p_{1I}$, we obtain

$$g_{2D} = \rho_{11} \exp(\eta_1 + \eta_3) + \rho_{12} \exp(\eta_2 + \eta_3) + \rho_{21} \exp(\eta_1 + \eta_1^* + \eta_2 + \eta_3) + \rho_{22} \exp(\eta_1 + \eta_2 + \eta_2^* + \eta_3), \quad (2.91)$$

where the real parameters $\rho_{11}, \rho_{12}, \rho_{21}$ and ρ_{22} can be chosen appropriately in terms of the parameters $A, B, C, D, E, F, G, H, I, p_{1R}, p_{2R}$ and q_{1R} . Thus, the two-dromion solution can be expressed as

$$F_{2D} = \frac{g_{2D}}{f_{2D}} = \frac{\left\{ \begin{array}{l} \rho_{11} \exp(\eta_1 + \eta_3) + \rho_{12} \exp(\eta_2 + \eta_3) + \rho_{21} \exp(\eta_1 + \eta_1^* + \eta_2 + \eta_3) \\ + \rho_{22} \exp(\eta_1 + \eta_2 + \eta_2^* + \eta_3) \end{array} \right\}}{\left\{ \begin{array}{l} 1 + A \exp(\eta_1 + \eta_1^*) + B \exp(\eta_2 + \eta_2^*) + C \exp(\eta_3 + \eta_3^*) \\ + D[\exp(\eta_1 + \eta_2^*) + \exp(\eta_2 + \eta_1^*)] \\ + E[\exp(\eta_1 + \eta_2^* + \eta_3 + \eta_3^*) + \exp(\eta_2 + \eta_1^* + \eta_3 + \eta_3^*)] \\ + F \exp(\eta_1 + \eta_1^* + \eta_2 + \eta_2^*) + G \exp(\eta_2 + \eta_2^* + \eta_3 + \eta_3^*) \\ + H \exp(\eta_1 + \eta_1^* + \eta_3 + \eta_3^*) + I \exp(\eta_1 + \eta_1^* + \eta_2 + \eta_2^* + \eta_3 + \eta_3^*) \end{array} \right\}}, \quad (2.92)$$

where $\eta_1 = p_1 X + iap_1^2 \tau + \eta_{01}$, $\eta_2 = p_2 X + iap_2^2 \tau + \eta_{02}$, $\eta_3 = q_1 Y + iaq_1^2 \tau + \eta_{03}$. Interaction properties of these localized structures (two-dromion like structures) which are expected to be quite similar to that of the DSI equation [188–190] can be analysed in the same way.

2.4 Numerical methods

The nonlinear Schrödinger equation (NLS) obtained in the previous section (equation (2.20)) is a nonlinear partial differential equation which generally does not admit of an analytical solution except for certain well-specified cases such as solitons for which the effects dispersion are compensated by the optical Kerr effects. Similarly, the equations governing the dynamics of the parameters of the test function do not admit analytical solutions, except for fairly simple cases. A numerical approach is often necessary to describe the studied systems. There are several numerical models: pseudo-spectral methods, Runge-kutta (RK4) methods, finite difference methods, etc. The use of a numerical

method depends on the equation to be solved. A numerical approach is therefore often necessary for an understanding of nonlinear effects in magnetized electronegative plasma. A large number of numerical methods can be used for this purpose [191, 192]. These can be classified into two broad categories known as: (i) the finite-difference methods; and (ii) the pseudospectral methods. Generally speaking, pseudospectral methods are faster by up to an order of magnitude to achieve the same accuracy [193]. The one method that has been used extensively to solve the pulse-propagation problem in nonlinear dispersive or dissipative media is the split-step Fourier method [194, 195]. The relative speed of this method compared with most finite-difference schemes can be attributed in part to the use of the finite-Fourier-transform (FFT) algorithm [196]. This section describes various numerical techniques used to study the IAWs-propagation problem with emphasis on the split-step Fourier method and its modifications.

2.4.1 Fourth-order Runge-Kutta method

In this subsection, we use the fourth-order Runge-Kutta method to study the dynamics of gaussian function parameters numerically. It is a single-step method, directly derived from Euler's method and very commonly used for the numerical resolution of differential equations. This method is easy to program and stable enough for common physics functions. Numerically, it requires only the knowledge of the initial values, but quite consuming calculation time. The idea of this method is to try to distribute the places where the function $f(x)$ is evaluated between the abscissas x and $x + h$ of iteration step h , rather than to calculate the successive derivatives up to a certain order n in one point. Overall, this method is based on the principle of iteration, i.e. a first estimate of the solution is used to calculate a second, more precise estimate, and so on.

Consider the following problem defined by the first derivative form and the initial condition:

$$\frac{dy}{dx} = y' = f(x, y), \quad y(x_0) = y_0. \quad (2.93)$$

The fourth-order Runge-Kutta method is given by the following equation

$$y(i+1) = y(i) + \frac{1}{6} (K_1 + 2K_2 + 2K_3 + K_4), \quad (2.94)$$

where $x(i+1) = x(i) + h$ with The iteration algorithm i of this method is as follows:

$$\begin{aligned}
 K_1 &= hf(x(i), y(i)), \\
 K_2 &= hf(x(i) + h/2, y(i) + K_1/2), \\
 K_3 &= hf(x(i) + h/2, y(i) + K_2/2,) \\
 K_4 &= hf(x(i) + h, y(i) + K_3).
 \end{aligned} \tag{2.95}$$

Here, the slope is obtained by a weighted average of slopes:

- K_1 is the slope at the beginning of the interval;
- K_2 is the slope in the middle of the interval using the slope K_1 to calculate the value of y at the point $x(i) + h/2$ through the Euler's method;
- K_3 is the slope in the middle of the interval, but this time obtained by using the slope K_2 to calculate the value of y ;
- K_4 is the slope at the end of the interval, with the value of y calculated using the slope K_3 .

2.4.2 Split-step fourier method

The Split-step Fourier method (SSFM) is based on the pseudo-spectral method and used to solve time dependent nonlinear partial differential equation. The nonlinear PDE is divided into related sub-problems of the original equation involving calculating the dispersive and nonlinear terms in the dynamical equations governing the propagation of IAWs in magnetized electronegative plasma. The method is easy to understand and with the use of MATLAB the implementation is straight forward [197, 198]. This method provides an excellent methodology for learning and teaching how to solve time dependent PDEs. In numerical analysis, the Split-step Fourier method is a pseudo-spectral numerical method used to solve nonlinear PDEs like the NLS equation [199, 200]. However, the split-step method provides a numerical solution to the problem. It is the most popular algorithm because of its good accuracy and relatively modest computing cost. Overall, the Linear and Nonlinear Schrödinger Equation and with the aid of MATLAB [197]. Here, below, is the description of the method.

Let us consider for example, the NLS equation [197]

$$i \frac{\partial u}{\partial t} = -\frac{1}{2} \left(\frac{\partial^2 u}{\partial x^2} + \frac{\partial^2 u}{\partial y^2} \right) + V(x, y)u \implies \frac{\partial u}{\partial t} = i \frac{1}{2} \left(\frac{\partial^2 u}{\partial x^2} + \frac{\partial^2 u}{\partial y^2} \right) - iV(x, y)u, \tag{2.96}$$

where $u(t, x)$ is a complex valued function, $V(x, y)$ a real function and $i^2 = -1$. The Split-step Fourier method is employed by letting

$$L = \frac{1}{2} \left(\frac{\partial^2}{\partial x^2} + \frac{\partial^2}{\partial y^2} \right), \quad (2.97a)$$

$$N = -V(x, y), \quad (2.97b)$$

where L and N time independent linear and nonlinear operators, respectively. Consider a small interval of time, say $[t, t + \Delta t]$. Now assume that $u(t, x, y)$ is known and assume that L is negligible, that is $u_{xx} \approx 0$ and $u_{yy} \approx 0$. Then Eq. (2.96) reduces to

$$\frac{\partial u}{\partial t} = iNu. \quad (2.98)$$

This approximation leads to an ordinary differential equation (ODE) in time. The solution to this ODE is known and the solution at time $t = t + \Delta t$ is given by

$$u(x, y, t + \Delta t) = \exp(i\Delta t N)u(x, y, t). \quad (2.99)$$

Next, we redo the problem but neglect the contribution of N . For this case the PDE is linear with no variable coefficients,

$$\frac{\partial u}{\partial t} = iLu. \quad (2.100)$$

This equation will be solved in the interval $[t, t + \Delta t]$ and use $u(x, y, t + \Delta t)$ as the initial condition. An analytical solution to this equation can be by taking the Fourier Transform

$$\frac{\partial \hat{u}}{\partial t} = iF(Lu) = iF\left(\frac{1}{2} \left(\frac{\partial^2}{\partial x^2} + \frac{\partial^2}{\partial y^2} \right)\right) = -i(k_x^2 + k_y^2)\hat{u}. \quad (2.101)$$

The following Fourier and Inverse Fourier Transform definitions have been used

$$\hat{h}(k) = F(h) = \int_{-\infty}^{-\infty} \int_{-\infty}^{-\infty} h(x) e^{-2i\pi(k_x x + k_y y)} dx dy, \quad (2.102a)$$

$$h(x) = F(\hat{h}) = \int_{-\infty}^{-\infty} \int_{-\infty}^{-\infty} \hat{h}(k) e^{2i\pi(k_x x + k_y y)} dk_x dk_y. \quad (2.102b)$$

The partial derivatives are now gone and the equation becomes an ODE. The analytical solution can be computed and value of $\hat{u}(k_x, k_y, t + \Delta t)$ is given by

$$\hat{u}(k_x, k_y, t + \Delta t) = \exp -i(k_x^2 + k_y^2)\Delta t \hat{u}(k_x, k_y, t). \quad (2.103)$$

The solution in the x domain can be calculated by inverse of the Fourier Transform:

$$\widehat{u}(x, y, t + \Delta t) = F^{-1}(\exp(-i(k_x^2 + k_y^2)\Delta t)\widehat{u}(k_x, k_y, t + \Delta t)). \quad (2.104)$$

The entire procedure can be stated in a single equation:

$$\widehat{u}(x, y, t + \Delta t) = F^{-1}(\exp(-i(k_x^2 + k_y^2)\Delta t)F(|\exp(i\Delta t V(x, y))u(x, y, t)|)). \quad (2.105)$$

The essence of the split method is to think of advancing in time and applying L and N one at a time to complete each time step.

A variation on this method is the symmetrized split-step Fourier method, which takes half a time step using one operator, then takes a full time step with only the other, and then takes a second half time step again with only the first. This method is an improvement upon the generic split-step Fourier method because its error is of order dt^3 for a time step dt . The Fourier transforms of this algorithm can be computed relatively fast using the Fast Fourier Transform (FFT). Compared to the typical finite difference methods [201], the split-step Fourier method can therefore be much faster.

Conclusion

This chapter was devoted to the presentation of the fluid model equations governing the dynamics of magnetized ENP system composed of electrons and negative ions, both in Boltzmann distribution, in addition to cold mobile positive ions and the external magnetic field. We have also presented analytical methods used in this thesis. Asymptotic expansion techniques, like the reductive perturbation and the multiple-scale expansion methods, have been presented. Using these methods, we have derived the amplitude equations (NLS and DS equations). We note that, coefficients of these equations do not depend only on electronegative parameters of the plasma, also on the magnetic field. Stability conditions have been discussed, using the MI analysis of the planar wave solution for these amplitude equations. Also, we have described the analytical and numerical methods of investigations. For example, we have performed the Hirota's bilinear method to show to derive the line solitons solutions. This last method allowed us to solve the DS-Equation and construct one- and two- dromion like structures.

Results and discussion

Introduction

This chapter is devoted to the results and discussion on the work carried out in this thesis. We mean to address comprehensively in $(2+1)$ -dimensional cases, the response of ion-acoustic waves to the effects of the electronegative parameters (the negative ion concentration ratio and the electron-to -negative ion temperature ratio) and magnetic field. We also show that under certain conditions, new classes of waves like ion-acoustic soliton, one- and two-dromions solutions may emerge. Solitonic structures have long been an attractive topic in nonlinear physics, since they arise in nonlinear physical systems and their importance has been discussed in a broad range of contexts that include non-exhaustively optic communication [66–71], Biophysics [72–75], Bose-Einstein condensates [76–78] and Plasma physics [79, 80]. In magnetized ENPs, the nonlinearity of the system is considerably affect and consequently the characteristics of ion-acoustic waves [202–204]. For instance, it has been well-established that they may appear in physical systems as the consequence of the interplay between nonlinear and dispersive effects, leading to the modulational instability phenomenon. Otherwise, under such effects, a plane wave solution breaks up into trains of solitonic objects. These investigations will allow us to have a precise idea of how plasma electronegative parameters and magnetic field impact the emergence, the propagation and the stability of solitary waves in such media.

3.1 Dynamics of modulated nonlinear IAW packets in magnetized ENP

3.1.1 Evolution of wave frequency of IAWs in NLS equation

The following partial differential equation (2.20) for a complex field (wave-amplitude ψ) obtained in the previous chapter

$$i \frac{\partial \psi}{\partial \tau} + P \frac{\partial^2 \psi}{\partial \eta^2} + Q |\psi|^2 \psi - S \frac{\partial^2 \psi}{\partial \xi^2} = 0, \quad (3.1)$$

$$\begin{aligned} P &= \frac{1}{2} \frac{\partial^2 \omega}{\partial k^2} = -\frac{3c_1}{2} \frac{\omega^5}{k^4} = -\frac{3\omega^3}{2k^2} (1 - \omega^2), \\ Q &= -k(\alpha_{v_z} + \beta_{v_z}) - \frac{\omega}{2}(\alpha_n + \beta_n) + \frac{\omega^3}{k^2} \left(c_2(\alpha_\phi + \beta_\phi) + \frac{3}{2}c_3 \right), \\ S &= \frac{\omega^3}{2k^2} \frac{1 + \omega_p^2 - \omega^2}{\omega_p^2 - \omega^2} \end{aligned} \quad (3.2)$$

is well-known as the (2+1)-dimensional nonlinear Schrödinger equation, with P , Q and S the longitudinal dispersive coefficient, cubic nonlinear coefficient and the transverse dispersive coefficient depending on the external magnetic field, respectively. It describes the amplitude modulation of the electronegative plasma amplitude ψ of positive ion acoustic wave packets along the external magnetic field. We note that the coefficients of the obtained NLS equation depend on the system parameters specially, not only on the electronegative parameters such as the negative ion concentration ratio and the electron-to-negative ion temperature ratio (α and σ_n , respectively), but also on the magnetic field (ω_p). In Eq. (3.2), $n = \frac{n_p}{n_{p0}}$ is the normalized number-density of positive ions, with charge neutrality condition at equilibrium defined by $Z_p n_{p0} = Z_n n_{n0} + n_{e0}$, $\Omega = \frac{\Omega_i}{w_{pi}}$ is the normalized parameter of ion cyclotron and ion plasma frequency ratio, with $w_{pi} = \sqrt{\frac{4\pi n_{p0} Z_p^2 e^2}{m_i}}$ and $\Omega_i = \frac{eB}{m_i c}$. $c_1 = \mu_e + \mu_n \sigma_n$, $c_2 = \frac{\mu_e + \mu_n \sigma_n^2}{2}$ and $c_3 = \frac{\mu_e + \mu_n \sigma_n^3}{6}$ are constants. Here, $\mu_e = \frac{n_{e0}}{Z_p n_{p0}} = \frac{1}{1+\alpha}$, and $\mu_n = \frac{Z_n n_{n0}}{Z_p n_{p0}} = \frac{\alpha}{1+\alpha}$ which assumes the neutrality condition of the plasma $\mu_e + \mu_n = 1$, with $\alpha = \frac{Z_n n_{n0}}{n_{e0}}$ being the negative ion-to-electron density ratio. The parameters $\alpha_\phi = \frac{k^2}{2\omega^4} - \frac{c_2^2}{3k^2}$, $\alpha_n = (4k^2 + c_1)\alpha_\phi + c_2$, $\alpha_{v_z} = \frac{\omega}{k}(\alpha_n - (k^2 + c_1)^2)$, $\beta_\phi = \frac{2v_g^2 c_2 - (k^2 + 3c_1)}{1 - c_1 v_g^2}$, $\beta_n = c_1 \beta_\phi + 2c_2$, $\beta_{v_z} = v_g \beta_n - \frac{2\omega}{k}(k^2 + c_1)^2$ depend on the following wave frequency Eqs. (3.3) and the group velocity Eqs. (3.4) of carrier wave (see Eqs. (2.11) and (2.14) obtained in the previous chapter): the dispersion relation is

$$\omega^2 = \frac{k^2}{k^2 + c_1}, \quad (3.3)$$

and the group velocity is

$$v_g = c_1 \frac{\omega^3}{k^3}. \quad (3.4)$$

In Fig. 3.1, we present the wave frequency ω given by Eq. (3.3) and the group velocity

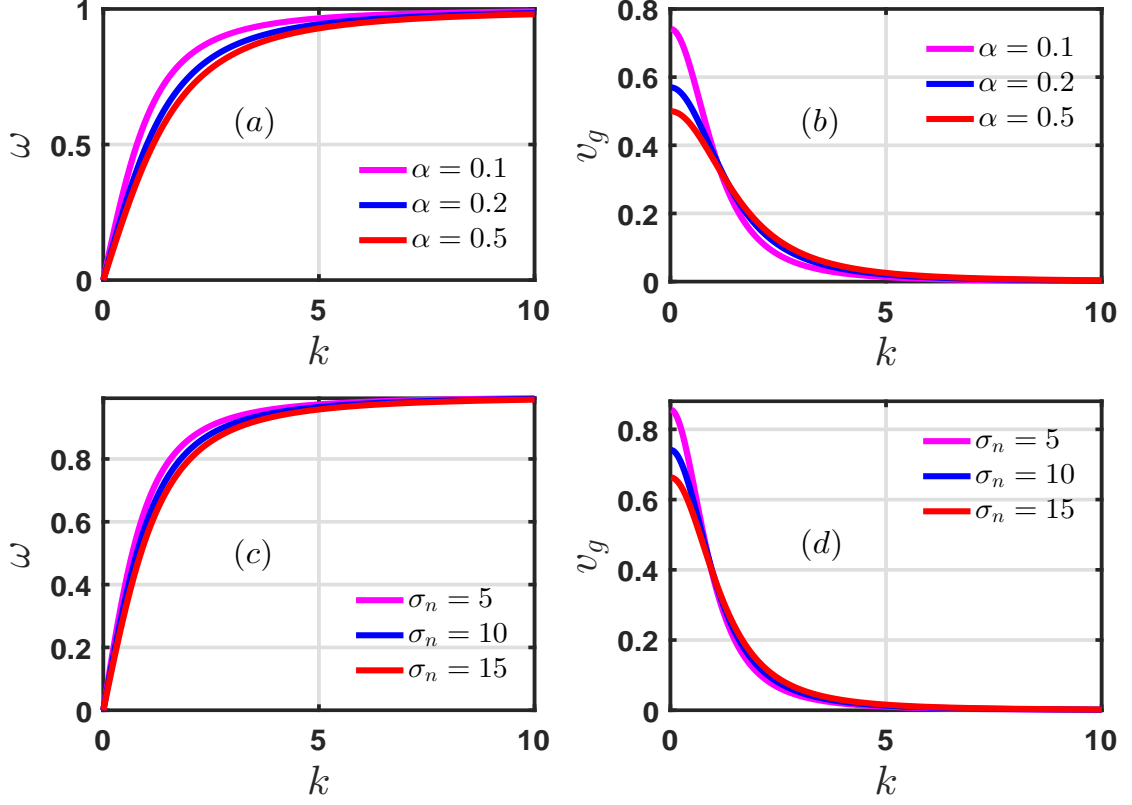


Figure 3.1: Plot of the frequency ω against k in panels (a) and (c), and the group velocity v_g versus k in panels (b) and (d) of wave packets for different values of α (upper panels for $\sigma_n = 5$) and σ_n (down panels for $\alpha = 0.1$).

v_g given by Eq. (3.4) against the wave number k for different values of the electronegativity parameters (negative ion-to-electron density ratio α and electron-to-negative ion temperature ratio σ_n). From the two panels (Fig. 3.1a and 3.1c), which allow to explain the linear dispersion of features ion-acoustic waves, we find that as k increases, the wave frequency ω increases and it approaches an asymptotic value around 1 at higher wavenumber k . It approaches a zero frequency value for the values of k tending towards zero. Moreover, for a fixed value of σ_n (α), as the values of the negative ion-to-electron density ratio α increase, the wave frequency ω decreases. This implies that to maintain the charge neutrality, the equilibrium negative ion density value will increase as the electron density increases. Moreover, this curve represents the relationship between the wavelength and

the frequency of the wave, and it is useful in understanding the behavior of wave packets in the plasma system. Physically, the system gained more energy with greater values of the wavenumber, and this energy has a limit value for highest wavenumber. Such negative ion-to-electron density ratio α (σ_n) has also a significant effect on the group velocity of waves as shown in the two other panels (Fig. 3.1b and 3.1d). The group velocity of waves (v_g) decreases and approaches the zero value with increasing wave number (k) for different values of α (σ_n). One can see that v_g decreases with an increasing value of α (σ_n) and its behavior continues until reaching a certain value of k ($k = 1.12$), and then, (v_g) turns to increase by increasing α (σ_n). This leads to improve the speed of the information carried by the propagating wave packets in our plasma system.

3.1.2 Modulational instability analysis of IAWs in NLS equation

In this section, we are interested on the study of modulational instability (MI) considering (2+1)-dimensional ion acoustic waves governed by the nonlinear Schrödinger equation Eq. (3.1). The plane homogeneous solution of this equation is given by [1, 82–85]

$$\psi = \psi_0 e^{i(Q|\psi_0|^2\tau)}, \quad (3.5)$$

where the constant ψ_0 represents the amplitude of the carrier wave. The stability of the solution (3.5) is studied by adding the small modulation $\delta\psi$ in the amplitude according to :

$$\psi = (\psi_0 + \delta\psi) e^{i(Q|\psi_0|^2\tau)}. \quad (3.6)$$

Substituting Eq. (3.6) into Eq. (3.1), collecting and linearizing terms in the first order, we obtain

$$i\frac{\partial\delta\psi}{\partial\tau} + P\frac{\partial^2\delta\psi}{\partial\eta^2} + Q|\psi_0|^2(\delta\psi + \delta\psi^*) - S\frac{\partial^2\delta\psi}{\partial\xi^2} = 0, \quad (3.7)$$

with $\delta\psi^*$, the complex conjugate of $\delta\psi$.

Introducing $\delta\psi = U + iV$, with $(U, V) = (U_0, V_0)e^{i(K_x\xi + K_z\eta - \Omega\tau)} + c.c$ in Eq. (3.1), where $K_x\xi + K_z\eta - \Omega\tau$ is the modulation phase with Ω the frequency of the modulation and K_x, K_z the modulation wave numbers in x and z directions, respectively, and separating the real and imaginary parts, we obtain the coupled equations as follows:

$$\begin{aligned} i\Omega V_0 + [2Q|\psi_0|^2 + SK_x^2 - PK_z^2]U_0 &= 0, \\ i\Omega U_0 + [-SK_x^2 + PK_z^2]V_0 &= 0. \end{aligned} \quad (3.8)$$

From Eq. (3.8), we obtain the following nonlinear dispersion relation for the amplitude modulation of the ion acoustic waves modes:

$$\Omega^2 = [PK_z^2 - SK_x^2]^2 \left[1 - \frac{2Q|\psi_0|^2}{PK_z^2 - SK_x^2} \right]. \quad (3.9)$$

The MI will be set in if the following condition is satisfied:

$$\frac{2Q|\psi_0|^2}{PK_z^2 - SK_x^2} > 1. \quad (3.10)$$

Letting $K^2 = K_x^2 + K_z^2$, the modulation wave number and $\alpha_\theta = \frac{K_z}{K_x}$ the parameter related to the modulational obliqueness θ ($\theta = \arctan(\alpha_\theta)$) and the nonlinear dispersion relation Eq. (3.9) reduces to

$$\Omega^2 = K^4 \left(\frac{P\alpha_\theta^2 - S}{1 + \alpha_\theta^2} \right)^2 \left[1 - \frac{2|\psi_0|^2(1 + \alpha_\theta^2)}{K^2} \frac{Q/P}{\alpha_\theta^2 - S/P} \right]. \quad (3.11)$$

From Eq. (3.11), we find that there exists a critical wave number K_c such that

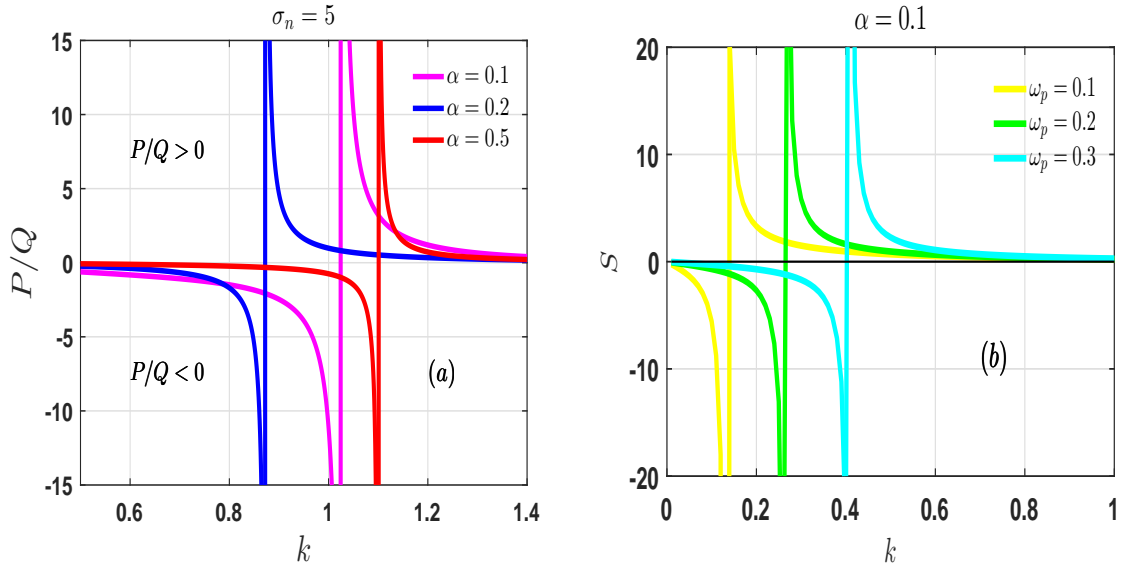


Figure 3.2: Panels show P/Q against the carrier wave number k for different values of negative ion to electron density ratio α (a) as in Fig. 3.1 and S versus the carrier wave number k for different values of plasma frequency ω_p (b).

$$K_c^2 = 2|\psi_0|^2(1 + \alpha_\theta^2) \frac{Q/P}{\alpha_\theta^2 - S/P} > K^2, \quad (3.12)$$

and the instability growth rate Γ ($\Omega = i\Gamma$) is given by

$$\Gamma = K^2 \left(\frac{P\alpha_\theta^2 - S}{1 + \alpha_\theta^2} \right) \left[\frac{K_c^2}{K^2} - 1 \right]^{1/2}. \quad (3.13)$$

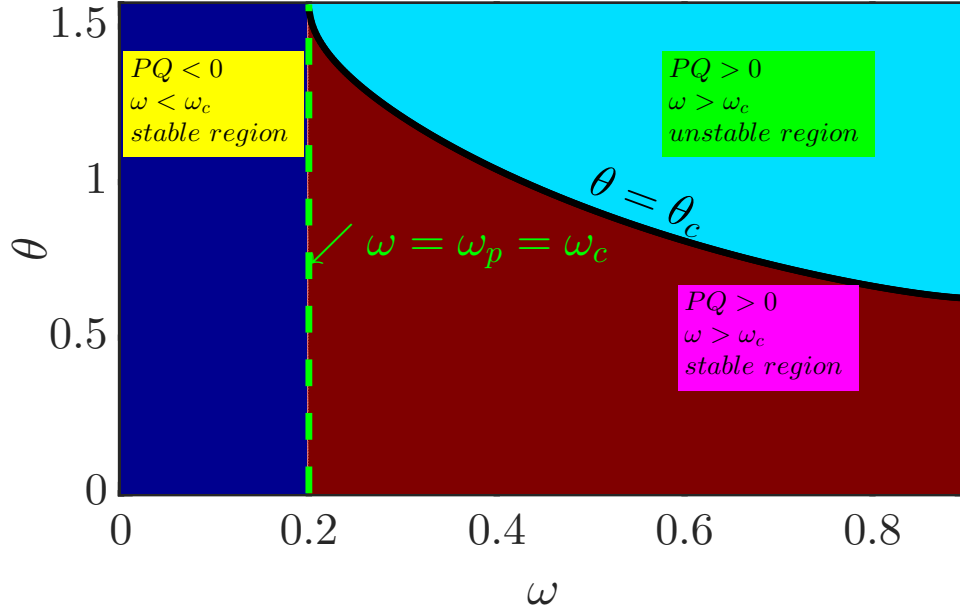


Figure 3.3: The stable/unstable regions for fixed values of the system parameters $\alpha = 0.1$, $\sigma_n = 5$ and $\omega_p = 0.2$ is shown by the contour plots of $P/Q = 0$ against the wave frequency ω and the modulation angle θ .

From Eq. (3.9), the maximum growth rate $\Gamma_{max} = \text{Im}(\Omega)_{max}$ can be obtained as $\Gamma_{max} = Q|\psi_0|^2$ provided $Q|\psi_0|^2 = PK_z^2 - SK_x^2$ is satisfied. The MI may be observed if one of the following two conditions is verified

$$QP > 0, \quad \alpha_\theta^2 > S/P = \frac{1 + \omega_p^2 - \omega^2}{3(\omega^2 - 1)(\omega_p^2 - \omega^2)}, \quad (3.14)$$

or

$$QP < 0, \quad \alpha_\theta^2 < S/P = \frac{1 + \omega_p^2 - \omega^2}{3(\omega^2 - 1)(\omega_p^2 - \omega^2)}. \quad (3.15)$$

It is clear that there also exists a critical value of θ , as $\theta_c = \arctan(S/P)^{1/2}$ resulting from Eq. (3.14) and Eq. (3.15) such that the MI occurs when either $PQ > 0$ and $\theta > \theta_c$ or $PQ < 0$ and $\theta < \theta_c$ holds and also indicate that $\omega > \omega_p$ and $\omega < \omega_p$, respectively. Hence, the instability condition depends on the sign of the product PQ and Figs. 3.2(a) and 3.2(b) show numerically the variations of the coefficients S and P/Q given by Eq. (3.2) with the different physical parameters (α , ω_p and σ_n). According to the choice of these physical parameters, one can see that the coefficient S gains its sign. The expression of S clearly shows that there is a cutoff at $\omega = \omega_p$ corresponding to the simple ion cyclotron oscillations (dimensional form) in electronegative plasma, which does not participate in the wave group dynamics and that ω_p plays a decisive role in the propagation dynamics

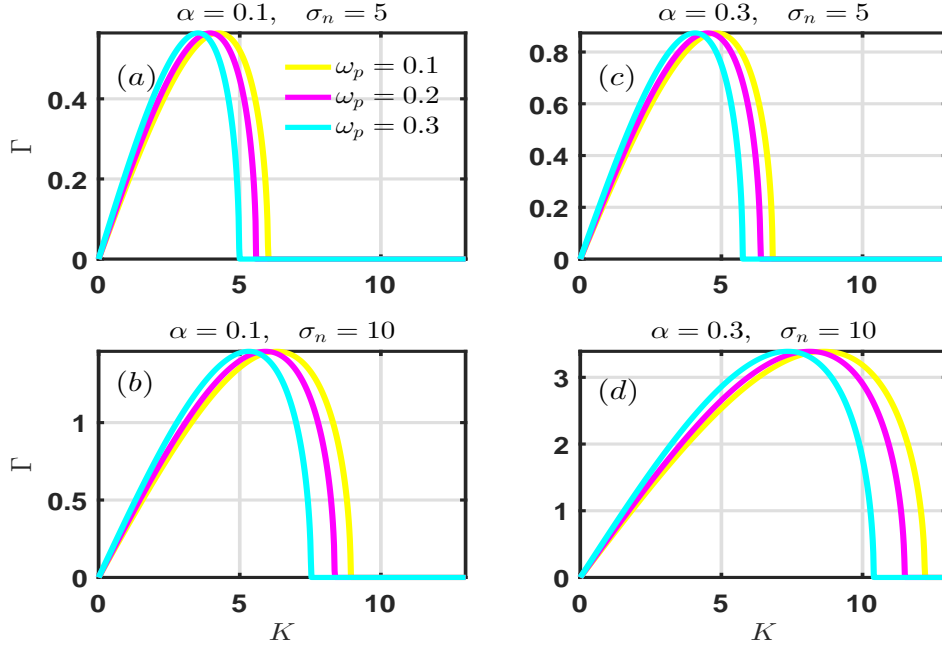


Figure 3.4: Plot of the modulational instability growth rate against the modulation wave number K for different values of ω_p and fixed values of α and σ_n : $\alpha = 0.1$ and $\sigma_n = 5$ (see the panel (a)), $\alpha = 0.1$ and $\sigma_n = 10$ (see the panel (b)), $\alpha = 0.3$ and $\sigma_n = 5$ (see the panel (c)) and $\alpha = 0.3$ and $\sigma_n = 10$ (see the panel (d)).

of the nonlinear ion acoustic waves [87]. The curves of P/Q in (ω, θ) -plane presented in Fig. 3.3 show the information about the positive and negative regions of product PQ according to the analytical expressions given in Eqs. (3.14) and (3.15) and the stable/unstable regions for fixed values of the system parameters. One can see that dispersion coefficients P , S and nonlinearity coefficient Q are related to α , σ_n and ω_p . It turns out that these physical parameters could significantly affect the stability characteristics of IAWs in our plasma system. Therefore, the modulation instability can be studied numerically. For that, the MI growth rate is shown in Fig. 3.4. The panels of Fig. 3.4 show the evolution of the growth rate of the MI for different values of the magnetic field ω_p in the case of some values of α and σ_n . As it increases, one clearly notices an extension of the zone of instability in the plane and the increasing of the maximum growth rate. We find that effect of increasing values of α and σ_n is to increase the modulational instability growth rate with cutoffs at higher wave numbers of modulation for different values of ω_p . We should precise that some studies were carried out recently that showed the strong impact of parameters such as the negative ion to electron concentration ratio and electron-to-negative ion temperature ratio [20–23, 52]. It is therefore, of high importance here to

insist on the combined effects due to such parameters and the magnetic field. Therefore, this implies that the unstable regions will also be modified with the changing of α , σ_n and ω_p .

3.1.3 Dynamics of IAWs characteristic parameters

In this section, we follow the standard variational approach [65,164,165] for the analysis of Eq. (3.1). Mathematically, this approach makes use of the Lagrangian density L defined by:

$$L = L \left(\psi, \psi^*, \frac{\partial \psi}{\partial \tau}, \frac{\partial \psi^*}{\partial \tau}, \frac{\partial \psi}{\partial \xi}, \frac{\partial \psi^*}{\partial \xi}, \frac{\partial \psi}{\partial \eta}, \frac{\partial \psi^*}{\partial \eta}, \tau, \xi, \eta \right) \quad (3.16)$$

$\psi, \psi^*, \frac{\partial \psi}{\partial \tau}, \frac{\partial \psi^*}{\partial \tau}, \frac{\partial \psi}{\partial \xi}, \frac{\partial \psi^*}{\partial \xi}, \frac{\partial \psi}{\partial \eta}, \frac{\partial \psi^*}{\partial \eta}, \tau, \xi$ and η are the generalized coordinates and the principle of least action applied to this functional Lagrangian is written in the following form:

$$\delta \iint L \left(\psi, \psi^*, \frac{\partial \psi}{\partial \tau}, \frac{\partial \psi^*}{\partial \tau}, \frac{\partial \psi}{\partial \xi}, \frac{\partial \psi^*}{\partial \xi}, \frac{\partial \psi}{\partial \eta}, \frac{\partial \psi^*}{\partial \eta}, \tau, \xi, \eta \right) = 0 \quad (3.17)$$

Let's consider the following Euler-Lagrange equation:

$$\frac{\partial}{\partial \tau} \left(\frac{\partial L}{\partial \psi^*} \right) + \frac{\partial}{\partial \eta} \left(\frac{\partial L}{\partial \psi^*} \right) + \frac{\partial}{\partial \xi} \left(\frac{\partial L}{\partial \psi^*} \right) - \frac{\partial L}{\partial \psi^*} = 0. \quad (3.18)$$

where the first three terms designate respectively the acceleration along the direction of propagation τ and the spatial coordinates ξ and η , and the last term represents the gradient of the potential along the coordinate τ . This last equation is equivalent to Eq. (3.1). Using Eq. (3.18), we find the following Lagrangian of Eq. (3.1)

$$L = \frac{i}{2} \left(\psi \frac{\partial \psi^*}{\partial \tau} - \psi^* \frac{\partial \psi}{\partial \tau} \right) + P \left| \frac{\partial \psi}{\partial \eta} \right|^2 - S \left| \frac{\partial \psi}{\partial \xi} \right|^2 - \frac{Q}{2} |\psi|^4. \quad (3.19)$$

We now proceed by assuming a trial function solution of Eq. (3.1) of the form

$$\psi(\xi, \eta, \tau) = C(\tau) e^{-\frac{\xi^2}{2X^2(\tau)} - \frac{\eta^2}{2Y^2(\tau)} + ia(\tau)\xi^2 + ib(\tau)\eta^2 + i\varphi(\tau)}, \quad (3.20)$$

where $C(\tau)$ is the complex amplitude, $(X(\tau), Y(\tau))$ the spacial width, $(a(\tau), b(\tau))$ the frequency chirp and $\varphi(\tau)$ the phase of the carrier wave.

Inserting the trial solution Eq. (3.20) into Eq. (3.19), we obtain the following reduced Lagrangian

$$\begin{aligned} \langle L \rangle &= \int_{-\infty}^{+\infty} \int_{-\infty}^{+\infty} L d\xi d\eta \\ &= \frac{\pi}{2} \left[i \left(C \frac{\partial C^*}{\partial \tau} - C^* \frac{\partial C}{\partial \tau} \right) XY + |\psi|^2 \frac{\partial a}{\partial \tau} X^3 Y \right. \\ &\quad \left. + |\psi|^2 \frac{\partial b}{\partial \tau} XY^3 - S |\psi|^2 \left(\frac{1}{X^4} + 4a^2 \right) X^3 Y \right. \\ &\quad \left. + P |\psi|^2 \left(\frac{1}{Y^4} + 4b^2 \right) XY^3 - Q |\psi|^4 XY \right]. \end{aligned} \quad (3.21)$$

Now, we can find the variation of $\langle L \rangle$ with respect to the various characteristic of Gaussian parameters of the carrier wave $C(\tau)$, $X(\tau)$, $Y(\tau)$, $a(\tau)$, $b(\tau)$ and $\varphi(\tau)$.

Using the Euler-Lagrange equations for each parameter, we obtain progressively:

$$\begin{aligned} \frac{\delta \langle L \rangle}{\delta C^*} &= \frac{\partial}{\partial \tau} \left(\frac{\partial \langle L \rangle}{\partial C_\tau^*} \right) - \frac{\partial \langle L \rangle}{\partial C^*} = 0 \Leftrightarrow \frac{\partial}{\partial \tau} (iCXY) = -iC_\tau XY + Ca_\tau X^3 Y \\ &+ Cb_\tau XY^3 - SC \left(\frac{1}{X^4} + 4a^2 \right) X^3 Y + PC \left(\frac{1}{Y^4} + 4b^2 \right) XY^3 - 2|C|^2 CXY \end{aligned} \quad (3.22)$$

$$\begin{aligned} \frac{\delta \langle L \rangle}{\delta C} &= \frac{\partial}{\partial \tau} \left(\frac{\partial \langle L \rangle}{\partial C_\tau} \right) - \frac{\partial \langle L \rangle}{\partial C} = 0 \Leftrightarrow \frac{\partial}{\partial \tau} (-iC^* XY) = iC_\tau^* XY + C^* a_\tau X^3 Y \\ &+ C^* b_\tau XY^3 - SC^* \left(\frac{1}{X^4} + 4a^2 \right) X^3 Y + PC^* \left(\frac{1}{Y^4} + 4b^2 \right) XY^3 - 2|C|^2 C^* XY \end{aligned} \quad (3.23)$$

$$\frac{\delta \langle L \rangle}{\delta b} = \frac{\partial}{\partial \tau} \left(\frac{\partial \langle L \rangle}{\partial b_\tau} \right) - \frac{\partial \langle L \rangle}{\partial b} = 0 \Leftrightarrow \frac{\partial}{\partial \tau} (|C|^2 X^3 Y) = -8S|C|^2 a X^3 Y \quad (3.24)$$

$$\frac{\delta \langle L \rangle}{\delta b} = \frac{\partial}{\partial \tau} \left(\frac{\partial \langle L \rangle}{\partial b_\tau} \right) - \frac{\partial \langle L \rangle}{\partial b} = 0 \Leftrightarrow \frac{\partial}{\partial \tau} (|C|^2 XY^3) = -8S|C|^2 b XY^3 \quad (3.25)$$

$$\begin{aligned} \frac{\delta \langle L \rangle}{\delta X} &= \frac{\partial}{\partial \tau} \left(\frac{\partial \langle L \rangle}{\partial X_\tau} \right) - \frac{\partial \langle L \rangle}{\partial X} = 0 \Leftrightarrow i(CC_\tau^* - C^*C_\tau) + 3|C|^2 a_\tau X^2 + |C|^2 b_\tau Y^2 \\ &- 3S|C|^2 \left(\frac{1}{X^4} + 4a^2 \right) X^2 + 4S|C|^2 \left(\frac{1}{X^2} \right) + P|C|^2 \left(\frac{1}{Y^4} + 4b^2 \right) Y^2 - Q|C|^4 = 0 \end{aligned} \quad (3.26)$$

$$\begin{aligned} \frac{\delta \langle L \rangle}{\delta Y} &= \frac{\partial}{\partial \tau} \left(\frac{\partial \langle L \rangle}{\partial Y_\tau} \right) - \frac{\partial \langle L \rangle}{\partial Y} = 0 \Leftrightarrow i(CC_\tau^* - C^*C_\tau) + |C|^2 a_\tau X^2 + 3|C|^2 b_\tau Y^2 \\ &- S|C|^2 \left(\frac{1}{X^4} + 4a^2 \right) X^2 + 3P|C|^2 \left(\frac{1}{Y^4} + 4b^2 \right) Y^2 - 4P|C|^2 \left(\frac{1}{Y^2} \right) - Q|C|^4 = 0 \end{aligned} \quad (3.27)$$

Now, multiplying the Eqs. (3.22) and (3.23) by $C^*(z)$ and $C(z)$, respectively, we obtain the following equations:

$$\begin{aligned} C^* \frac{\partial}{\partial \tau} (iCXY) &= -iC^*C_\tau XY + |C|^2 a_\tau X^3 Y + |C|^2 b_\tau XY^3 - S|C|^2 \left(\frac{1}{X^4} + 4a^2 \right) X^3 Y \\ &+ P|C|^2 \left(\frac{1}{Y^4} + 4b^2 \right) XY^3 - 2|C|^4 XY \end{aligned} \quad (3.28a)$$

$$\begin{aligned} C \frac{\partial}{\partial \tau} (-iC^* XY) &= iCC_\tau^* XY + |C|^2 a_\tau X^3 Y + |C|^2 b_\tau XY^3 - S|C|^2 \left(\frac{1}{X^4} + 4a^2 \right) X^3 Y \\ &+ P|C|^2 \left(\frac{1}{Y^4} + 4b^2 \right) XY^3 - 2|C|^4 XY \end{aligned}$$

(3.28b)

By subtracting and adding the Eqs. (3.28a) and (3.28b), respectively, we obtain the following equations:

$$C \frac{\delta \langle L \rangle}{\delta C} - C^* \frac{\delta \langle L \rangle}{\delta C^*} = 0 \Leftrightarrow \frac{d}{d\tau} (|C|^2 XY) = 0 \quad (3.29a)$$

$$\begin{aligned} C \frac{\delta \langle L \rangle}{\delta C} + C^* \frac{\delta \langle L \rangle}{\delta C^*} = 0 &\Leftrightarrow i(C^* C_\tau - C C_\tau^*) = |C|^2 a_\tau X^2 + |C|^2 b_\tau Y^2 \\ &- S|C|^2 \left(\frac{1}{X^4} + 4a^2 \right) X^2 + P|C|^2 \left(\frac{1}{Y^4} + 4b^2 \right) Y^2 - 2|C|^4 \end{aligned} \quad (3.29b)$$

Equation (3.29a) implies a constant of motion, which express the fact that the energy of wave does not change:

$$|C|^2 XY = \text{const} = E_0 = |C_0|^2 X_0 Y_0, \quad (3.30)$$

where $X_0 = w(0)$, $X_0 = w(0)$ and $C_0 = C(0)$ at $\tau = 0$, with E_0 the conserved quantity related to the wave energy. This result (Eq. (3.30)) could also have been obtained from the well-known invariant of the NLS equation:

$$\int_{-\infty}^{+\infty} \int_{-\infty}^{+\infty} |\psi(\xi, \eta, \tau)|^2 d\xi d\eta = \text{const}. \quad (3.31)$$

From Eq. (3.24) and (3.25), using the fact the $|C|^2 XY$ is constant, we obtain:

$$\frac{dX}{d\tau} = -4SaX \quad (3.32a)$$

$$\frac{dY}{d\tau} = 4PbY \quad (3.32b)$$

By comparing Eqs. (3.26) and (3.29b), Eqs. (3.27) and (3.29b), respectively, we obtain:

$$\frac{da}{d\tau} = 4Sa^2 - \frac{S}{X^4} - \frac{Q|C|^2}{2X^2} = 4Sa^2 - \frac{S}{X^4} - \frac{QE_0}{2X^3Y} \quad (3.33a)$$

$$\frac{db}{d\tau} = -4Pb^2 + \frac{P}{Y^4} - \frac{Q|C|^2}{2Y^2} = -4Pb^2 + \frac{P}{Y^4} - \frac{QE_0}{2XY^3} \quad (3.33b)$$

By deriving Eqs. (3.32a) and (3.32b) and using Eqs. (3.33a) and (3.33b), we obtain:

$$\frac{d^2 X}{d\tau^2} = \frac{4S^2}{X^3} + \frac{2QS|C|^2}{X} = \frac{4S^2}{X^3} + \frac{2QSE_0}{X^2Y} \quad (3.34a)$$

$$\frac{d^2Y}{d\tau^2} = \frac{4P^2}{Y^3} - \frac{2QP|C|^2}{Y} = \frac{4P^2}{Y^3} - \frac{2QPE_0}{XY^2} \quad (3.34b)$$

Considering the complexe amplitude $C(\tau)$, as follows: $C(\tau) = |C(\tau)|e^{i\phi(\tau)}$ and $C^*(\tau) = |C(\tau)|e^{(-i\phi)}$ its complexe conjuguate, we have:

$$\frac{dC}{d\tau} = \left(\frac{d|C|}{d\tau} + i|C|\frac{d\phi}{d\tau} \right) e^{i\phi}, \quad \frac{dC^*}{d\tau} = \left(\frac{d|C|}{d\tau} - i|C|\frac{d\phi}{d\tau} \right) e^{-i\phi} \quad (3.35)$$

By inserting Eq. (3.35) into Eq. (3.29b) and using Eqs. (3.33a) and (3.33b), we obtain:

$$\frac{d\phi}{d\tau} = \frac{S}{X^2} - \frac{P}{Y^2} + \frac{3Q|C|^2}{2} = \frac{S}{X^2} - \frac{P}{Y^2} + \frac{3QE_0}{2XY} \quad (3.36)$$

Equations (3.30), (3.33a), (3.33b), (3.34a), (3.34b) and (3.36) lead to the following dy-

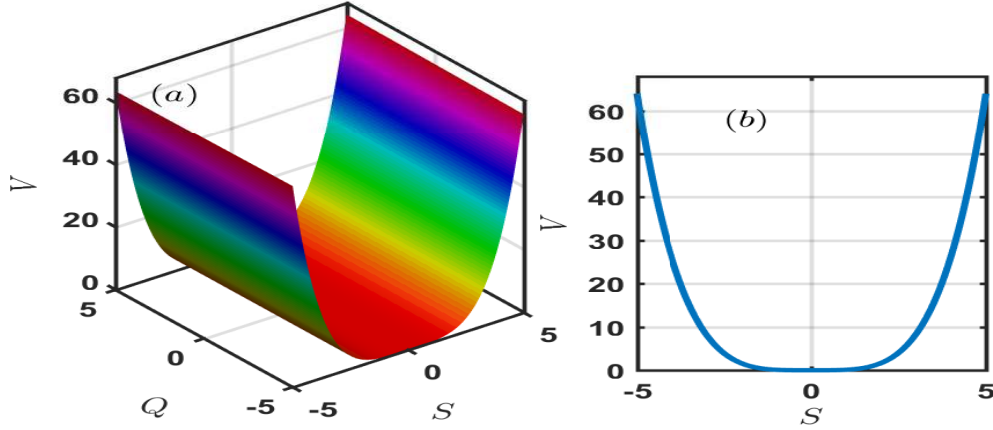


Figure 3.5: Plot of the potential function given by Eq. (3.39) versus the (S,Q)-plane for $\alpha = 0.1$, $\sigma_n = 5$ and $\omega_p = 0.2$.

namic system:

$$\left\{ \begin{array}{l} |C|^2 XY = |C_0|^2 X_0 Y_0, \\ \frac{da}{d\tau} = 4Sa^2 + \frac{S}{X^4} - \frac{QE_0}{2X^3Y}, \\ \frac{db}{d\tau} = -4Pb^2 + \frac{P}{Y^4} - \frac{QE_0}{2XY^3}, \\ \frac{\partial^2 X}{\partial \tau^2} = \frac{4S^2}{X^3} + \frac{2SQE_0}{X^2Y}, \\ \frac{\partial^2 Y}{\partial \tau^2} = \frac{4P^2}{Y^3} - \frac{2PQE_0}{XY^2}, \\ \frac{d\phi}{d\tau} = -\frac{S}{X^2} + \frac{P}{Y^2} - \frac{3QE_0}{2XY}. \end{array} \right. \quad (3.37)$$

where $E_0 = \int_{-\infty}^{+\infty} \int_{-\infty}^{+\infty} |\psi|^2 d\xi d\eta = |C|^2 XY = |C_0|^2 X_0 Y_0$ is the constant linked to the

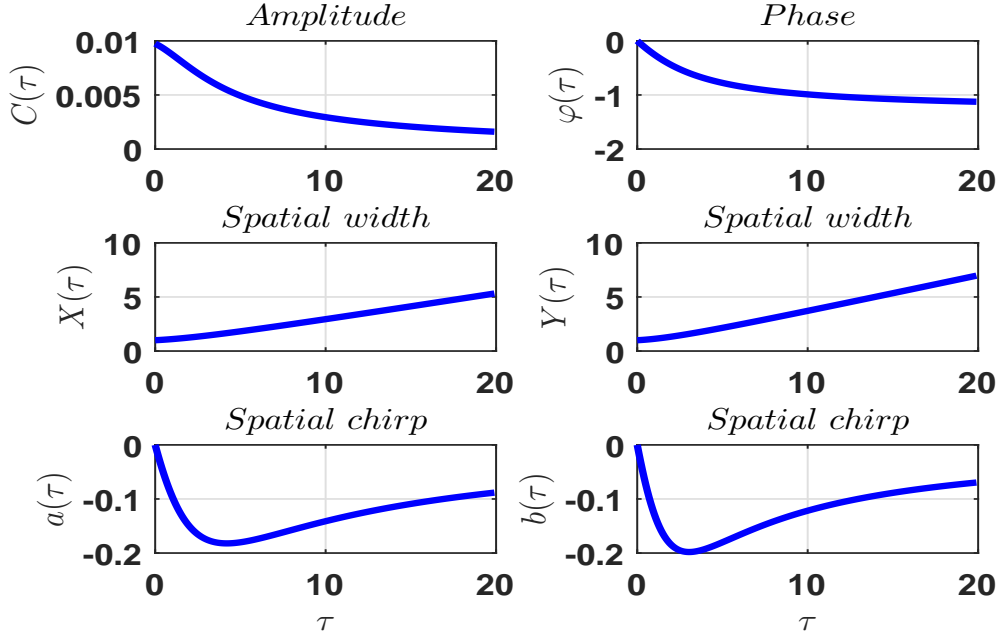


Figure 3.6: Evolution of Gaussian parameters: amplitude $C(\tau)$, spatial widths $X(\tau)$, $Y(\tau)$, spatial chirps $a(\tau)$, $b(\tau)$ and phase φ .

energy of the wave, with $C_0 = C(0)$, $X_0 = X(0)$ and $Y_0 = Y(0)$. The differential equations of the set of Eq. (3.37) represent the dynamical equations of the amplitude, widths, chirps and phase of the ion acoustic waves in electronegative plasma in the presence the external magnetic field. The associated potential of this system can be expressed as

$$V(X, Y) = -\frac{1}{2} \left(\frac{dX}{d\tau} \right)^2 - \frac{1}{2} \left(\frac{dY}{d\tau} \right)^2. \quad (3.38)$$

Inserting the fourth and fifth relations of Eq. (3.37), using the normalized variables $Z(\tau) = X(\tau)/X_0$, $T(\tau) = Y(\tau)/Y_0$, we finally obtain the following scalar potential of the system describing the movement of particles in the potential well:

$$V(Z, T) = \frac{\lambda_1}{Z^2} + \frac{\lambda_2}{T^2} + \frac{\lambda_1 + \lambda_2}{ZT} - (\lambda_1 + \beta_1 + \lambda_2 + \beta_2), \quad (3.39)$$

where the constants λ_1 , β , λ_2 and β_2 are defined as follows $\lambda_1 = \frac{2S^2}{X_0^4}$, $\beta_1 = \frac{2P^2}{Y_0^4}$, $\lambda_2 = \frac{2SQE_0}{X_0^3Y_0}$ and $\beta_2 = -\frac{2PQE_0}{X_0Y_0^3}$. Moreover, Fig. 3.5 shows the plot of the potential function given by Eq. (3.39). The figure presents a potential well of almost parabolic shape with a fairly steep slope. We note that a stable dynamical behavior can be obtained when considering values of nonlinear and magnetic field parameters (Q, S) around the bottom of the potential well. Consequently, a stable propagation of ion-acoustic wave can be achieved in the plasma. The time evolution of the solution parameters has been numerically investigated

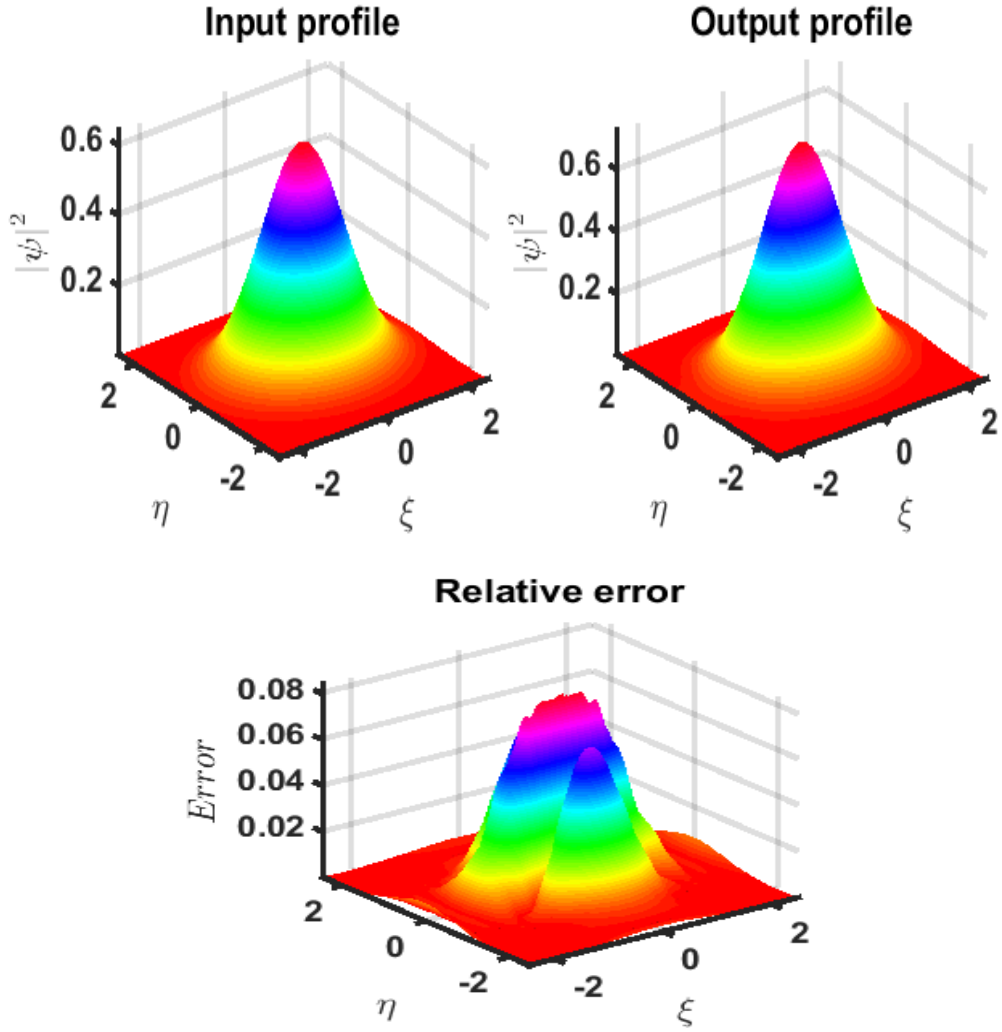


Figure 3.7: Exact solution (input profile) in left panel, numerical solution (output profile) in right panel and relative error in down panel of modified NLS Eq. (3.1).

using the fourth-order Runge-Kutta computational method, which allows to integrate the system of equations obtained through the variational approach. Panels of Fig. 3.6 show the evolution of the Gaussian parameters using Eq. (3.37) as a function of the direction of propagation τ : the amplitude $C(\tau)$, the spatial widths $X(\tau)$, $Y(\tau)$, the spatial chirps $a(\tau)$, $b(\tau)$ and the phase $\varphi(\tau)$ of the carrier wave. In this figure, when the amplitude $C(\tau)$ decreases, the spatial widths $X(\tau)$, $Y(\tau)$ increase, this leads to the fact that such wave can propagate in our plasma model. In order to confirm the results from the variational approach, we studied the system numerically using the Split Step Fourier Method (SSFM). For this numerical simulation, the solution obtained using the variational approach was used as the input solution. Fig. 3.7 presents the exact (input profile), numerical (output profile) solutions and relative error of Eq. (3.1). These two profiles are almost similar in

amplitude, but with a spatial spreading of soliton in the zone of modulational instability. Therefore, a good agreement between analytical and numerical results are observed. We can clearly see that the ion-acoustic wave can propagate through the plasma system maintain its profile. Basically, this arises under the interplay between dispersion and nonlinearity for the system parameters taken in the modulational instability zone.

3.2 Dynamics of propagation of ion-acoustic dromions in a magnetized ENP

3.2.1 Evolution of wave frequency of IAWs in the DS equations

The following partial differential equations (2.32) for a complex field (wave-amplitude ψ), and a real field, for a mean-flow ψ_2 obtained in the previous chapter

$$\begin{aligned} i \frac{\partial \psi_1}{\partial \tau} + \gamma_1 \frac{\partial^2 \psi_1}{\partial \xi^2} + \gamma_2 \frac{\partial^2 \psi_1}{\partial \eta^2} + (\gamma_3 |\psi_1|^2 + \gamma_4 \psi_2) \psi_1 &= 0, \\ \delta_1 \frac{\partial^2 \psi_2}{\partial \xi^2} + \frac{\partial^2 \psi_2}{\partial \eta^2} + \delta_2 \frac{\partial^2 |\psi_1|^2}{\partial \xi^2} + \delta_3 \frac{\partial^2 |\psi_1|^2}{\partial \eta^2} &= 0, \end{aligned} \quad (3.40)$$

are known as the DS equations [101] that couples a complex field, for the wave-amplitude ψ_1 , and a real field, for a mean-flow ψ_2 . Seminally, the DS equations was derived to describe nonlinear evolution of (2+1)-dimensional waves packets in water of finite depth [101]. The first equation this set of equations is called Potential equation and the second equation is Amplitude equation. We note that all the coefficients of theses equations are given in appendix (Eq. (61)). Specifically, DSEs were shown in Ref. [160] to arise in multi-dimensional plasmas under the assumption that ion waves were parallel to the magnetic field. In the context of the present thesis, one should notice that the different coefficients of DS equations (Eq. (3.40)) depend on the system parameters. This renders easier the evolution of the contribution of both nonlinear and dispersive effects to the emergence of nonlinear waves and solitons. In the meantime, it should be noted that the dispersion relation (Eq. (2.28)) and the group velocity v_g (Eq. (2.29)), respectively represented in Figs. 3.8(a) and 3.8(b), are very sensitive to the changes in the magnetic field reflected by Ω . In general, the frequency ω is an increasing function of the magnetic field, while the group velocity shows a reverse behavior. However, there has been little discussion on the effect of a magnetic field on the nonlinear evolution of ion-acoustic waves governed by the Davey-Stewartson equations.

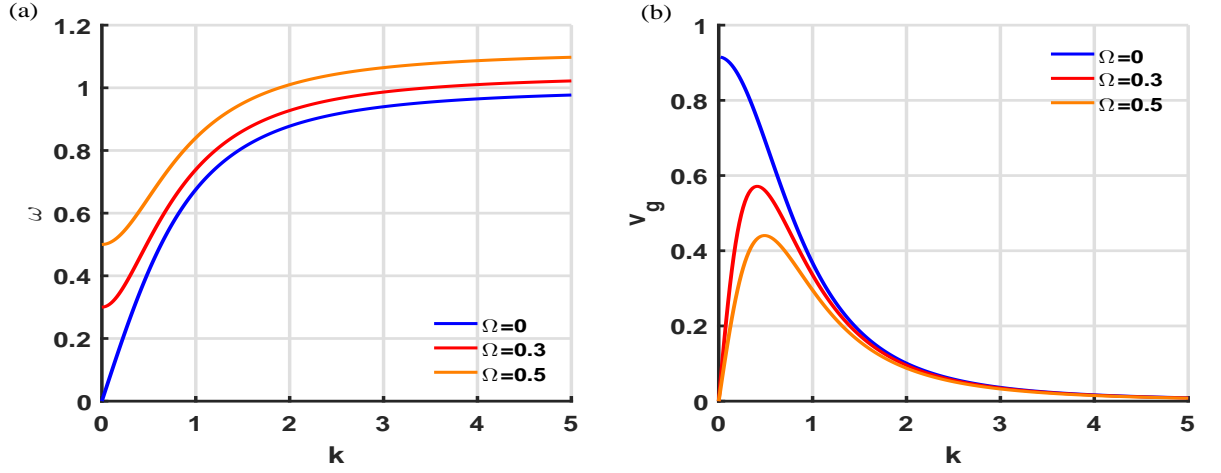


Figure 3.8: Panel (a) shows the variation of the wave frequency ω versus the wavenumber k , and panel (b) the variation of the group velocity, both under the changing effect of the magnetic field. The electron-to-negative ion temperature ratio σ_n and the negative-ion concentration ratio α take the respective values $\sigma_n = 2.5$ and $\alpha = 0.01$.

3.2.2 Modulational instability analysis of IAWs in the DS system

One of the direct mechanisms responsible for the formation of solitons in nonlinear media is MI. The latter occurs when a constant wave background becomes unstable and induces sinusoidal modulations under the competitive contribution of nonlinear and dispersive effects. Otherwise, under such effects, a plane wave solution breaks up into trains of solitonic objects. In this section, we consider the DS system (2.32) with the trial plane wave solutions [21, 168, 169]

$$\psi_1 = \psi_{10} e^{i(\alpha_1 \xi + \alpha_2 \eta - R\tau + \varphi)}, \quad \psi_2 = \psi_{20}, \quad (3.41)$$

where ψ_{10} , ψ_{20} , α_1 , α_2 and φ are real constants. Indubitably, such trial solutions will propagate in the system if the condition

$$R = \gamma_1 \alpha_1^2 + \gamma_2 \alpha_2^2 - \gamma_3 \psi_{10}^2 - \gamma_4 \psi_{20}, \quad (3.42)$$

is satisfied. Here, R obtained by substituting Eq. (3.41) in the DS system (3.40), is so-called linear dispersion relation or unperturbed dispersion relation. To further proceed, we study the stability of the plane wave solution by introducing small perturbations so that

$$\psi_1 = (\psi_{10} + \delta\psi_1) e^{i(\alpha_1 \xi + \alpha_2 \eta - R\tau + \varphi + \delta\varphi)}, \quad \psi_2 = \psi_{20} + \delta\psi_2, \quad (3.43)$$

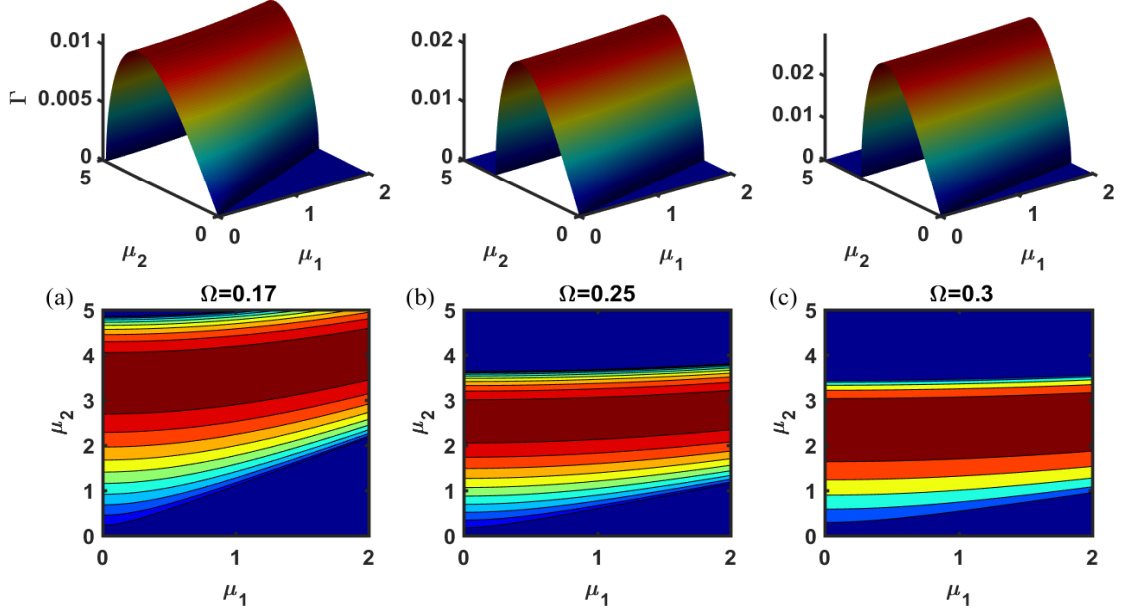


Figure 3.9: Panels show the MI growth rate in the (μ_1, μ_2) -plane for a fixed value of $\alpha = 0.2$ and the ion cyclotron frequency taking the values: (a) $\Omega = 0.17$, (b) $\Omega = 0.25$ and (c) $\Omega = 0.3$. The other parameters are: $\sigma_n = 20.5$, $k = 2.4$, $\alpha_1 = 2.5$, $\alpha_2 = 2.5$, $\psi_{10} = 0.06$, and $\psi_{20} = 0.025$.

where the small perturbations $\delta\psi_1$, $\delta\psi_2$ and $\delta\varphi$ are taken to be

$$\begin{pmatrix} \delta\psi_1 \\ \delta\psi_2 \\ \delta\varphi \end{pmatrix} = \begin{pmatrix} \Delta\psi_1 \\ \Delta\psi_2 \\ \Delta\varphi \end{pmatrix} \text{Re} \left(e^{i(\mu_1\xi + \mu_2\eta - \nu\tau)} \right), \quad (3.44)$$

with $\Delta\psi_1$, $\Delta\psi_2$, $\Delta\varphi$, μ_1 , μ_2 being real constants. Inserting Eqs. (3.43) and 3.44 into (3.40) and making use of the dispersion relation (3.42), we obtain a homogeneous system in $\Delta\psi_1$, $\Delta\psi_2$ and $\Delta\varphi$, which admits non-trivial solutions if its determinant is non-zero. This leads to the following nonlinear dispersion relation:

$$(N_D)^2 = (\gamma_1\mu_1^2 + \gamma_2\mu_2^2) \left(\gamma_1\mu_1^2 + \gamma_2\mu_2^2 - 2\gamma_3\psi_{10}^2 + 2\gamma_4\psi_{10}^2 \frac{\delta_2\mu_1^2 + \delta_3\mu_2^2}{\delta_1\mu_1^2 + \mu_2^2} \right), \quad (3.45)$$

where $N_D = \nu - 2\gamma_1\alpha_1\mu_1 - 2\gamma_2\alpha_2\mu_2$. The plane wave solutions (3.41) will be unstable if $N_D^2 < 0$, which amounts to the explicit condition

$$(\gamma_1\mu_1^2 + \gamma_2\mu_2^2)^2 \left(1 - 2\psi_{10}^2 \frac{\gamma_3(\delta_1\mu_1^2 + \mu_2^2) - \gamma_4(\delta_2\mu_1^2 + \delta_3\mu_2^2)}{(\gamma_1\mu_1^2 + \gamma_2\mu_2^2)(\delta_1\mu_1^2 + \mu_2^2)} \right) < 0. \quad (3.46)$$

Obviously, the stability/instability condition of the plane wave only depends on the terms $\left(1 - 2\psi_{10}^2 \frac{\gamma_3(\delta_1\mu_1^2 + \mu_2^2) - \gamma_4(\delta_2\mu_1^2 + \delta_3\mu_2^2)}{(\gamma_1\mu_1^2 + \gamma_2\mu_2^2)(\delta_1\mu_1^2 + \mu_2^2)} \right)$, which also fixes the threshold amplitude above which

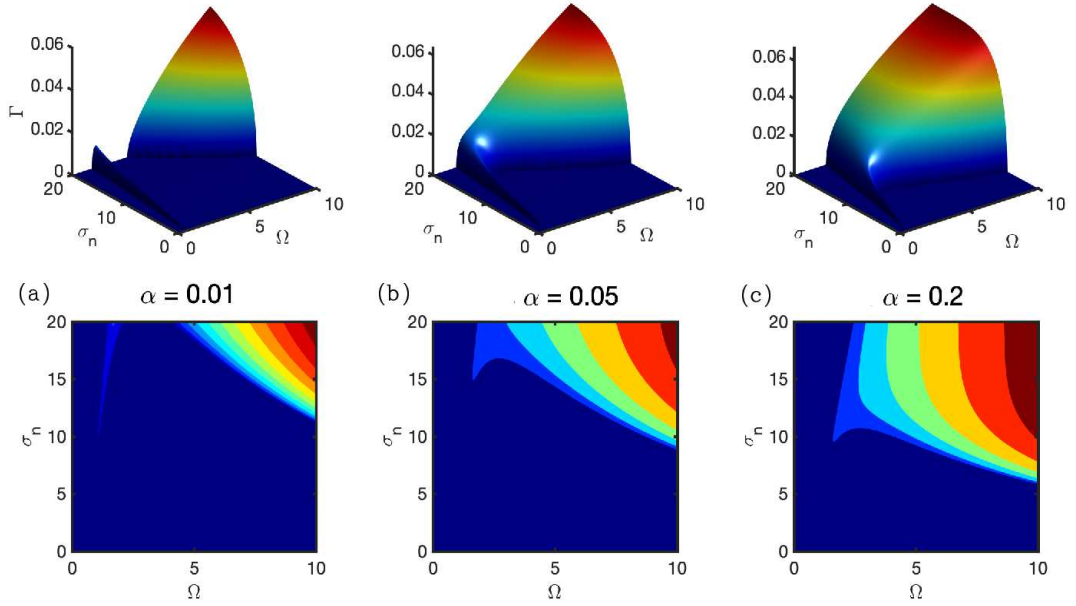


Figure 3.10: Panels show the growth rate of MI versus the electron-to-negative ion temperature ratio σ_n and the frequency Ω when the negative-ion concentration ratio α takes the respective values (a) $\alpha = 0.01$, (b) $\alpha = 0.05$ and (c) $\alpha = 0.2$, with the other parameter values being: $\sigma_n = 20.5$, $k = 2.4$, $\alpha_1 = 2.5$, $\alpha_2 = 2.5$, $\psi_{10} = 0.06$, and $\psi_{20} = 0.025$.

the plane wave is expected to break up into solitary structures, i.e.,

$$\psi_{10,cr}^2 = \frac{(\gamma_1 \mu_1^2 + \gamma_2 \mu_2^2)(\delta_1 \mu_1^2 + \mu_2^2)}{2\gamma_3(\delta_1 \mu_1^2 + \mu_2^2) - 2\gamma_4(\delta_2 \mu_1^2 + \delta_3 \mu_2^2)}. \quad (3.47)$$

For the above, one can deduce the MI growth rate $\Gamma = \sqrt{-N_D^2}$ that will be used in this section to characterize the emergence of unstable wave patterns in the magnetized ENP under study. It is, therefore, of high importance here to insist on the combined effects due to such parameters and the magnetic field. The panels of Fig. 3.9 show, for example, how changing the frequency Ω influences the instability domain. As it increases, one clearly notices a reduction of the zone of instability in the (μ_1, μ_2) -plane, with fixed values of the other control parameters $\sigma_n = 20.5$ and $\alpha = 0.01$. Recent contributions in 2D and 3D showed that the two later parameters could control ENP plasma instability. Under relativistic effects, the negative ion-electron concentration ratio and electron-to-negative ion temperature ratio were found to contribute to a suitable balance between nonlinear and dispersive effects for rogue waves to appear. At this point, one question arises: what could be the behaviors of the MI growth rate under the influence of changing α and σ_n ? Comprehensive answers to the previous question are given by the plots of Figs. 3.10-3.12. In Fig. 3.10, the MI growth rate takes place in the (Ω, σ_n) -plane with

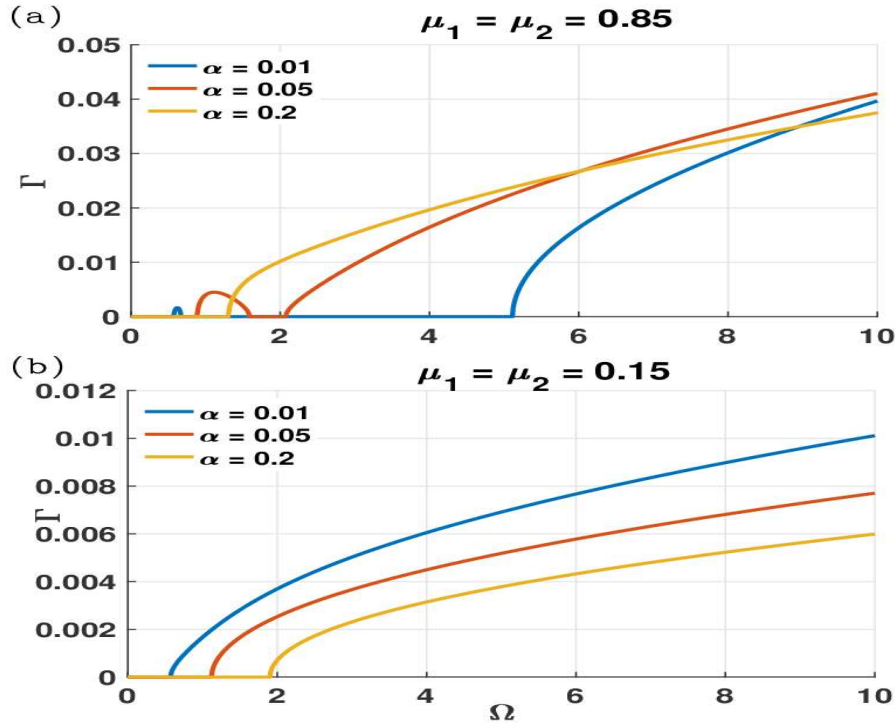


Figure 3.11: Panels show the growth rate of MI versus the frequency Ω for two sets of the wavenumbers (a) $\mu_1 = \mu_2 = 0.85$ and (b) $\mu_1 = \mu_2 = 0.15$. In each of the panels, the negative-ion concentration ratio α takes increasing values, while the other parameters are fixed as: $\sigma_n = 20.5$, $k = 2.4$, $\alpha_1 = 2.5$, $\alpha_2 = 2.5$, $\psi_{10} = 0.06$, and $\psi_{20} = 0.025$.

panels corresponding to different values of the negative ion concentration ratio. It is for example observed that for $\alpha = 0.01$, there are two regions of instability (see Fig. 3.10(a)) that merge with increasing α . Interestingly, most of the instability occurs for high values of σ_n , while instability is possible in a very restrained area of small magnetic field values. This is drastically modified for $\alpha = 0.05$ and 0.2 , where after merging, the common single region of instability expands. However, instability does not still occur for small values of the electron-to-negative-ion temperature ratio σ_n . However, the growth rate maximum takes place for high values of both σ_n and the magnetic field. In Fig. 3.11, for two sets of the wavenumber μ_1 and μ_2 , the effect of the negative-ion concentration ratio α on the MI growth rate appears clearly and concurs with the instability windows obtained in Fig. 3.10. Additional information on the appearance of instability due to the plasma parameters and the magnetic field is recorded in Fig. 3.12, this time in the (Ω, α) -plane with changing the electron-to-negative ion temperature ratio σ_n . Contrarily to the features of Fig. 3.10, there is only one region of instability for all values of σ_n .

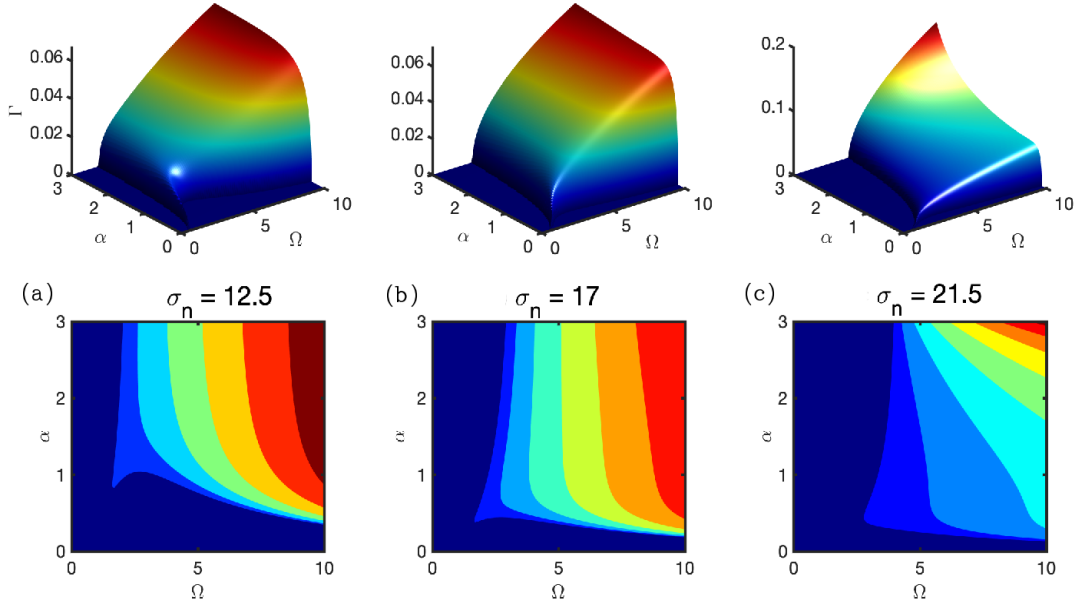


Figure 3.12: Panels show the MI growth rate versus the negative-ion concentration ratio α and the frequency Ω when the electron-to-negative ion temperature ratio takes the respective values: $\sigma_n = 12.5$, (b) $\sigma_n = 17$ and (c) $\sigma_n = 21.5$. The other parameter values are: $k = 2.4$, $\alpha_1 = 2.5$, $\alpha_2 = 2.5$, $\psi_{10} = 0.06$, and $\psi_{20} = 0.025$.

However, increasing the latter's value increasingly involves small values of α in the MI process. Nevertheless, the zone of instability gets reduced for high values of σ_n , even though the growth rate intensity increases. Indeed, such results confirm the existence of IAWs in the studied plasma system, especially in the presence of the magnetic field, which probably will contribute to the emergence of more complex patterns under the simultaneous effect of nonlinearity and dispersion. Therefore, when this is fulfilled, a random amplitude perturbation will grow, leading to the generation of IAWs. This is supported in the background by the physical information contained in the coefficients of the DS equations, which are functions of relevant plasma parameters as indicated by the above parametric analysis of MI. In such regions, exact solutions exist and can be obtained using different methods for different applications. In what follows, we propose solutions to the DS system (2.32) using Hirota's Bilinear method.

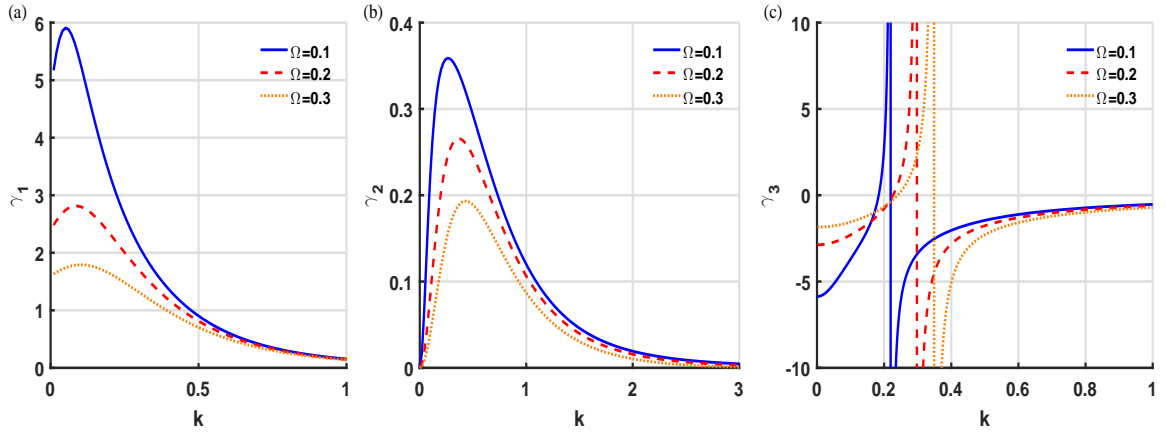


Figure 3.13: Panels show the plotted of γ_1 , γ_2 and γ_3 versus k (Eqs. (61b), (61d)) and (61e) for $\alpha = 0.01$, and $\sigma_n = 5.5$ and different values of Ω .

3.2.3 One- and two-dromion solutions of the Davey-Stewartson equations

During the last decades, the research on exact solutions for nonlinear evolution equations has attracted a lot of interests. In this regard, a collection of analytical methods for investigating exact solutions to nonlinear PDEs have been proposed, amongst which are the Backlund and Darboux transformation method [171], the inverse scattering method [170], the Hirota bilinear method [113, 166], pseudo-spectral method [172], the hyperbolic function method [173, 174], the homogeneous balance method and formal variable separation method [175–177], the generalized Riccati equation method [178] unified algebraic method and varied Jacobi elliptic function methods [179, 180]. Interestingly, The Hirota bilinear method [113, 166] has been used to construct dromions-like solutions to a system of equations similar to the DS system. More recently, Panguetna [21] used the Hirota’s bilinear method to obtain one- and two-dromion solutions for the DS system of equations. We should indicate that there exist types I and II DS equations depending on the sign of their coefficients [181, 182]. However, from the results of Sec. 3.1.2, one may obtain the two types of systems. It has been shown that the system of Eq. (3.40) may display DS-I behaviors if the conditions $\gamma_1/\gamma_2 > 0$ and $\gamma_3 > 0$ are satisfied [183, 184]. The Fig. 3.13 shows the parameters γ_1 , γ_2 and γ_3 versus k . For any $k > 0$, all the values of γ_1 and γ_2 are positives, $\gamma_3 > 0$ for DS-I, while $\gamma_3 < 0$ gives the DS-II equations. The solutions of Eq. (2.32) are exponentially localized and called dromions. Using the Hirota’s bilinear method, we will proceed to find the solutions of the system. Such solutions

are investigated by first studying their domain of existence. Therefore, we first rescale dependent and independent variables as follows:

$$\xi' = \frac{1}{(\delta_1\gamma_3 - \delta_2\gamma_4)^{1/2}}\xi, \quad \eta' = \frac{1}{(\delta_3\gamma_4 - \gamma_3)^{1/2}}\eta, \quad \psi = \gamma_3 |\psi_1|^2 + \gamma_4\psi_2. \quad (3.48)$$

We also introduce the following new independent variables through a coordinate axis rotation by 45° :

$$X = \frac{1}{\sqrt{2}}(\xi' + \eta'), \quad Y = \frac{1}{\sqrt{2}}(\xi' - \eta'). \quad (3.49)$$

Substituting the relations (3.48) and (3.49) into Eqs. (3.40), we obtain the following set of equations

$$i\psi_{1\tau} + a(\psi_{1XX} + \psi_{1YY}) + b\psi_{1XY} + \psi_1\psi = 0, \quad (3.50a)$$

$$c(\psi_{XX} + \psi_{YY}) + d\psi_{XY} = 2(|\psi_1|^2)_{XY}, \quad (3.50b)$$

where,

$$a = \frac{1}{2} \left(\frac{\gamma_1}{\delta_1\gamma_3 - \delta_2\gamma_4} + \frac{\gamma_2}{\delta_3\gamma_4 - \gamma_3} \right), \quad b = \frac{1}{2} \left(\frac{\gamma_1}{\delta_1\gamma_3 - \delta_2\gamma_4} - \frac{\gamma_2}{\delta_3\gamma_4 - \gamma_3} \right), \quad c = \frac{1}{2} \left(\frac{\delta_1}{\delta_1\gamma_3 - \delta_2\gamma_4} - \frac{1}{\delta_3\gamma_4 - \gamma_3} \right),$$

$$d = \frac{1}{2} \left(\frac{\delta_1}{\delta_1\gamma_3 - \delta_2\gamma_4} + \frac{1}{\delta_3\gamma_4 - \gamma_3} \right).$$

We note that the above constants depend on the magnetized electronegative plasma parameters such as Ω , σ_n and α . Solutions for system (3.50) are investigated by introducing the new dependent variables F (real) and G (complex) so that

$$\psi_1 = \sqrt{2bd} \left(\frac{G}{F} \right), \quad \text{and} \quad \psi = 2b(\ln f)_{XY}. \quad (3.51)$$

This leads to the bilinear form, with assumption

$$\frac{\gamma_1}{\delta_1\gamma_3 - \delta_2\gamma_4} = \frac{\gamma_2}{\gamma_3 - \delta_3\gamma_4}$$

$$(iD_\tau + a(D_{XX} + D_{YY}))(G \cdot F) = 0, \quad (3.52a)$$

$$D_{XY}F \cdot F = 4G \cdot G^*, \quad (3.52b)$$

where D is an operator defined by

$$D_x^n G \cdot F = (\partial_{x_1} - \partial_{x_2})^n F(x_1)G(x_2) \big|_{x_2=x_1=x}, \quad (3.53)$$

which is also known as the Hirota bilinear operator. We further expand the new variables

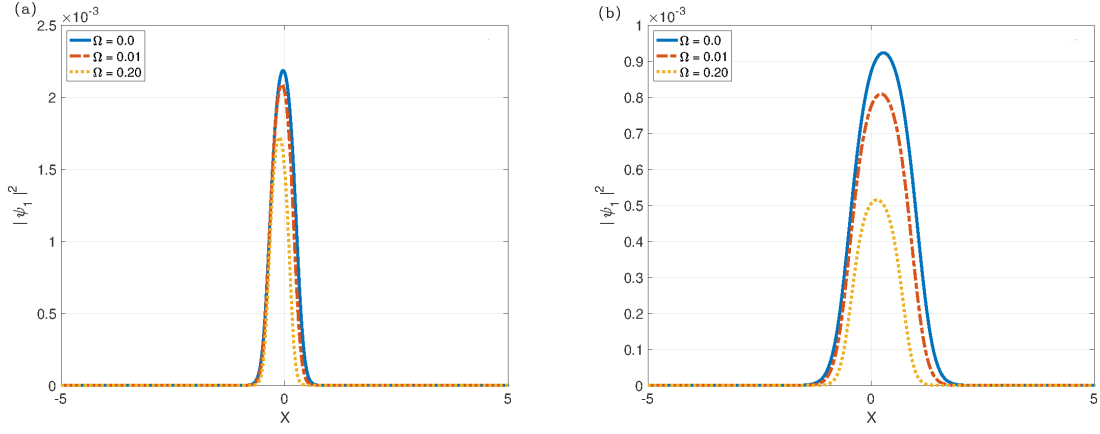


Figure 3.14: Panels show the behaviors of the one-dromion solution with increasing the magnetic field. For (a), the negative ion concentration ratio is fixed as $\alpha = 0.01$, while (b) corresponds to $\alpha = 0.08$, with Ω taking the increasing values 0, 0.01 and 0.2 in each of the panels. The other parameters are $\sigma_n = 5.5$, and $J = K = L = 1$.

F and G in the power series of small parameter δ as $G = \delta G_1 + \delta^3 G_3 + \dots$, and $F = 1 + \delta^2 F_2 + \delta^4 F_4 + \dots$ in order to obtain the dromion-like solutions [21, 183]. This is introduced into (3.52) to find G_1 , G_3 , F_2 and F_4 . Taking G_1 to be in the form

$$G_1 = \sum_{j=1}^N e^{\eta_j}, \quad \eta_j = p_j X + q_j Y + ia(p_j^2 + q_j^2)\tau + \eta_{0j}, \quad (3.54)$$

with p_j , q_j , and η_{0j} being the complex constants, the generalized form of one-dromion solution is obtained as

$$\psi_{11D} = \frac{G_{1D}}{F_{1D}} = \frac{\rho \exp(\eta_1 + \eta_2)}{\left\{ 1 + J \exp(\eta_1 + \eta_1^*) + K \exp(\eta_2 + \eta_2^*) + L \exp(\eta_1 + \eta_1^* + \eta_2 + \eta_2^*) \right\}},$$

$$\eta_1 = pX + iap^2\tau + \eta_{01}, \quad \eta_2 = qY + iaq^2\tau + \eta_{02}. \quad (3.55)$$

Moreover, in Eq. (3.55), J , K and L are real constants, $p = p_1$, $q = q_1$ and $|\rho|^2 = 2L(p + p^*)(q + q^*) = 8Lp_R q_R$.

It is interesting to see now if the presence of the magnetic field in the system impacts the structure and the propagation of the dromions in such a system. In Fig. 3.14, for example, the one-dromion solution is plotted versus X , with panels (a) and (b) corresponding, respectively to $\alpha = 0.01$ and $\alpha = 0.08$. In each of the cases, the solution decreases with increasing the value of the magnetic field, with the value $\Omega = 0$ corresponding to the unmagnetized plasma. On one hand, a behavior that was already obtained is the increase of the base width of the solution with increasing the negative-ion

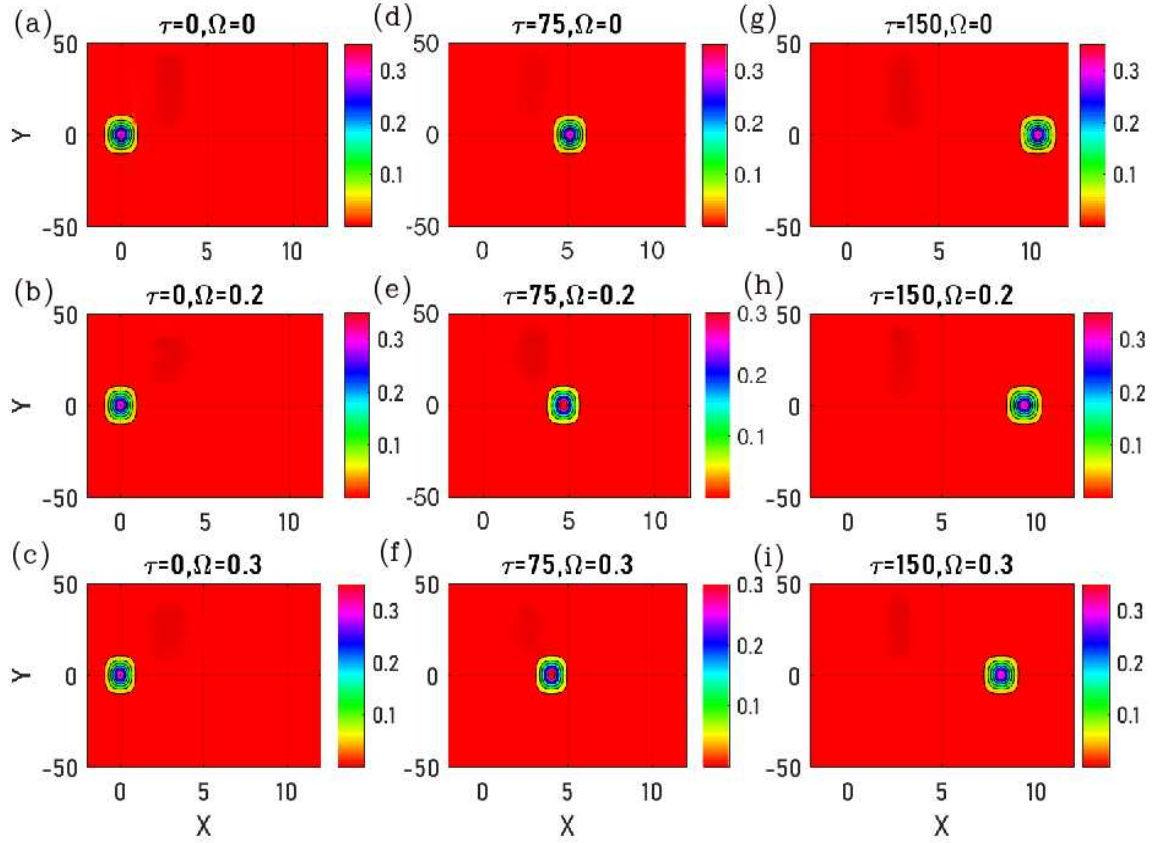


Figure 3.15: Panels show the propagation of one-dromion solutions (3.55) for increasing values of the magnetic field Ω and at different instants τ when $\alpha = 0.01$, $\sigma_n = 5.5$, and $J = K = L = 1$.

concentration ratio α . Additionally, the same base width gets decreased, together with the wave amplitude, when the strength of the magnetic field increases. In general, with increasing the magnetic field, dispersive effects get dominated by the nonlinearity effects leading to more spiky dromions in the studied plasma system. The panels of Fig. 3.15 show the propagation of the one-dromion solution of Eq. (3.40) for different values of the magnetic field at different instants. We observe that in the absence of the magnetic field, the dromion can propagate with speed v_g . The speed of propagation decreases when the value of the magnetic field increases. For example, at the instant $t = 150$, the peak of the dromion is at position $X = 9.4$ (see Fig. 3.15(c)) for $\Omega = 0.2$, while at the same instant and for $\Omega = 0.3$, the peak of the dromion is at position $X = 8.2$. Therefore, it is clear that the presence of the magnetic field has a slowing effect on the propagation of the dromion solution. Similarly, we can proceed and find the two-dromion solutions in the form

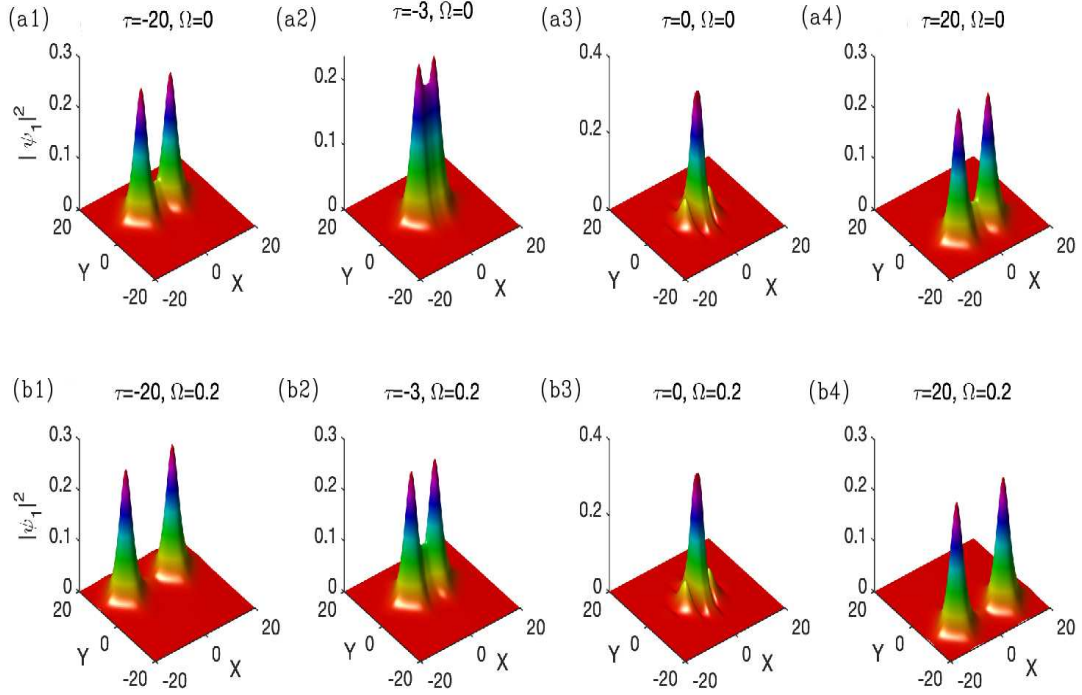


Figure 3.16: Panels show elastic collision of the two-dromion solution (3.56) in a moving frame, where panels (a)_{j=1,2,3,4} display results in the absence of the magnetic field ($\Omega = 0$) and panels (b)_{j=1,2,3,4} show results in the presence of the magnetic field. In the process, two identical dromions interact and keep their shapes after collision. However, the presence of the magnetic field accelerates such a collision, with the other parameters being $\alpha = 0.01$, $\sigma_n = 20.5$, and $A = B = C = D = E = F = G = H = I = 1$.

$$\psi_{12D} = \frac{G_{2D}}{F_{2D}} = \frac{\left\{ \begin{aligned} &\rho_{11} \exp(\eta_1 + \eta_3) + \rho_{12} \exp(\eta_2 + \eta_3) + \rho_{21} \exp(\eta_1 + \eta_1^* + \eta_2 + \eta_3) \\ &+ \rho_{22} \exp(\eta_1 + \eta_2 + \eta_2^* + \eta_3) \end{aligned} \right\}}{\left\{ \begin{aligned} &1 + A \exp(\eta_1 + \eta_1^*) + B \exp(\eta_2 + \eta_2^*) + C \exp(\eta_3 + \eta_3^*) \\ &+ D [\exp(\eta_1 + \eta_2^*) + \exp(\eta_2 + \eta_1^*)] \\ &+ E [\exp(\eta_1 + \eta_2^* + \eta_3 + \eta_3^*) + \exp(\eta_2 + \eta_1^* + \eta_3 + \eta_3^*)] \\ &+ F \exp(\eta_1 + \eta_1^* + \eta_2 + \eta_2^*) + G \exp(\eta_2 + \eta_2^* + \eta_3 + \eta_3^*) \\ &+ H \exp(\eta_1 + \eta_1^* + \eta_3 + \eta_3^*) + I \exp(\eta_1 + \eta_1^* + \eta_2 + \eta_2^* + \eta_3 + \eta_3^*) \end{aligned} \right\}},$$

$$\eta_1 = p_1 X + i a p_1^2 \tau + \eta_{01}, \quad \eta_2 = p_2 X + i a p_2^2 \tau + \eta_{02}, \quad \eta_3 = q_1 Y + i a q_1^2 \tau + \eta_{03},$$

(3.56)

where A, B, C, D, E, F, G, H and I are real, positive constants.

The panels of Fig. 3.16 show the evolution of two dromions solutions and their elastic

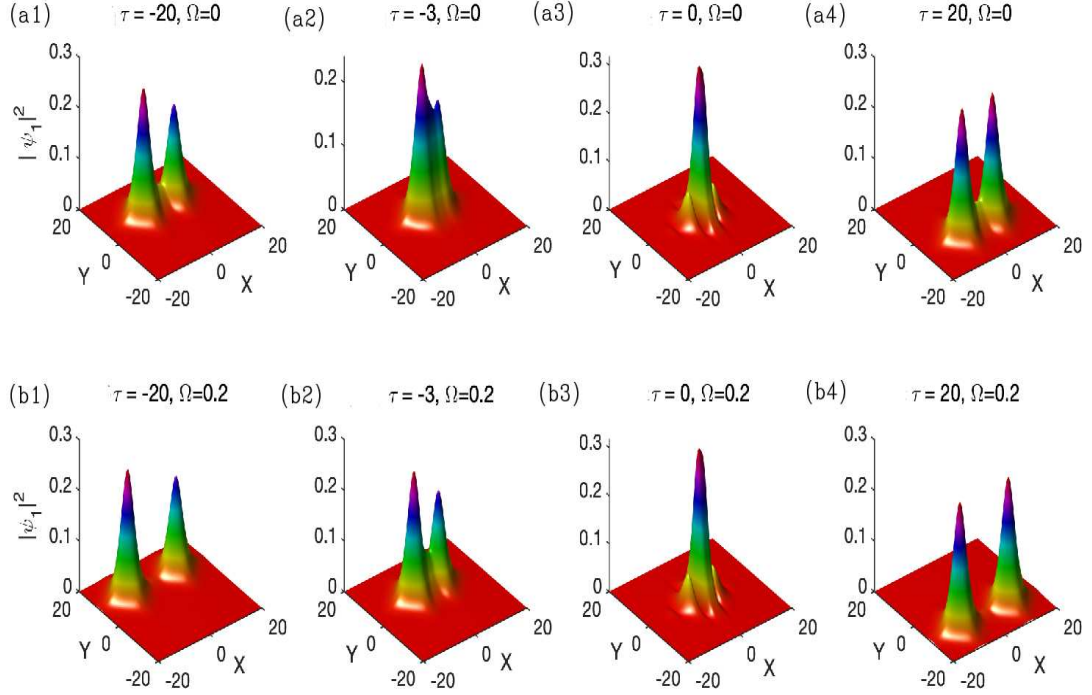


Figure 3.17: Panels show elastic collision of two dromions with energy exchange both in absence (panels (a)_{j=1,2,3,4}) and in presence (panels (b)_{j=1,2,3,4}) of the magnetic field. The colliding objects involve two dromions of different amplitudes which, after collision, give rise to entities with equal amplitudes. The parameters are $\alpha = 0.01$, $\sigma_n = 20.5$, and $A = B = C = D = E = F = G = H = I = 1$.

collision in the absence and presence of the magnetic field. Obviously, in the absence of the magnetic field, the collision happens with a delay [see Fig. 3.16(a)_{j=1,2,3,4}], while in the presence of the magnetic field, the collision process is accelerated [see Fig. 3.16(b)_{j=1,2,3,4}]. However, in the two cases, the colliding objects keep their initial characteristics after the collision, implying no energy exchange. Nevertheless, it should be indicated that when two dromions interact, there might be energy exchange which may affect their amplitude and some other characteristics [21, 205]. This is for example the case in Fig. 3.17, where the two dromions of unequal amplitudes collide, share energies, and end up displaying the same features. The dromion with the highest amplitude has shared its energy with the small dromion, which resulted in identical objects under elastic collision. We notice that even in this context, the impact of the magnetic field in the collision process, similar to what was already discussed in Fig. 3.16. Another possibility in the process of wave collision is that the colliding entities merge into one, a phenomenon that is also known as an inelastic collision. This is depicted in Fig. 3.18, where initially, there are two dromions of different

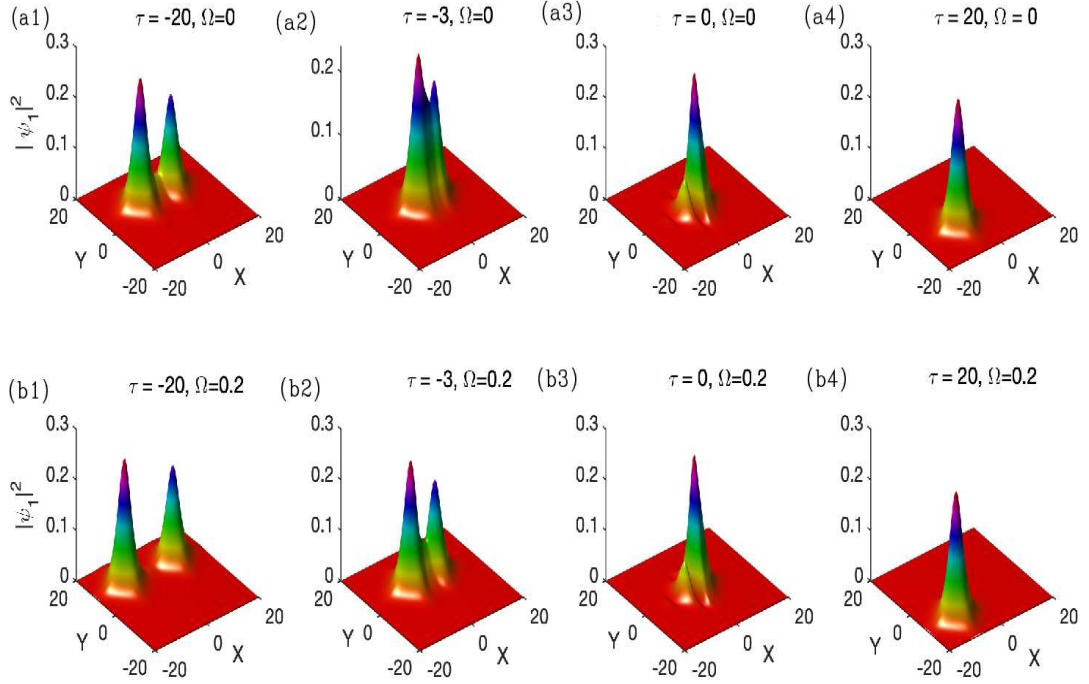


Figure 3.18: Panels show inelastic collision of two dromions both in absence (panels (a)_{j=1,2,3,4}) and in presence (panels (b)_{j=1,2,3,4}) of the magnetic field. In both cases, the dromions after collision combine and give rise to one soliton, but the presence of the magnetic field accelerates such a process. The parameters are $\alpha = 0.01$, $\sigma_n = 20.5$, and $A = B = C = D = E = F = G = H = I = 1$.

amplitudes that interact and form a single solitonic object. This particular case is typical in plasma systems where several components are involved, which is useful in producing plasma particles in a process known as energy recombination. This is inherently facilitated by the presence of different dynamical modes [206, 207]. However, the results obtained here confirm that such the recombination process is accelerated by the magnetic field, which enhances the collision process. Many other scenarios can be explored, especially when plasma parameters change, as was already reported by Panguetna et al. [21] who showed that dromions and their interactions were very sensitive to changes in the electron-to-negative-ion temperature ratio and the negative-ion concentration ratio. Some other contributions also introduced the modulation angle, an important factor to be included when three-dimensional components are involved, a scenario that may enrich the features inherent to the presence of the magnetic field applied to two-negative ion plasmas such as $\text{Xe}^+ - \text{F}^- - \text{SF}_6^-$ and $\text{Ar}^+ - \text{F}^- - \text{SF}_6^-$, for example.

Conclusion

This chapter was devoted to the presentation of the main results and discussion of this thesis. These results concern the $(2+1)$ -dimensional modulated nonlinear ion-acoustic soliton packets and two-dimensional dynamics of ion-acoustic dromions, both in magnetized electronegative plasma. We have presented the influence of MI in NLS equation. The variational approach involving trial functions to describe the main characteristics of pulse evolution has been investigated. Numerically, the exact solution (input profile) and numerical solution (output profile) have been also discussed. Moreover, the MI analysis has been performed in DS equations. Results are presented based on the competitive effects between the magnetic field and the other essential system parameters, namely the electron-to-negative-ion temperature ratio and the negative-ion concentration ratio. Dromion-like solutions for the DS equations have also discussed along with their response to the change of parameters. As some previous theoretical studies conducted in electronegative plasma, the present work has also the potential to enhance in the real world, several applications across various fields such as plasma etching (dry etching) or thin film deposition, ion implantation (semiconductor doping), surface treatment (cleaning of surfaces by sputtering), and fabrication of semiconductor devices [58,138–140]. Moreover, the performance of these processes can be improved by confining the plasma and increasing the reaction rate due to the presence of the magnetic field.

♣ General conclusion ♣

Summary and Contributions

In this thesis, we have investigated the dynamics of propagation of $(2+1)$ -dimensional nonlinear ion-acoustic solitons and dromions in magnetized electronegative plasma made of a significant number of negative ions, with electrons both in Boltzmann distribution, cold mobile positive ions and the external magnetic field. Specific analytical and numerical analysis methods have been formulated to evaluate the response of the system. In our contribution, we have started with the system of four equations namely: continuity equation, momentum equation and Poisson's equation describing the response of the nonlinear medium to the ion-acoustic wave. Then we have reported on the derivation of the $(2+1)$ -dimensional NLS equation on the one hand and DS equations on the other hand by using the standard reductive perturbation method. To understand the process of the emergence and propagation of IAWs in such system, it was necessary to explain in detail the different notions that we have used in our investigations. The main results obtained in this work are summarized as follows:

In chapter I, we have presented the literature review on the generalities related plasma theory and some of their useful properties and characteristics. We have also discussed the plasma fluid models with emphasis on magnetized ENPs that have been the starting-point for studying plasmas dynamics.

In chapter II, we have derived the model description of the governing equations for the propagation of ion-acoustic waves along the external magnetic field in an electronegative plasma by using the reductive perturbation method. We have also presented the analytical and numerical method used along the thesis.

In chapter III, we have presented and discussed the results reported in this thesis concerning $(2+1)$ -dimensional modulated nonlinear ion-acoustic soliton packets and two-dimensional dynamics of ion-acoustic dromions, both in magnetized electronegative plasma.

We have also investigated analytically and numerically the modulational instability of in nonlinear media. Indeed, in the case of the NLS equation, the modulational instability of planes waves has been investigated based on the magnetic field, the negative ion concentration ratio and the electron-to-negative temperature ratio. The effect of increasing values of α and σ_n is to increase the modulational instability growth rate with cutoffs at higher wave numbers of modulation of different values of the magnetic field. Therefore, it comes that this plasma system can support propagation of ion-acoustic solitons as informations carrier. The variational method has been performed in order to describe the main characteristics of IAWs, involving trial function solution of NLS equation. It shows that when the amplitude $C(\tau)$ decreases, the spatial widths $X(\tau)$, $Y(\tau)$ increase, this leads to the fact that such wave can propagate in our plasma model. In addition, the exact solution (input profile) and numerical solution (output profile) have been also discussed. These solutions have been investigated and the emergence and propagation of stable ion-acoustic wave have been confirmed in electronegative plasma in the presence of the external magnetic field.

In the case of DS equation, the linear stability analysis of MI has been adopted to discuss the existence of solitonic-like structures. The MI growth rate behaviors have mainly been discussed based on the system parameters. Principally the joined effects of the electron-to-negative ion temperature ratio σ_n and the negative-ion concentration ratio α have been confronted to the change in the external magnetic field to show that MI can take place in some interval of such parameters under the suitable balance between nonlinear and dispersive effects. Under specific conditions, we have shown, using the bilinear Hirota method, that the solutions for the derived DS equation can be found as one- and two-dromion ion-acoustic solutions. The combined effects of various physical parameters such as the electron-to-negative-ion temperature ratio, the negative-ion concentration ratio, and the strength of magnetic field have been studied on the existence regions and propagation properties of ion-acoustic dromions. We have noted that the shape of the obtained solutions depends both on the system parameters and the magnetic field. Increasing the values of the magnetic field magnitude has generated solitonic profiles such as dromions-like shapes. The parametric analysis has been extended to two-dromion dynamics under different interaction scenarios. We have noticed the strong impact of the magnetic field on the energy exchange and recombination processes.

The current findings are useful for understanding the propagation characteristics of ion-acoustic solitons in the magnetized electronegative plasma. This present work can be

useful in various fields such as plasma etching, surface treatment, ion implantation, and fabrication of semiconductor devices.

Open problems and future directions

Although very significant results on the impact of the electronegative plasma parameters and the magnetic field have been obtained in this present work, possible development may be done in near future:

- In this present work, we considered in the case of the $(2+1)$ -dimensional plasma analysis. However, we believe that the extension of this analysis to $(3+1)$ -dimensional space will make it possible to better appreciate the impact of the electronegative parameters and the magnetic field on the emergence and propagation of ion-acoustic waves.
- Future research should be devote to the development of a magnetized electronegative plasma model, in the case of magnetized dusty electronegative plasma.
- More suitable electronegative plasma environments with multi-compenents in the non-relativistic and the relativistic context should be extended to include the external magnetic field.
- Since the ion or electron acoustic waves in plasmas are strongly influenced by electronegative parameters the magnetic field, it is interesting to analyze the behavior of these waves in one or more dimensional unmagnetized plasma by considering other distribution than the boltzmann distribution.

♣ Appendix ♣

.1 Various coefficients

The coefficients appearing in various equations are defined as follows

$$\begin{aligned}
\beta_1 &= \omega^2(k^2 + a_1) - k_z^2, & \beta_2 &= \omega^2(4k^2 + a_1) - k_z^2, \\
u_{x\phi} &= \frac{\beta_1}{k_x\omega}, & u_{z\phi} &= \frac{k_z}{\omega}, & u_{y\phi} &= -\frac{i\beta_1\Omega}{k_x\omega^2}, \\
u_{x\xi} &= -\frac{2\omega}{k^2 + a_1} + \frac{\beta_1}{k_x^2\omega(k^2 + a_1)} - \frac{\beta_2 v_{gx}}{k_x\omega^2(k^2 + a_1)}, \\
u_{x\eta} &= -\frac{2k_z\omega}{k_x(k^2 + a_1)} + \frac{2k_z}{k_x\omega(k^2 + a_1)} - \frac{\beta_2 v_{gz}}{k_x\omega^2(k^2 + a_1)}, \\
u_{y\xi} &= -\frac{2\Omega}{k^2 + a_1} + \frac{\beta_1\Omega}{k_x^2\omega^2(k^2 + a_1)} - \frac{2k_z^2\Omega v_{gx}}{k_x\omega^3(k^2 + a_1)}, \\
u_{z\xi} &= \frac{k_z v_{gx}}{\omega^2(k^2 + a_1)}, & u_{z\eta} &= -\frac{1}{\omega(k^2 + a_1)} \left(v_{gz} \frac{k_z}{\omega} - 1 \right),
\end{aligned} \tag{57}$$

$$\begin{aligned}
\alpha_\phi &= \frac{\left\{ (4\omega^2 - \Omega^2)(2(k^2 + a_1)^2\omega^2 + k_z^2(k^2 + a_1) - 2a_2\omega^2) \right.}{2(k^2 + a_1)^2(\beta_2(4\omega^2 - \Omega^2) - 4k_x^2\omega^2)}, \\
&\quad \left. + 2\beta_1(k^2 + a_1)(2\omega^2 + \Omega^2) \right\} \\
\alpha_n &= (4k^2 + a_1)\alpha_\phi + \frac{a_2}{(k^2 + a_1)^2}, & \alpha_{u_x} &= \frac{\omega}{k_x}(\alpha_n - 1) - \frac{k_z}{k_x}\alpha_{u_z}, \\
\alpha_{u_y} &= -\frac{\Omega}{2\omega}(\alpha_{u_x} - \frac{\beta_1}{k_x\omega(k^2 + a_1)}), & \alpha_{u_z} &= \frac{k_z}{\omega}\alpha_\phi + \frac{k_z}{2\omega(k^2 + a_1)}.
\end{aligned} \tag{58}$$

.2 Equations and other coefficients

The third-order (ε^3) reduced equations for $l = 0$ are obtained as set of couple equations

$$\begin{aligned}
-v_{gx} \frac{\partial \phi_0^{(2)}}{\partial \xi} - v_{gz} \frac{\partial \phi_0^{(2)}}{\partial \eta} + \frac{\partial u_{z0}^{(2)}}{\partial \eta} &= A_\xi \frac{\partial |n_1^{(1)}|^2}{\partial \xi} + A_\eta \frac{\partial |n_1^{(1)}|^2}{\partial \eta}, \\
-v_{gx} \frac{\partial u_{z0}^{(2)}}{\partial \xi} - v_{gz} \frac{\partial u_{z0}^{(2)}}{\partial \eta} + \frac{\partial \phi_0^{(2)}}{\partial \eta} &= B_\xi \frac{\partial |n_1^{(1)}|^2}{\partial \xi} + B_\eta \frac{\partial |n_1^{(1)}|^2}{\partial \eta},
\end{aligned} \tag{59}$$

where $A_\xi = \frac{2v_{gx}a_2}{(k^2+a_1)^2}$, $B_\eta = \frac{1}{(k^2+a_1)^2} \left[\frac{\beta_1}{\omega^2} - \frac{3k_z^2}{\omega^2} + 2k_z^2 + \frac{k_z v_{gz}}{\omega^3} (\beta_2 - \beta_1) \right]$,
 $A_\eta = \frac{2v_{gz}a_2}{(k^2+a_1)^2} - \frac{2k_z}{\omega(k^2+a_1)}$, $B_\xi = \frac{2}{(k^2+a_1)^2} \left[-\frac{k_z\beta_1}{k_x\omega^2} + k_x k_z + \frac{k_z v_{gz}}{2\omega^3(k^2+a_1)^2} (\beta_1 + \beta_2) \right]$.

The coefficients of Eq. 2.30 are as follows

$$\begin{aligned} \delta_1 &= -v_{gx}^2 a_1, & \delta_{\xi\eta} &= -2v_{gx}v_{gz}a_1, & \delta_\eta &= 1 - v_{gz}^2 a_1, & \delta_2 &= -v_{gx}A_\xi, \\ \delta_{23} &= -v_{gx}A_\eta - v_{gz}A_\xi - B_\xi, & \delta_3 &= -v_{gz}A_\eta + B_\eta. \end{aligned} \quad (60)$$

.3 Coefficients of DSEs

The coefficients of Eq. (2.31) are as follows

$$\gamma_\tau = \frac{2}{\omega} (\Omega^4(k^2 + a_1) + k_z^2 \Omega^2), \quad (61a)$$

$$\gamma_1 = \frac{1}{\gamma_\tau} \left[\begin{array}{c} v_{gx} \left(\begin{array}{c} -2k_x\omega(\omega^2 - \Omega^2) + k_x\omega^2(k^2 + a_1)u_{x\xi} + k_x\omega\Omega(k^2 + a_1)u_{y\xi} \\ + k_z(\omega^2 - \Omega^2)(k^2 + a_1)u_{z\xi} \end{array} \right) \\ -\omega(\omega^2 - \Omega^2)(k^2 + a_1)u_{z\xi} - \omega^2(\omega^2 - \Omega^2) \end{array} \right], \quad (61b)$$

$$\gamma_{12} = \frac{1}{\gamma_\tau} \left[\begin{array}{c} -2\omega(\omega^2 - \Omega^2)(k^2 + a_1)(k_z v_{gx} + k_x v_{gz}) - \omega(\omega^2 - \Omega^2)(k^2 + a_1)(u_{x\eta} \\ + u_{z\xi}) + k_x\omega^2(k^2 + a_1)(v_{gx}u_{x\eta} + v_{gz}u_{x\xi}) + k_x\omega\Omega(k^2 + a_1)(v_{gx}u_{y\eta} \\ + v_{gz}u_{x\xi}) + k_z(\omega^2 - \Omega^2)(k^2 + a_1)(v_{gx}u_{z\eta} + v_{gz}u_{z\xi}) \end{array} \right], \quad (61c)$$

$$\gamma_2 = \frac{1}{\gamma_\tau} \left[\begin{array}{c} v_{gz} \left(\begin{array}{c} -2k_z\omega(\omega^2 - \Omega^2) + k_x\omega^2(k^2 + a_1)u_{x\eta} + k_x\omega\Omega(k^2 + a_1)u_{y\eta} \\ + k_z(\omega^2 - \Omega^2)(k^2 + a_1)u_{z\eta} \end{array} \right) \\ -\omega(\omega^2 - \Omega^2)(k^2 + a_1)u_{z\eta} - \omega^2(\omega^2 - \Omega^2) \end{array} \right], \quad (61d)$$

$$\gamma_3 = \frac{1}{\gamma_\tau} \left[\begin{array}{c} -\omega(\omega^2 - \Omega^2) \left(\begin{array}{c} (k^2 + a_1)(k_x\alpha_{u_x} + k_z\alpha_{u_z}) \\ + \frac{1}{\omega} (\alpha_n(\beta_1 + k_z^2) - 2\beta_1) + \frac{a_2}{\omega(k^2+a_1)} (2\beta_1 + k_z^2) \end{array} \right) \\ + k_x\omega^2 \left(\alpha_{u_x} \left(\frac{2k_z^2\Omega}{\omega} - \frac{\beta_1}{\omega} \right) + \frac{\beta_1\alpha_{u_z}}{\omega} + \frac{2\beta_1^2}{k_x\omega^2(k^2+a_1)} \right) \\ + k_x\omega\Omega \left(\begin{array}{c} -2\alpha_{u_y} \left(\frac{\beta_1\Omega}{\omega} + \frac{k_z^2}{\omega} \right) + \frac{\beta_1\Omega\alpha_{u_x}}{\omega^2} + \frac{2\Omega\beta_1^2}{k_x\omega^3(k^2+a_1)} \\ + \frac{k_z\beta_1\Omega\alpha_{u_z}}{k_x\omega^2} \end{array} \right) \\ + k_z(\omega^2 - \Omega^2) \left(-\alpha_{u_z} \left(\frac{2\beta_1}{\omega} + \frac{k_z^2}{\omega} \right) + \frac{2k_z\beta_1}{\omega^2(k^2+a_1)} + \frac{k_x k_z \alpha_{u_x}}{\omega} \right) \\ + \omega^2(\omega^2 - \Omega^2) \left(2a_2\alpha_\phi - \frac{3a_3}{(k^2+a_1)^2} \right) \end{array} \right], \quad (61e)$$

$$\gamma_4 = -\frac{(\omega^2 - \Omega^2)}{\gamma_\tau} (2k_z\omega v_{gz} - 1 + 2a_2\omega^2). \quad (61f)$$

♣ Bibliography ♣

- [1] A. P. Misra and C. Bhowmik, *Physics of Plasmas* **14**, 012309 (2007).
- [2] A. P. Misra, C. Bhowmik and P. K. Shukla, *Physics of Plasmas* **16**, 1072116 (2009).
- [3] A. Saha and S. Banerjee, Dynamical systems and nonlinear waves in plasmas, *CRC Press*, (2021).
- [4] S. Ali, W. M. Moslem, P. K. Shukla and R. Schlickeiser, *Phys. Plasmas* **14**, 082307 (2007).
- [5] I. Paul, A. Chatterjee and S. N. Paul, *Las. Part. beams* **37**, 378-380 (2019).
- [6] X.-W. Cheng, Z.-G. Zhang and H.-W. Yang, *Chin. Phys. B* **29**, 124501 (2020).
- [7] K. N. Ostrikov, S. Kumar and H. Sugai, *Phys. Plasmas* **7**, 3490 (2001).
- [8] M. Djebli, *Phys. Plasmas* **10**, 4910 (2003).
- [9] A. A. Marmun and P. K. Shukla, *Phys. Plasmas* **10**, 1518 (2003).
- [10] K. A. Islam, F. Deebea and Md. Kamal-Al-Hassan, *Heliyon* **6**, (2020) e05373.
- [11] M. R. Hassan, S. Biswas, K. Habib and S. Sultana, *Results in Physics* **33**, (2022) 105106.
- [12] N. Shahmohammadi and D. Dorrnian, *Contrib. Plasma Phys.* **55**, 643-657 (2015).
- [13] K. Annou and R. Annou, *Phys. Plasmas* **19**, 043705 (2012).
- [14] J.-C. Sun, Z.-G. Zhang, H.-H. Dong and H.-W. Yang, *Commun. Theor. Phys.* **72**, 125001 (2020)

- [15] A. Mushtaq, R. Saeed and Q. Haque, *Phys. Plasmas* **16**, 084501 (2009).
- [16] A. P. Misra, *Phys. Plasmas* **16**, 033702 (2009).
- [17] M. Kono, J. Vranjes, and N. Batool, *Phys. Rev. Lett.* **112**, 105001 (2014).
- [18] S. Guo and L. Mei, *Phys. Plasmas* **21**, 082303 (2014).
- [19] S. Jahan, R. K. Shikha, A. Mannan and A. A. Mamun, *Plasma* **5**, 1-11 (2021).
- [20] Z. X. Wang, J. Y. Liu, X. Zou, Y. Liu and X. G. Wang, *Chin. Phys. Lett.* **20**, 1537 (2003).
- [21] C. S. Panguetna, C. B. Tabi and T. C. Kofané, *Physics of Plasmas* **24**, 092114 (2017).
- [22] C. S. Panguetna, C. B. Tabi and T. C. Kofané, *Commun. Nonl. Sci. Numer. Simulat.* **55**, 326 (2018).
- [23] C. S. Panguetna, C. B. Tabi and T. C. Kofané, *J. Theor. Appl. Phys.* **13** (3), 237-249 (2019).
- [24] X. Zou, J. Y. Liu, Z. X. Wang, Y. Gong, Y. Liu and X. G. Wang, *Chin. Phys. Lett.* **21**, 1572 (2004).
- [25] X. Zou, H.-P. Liu and X. S. Hang, *Chin. Phys. Lett.* **28**, 125201 (2011).
- [26] M. Aslaninejad and K. Yasserian, *Phys. Plasmas* **19**, 033504 (2012).
- [27] S. K. El-Labany, E. F. El-Shamy and E. E. Behery, *Phys. Plasmas* **20**, 122114 (2013).
- [28] A. Aanesland, J. Bredin and P. Chabert, *Plasma Sources Sci. Technol.* **23**, 044003 (2014).
- [29] O. Rahman and M. M. Haider, *Theoretical Phys.* **4** (2), 47-56 (2019).
- [30] S. K. El-Labany, E. E. Behery, H. N. A. El-Razek and L. A. Abdelrazek, *Eur. Phys. J. D* **74**, 104 (2020).
- [31] J.-J. Li, J. X. Ma and Z.-A. Wei, *Phys. Plasmas* **20**, 063503 (2013).
- [32] K. Yasserian and M. Aslaninejad, *J. Theor. Appl. Phys.* **13**, 251261 (2019).

- [33] R. Paul, S. Adhikari, R. Moulick, S. S. Kausik and B. K. Saikia, *Phys. Plasmas* **27**, 063520 (2020).
- [34] L. Wang, M. Vass, Z. Donko, P. Hartmann, A. Dersi, Y.-H. Song and J. Schulze, *Plasmas Sources Sci. Technol.* **31**, 06LT01 (2022).
- [35] M. A. Akbar, Md. Abdus Salam and M. Zulfikar Ali, *Results in Physics* **51**, 106682 (2023).
- [36] I. Langmuir, *Proc. Nat. Acad. Sci.* **14** , 627-637 (1928).
- [37] F. F. Chen, Introduction to Plasma Physics and controlled fusion, (*Springer International Publishing*, Third Edition, 2016).
- [38] P. Chatterjee, K. Roy and U. N. Ghosh, Waves and Wave Interaction in Plasmas, *World Scientific* (India, 2022).
- [39] S. V. Vladimirov, K. Ostrikov, M. Y. Yu and G. E. Morfill, *Phys. Rev. E* **67**, 036406 (2003).
- [40] T.-L. Liu, Y.-L. Wang and Y.-Z. Lu, *Chin. Phys. B* **24**, 025202 (2015).
- [41] M. M. Selim, *Eur. Phys. J. Plus* **131**, 93 (2016).
- [42] N. A. Chowdhury, A. Mannan, M. M. Hasan and A. A. Mamun, *Chaos* **27**, 093105 (2017).
- [43] O. Rahman, A. Mamun and K. S. Ashrafi, *Astrophys. Space. Sci.* **335**, 425-433 (2011).
- [44] H. Massey, Negative Ions, 3rd ed., *Cambridge University Press*, Cambridge, UK (1976).
- [45] S. Khondaker, A. Mannan, N. A. Chowdhury and A. A. Mamun, *Contrib. Plasma Phys.* **59**, e201800125 (2019).
- [46] M. K. Mishra, A. K. Arora and R. S. Chhabra, *Phys. Rev. E* **66**, 046402 (2002).
- [47] M. K. Mishra, R. S. Chhabra and S. R. Sharma, *Phys. Rev. E* **51**, 4790 (1995).
- [48] A. Pedersen, *Tellus* **17**, 02 (1965).
- [49] R. Sabry, W. M. Moslem, P. K. Shukla, *Phys. Plasmas* **16**, 032302 (2009).

- [50] H. G. Abdelwahed, E. K. El-Shewy, M. A. Zahran, S. A. Elwakil, *Phys. Plasmas* **23**, 022102 (2016).
- [51] O. R. Rufai, *Heliyon* **5**, e01976 (2019).
- [52] C. B. Tabi, C. S. Panguetna and T. C. Kofané, *Physica B: Condens. Matt.* **545**, 370 (2018).
- [53] J. Jacquinet, B. D. McVey, J. E. Scharer, *Phys. Rev. Lett.* **39**, 88 (1977).
- [54] I. Kourakis and P. K. Shukla, *Nonlinear Proc. Geophys.* **12**, 407 (2005).
- [55] T. Kimura, K. Imagaki, and K. Ohe, *J. Phys. D: Appl. Phys.* **31**, 2295 (1998).
- [56] D. Vender, W. W. Stoffels, E. Stoffels, G. M. W. Kroesen, and F. J. de Hoog, *Phys. Rev. E* **51**, 2436 (1995).
- [57] R. N. Franklin, *Plasma Sources Sci. Technol.* **11**, A31 (2002).
- [58] M. A. Lieberman and A. Lichtenberg, *Principle of Plasma Discharges and Materials Processing*, 2nd ed. (Wiley, New York, (2005)).
- [59] P. Chabert, A. J. Lichtenberg, and M. A. Lieberman, *Phys. Plasmas* **14**, 093502 (2007).
- [60] N. Plihon, P. Chabert, and C. S. Corr, *Phys. Plasmas* **14**, 013506 (2007).
- [61] A. Meige, N. Plihon, G. J. M. Hagelaar, J.-P. Boeuf, P. Chabert, R. W. Boswell, *Phys. Plasmas* **14**, 053508 (2007).
- [62] T. H. Chung, *Phys. Plasmas* **16**, 063503 (2009).
- [63] M. G. Anowar, K. S. Ashrafi, and A. A. Mamun, *J. Plasma Phys.* **77**, 133 (2011).
- [64] S. Duha, M. S. Rahman, A. A. Mamun, and G. M. Anowar, *J. Plasma Phys.* **78**, 279 (2012).
- [65] D. Anderson, *Phys. Rev. Lett. A* **27**, 6 (1983).
- [66] D. Mihalache, D. Mazilu, F. Lederer, Y. V. Kartashov, L.-C. Crasovan, L. Torner and B. A. Malomed, *Phys. Rev. Lett.* **97**, 073904 (2006).
- [67] D. D. E. Temgoua and T. C. Kofané, *Phys. Rev. E* **93**, 062223 (2016).

- [68] M. Djoko and T. C. Kofané, *Opt. Commun.* **416**, 198 (2018).
- [69] A. Djazet, S. I. Fewo, E. B. N. Nkouankam and T. C. Kofané, *Eur. Phys. J. D* **74**, 67 (2020).
- [70] L. T. Megne, C. B. Tabi and T. C. Kofané, *Phys. Rev. E* **102**, 042207 (2020).
- [71] J. A. A. Otsobo, L. T. Megne, C. B. Tabi and T. C. Kofané, *Chaos, Sol. Frac.* **158**, 112034 (2022).
- [72] J. B. Okaly, A. Mvogo, C. B. Tabi, H. P. Ekobena Fouda and T. C. Kofané, *Phys. Rev. E* **102**, 062402 (2020).
- [73] A. S. Etémé, C. B. Tabi and A. Mohamadou, *Commun. Nonl. Sci. Num. Simul.* **43**, 211 (2017).
- [74] C. B. Tabi, R. Y. Ondoua, H. P. Ekobena, A. Mohamadou and T. C. Kofané, *Phys. Lett. A* **380**, 2374 (2016).
- [75] G. R. Y. Mefire, C. B. Tabi, A. Mohamadou, H. P. F. Ekobena and T. C. Kofané, *Chaos* **23**, 033128 (2013).
- [76] A. X. Zhang and J. K. Xue, *Phys. Rev. A* **75**, 013624 (2007).
- [77] P. Otlaadisa, C. B. Tabi and T. C. Kofané, *Phys. Rev. E* **103**, 052206 (2021).
- [78] P. A. Andreev and L. S. Kuzmenkov, *Phys. Rev. A* **78**, 053624 (2008).
- [79] E. A. Kuznetsov, A. M. Rubenchik and V. E. Zakharov, *Phys. Rep.* **142**, 103 (1986).
- [80] J. Borhanian, I. Kourakis and S. Sobhanian, *Phys. Lett. A* **373**, 3667 (2009).
- [81] H. Washimi and T. Taniuti, *Phys. Rev. Lett.* **17**, 996 (1966).
- [82] J.-K. Xue, *Physics of Plasmas* **12**, 062313 (2005).
- [83] A. P. Misra, P. K. Shukla, *Physics of Plasmas* **15**, (2008) 122107.
- [84] A. S. Bains, A. P. Misra, N. S. Saini, T. S. Gill, *Physics of Plasmas* **17**, (2010) 012103.
- [85] Shalini, A. P. Misra, N. S. Saini, *J. Theor. Appl. Phys.* **11**, (2017) 217-224.

- [86] A. Abdikian, *Phys. Plasmas* **24**, 052123 (2017).
- [87] A. Biswas, D. Chakraborty, S. Pramanik, and S. Ghosh, *Phys. Plasmas* **28**, 062105 (2021).
- [88] V. Berezhnoj, C. B. Shin, U. Buddemeier, and I. Kaganovich, *Appl. Phys. Lett.* **77**, 800 (2000).
- [89] E. N. Kenkeu, A. B. T. Motcheyo, T. Kanaa and C. Tchawoua, *Phys Plasmas*. **29**, 043702 (2022).
- [90] R. Ichiki, S. Yoshimura, T. Watanabe, Y. Nakamura and Y. Kawai, *Phys. Plasmas* **9**, 4481 (2002).
- [91] R. A. Gottscho and C. E. Gaebe, *IEEE Trans. Plasma Sci.* **14**, 92 (1986).
- [92] Y. I. Portnyagin, O. F. Klyuev, A. A. Shidlovsky, A. N. Evdokimov, T. W. Buzdigar, P. G. Matukhin, S. G. Pasyunkov, K. N. Shamshev, V. V. Sokolov and N. D. Semkin, *Adv. Space Res.* **11**, 89 (2011).
- [93] R. Sabry, W. M. Moslem and P. K. Shukla, *Phys. Plasmas* **16**, 032302 (2009).
- [94] A. J. Coates, F. J. Crary, G. R. Lewis, D. T. Young, J. H. Waite Jr and E. C. Sittler Jr, *Geophys. Res. Lett.* **34**, L22103 (2007).
- [95] A. A. Mamun, P. K. Shukla and B. Eliasson, *Phys. Rev. E* **80**, 046406 (2009).
- [96] C. B. Tabi, C. S. Panguetna and T C Kofané, *Physica B* **545**, 70 (2018).
- [97] U. M. Abdelsalam, *Ain Shams Eng J.* **12**, 4111-4118 (2021).
- [98] A. R. Alharbi, *Comput. Model. Eng. Sci.* **134**(3), 2193 (2022).
- [99] A. R. Alharbi, *AIMS Math.* **8**(1), 1230-1250 (2022).
- [100] S. Frassu, T. Li and G. Viglialoro, *Math Meth Appl Sci.* **45**(17) 11067-11078 (2022).
- [101] A. Davey and K. Stewartson, *Proc. R. Soc. London-Ser. A* **338**, 101 (1974).
- [102] A. C. Newell and J. V. Moloney, *Nonlinear Optics*. Addison-Wesley, Redwood City, (1992).

- [103] G. Huang, L. Deng and C. Hang, *Phys. Rev. E* **72**, 036621 (2005).
- [104] H. Leblond, *J. Phys. A: Math. Gen.* **32**, 7907 (1999).
- [105] L. Y. Sung, *J. Math. Anal. Appl.* **183**, 121 (1994a).
- [106] L. Y. Sung, *J. Nonlinear Sci.* **5**, 433 (1995).
- [107] Y. Ohta and J. Yang, *Phys. Rev. E* **86**, 036604 (2012).
- [108] Y. Ohta and J. Yang, *J. Phys. A: Math. Theor* **46**, 105202 (2013).
- [109] H.-X. Jia, D.-W. Zuo, X.-H. Li and X.-S. Xiang, *Phys. Lett. A* **405**, 127426 (2021).
- [110] H. G. Abdelwahed, E. K. El-Shewy, S. Alghanim and M. A. E. Abdelrahman, *Fractal Fract.* **6**, 430 (2022).
- [111] H. G. Abdelwahed, A. F. Alsarhana, E. K. El-Shewy and M. A. E. Abdelrahman, *Phys. Fluids* **35**, 037129 (2023).
- [112] E. K. El-Shewy, Y. F. Alharbi and M. A. E. Abdelrahman, *Chaos, Solitons and Fractals* **170**, 113324 (2023).
- [113] J. Hietarinta and R. Hirota, *Phys Lett A.* **145**, 5 (1990).
- [114] R. H. Heredero, L. M. Alonso and E. M. Reus, *Phys. Lett. A* **152**, 1-2 (1991).
- [115] M. Boiti, J. J.-P. Leon, L. Martina and F. Pempinelli, *Phys. Lett. A* **132**, 8-9 (1988).
- [116] T.-C. Xia and D.-Y. Chen, *Chaos, Solitons and Fractals* **22**, 577-582 (2004).
- [117] G. Xu, *Chaos, Solitons and Fractals* **30**, 71-76 (2006).
- [118] N. Prathap, S. Arunprakash, M. S. M. Rajan and K. Subramanian, *Optik* **158** 1179-1185 (2018).
- [119] S. Veni and M. S. M. Rajan, *Opt. Quant. electron.* **55**, 107 (2023).
- [120] L. Rezeau, G. Belmont, Quelques propriétés des plasmas, **3** (2007).
- [121] S. Ali, Plasma Physics and its Applications, March 2019: DOI: 10.13140/RG.2.2.16890.54724.

- [122] A. Talebpour, J. Young, S. L. Chin, *Opt. Commun.* **163**, 29 (1999).
- [123] L. V. Keldysh, *Sov. Phys. JETP* **20**, 1307 (1965).
- [124] L. Bergé, A. Couairon, *Phys. Rev. Lett.* **86**, 1003 (2001).
- [125] N. A. Krall A. W. Trivelpiece, Principles of Plasma Physics, (*McGraw-Hill*, New York 1973).
- [126] A. S. Eddington, The Internal Constitution of the Stars, (*Cambridge University Press*, 1926).
- [127] P. Debye and E. Hückel, *Phys. Z.* **24**, 183 (1923).
- [128] P. Gibbon, Introduction to Plasma Physics, *Proceedings of the 2014 CAS-CERN Accelerator School: Plasma Wake Acceleration*, Vol. 1 (2016).
- [129] K. Nishikawa and M. Wakatani, Plasma Physics: Basic Theory with Fusion Applications, (*Springer-Verlag* Berlin Heidelberg, New York, 1990).
- [130] B. Ghosh, Basic Plasma Physics, *Alpha science International Ltd. Oxford*, U.K (2014).
- [131] Gay-Mimbrera, J. García, M. C. Isla-Tejera, B. Rodero-Serrano, A. García-Nieto, A. V. Ruano, *J. Adv. in Ther.* textbf33, 894 (2016).
- [132] R. E. J. Sladek, Plasma needle : *non-thermal atmospheric plasmas in dentistry* (PhD thesis, 2006). doi:10.6100/IR613009.
- [133] W. Schottky, *Phys. Z.* **25**, 635 (1924).
- [134] M. H. Corbett, *Proc. 31st Int. Electr. Propuls. Conf.* 151 (2009).
- [135] D. J. Economou, *Appl. Surf. Sci.* **253**, 6672 (2007).
- [136] U. Fantz, *Nucl. Fusion* **49**, 125007 (2009).
- [137] D. L. Flamm, *Pure and Appl. Chem.* **62**, 170 (1990).
- [138] S. Basnet, A. Patel and R. Khanal, *Plasma Phys. Control. Fusion* **62**, 115011 (2020).
- [139] M. M. Hatami, *Sci. Rep.* **11**, 9531 (2021).

- [140] S. Ganyou, S. I. Fewo, C. S. Panguetna, T. C. Kofané, *Results in Physics* **52**, 106821 (2023).
- [141] T. H. Stix, *Waves in Plasmas*, (*Springer-Verlag* New York, 1992).
- [142] D. G. Swanson, *Plasma Waves*, (*Institute of Physics Bristol*, Second Edition, 2003).
- [143] F. Anderegg, C. F. Driscoll, D. H. E. Dubin, T. M. O’Neil and F. Valentini, *Phys. Plasmas* **16**, 055705 (2009).
- [144] N. S. Suryanarayana, J. Kaur and V. Dubey, *J. Mod. Phys.* **1**, 281 (2010).
- [145] L. Oksuz, D. Lee and N. Hershkowitz, *Plasma Sources Sci. Techn.* **17**, 015012 (2008).
- [146] N. J. Zabusky and M. D. Kruskal, *Phys. Rev. Lett.* **15**, 240 (1965).
- [147] M. A. Allen and G. Rowlands, *J. Plasma Phys.* **50**, 413 (1993).
- [148] J. S. Russel, Report on Waves, (Report of the Fourteenth Meeting of the British Association for the Advancement of Science, *John Murray*, Londres, 1844).
- [149] D. J. Korteweg and G. de Vries, On the change of form of long waves advancing in a rectangular canal and on a new type of long stationary waves, (*Philosophical Magazine* 5th Series, 36, 1895).
- [150] C. S. Gardner, J. M. Greene, M. D. Kruskal and R. M. Miura, *Phys. Rev. Lett.* **19**, 1095 (1967).
- [151] B.-X. Gan, Y.-H. Chen, and M. Y. Yu, *J. Appl. Phys.* **101**, 113310 (2007).
- [152] X. Zheng, Y. Chen, H. Hu, G. Wang, F. Huang, C. Dong, and M. Y. Yu, *Phys. Plasmas* **16**, 023701 (2009).
- [153] H. Leblond, *J. Phys. B: At. Mol. Opt. Phys.* **41** 043001 (2008).
- [154] R. Sabry, W. M. Moslem and P. K. Shukla, *Plasma Phys. Control. Fusion* **54**, 035010 (2012).
- [155] M. N. Haque and A. Mannan, *Contrib. Plasma Phys.* **61**, e202000161 (2020).

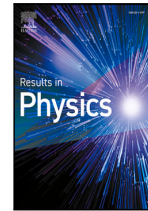
- [156] W. F. El-Taibany, N. A. El-Bedwehy, N. A. El-Shafeay and S. K. El-Labany, *Galaxies*, **9**,48 (2021) .
- [157] T. S. Gill, C. Bedi and A. S. Bains, *Phys. Plasmas* **16**, 032111 (2009).
- [158] M. Bacha, L. A Gougama, M. Tribeche, *Physica A* **466**, 199-210 (2017).
- [159] W. Craig, U. Schanz and C. Sulem, *Ann. I. H. P. Sec. C* **14**, 615 (1977).
- [160] K. Nishinari, K. Abe and J. Satsuma, *Phys. Plasmas* **1**, 2559 (1994).
- [161] J.-K. Xue, *Phys. Lett. A* **330**, 390 (2004).
- [162] C. Bedi and T. S. Gill, *Phys. Plasmas* **19**, 062109 (2012).
- [163] P. Carbonaro, Chaos, *Solitons Fractals* **45**, 959 (2012).
- [164] N. Aközbek, C. M. Bowden, A. Talebpour, and S. L. Chin, *Phys. Rev. E* **61** (4), 4540 (2000).
- [165] C. P. Jisha, V. C. Kuriakose, K. Porsezian, *Phys. Lett. A* **352**, 496-499 (2006).
- [166] J. Hietarinta, *Springer*, Berlin, Heidelberg 1997.
- [167] H. G. Abdelwahed, R. Sabry, *Astrophys. Space Sci.* **362**, 92 (2017).
- [168] K. Nishinari, K. Abe, and J. Satsuma, *J. Phys. Soc. Japan* **6**, 2021-2029 (1993).
- [169] K. Nishinari, K. Abe and J. Satsuma, *Theor. Math. Phys.* **99**,745-753 (1994).
- [170] M. J. Ablowitz and P. A. Clarkson, *Cambridge University Press*, Cambridge, (1991)
- [171] V. B. Matveev and M. A. Salle, *Springer-Verlag*, Berlin, (1991).
- [172] M. Saravi, E. Babolian, R. England and M. Bromilow, *Comput. Math. Appl.* **59**, 1524 (2010).
- [173] W. Malfliet and W. Hereman, *Phys. Scr.* **54**, 563 (1996).
- [174] Q. Wang, Y. Chen and H. Zhang, *Appl. Math. Comput.* **181**, 247 (2006).
- [175] E. Fan and H. Zhang, *Phys. Lett. A* **246**, 403 (1998).
- [176] S. Lou, *Phys. Scr.* **65**, 7 (2002).

- [177] S. Lou and J. Lu, *J. Phys. A* **29**, 4209 (1996).
- [178] Z. Yan and H. Q. Zhang, *Phys. Lett. A* **285**, 355 (2001).
- [179] C. B. Tabi, A. Mohamadou and T. C. Kofané, *Phys. Lett. A* **373**, 2476 (2009).
- [180] C. B. Tabi, A. Mohamadou and T. C. Kofané, *Physica Scripta* **77**, 045002 (2008).
- [181] M. J. Ablowitz and H. Segur, *SIAM*, Philadelphia, (1981).
- [182] R. Radha and M. Lakshmanan, *J. Phys. A: Math. Gen.* **30**, 3229 (1997).
- [183] S. S. Ghosh, A. Sen and G. S. Lakhina, *Nonlinear Processes Geophys.* **9**, 463 (2002).
- [184] N. S. Saini, Y. Ghai and R. Kohli, *J. Geophys. Res.* **121**, 5944 (2016).
- [185] J. Hietarinta, *Phys. Lett. A* **145**, 237 (1990).
- [186] J. Hietarinta, *Phys. Lett. A* **149**, 113 (1990).
- [187] R. Radha and M. Lakshmanan *Chaos, Solitons and Fractals* **8** (1), 17-25 (1997).
- [188] A. S. Fokas and P. M. Santini, *Physica D* **44**, 99 (1990).
- [189] C. R. Gilson and J. J. C. Nimmo, *Proc. Roy. Soc. A* **435**, 339 (1991).
- [190] C. R. Gilson, *Phys. Lett. A* **161**, 423 (1992).
- [191] V. I. Karpman and E. M. Krushkal, *Sov. Phys. JETP* **28**, 277 (1969).
- [192] Q. Chang, E. Jia, and W. Sun, *J. Comput. Phys.* **148**, 397 (1999).
- [193] T. R. Taha and M. J. Ablowitz, *J. Comput. Phys.* **55**, 203 (1984).
- [194] R. H. Hardin and F. D. Tappert, *SIAM Rev. Chronicle* **15**, 423 (1973).
- [195] R. A. Fisher and W. K. Bischel, *Appl. Phys. Lett.* **23**, 661 (1973); *J. Appl. Phys.* **46**, 4921 (1975).
- [196] J. W. Cooley and J. W. Tukey, *Math. Comput.* **19**, 297 (1965).
- [197] P Suarez, An introduction to the Split Step Fourier Method using MATLAB, (2015) DOI: 10.13140/RG.2.1.1394.0965.

- [198] X.-S. Yang. An Introduction to Computational Engineering with MATLAB. *Cambridge International Science Publishing*, 1st edition, (2006).
- [199] T. R. Taha and X Xu, *The Journal of Supercomputing* **5**, 5?23, (2005).
- [200] J A C Weideman and B M Herbst, *SIAM Journal on Numerical Analysis* **23**, 485?507, (1986).
- [201] K. S. Yee, *IEEE Trans. Antennas Propagat.*, **AP-14**, 302 (1966).
- [202] G. C. Das and A. Nag, *Assam Univ. J. Sci. Technol.* **5** (2010) 169.
- [203] S. A. Shan and N. Akhtar, *Astrophys. Space Sci.* **346** (2013) 367.
- [204] S. Hussain, S.A. Shan, N. Akhtar and M.M. Masud, *Astrophys. Space Sci.* **352** (2014) 605.
- [205] M. A.-Moghanjoughi, *Phys. Plasmas* **17**, 092304 (2010).
- [206] H. P. Le and J.-L. Cambier, *Phys. Plasmas* **23**, 063505 (2016).
- [207] J. Vranjes, M. Kono, D. Petrovic, S. Poedts, A. Okamoto, S. Yoshimura and M. Y. Tanaka, *Plasma Sour. Sci. Technol.* **15**, S1-S7 (2006).

♣ List of publications ♣

1. **Stéphanie Ganyou**, Serge I. Fewo, Chérif S. Panguetna, and Timoléon C. Kofané, (2+1)-dimensional modulated nonlinear ion-acoustic soliton packets in magnetized electronegative plasma, *Results in Physics* **52**, 106821 (2023).
doi: <https://doi.org/10.1016/j.rinp.2023.106821>
2. **Stéphanie Ganyou**, Chérif S. Panguetna, Serge I. Fewo, Conrad B. Tabi, and Timoléon C. Kofané, Two-dimensional dynamics of ion-acoustic waves in a magnetized electronegative plasma, *Pramana Journal of Physics*, **98**, 30 (2024).
doi: <https://doi.org/10.1007/s12043-023-02704-z>



(2+1)-dimensional modulated nonlinear ion-acoustic soliton packets in magnetized electronegative plasma

Stéphanie Ganyou, Serge I. Fewo^{*}, Chérif S. Panguetna, Timoléon C. Kofané

Laboratory of Mechanics, Materials and Structures, Department of Physics, Faculty of Science, The University of Yaounde I, P.O. Box 812, Yaounde, Cameroon

ARTICLE INFO

Keywords:

Magnetized electronegative plasma
Nonlinear Schrödinger equation
Modulational instability
Variational approach

ABSTRACT

The dynamics of propagation of (2+1)-dimensional ion-acoustic wave (IAW) packets in magnetized electronegative plasma made of negative ions with electrons, both in Boltzmann distribution and cold mobile positive ions is studied. For this purpose, the standard reductive perturbation method is used to derive the (2+1)-dimensional nonlinear Schrödinger (NLS) equation, which governs the modulation of positive IAW packets. The coefficients of the obtained NLS equation do not only depend on the system parameters specially the electronegative parameters such as the negative ion concentration ratio and the electron-to-negative ion temperature ratio (α and σ_n , respectively), but also on the magnetic field (ω_p). The modulational instability is studied to analyze the areas of the emergence of waves. In order to describe the main characteristics of IAWs, the variational method is performed involving trial function solution of NLS equation and the exact (input profile) and numerical (output profile) solutions are also discussed.

Introduction

During recent years, the effect of positive (negative) ions on the plasma properties such as quantum plasma [1–3], dust plasma [4–8], pair-ion plasma [9–13], electronegative plasma [14–17], magnetized electronegative plasma [18–25], just to name a few, has long been the subject of significant interest. The solar system is made up of planets surrounded by plasma with various characteristics (electron density, temperature, collision frequency...).

Plasmas are considered as one of the four states of matter, just like solids, liquids, and gas. They are composed of positive ions in addition to negative ions and electrons. In the presence of a significant amount of negative ions, they are said to be electronegative plasmas (ENPs) [26–30]. The latter nowadays has become a fascinating topic because of fundamental scientific interest, and it is observed in astrophysical objects (Earth's ionosphere [31,32]), (D-region [33–35] and F-region [36]), Solar wind magnetosphere [37,38], in industries [39] and laboratory experiment [40]. However, Plasmas, which are nonlinear and dispersive media, have vast opportunities to observe different nonlinear wave phenomena such as ion acoustic solitons (IASs), shock waves and different kinds of instabilities. Due to the suitable balance between nonlinearity and dispersion, ion acoustic waves (IAWs), and solitons in general, can spread over long distances, keeping intact their characteristics and shape. Various applications in plasma science and industry [41,42], and the proof of its existence in astrophysics,

space, and laboratory experiments make ENPs a subject of growing interest as witnessed by recent contributions both in one-dimensional and multidimensional contexts [43–49]. In some previous works, the study of negative ions including charge evolution in dust plasmas and ion-acoustics (IA) waves were investigated [33,50,51]. The structure of electronegative plasmas sheath without magnetic field [14–17] and with magnetic field [18] are investigated. For ion-acoustic waves in electronegative plasma in the presence of the magnetic field, the solitary wave which is described by the well-known nonlinear Schrödinger equation can propagate. The study of other aspects and characteristics of such plasmas waves, related to their response to external magnetic fields using the hydrodynamic equations, in one or more dimensions [16,17] can be reduced to nonlinear Schrödinger (NLS) equations by introducing the reductive perturbation approximation.

One of the direct mechanisms responsible for the formation of solitons in nonlinear media is the modulational instability (MI). The latter occurs when a constant wave background becomes unstable and induces sinusoidal modulations under the competitive contribution of nonlinear and dispersive effects. The result is a self-organization of the system that leads to the emergence of nonlinear structures and solitons. Due to its importance in stable wave propagation, the MI of different waves modes in plasma systems has gained a great attention. Recently, the MI of IAWs in electronegative plasma and other types of plasma has been investigated in some previous works [1,16,52–57].

^{*} Corresponding author.

E-mail addresses: stephanieganyou@gmail.com (S. Ganyou), sergefewo@yahoo.fr (S.I. Fewo), cherifps@yahoo.fr (C.S. Panguetna), tckofane@gmail.com (T.C. Kofané).

<https://doi.org/10.1016/j.rinp.2023.106821>

Received 15 May 2023; Received in revised form 12 July 2023; Accepted 30 July 2023

Available online 2 August 2023

2211-3797/© 2023 The Author(s). Published by Elsevier B.V. This is an open access article under the CC BY-NC-ND license (<http://creativecommons.org/licenses/by-nc-nd/4.0/>).

In this work, we used the standard reductive perturbation technique in order to obtain the (2+1)-dimensional NLS equation modeling the dynamics of propagation of IAWs in magnetized electronegative plasma. An analytical approach such as the variational method can be applied to NLS equation in order to study the dynamics of the relevant parameters of IAWs in plasma medium. This method is well known in classical mechanics and can be used in various contexts. To remind, in nonlinear optics in general and the propagation of pulses in optical fibers in particular, it was applied for the first time in 1983 by Anderson [58]. The basic physical assumption of this approach is based on the fact that a propagating pulse retains its initial shape or profile while only its characteristics such amplitude, width, chirp and phase can change continuously according to the propagation distance.

In our investigation, we are interested by the dynamics of propagation of ion-acoustic solitons in electronegative plasma in the presence of external magnetic field, because magnetized plasmas play a very important role in the study of plasma physics. Indeed, the introduction of a magnetic field considerably enriches the physical phenomena that can be generated in plasmas. One of our interests in magnetized plasma has concerned the anisotropic characteristic of plasma in the presence of magnetic field and the properties of waves which depend on the direction of wave vector relative to the magnetic field vector. Moreover, the presence of the external magnetic field can be used to control the directions, the velocity and the electrical properties of the plasma and improve the performance of these processes by confining the plasma and increasing the reaction rate. Working with the electronegative plasma in the presence of external magnetic field, we study the dynamics of propagation of ion-acoustic solitons in the system. We analytically show that the electronegative plasma hydrodynamical equation can lead to the (2+1)-dimensional nonlinear Schrödinger equation, where the transverse dispersive coefficient depends on the external magnetic field. Thereafter, we pay attention to wave modulation via the activation of modulational instability using the linear stability analysis of plane wave solutions, which allows obtaining an expression for the MI growth rate. The descriptions are made taking into account some physical system parameters such as the negative ion concentration ratio, the electron-to-negative ion temperature ratio and the magnetic field. In addition, in order to describe the main characteristics of IAWs, the variational method is performed involving a function solution of NLS equation. The evolution of relevant parameters is presented. The practical existence of the model is characterized by its potential to enhance several applications across various fields such as plasma etching, surface treatment, ion implantation, and fabrication of semiconductor devices [59,60].

We organize this present paper as follows: in Section “Problem formulation”, we describe the problem and we perform the reductive perturbation method in (2+1)-dimensional magnetized electronegative plasma model to derive the nonlinear (2+1)-dimensional Schrödinger equation. In Section “Modulational instability analysis of IAWs in NLS equation”, we present the influence of MI in NLS equation. We employ a variational approach involving trial functions to describe the main characteristics of pulse evolution in Section “Variational approach for NLS equation”. The paper ends with concluding discussions in Section “Conclusion”.

Problem formulation

In this section, we present the (2+1)-dimensional mathematical model for the propagation of positive ion-acoustic waves along the external magnetic field $\mathbf{B} = B_0 \mathbf{z}$ in an electronegative plasma. For that, we use a plasma system composed of electrons and negative ions, both in Boltzmann distribution, in addition to cold mobile positive ions [61,62]. In plasma systems, the charge neutrality condition ($Z_p n_p = Z_n n_n + n_e$), is modified by the presence of negative ions, with n_e , n_p , and n_n the electron, positive, and negative ions densities,

respectively. Z_p and Z_n are the charge number of positive and negative ions.

Let us consider the following fluid continuity, momentum and Poisson's equations for the positive ions:

$$\frac{\partial n_p}{\partial t} + \nabla \cdot (n_p \mathbf{v}_p) = 0, \quad (1)$$

$$\frac{\partial \mathbf{v}_p}{\partial t} + (\mathbf{v}_p \cdot \nabla) \mathbf{v}_p = -\frac{q_p}{m_p} \nabla \Phi + \frac{q_p}{m_p} (\mathbf{v}_p \times \mathbf{B}), \quad (2)$$

$$\nabla^2 \Phi = -4\pi e (Z_p n_p - Z_n n_n - n_e). \quad (3)$$

Here, $n_e = n_{e0} e^{\frac{e\Phi}{k_B T_e}}$, $n_p = n_{p0} e^{\frac{e\Phi}{k_B T_p}}$, with the electron-to-negative ion temperature ratio $\sigma_n = \frac{T_e}{T_p}$, the positive ions charge $q_p = +Z_p e$ of mass m_p , the negative ions charge $q_n = -Z_n e$ of mass m_n and the electrons charge $q_e = -e$, mass m_e . \mathbf{v}_p , q_p , m_p and $\mathbf{E} = -\nabla \Phi$ are the positive ion mean velocity, ion charges, ion mass and the electrostatic potential, respectively. We also assume that in plane (x, z) , $\nabla = (\frac{\partial}{\partial x}, 0, \frac{\partial}{\partial z})$ and the normalized ion continuity, momentum and Poisson's equations take the form of a system of (scalar) equations:

$$\frac{\partial n}{\partial t} + \frac{\partial (nv_x)}{\partial x} + \frac{\partial (nv_z)}{\partial z} = 0, \quad (4)$$

$$\frac{\partial v_x}{\partial t} + (v_x \frac{\partial}{\partial x} + v_z \frac{\partial}{\partial z}) v_x = -\frac{\partial \phi}{\partial x} + \omega_p v_y \quad (5a)$$

$$\frac{\partial v_y}{\partial t} + (v_x \frac{\partial}{\partial x} + v_z \frac{\partial}{\partial z}) v_y = -\omega_p v_x \quad (5b)$$

$$\frac{\partial v_z}{\partial t} + (v_x \frac{\partial}{\partial x} + v_z \frac{\partial}{\partial z}) v_z = -\frac{\partial \phi}{\partial z} \quad (5c)$$

$$\frac{\partial^2 \phi}{\partial x^2} + \frac{\partial^2 \phi}{\partial z^2} = 1 + c_1 \phi + c_2 \phi^2 + c_3 \phi^3 - n \quad (6)$$

where $n = \frac{n_p}{n_{p0}}$ with charge neutrality condition at equilibrium defined

by $Z_p n_{p0} = Z_n n_{n0} + n_{e0}$, $\mathbf{v} = (v_x, v_y, v_z) = \frac{v_p}{C_s}$ with $C_s = (\frac{Z_p k_B T_e}{m_i})^{\frac{1}{2}}$ which is the characteristic speed scale used for velocity normalization, $\phi = \frac{e\Phi}{k_B T_e}$. The space (x, z) and time (t) variables are normalized by the Debye length $\lambda_{De} = (\frac{k_B T_e}{4\pi Z_p n_{p0} e^2})^{\frac{1}{2}}$, $\omega_p = \frac{\omega_i}{\omega_{pi}}$ is the normalized parameter of ion

cyclotron and ion plasma frequency ratio, with $\omega_{pi} = (\frac{4\pi n_{p0} Z_p^2 e^2}{m_i})^{\frac{1}{2}}$ and $\omega_i = \frac{e B_0}{m_i c}$. The constants $c_1 = \mu_e + \mu_n \sigma_n$, $c_2 = \frac{\mu_e + \mu_n \sigma_n^2}{2}$ and $c_3 = \frac{\mu_e + \mu_n \sigma_n^3}{6}$ are obtained by using the power series expansion of the exponential factor around zero in n_p and n_n . Here, $\mu_e = \frac{n_{e0}}{Z_p n_{p0}} = \frac{1}{1+\alpha}$, $\mu_n = \frac{Z_n n_{n0}}{Z_p n_{p0}} = \frac{\alpha}{1+\alpha}$ which assumes the neutrality condition of the electronegative plasma: $\mu_e + \mu_n = 1$, where $\alpha = \frac{Z_n n_{n0}}{n_{e0}}$ being the density ratio of negative ion to electron (negative ion-to-electron density ratio).

In order to investigate the dynamics of propagation of positive IAWs and derive the nonlinear Schrödinger (NLS) equation, we employ the standard reductive perturbation expansion. The stretched coordinates in space and time may be introduced as [15,63]:

$$\xi = \epsilon x, \quad \eta = \epsilon(z - v_g t), \quad \tau = \epsilon^2 t, \quad (7)$$

where v_g is the group velocity that will be found later by the solvability condition of Eqs. (4)–(5c). ϵ is a small expansion parameter ($0 < \epsilon \ll 1$) that measures the strength of nonlinearity [3,56,64–66]. The condition about ϵ implies that the plasma dimension must be much larger than the Debye length, which is satisfied in most cases of interest [67]. The dependent physical variables around their equilibrium values are expanded as follows [39,68]:

$$\begin{pmatrix} n \\ v_x \\ v_y \\ v_z \\ \phi \end{pmatrix} = \begin{pmatrix} 1 \\ 0 \\ 0 \\ 0 \\ 0 \end{pmatrix} + \sum_{p=1}^{+\infty} \epsilon^p \sum_{l=-\infty}^{+\infty} \begin{pmatrix} n_l^{(p)}(\xi, \eta, \tau) \\ v_{xl}^{(p)}(\xi, \eta, \tau) \\ v_{yl}^{(p)}(\xi, \eta, \tau) \\ v_{zl}^{(p)}(\xi, \eta, \tau) \\ \phi_l^{(p)}(\xi, \eta, \tau) \end{pmatrix} A^l(z, t). \quad (8)$$

We note that the above series include $A^l(z, t) = e^{il(kz - \omega t)}$, up to order p . These are generated by the nonlinear terms, which means that the corresponding coefficients are of maximum order ε^p . The state variables n , v_{x1} , v_{y1} , v_{z1} and ϕ must satisfy the following condition $(n_l^{(p)})^* = n_{-l}^{(p)}$, $(v_{x1}^{(p)})^* = v_{x-1}^{(p)}$, $(v_{y1}^{(p)})^* = v_{y-1}^{(p)}$, $(v_{z1}^{(p)})^* = v_{z-1}^{(p)}$, $(\phi_l^{(p)})^* = \phi_{-l}^{(p)}$, respectively. The asterisk (*) denotes the complex conjugate. Substituting the trial solutions (8) into Eqs. (4)–(6), and equating the quantities with equal power of ε , we obtain several coupled equations in different orders of ε .

At the first harmonic of perturbation (ε^1), we obtain the following relations:

For $l = 0$, we obtain

$$n_0^{(1)} = v_{x0}^{(1)} = v_{y0}^{(1)} = v_{z0}^{(1)} = \phi_0^{(1)} = 0 \quad (9)$$

For $l = 1$, we find

$$\begin{cases} n_1^{(1)} = \frac{k^2}{\omega^2} \phi_1^{(1)} \\ v_{x1}^{(1)} = v_{y1}^{(1)} = 0 \\ v_{z1}^{(1)} = \frac{k}{\omega} \phi_1^{(1)} \end{cases} \quad (10)$$

under the condition that the dispersion relation

$$\omega^2 = \frac{k^2}{k^2 + c_1} \quad (11)$$

is verified, leading to the first harmonic of perturbation.

At the second harmonic of perturbation (ε^2), we obtain the following relations:

For $l = 0$,

$$\begin{cases} v_{x0}^{(2)} = v_{y0}^{(2)} = 0 \\ n_0^{(2)} - c_1 \phi_0^{(2)} = 2c_2 |\phi_1^{(1)}|^2 \end{cases} \quad (12)$$

For $l = 1$,

$$\begin{cases} n_1^{(2)} = (k^2 + c_1) \phi_1^{(2)} - 2ik \frac{\partial \phi_1^{(1)}}{\partial \eta} \\ v_{x1}^{(2)} = -\frac{i\omega}{\omega^2 - \omega_p^2} \frac{\partial \phi_1^{(1)}}{\partial \xi} \\ v_{y1}^{(2)} = -\frac{\omega_p}{\omega^2 - \omega_p^2} \frac{\partial \phi_1^{(1)}}{\partial \xi} \\ v_{z1}^{(2)} = \frac{k}{\omega} \phi_1^{(2)} + \frac{i}{\omega} \left(v_{g\frac{k}{\omega}} - 1 \right) \frac{\partial \phi_1^{(1)}}{\partial \eta} \end{cases} \quad (13)$$

The group velocity is

$$v_g = c_1 \frac{\omega^3}{k^3}. \quad (14)$$

For $l = 2$,

$$\begin{cases} n_2^{(2)} = \alpha_n (\phi_1^{(1)})^2 \\ v_{x2}^{(2)} = v_{y2}^{(2)} = 0 \\ v_{z2}^{(2)} = \alpha_{v_z} (\phi_1^{(1)})^2 \\ \phi_2^{(2)} = \alpha_\phi (\phi_1^{(1)})^2 \end{cases} \quad (15)$$

with $\alpha_\phi = \frac{k^2}{2\omega^4} - \frac{c_2^2}{3k^2}$, $\alpha_n = (4k^2 + c_1) \alpha_\phi + c_2$, $\alpha_{v_z} = \frac{\omega}{k} (\alpha_n - (k^2 + c_1)^2)$.

In the case of the third-order of perturbation (ε^3), we obtain

For $l = 0$

$$\begin{cases} -v_{g\frac{k}{\omega}} n_0^{(2)} + v_{z0}^{(2)} = -\frac{2k^3}{\omega^2} |\phi_1^{(1)}|^2, \\ -v_{g\frac{k}{\omega}} v_{z0}^{(2)} + \phi_0^{(2)} = -\frac{k^2}{\omega^2} |\phi_1^{(1)}|^2. \end{cases} \quad (16)$$

Using the last relation of Eq. (12) from the order (ε^2 , $l = 0$) and the Eq. (16), we obtain

$$\begin{cases} n_0^{(2)} = \beta_n |\phi_1^{(1)}|^2 \\ v_{z0}^{(2)} = \beta_{v_z} |\phi_1^{(1)}|^2 \\ \phi_0^{(2)} = \alpha_\phi |\phi_1^{(1)}|^2 \end{cases} \quad (17)$$

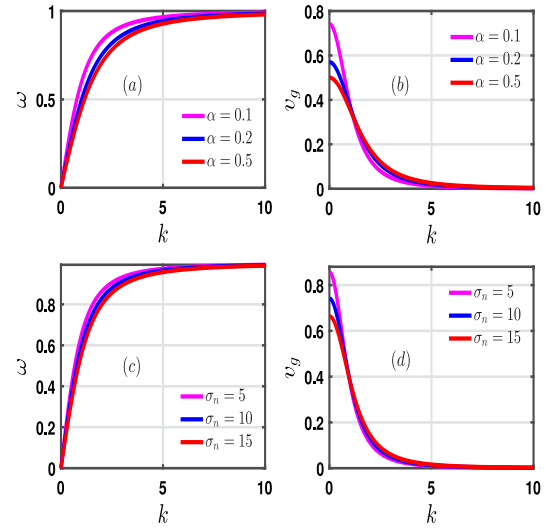


Fig. 1. (Color online) Plot of the frequency ω against k in panels (a) and (c), and the group velocity v_g versus k in panels (b) and (d) of wave packets for different values of α (upper panels for $\sigma_n = 5$) and σ_n (down panels for $\alpha = 0.1$).

with $\beta_\phi = \frac{2v_{g\frac{k}{\omega}}^2 c_2 - (k^2 + 3c_1)}{1 - c_1 v_{g\frac{k}{\omega}}^2}$, $\beta_n = c_1 \beta_\phi + 2c_2$, $\beta_{v_z} = v_{g\frac{k}{\omega}} \beta_n - \frac{2\omega}{k} (k^2 + c_1)^2$.

For $l = 1$, we find the following equation

$$i \frac{\partial \phi_1^{(1)}}{\partial \tau} + P \frac{\partial^2 \phi_1^{(1)}}{\partial \eta^2} + Q |\phi_1^{(1)}|^2 \phi_1^{(1)} - S \frac{\partial^2 \phi_1^{(1)}}{\partial \xi^2} = 0, \quad (18)$$

where

$$\begin{aligned} P &= \frac{1}{2} \frac{\partial^2 \omega}{\partial k^2} = -\frac{3c_1}{2} \frac{\omega^5}{k^4} = -\frac{3\omega^3}{2k^2} (1 - \omega^2), \\ Q &= -k \left(\alpha_{v_z} + \beta_{v_z} \right) - \frac{\omega}{2} (\alpha_n + \beta_n) \\ &\quad + \frac{\omega^3}{k^2} \left(c_2 (\alpha_\phi + \beta_\phi) + \frac{3}{2} c_3 \right), \\ S &= \frac{\omega^3}{2k^2} \frac{1 + \omega_p^2 - \omega^2}{\omega_p^2 - \omega^2}, \end{aligned} \quad (19)$$

Introducing the notation $\psi = \phi_1^{(1)}$, Eq. (18) become:

$$i \frac{\partial \psi}{\partial \tau} + P \frac{\partial^2 \psi}{\partial \eta^2} + Q |\psi|^2 \psi - S \frac{\partial^2 \psi}{\partial \xi^2} = 0. \quad (20)$$

This partial differential equation (20) for a complex field (wave-amplitude ψ) is well-known as the (2+1)-dimensional nonlinear Schrödinger equation, with P , Q and S the longitudinal dispersive coefficient, cubic nonlinear coefficient and the transverse dispersive coefficient depending on the external magnetic field, respectively. It describes the amplitude modulation of the electronegative plasma amplitude ψ of positive ion acoustic wave packets along the external magnetic field. We note that the coefficients of the obtained NLS equation depend on the system parameters specially, not only on the electronegative parameters such as the negative ion concentration ratio and the electron-to-negative ion temperature ratio (α and σ_n , respectively), but also on the magnetic field (ω_p).

In Fig. 1, we present the wave frequency ω given by Eq. (11) and the group velocity v_g given by Eq. (14) against the wave number k for different values of the electronegativity parameters (negative ion-to-electron density ratio α and electron-to-negative ion temperature ratio σ_n). From the two panels (Fig. 1a and 1c), which allow to explain the linear dispersion of features ion-acoustic waves, we find that as k increases, the wave frequency ω increases and it approaches an asymptotic value around 1 at higher wavenumber k . It approaches a zero frequency value for the values of k tending towards zero. Moreover, for a fixed value of σ_n (α), as the values of the negative ion-to-electron density ratio α increase, the wave frequency ω decreases. This implies

that to maintain the charge neutrality, the equilibrium negative ion density value will increase as the electron density increases. Moreover, this curve represents the relationship between the wavelength and the frequency of the wave, and it is useful in understanding the behavior of wave packets in the plasma system. Physically, the system gained more energy with greater values of the wavenumber, and this energy has a limit value for highest wavenumber. Such negative ion-to-electron density ratio α (σ_n) has also a significant effect on the group velocity of waves as shown in the two other panels (Fig. 1b and 1d). The group velocity of waves (v_g) decreases and approaches the zero value with increasing wave number (k) for different values of α (σ_n). One can see that v_g decreases with an increasing value of α (σ_n) and its behavior continues until reaching a certain value of k ($k = 1.12$), and then, (v_g) turns to increase by increasing α (σ_n). This leads to improve the speed of the information carried by the propagating wave packets in our plasma system.

Modulational instability analysis of IAWs in NLS equation

In this section, we are interested on the study of modulational instability (MI) considering (2+1)-dimensional ion acoustic waves governed by the nonlinear Schrödinger equation Eq. (20). The plane homogeneous solution of this equation is given by [1,52–55]

$$\psi = \psi_0 e^{i(Q|\psi_0|^2 \tau)} \quad (21)$$

where the constant ψ_0 represents the amplitude of the carrier wave. The stability of the solution (21) is studied by adding the small modulation $\delta\psi$ in the amplitude according to:

$$\psi = (\psi_0 + \delta\psi) e^{i(Q|\psi_0|^2 \tau)} \quad (22)$$

Substituting Eq. (22) into Eq. (20), collecting and linearizing terms in the first order, we obtain

$$i \frac{\partial \delta\psi}{\partial \tau} + P \frac{\partial^2 \delta\psi}{\partial \eta^2} + Q|\psi_0|^2 (\delta\psi + \delta\psi^*) - S \frac{\partial^2 \delta\psi}{\partial \xi^2} = 0 \quad (23)$$

with $\delta\psi^*$, the complex conjugate of $\delta\psi$.

Introducing $\delta\psi = U + iV$, with $(U, V) = (U_0, V_0) e^{i(K_x \xi + K_z \eta - \Omega \tau)} + c.c$ in Eq. (20), where $K_x \xi + K_z \eta - \Omega \tau$ is the modulation phase with Ω the frequency of the modulation and K_x, K_z the modulation wave numbers in x and z directions, respectively, and separating the real and imaginary parts, we obtain the coupled equations as follows:

$$\begin{aligned} i\Omega V_0 + [2Q|\psi_0|^2 + SK_x^2 - PK_z^2]U_0 &= 0 \\ i\Omega U_0 + [-SK_x^2 + PK_z^2]V_0 &= 0 \end{aligned} \quad (24)$$

From Eq. (24), we obtain the following nonlinear dispersion relation for the amplitude modulation of the ion acoustic waves modes:

$$\Omega^2 = [PK_z^2 - SK_x^2] \left[1 - \frac{2Q|\psi_0|^2}{PK_z^2 - SK_x^2} \right]. \quad (25)$$

The MI will be set in if the following condition is satisfied:

$$\frac{2Q|\psi_0|^2}{PK_z^2 - SK_x^2} > 1. \quad (26)$$

Letting $K^2 = K_x^2 + K_z^2$, the modulation wave number and $\alpha_\theta = \frac{K_z}{K_x}$ the parameter related to the modulational obliqueness θ ($\theta = \arctan(\alpha_\theta)$) and the nonlinear dispersion relation Eq. (25) reduces to

$$\Omega^2 = K^4 \left(\frac{P\alpha_\theta^2 - S}{1 + \alpha_\theta^2} \right)^2 \left[1 - \frac{2|\psi_0|^2(1 + \alpha_\theta^2)}{K^2} \frac{Q/P}{\alpha_\theta^2 - S/P} \right] \quad (27)$$

From Eq. (27), we find that there exists a critical wave number K_c such that

$$K_c^2 = 2|\psi_0|^2(1 + \alpha_\theta^2) \frac{Q/P}{\alpha_\theta^2 - S/P} > K^2, \quad (28)$$

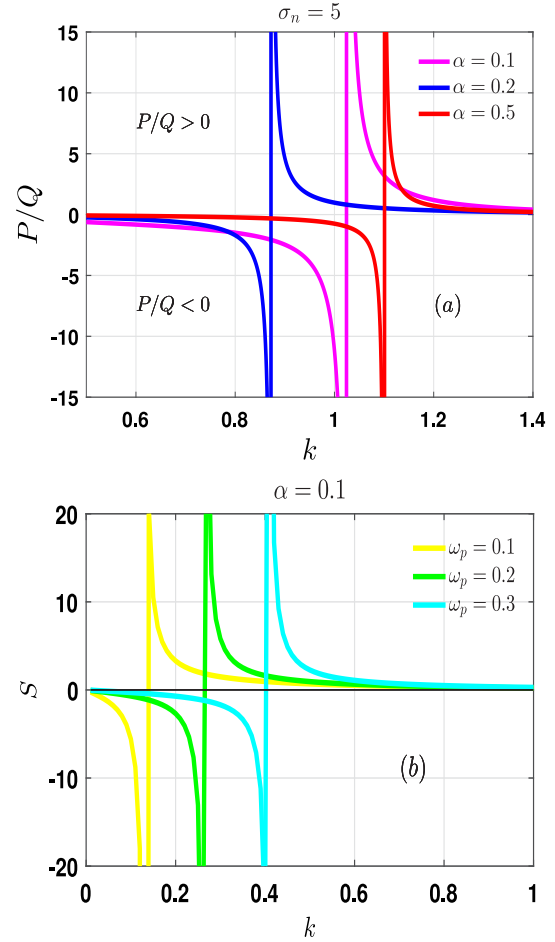


Fig. 2. (Color online) Panels show P/Q against the carrier wave number k for different values of negative ion to electron density ratio α (a) as in Fig. 1 and S versus the carrier wave number k for different values of plasma frequency ω_p (b).

and the instability growth rate Γ ($\Omega = i\Gamma$) is given by

$$\Gamma = K^2 \left(\frac{P\alpha_\theta^2 - S}{1 + \alpha_\theta^2} \right) \left[\frac{K_c^2}{K^2} - 1 \right]^{1/2} \quad (29)$$

From Eq. (25), the maximum growth rate $\Gamma_{max} = Im(\Omega)_{max}$ can be obtained as $\Gamma_{max} = Q|\psi_0|^2$ provided $Q|\psi_0|^2 = PK_z^2 - SK_x^2$ is satisfied.

The MI may be observed if one of the following two conditions is verified

$$QP > 0, \quad \alpha_\theta^2 > S/P = \frac{1 + \omega_p^2 - \omega^2}{3(\omega^2 - 1)(\omega_p^2 - \omega^2)}, \quad (30)$$

or

$$QP < 0, \quad \alpha_\theta^2 < S/P = \frac{1 + \omega_p^2 - \omega^2}{3(\omega^2 - 1)(\omega_p^2 - \omega^2)}. \quad (31)$$

It is clear that there also exists a critical value of θ , as $\theta_c = \arctan(S/P)^{1/2}$ resulting from Eqs. (30) and (31) such that the MI occurs when either $PQ > 0$ and $\theta > \theta_c$ or $PQ < 0$ and $\theta < \theta_c$ holds and also indicate that $\omega > \omega_p$ and $\omega < \omega_p$, respectively. Hence, the instability condition depends on the sign of the product PQ and Figs. 2(a) and 2(b) show numerically the variations of the coefficients S and P/Q given by Eq. (19) with the different physical parameters (α , ω_p and σ_n). According to the choice of these physical parameters, one can see that the coefficient S gains its sign. The expression of S clearly shows that there is a cutoff at $\omega = \omega_p$ corresponding to the simple ion cyclotron oscillations (dimensional form) in electronegative plasma, which does not participate in the wave group dynamics and that ω_p plays a decisive role in the propagation dynamics of the nonlinear

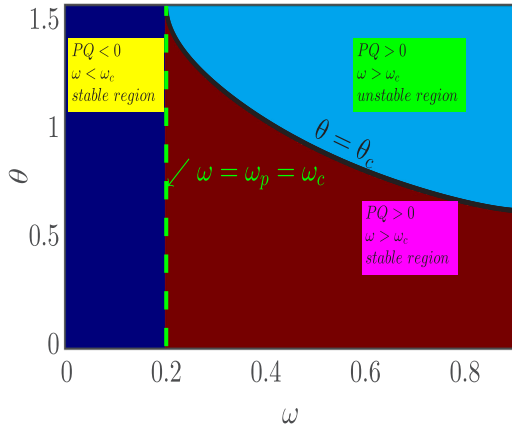


Fig. 3. The stable/unstable regions for fixed values of the system parameters $\alpha = 0.1$, $\sigma_n = 5$ and $\omega_p = 0.2$ is shown by the contour plots of $P/Q = 0$ against the wave frequency ω and the modulation angle θ .

ion acoustic waves [57]. The curves of P/Q in (ω, θ) -plane presented in Fig. 3 show the information about the positive and negative regions of product PQ according to the analytical expressions given in Eqs. (30) and (31) and the stable/unstable regions for fixed values of the system parameters. One can see that dispersion coefficients P , S and nonlinearity coefficient Q are related to α , σ_n and ω_p . It turns out that these physical parameters could significantly affect the stability characteristics of IAWs in our plasma system. Therefore, the modulation instability can be studied numerically. For that, the MI growth rate is shown in Fig. 4. The panels of Fig. 4 show the evolution of the growth rate of the MI for different values of the magnetic field ω_p in the case of some values of α and σ_n . As it increases, one clearly notices an extension of the zone of instability in the plane and the increasing of the maximum growth rate. We find that effect of increasing values of α and σ_n is to increase the modulational instability growth rate with cutoffs at higher wave numbers of modulation for different values of ω_p . We should precise that some studies were carried out recently that showed the strong impact of parameters such as the negative ion to electron concentration ratio and electron-to-negative ion temperature ratio [14–17,39]. It is therefore, of high importance here to insist on the combined effects due to such parameters and the magnetic field. Therefore, this implies that the unstable regions will also be modified with the changing of α , σ_n and ω_p .

Variational approach for NLS equation

In this section, we follow the standard variational approach [58,69,70] for the analysis of Eq. (20). Let us consider the following Euler-Lagrange equation:

$$\frac{\partial}{\partial \tau} \left(\frac{\partial L}{\partial \psi^*} \right) + \frac{\partial}{\partial \eta} \left(\frac{\partial L}{\partial \psi^*} \right) + \frac{\partial}{\partial \xi} \left(\frac{\partial L}{\partial \psi^*} \right) - \frac{\partial L}{\partial \psi^*} = 0 \quad (32)$$

Using Eq. (32), we find the following Lagrangian of Eq. (20)

$$L = \frac{i}{2} \left(\psi \frac{\partial \psi^*}{\partial \tau} - \psi^* \frac{\partial \psi}{\partial \tau} \right) + P \left| \frac{\partial \psi}{\partial \eta} \right|^2 - S \left| \frac{\partial \psi}{\partial \xi} \right|^2 - \frac{Q}{2} |\psi|^4 \quad (33)$$

We now proceed by assuming a trial function solution of Eq. (20) of the form

$$\psi(\xi, \eta, \tau) = C(\tau) e^{-\frac{\xi^2}{2X^2(\tau)} - \frac{\eta^2}{2Y^2(\tau)} + i a(\tau) \xi^2 + i b(\tau) \eta^2 + i \varphi(\tau)}, \quad (34)$$

where $C(\tau)$ is the complex amplitude, $(X(\tau), Y(\tau))$ the spacial width, $(a(\tau), b(\tau))$ the frequency chirp and $\varphi(\tau)$ the phase of the carrier wave.

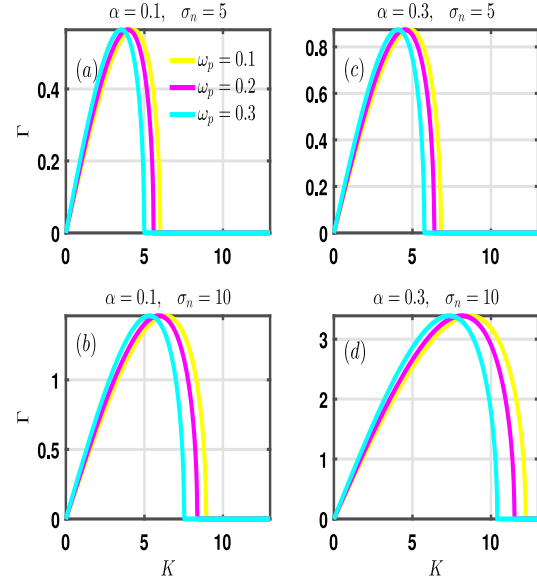


Fig. 4. (color online) Plot of the modulational instability growth rate against the modulation wave number K for different values of ω_p and fixed values of α and σ_n : $\alpha = 0.1$ and $\sigma_n = 5$ (see the panel (a)), $\alpha = 0.1$ and $\sigma_n = 10$ (see the panel (b)), $\alpha = 0.3$ and $\sigma_n = 5$ (see the panel (c)) and $\alpha = 0.3$ and $\sigma_n = 10$ (see the panel (d)).

Inserting the trial solution Eq. (34) into Eq. (33), we obtain the following reduced Lagrangian

$$\begin{aligned} \langle L \rangle &= \int_{-\infty}^{+\infty} \int_{-\infty}^{+\infty} L d\xi d\eta \\ &= \frac{\pi}{2} \left[i \left(C \frac{\partial C^*}{\partial \tau} - C^* \frac{\partial C}{\partial \tau} \right) XY + |\psi|^2 \frac{\partial a}{\partial \tau} X^3 Y \right. \\ &\quad \left. + |\psi|^2 \frac{\partial b}{\partial \tau} XY^3 - S |\psi|^2 \left(\frac{1}{X^4} + 4a^2 \right) X^3 Y \right. \\ &\quad \left. + P |\psi|^2 \left(\frac{1}{Y^4} + 4b^2 \right) XY^3 - Q |\psi|^4 XY \right] \end{aligned} \quad (35)$$

Now, we can find the variation of $\langle L \rangle$ with respect to the various characteristic of Gaussian parameters of the carrier wave $C(\tau)$, $X(\tau)$, $Y(\tau)$, $a(\tau)$, $b(\tau)$ and $\varphi(\tau)$.

Using the Euler-Lagrange equations of each parameter, we find the following dynamic equations:

$$\begin{cases} |C|^2 XY = |C_0|^2 X_0 Y_0, \\ \frac{da}{d\tau} = 4Sa^2 + \frac{S}{X^4} - \frac{QE_0}{2X^3Y}, \\ \frac{db}{d\tau} = -4Pb^2 + \frac{P}{Y^4} - \frac{QE_0}{2XY^3}, \\ \frac{\partial^2 X}{\partial \tau^2} = \frac{4S^2}{X^3} + \frac{2SQE_0}{X^2Y}, \\ \frac{\partial^2 Y}{\partial \tau^2} = \frac{4P^2}{Y^3} - \frac{2PQE_0}{XY^2}, \\ \frac{d\varphi}{d\tau} = -\frac{S}{X^2} + \frac{P}{Y^2} - \frac{3QE_0}{2XY}, \end{cases} \quad (36)$$

where $E_0 = \int_{-\infty}^{+\infty} \int_{-\infty}^{+\infty} |\psi|^2 d\xi d\eta = |C|^2 XY = |C_0|^2 X_0 Y_0$ is the constant linked to the energy of the wave, with $C_0 = C(0)$, $X_0 = X(0)$ and $Y_0 = Y(0)$. The differential equations of the set of Eq. (36) represent dynamical equations of the amplitude, widths, chirps and phase of the ion acoustic waves in electronegative plasma in the presence of the external magnetic field. The associated potential of this system can be expressed as

$$V(X, Y) = -\frac{1}{2} \left(\frac{dX}{d\tau} \right)^2 - \frac{1}{2} \left(\frac{dY}{d\tau} \right)^2 \quad (37)$$

Inserting the fourth and fifth relations of Eq. (36), using the normalized variables $Z(\tau) = X(\tau)/X_0$, $T(\tau) = Y(\tau)/Y_0$, we finally obtain the following scalar potential of the system describing the movement of

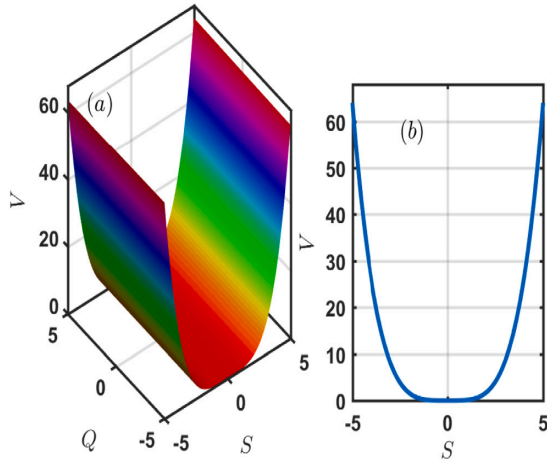


Fig. 5. Plot of the potential function given by Eq. (38) versus the (S, Q) -plane for $\alpha = 0.1$, $\sigma_n = 5$ and $\omega_p = 0.2$.

particles in the potential well:

$$V(Z, T) = \frac{\lambda_1}{Z^2} + \frac{\lambda_2}{T^2} + \frac{\lambda_1 + \lambda_2}{ZT} - (\lambda_1 + \beta_1 + \lambda_2 + \beta_2) \quad (38)$$

where the constants λ_1 , β , λ_2 and β_2 are defined as follows $\lambda_1 = \frac{2S^2}{X_0^4}$, $\beta_1 = \frac{2P^2}{Y_0^4}$, $\lambda_2 = \frac{2SQE_0}{X_0^3Y_0}$ and $\beta_2 = -\frac{2PQE_0}{X_0Y_0^3}$. Moreover, Fig. 5 shows the plot of the potential function given by Eq. (38). The figure presents a potential well of almost parabolic shape with a fairly steep slope. We note that a stable dynamical behavior can be obtained when considering values of nonlinear and magnetic field parameters (Q, S) around the bottom of the potential well. Consequently, a stable propagation of ion-acoustic wave can be achieved in the plasma. The time evolution of the solution parameters has been numerically investigated using the fourth-order Runge–Kutta computational method, which allows to integrate the system of equations obtained through the variational approach. Panels of Fig. 6 show the evolution of the Gaussian parameters using Eq. (36) as a function of the direction of propagation τ : the amplitude $C(\tau)$, the spatial widths $X(\tau)$, $Y(\tau)$, the spatial chirps $a(\tau)$, $b(\tau)$ and the phase $\varphi(\tau)$ of the carrier wave. In this figure, when the amplitude $C(\tau)$ decreases, the spatial widths $X(\tau)$, $Y(\tau)$ increase, this leads to the fact that such wave can propagate in our plasma model. In order to confirm the results from the variational approach, we studied the system numerically using the Split Step Fourier Method (SSFM). For this numerical simulation, the solution obtained using the variational approach was used as the input solution. Fig. 7 presents the exact (input profile) and numerical (output profile) solutions of Eq. (20). These two profiles are almost similar in amplitude, but with a spatial spreading of soliton in the zone of modulational instability. Therefore, a good agreement between analytical and numerical results are observed. We can clearly see that the ion-acoustic wave can propagate through the plasma system maintain its profile. Basically, this arises under the interplay between dispersion and nonlinearity for the system parameters taken in the modulational instability zone.

Conclusion

In this work, the nonlinear propagation of ion acoustic waves in magnetized electronegative plasma have been studied. Using the reductive perturbation method, the nonlinear Schrödinger equation modeling the evolution of (2+1)-dimensional ion-acoustic waves in electronegative plasma in the presence of external magnetic field has been obtained and analyzed. Indeed, the modulational instability of planar waves has been investigated based on the magnetic field, the negative ion concentration ratio and the electron-to-negative temperature ratio. The

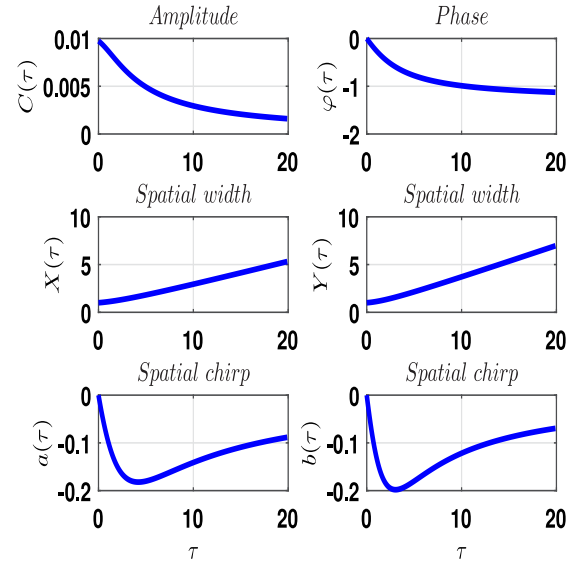


Fig. 6. Evolution of Gaussian parameters: amplitude $C(\tau)$, spatial widths $X(\tau)$, $Y(\tau)$, spatial chirps $a(\tau)$, $b(\tau)$ and phase φ .

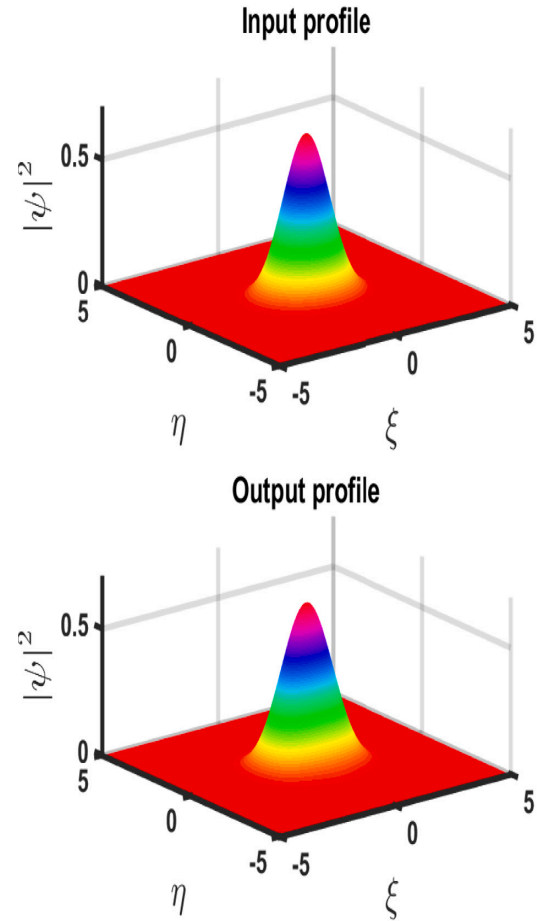


Fig. 7. Exact solution (input profile) in upper panel and numerical solution (output profile) in down panel of modified NLS Eq. (20).

instability areas have been studied via analytical and numerical investigation of modulational instability. The effect of increasing values of α and σ_n is to increase the modulational instability growth rate with cutoffs at higher wave numbers of modulation of different values of the magnetic field. Therefore, it comes that this plasma system can support propagation of ion-acoustic solitons as informations carrier. The variational method has been performed in order to describe the

main characteristics of IAWs, involving trial function solution of NLS equation. It shows that when the amplitude $C(\tau)$ decreases, the spatial widths $X(\tau)$, $Y(\tau)$ increase, this leads to the fact that such wave can propagate in our plasma model. In addition, the exact solution (input profile) and numerical solution (output profile) have been also discussed. These solutions have been investigated and the emergence and propagation of stable ion-acoustic wave have been confirmed in electronegative plasma in the presence of the external magnetic field. The current findings are useful for understanding the propagation characteristics of ion-acoustic solitons in the magnetized electronegative plasma. This present work can be useful in various fields such as plasma etching, surface treatment, ion implantation, and fabrication of semiconductor devices.

CRediT authorship contribution statement

Stéphanie Ganyou: Conceived the original idea, Developed the theory, Performed the analytic calculations, The numerical simulations and drafted the manuscript. **Serge I. Fewo:** Designed the study, Participated in the elaboration of the numerical simulations, The writing and the review editing of the paper. **Chérif S. Panguetna:** Conceived the original idea, Verified and contributed to the interpretation of the results. **Timoléon C. Kofané:** Supervised and validated the project.

Declaration of competing interest

The authors declare that they have no known competing financial interests or personal relationships that could have appeared to influence the work reported in this paper.

Data availability

Data will be made available on request.

References

- [1] Misra AP, Bhowmik C. *Phys Plasmas* 2007;14:012309.
- [2] Misra AP, Bhowmik C, Shukla PK. *Phys Plasmas* 2009;16:1072116.
- [3] Saha A, Banerjee S. *Dynamical systems and nonlinear waves in plasmas*. CRC Press; 2021.
- [4] Ostrikov KN, Kumar S, Sugai H. *Phys Plasmas* 2001;7:3490.
- [5] Djebli M. *Phys Plasmas* 2003;10:4910.
- [6] Marmun AA, Shukla PK. *Phys Plasmas* 2003;10:1518.
- [7] Islam KA, Deebe F, Kamal-Al-Hassan Md. *Heliyon* 2020;6:e05373.
- [8] Hassan MR, Biswas S, Habib K, Sultana S. *Results Phys* 2022;33:105106.
- [9] Mushtaq A, Saeed R, Haque Q. *Phys Plasmas* 2009;16:084501.
- [10] Misra AP. *Phys Plasmas* 2009;16:033702.
- [11] Kono M, Vranjes J, Batool N. *Phys Rev Lett* 2014;112:105001.
- [12] Guo S, Mei L. *Phys Plasmas* 2014;21:082303.
- [13] Jahan S, Shikha RK, Mannan A, Mamun AA. *Plasma* 2021;5:1–11.
- [14] Wang ZX, Liu JY, Zou X, Liu Y, Wang XG. *Chin Phys Lett* 2003;20:1537.
- [15] Panguetna CS, Tabi CB, Kofané TC. *Phys Plasmas* 2017;24:092114.
- [16] Panguetna CS, Tabi CB, Kofané TC. *Commun Nonlinear Sci Numer Simul* 2018;55:326.
- [17] Panguetna CS, Tabi CB, Kofané TC. *J Theor Appl Phys* 2019;13(3):237–49.
- [18] Zou X, Liu JY, Wang ZX, Gong Y, Liu Y, Wang XG. *Chin Phys Lett* 2004;21:1572.
- [19] Zou X, Liu H-P, Hang XS. *Chin Phys Lett* 2011;28:125201.
- [20] Aslaninejad M, Yasserian K. *Phys Plasmas* 2012;19:033504.
- [21] El-Labany SK, El-Shamy EF, Behery EE. *Phys Plasmas* 2013;20:122114.
- [22] Aanesland A, Bredin J, Chabert P. *Plasma Sources Sci Technol* 2014;23:044003.
- [23] Rahman O, Haider MM. *Theor Phys* 2019;4(2):47–56.
- [24] El-Labany SK, Behery EE, El-Razek HNA, Abdelrazek LA. *Eur Phys J D* 2020;74:104.
- [25] Akbar MA, Salam Md Abdus, Zulfikar Ali M. *Results Phys* 2023;51:106682.
- [26] Vladimirov SV, Ostrikov K, Yu MY, Morfill GE. *Phys Rev E* 2003;67:036406.
- [27] Rahman O, Mamun A, Ashrafi KS. *Astrophys Space Sci* 2011;335:425–33.
- [28] Liu T-L, Wang Y-L, Lu Y-Z. *Chin Phys B* 2015;24:025202.
- [29] Selim MM. *Eur Phys J Plus* 2016;131:93.
- [30] Chowdhury NA, Mannan A, Hasan MM, Mamun AA. *Chaos* 2017;27:093105.
- [31] Massey H. *Negative ions*. 3rd ed. Cambridge, UK: Cambridge University Press; 1976.
- [32] Khondaker S, Mannan A, Chowdhury NA, Mamun AA. *Contrib Plasma Phys* 2019;59:e201800125.
- [33] Mishra MK, Arora AK, Chhabra RS. *Phys Rev E* 2002;66:046402.
- [34] Mishra MK, Chhabra RS, Sharma SR. *Phys Rev E* 1995;51:4790.
- [35] Pedersen A. *Tellus* 1965;17:02.
- [36] Sabry R, Moslem WM, Shukla PK. *Phys Plasmas* 2009;16:032302.
- [37] Abdelwahed HG, El-Shewy EK, Zahran MA, Elwakil SA. *Phys Plasmas* 2016;23:022102.
- [38] Rufai OR. *Heliyon* 2019;5:e01976.
- [39] Tabi CB, Panguetna CS, Kofané TC. *Phys Rev B* 2018;545:370.
- [40] Jacquinet J, McVey BD, Scherer JE. *Phys Rev Lett* 1977;39:88.
- [41] Kourakis I, Shukla PK. *Nonlinear Process Geophys* 2005;12:407.
- [42] Kimura T, Imagaki K, Ohe K. *J Phys D* 1998;31:2295.
- [43] Vender D, Stoffels WW, Stoffels E, Kroesen GMW, de Hoog FJ. *Phys Rev E* 1995;51:2436.
- [44] Franklin RN. *Plasma Sources Sci Technol* 2002;11:A31.
- [45] Lieberman MA, Lichtenberg A. *Principle of plasma discharges and materials processing*. 2nd ed. New York: Wiley; 2005.
- [46] Chabert P, Lichtenberg AJ, Lieberman MA. *Phys Plasmas* 2007;14:093502.
- [47] Plihon N, Chabert P, Corr CS. *Phys Plasmas* 2007;14:013506.
- [48] Meige A, et al. *Phys Plasmas* 2007;14:053508.
- [49] Chung TH. *Phys Plasmas* 2009;16:063503.
- [50] Anowar MG, Ashrafi KS, Mamun AA. *J Plasma Phys* 2011;77:133.
- [51] Duha S, Rahman MS, Mamun AA, Anowar GM. *J Plasma Phys* 2012;78:279.
- [52] Xue J-K. *Phys Plasmas* 2005;12:062313.
- [53] Misra AP, Shukla PK. *Phys Plasmas* 2008;15:122107.
- [54] Bains AS, Misra AP, Saini NS, Gill TS. *Phys Plasmas* 2010;17:012103.
- [55] Shalini A, Misra P, Saini NS. *J Theor Appl Phys* 2017;11:217–24.
- [56] Abdikian A. *Phys Plasmas* 2017;24:052123.
- [57] Biswas A, Chakraborty D, Pramanik S, Ghosh S. *Phys Plasmas* 2021;28:062105.
- [58] Anderson D. *Phys Rev Lett A* 1983;27:6.
- [59] Basnet S, Patel A, Khanal R. *Plasma Phys Control Fusion* 2020;62:115011.
- [60] Hatami MM. *Sci Rep* 2021;11:9531.
- [61] Gan B-X, Chen Y-H, Yu MY. *J Appl Phys* 2007;101:113310.
- [62] Zheng X, Chen Y, Hu H, Wang G, Huang F, Dong C, et al. *Phys Plasmas* 2009;16:023701.
- [63] Leblond H. *J Phys B: At Mol Opt Phys* 2008;41:043001.
- [64] Sabry R, Moslem WM, Shukla PK. *Plasma Phys Control Fusion* 2012;54:035010.
- [65] Haque MN, Mannan A. *Contrib Plasma Phys* 2020;61:e202000161.
- [66] El-Taibany WF, El-Bedwehy NA, El-Shafeay NA, El-Labany SK. *Galaxies* 2021;9:48.
- [67] Gill TS, Bedi C, Bains AS. *Phys Plasmas* 2009;16:032111.
- [68] Bacha M, Gougama LA, Tribeche M. *Physica A* 2017;466:199–210.
- [69] Aközbek N, Bowden CM, Talebpour A, Chin SL. *Phys Rev E* 2000;61(4):4540.
- [70] Jisha CP, Kuriakose VC, Porsezian K. *Phys Lett A* 2006;352:496–9.



Two-dimensional dynamics of ion-acoustic waves in a magnetised electronegative plasma

STÉPHANIE GANYOU¹, CHÉRIF S PANGUETNA¹, SERGE I FEWO¹ , CONRAD B TABI²
and TIMOLÉON C KOFANÉ^{1,2}

¹Laboratory of Mechanics, Materials and Structures, Department of Physics, Faculty of Science,
The University of Yaounde I, P.O. Box 812, Yaounde, Cameroon

²Department of Physics and Astronomy, Botswana International University of Science and Technology,
Private Bag 16, Palapye, Botswana

*Corresponding author. E-mail: sergefewo@yahoo.fr

MS received 28 November 2022; revised 17 August 2023; accepted 19 September 2023

Abstract. We consider a plasma model made of negative ions and electrons in Boltzmann distribution and cold mobile positive ions, under the influence of an external magnetic field, to study the propagation of ion-acoustic waves (IAWs). From the hydrodynamic equations of the two-dimensional (2D) electronegative plasma, the dynamics of the system is reduced via the reductive perturbation method to the Davey–Stewartson (DS) equations. Using the linear stability analysis of planar waves, an expression of the modulational instability growth rate is derived, and its response to system parameters, such as the negative ion concentration ratio, the electron-to-negative ion temperature ratio and the magnetic field is discussed. It comes out that the instability occurs for high values of the negative ion concentration ratio and in a very restrained area of small magnetic field values. The growth rate is maximum for high values of both the electron-to-negative ion temperature ratio and the magnetic field. The existence of IAWs in the model is confirmed. One-dromion and two-dromion solutions are investigated analytically using the Hirota's bilinear method and numerically. The impact of the magnetic field is discussed in that context, and particular attention is given to dromion interactions under different scenarios. We noted a slowing effect on the propagation of the dromion solutions in the presence of the magnetic field. Elastic collision of two-dromion solutions is observed during their evolution, with an acceleration of the process in the presence of the magnetic field.

Keywords. Magnetised electronegative plasma; Davey–Stewartson equations; modulational instability; dromions solutions.

PACS Nos 52.35.Fp; 52.25.Xz; 52.35.Sb; 52.35.Mw

1. Introduction

Over the past 20 years, solitonic structures have been investigated in nonlinear physical systems and their importance has been discussed in a broad range of contexts that include non-exhaustively optic communication [1–6], biophysics [7–10], Bose–Einstein condensates [11–13] and plasma physics [14,15]. By supplying energy to a neutral gas, one can cause a formation of charged particles (electrons, ions), which with the non-ionised atoms or molecules of the gas, become the components of the generated plasma. Plasma is an ionised gas. The term plasma was first officially introduced in physics by Irving Langmuir in 1928 [16] to describe the

ionised gas by its behaviour in discharge tubes. Following this discovery, several scientific researchers became interested in the study of plasma physics. The way the energy is transferred depends not only on the method of production of plasma, but also on its physical properties and potential applications, both in the laboratory and in technology. On the scale of the Universe, plasma represents up to 99% of the available matter. One of its most important characteristics is that it displays high sensitivity to electric and magnetic fields. Many scientists are interested in studying plasma because of their temperature, density and the types of particles they contain which are its main characteristics. For many years now, the effects of charged particles (electrons, positive

or negative ions) on plasmas, such as quantum plasmas [17–19], dusty plasmas [20–25], electronegative plasmas [26–28], magnetised electronegative plasmas [29–38], just to name a few, have long been the subject of significant interest. From the seminal work of Washimi and Taniuti [39], who first derived the KdV equation for ion-acoustic waves (IAWs) in the plasmas, soliton theory has been the centre of interest for the plasma physics community with a particular interest in nonlinear phenomena related to structures, instabilities, wave interaction, wave–particle interaction and methodology related to plasma nonlinear oscillations. Resulting from the suitable balance between nonlinear and dispersive effects, IAWs and solitons in general, can spread over long distances, keeping intact their characteristics and shape. Considered as one of the four states of matter, just like solids, liquids and gas, plasmas are composed of positive ions in addition to negative ions and electrons and when a significant amount of negative ions is involved, they are known as electronegative plasma (ENP). Various applications in plasma science and industry [40–43] and the proof of its existence in astrophysics, space and laboratory experiments make ENPs a subject of growing interest, as witnessed by recent contributions both in one-dimensional and multi-dimensional contexts. ENPs have been generated in the laboratory by different methods [44–46], which corroborate their presence in many space observations, which include $(H^+ - H^-)$ and $(H^+ - O_2^-)$ and in the D- and F-regions of the Earth’s ionosphere [47,48]. Moreover, the dynamics and head-on collisions of IAWs in $Ar^+ - F^-$ plasmas have been reported experimentally [49], while Ichiki *et al* [44] addressed the propagation features of IAWs in $Ar^+ - SF_6^-$ plasma. Theoretically, based on such experimental observations, Mamun *et al* [50] regarded the existence of ion-acoustic (IA) and dust ion-acoustic (DIA) waves in an ENP constituted by Boltzmann negative ions, Boltzmann electrons and cold mobile positive ions. It was also highlighted recently by Tabi and co-workers that the negative ion concentration ratio and the electron-to-negative ion temperature ratio affect the modulational instability (MI) in one-, two- and three-dimensional contexts [27,28,51,52]. In addition to the above, the structure of the electronegative plasma sheath without a magnetic field was investigated in refs [26–28] and with magnetic field in ref. [29]. The study of other aspects and characteristics of such plasmas waves, related to their response to external magnetic fields [53–55] in the vicinity of the Korteweg–de Vries (KdV) equations are obtained from the reductive perturbation approximation. In the context of the present work, we show that when two and higher dimensions are considered, magnetised plasma can asymptotically be described by the Davey–Stewartson equations (DSEs).

It is, however, important to recall that DSEs are nonlinear partial differential equations, as the Riemann wave system [56], the Novikov–Veselov system [57], the chemotaxis models [58], just to name a few, that were first introduced in fluid dynamics to understand the evolution of three-dimensional wave packets in water of finite depth [59]. Since then, they have found application in many areas of physics, most notably in nonlinear optics [60] and related fields such as Bose–Einstein condensates [61] and electromagnetic waves in ferromagnets [62]. A surprising and interesting property of the DSEs is that they are among the few multidimensional systems whose inverse scattering transform is well known [63,64], and one can actually get a broad range of exact solutions among which are rogue waves [65–67], Langmuir waves [68–70] and dromions [27,71,72]. Dromions, defined by an exact and nonlinear solution of any of a large class of two-dimensional partial differential equations, were first time investigated theoretically by Boiti *et al* [73]. A particular and important characteristic of dromion solutions is that they are localised wave packets in various physical systems, such as plasma physics, fluid dynamics and nonlinear optics [74] and the interactions of dromions for the $(2 + 1)$ -dimensional equations may be elastic or inelastic [75–77]. On this basis, important additional features, compared to the NLS equation, may take place and describe very rich behaviours of the multidimensional MI activation and the resulting plasma modes, especially when system parameters are suitably chosen. The present paper pays attention to a comprehensive analysis of MI and additionally proposes exact solutions to the DS equations, using the Hirota’s bilinear method [71], and their response to changing system parameters, such as the electron-to-negative ion temperature ratio, the negative ion concentration ratio and more importantly, the magnetic field. The Hirota’s method was introduced for the first time by Hirota [78] to construct multisoliton solutions of integrable nonlinear evolution equations. The method is an algebraic one, based on the bilinear form of the nonlinear equation, used to solve nonlinear partial differential equations (PDEs). The main feature of the method is the derivation of multisoliton solutions of some physical systems [79–82].

In the present work, we extend the results of a previous model of electronegative plasma studied by Panguetna *et al* [27] by including the external magnetic field. This electronegative plasma, in the presence of the external magnetic field, is the so-called magnetised electronegative plasma. Made of a significant number of negative ions, with electrons both in Boltzmann distribution, cold mobile positive ions and the magnetic field, the dynamics of the system is reduced to the DS equations via the reductive perturbation method. Through the linear

stability analysis of planar waves, an expression of the modulational instability growth rate is derived, enabling the determination of instability/stability zones where the generation of stable solitary solutions is possible. Using the MI, the response to physical system parameters, such as the negative ion concentration ratio, the electron-to-negative ion temperature ratio and the magnetic field is investigated. Another major point of this work is the investigation of the impact of the magnetic field on the dromion-like solutions and their interactions under different scenarios. In addition, one-dromion and two-dromion-like solutions are studied analytically using the Hirota's bilinear method. Like some previous theoretical studies conducted in electronegative plasma, the present work also has the potential to enhance in the real world, several applications across various fields, such as plasma etching (dry etching) or thin film deposition, ion implantation (semiconductor doping), surface treatment (cleaning of the surfaces by sputtering) and fabrication of semiconductor devices [83–85]. Moreover, the performance of these processes can be improved by confining the plasma and increasing the reaction rate due to the presence of the magnetic field. The presented results are obtained using the Matlab software for numerical simulations and plotting.

The rest of the paper is outlined as follows. In §2, we present the governing model equations, and the reductive perturbation method is used to find its corresponding DS equations. In §3, the MI analysis is performed. Results are presented based on the competitive effects between the magnetic field and the other essential system parameters, namely the electron-to-negative-ion temperature ratio and the negative-ion concentration ratio. Dromion-like solutions for the DS equations are discussed in §4, along with their response to the change of parameters. Section 5 is devoted to some concluding remarks.

2. Model description

Plasmas consisting of positive ions, electrons and a significant number of negative ions have been the subject of intense theoretical and experimental interest over the last few years [40,42,86,87]. The so-called electronegative plasmas, which are generated in both laboratory and space environments [40,42,49,85–91] are of particular interest. Electronegative plasmas are contaminated in most cases by solid impurities, and are not practically neutral because they are charged by absorbing electronegative plasma electrons and positive as well as negative ions. Electronegative plasmas are, in fact, dusty electronegative plasmas [22,92–97], in which the density of heavy negative ions is much

larger than the electron density, by a factor of ~ 10 –1000. The particle velocity distributions play crucial roles in characterising the fundamental physical properties of the nonlinear phenomena in plasma systems. For instance, to understand the dynamics of collisionless and correlated particle systems, which are characterised by non-Maxwellian particle distribution, three-particle distributions, such as Vasyliunas distribution or kappa distribution [98], Cairns *et al* [99] and Tsallis [100] distributions, have been proposed. In this work, we have considered an electronegative plasma containing Boltzmann electrons and Boltzmann negative ions. The main physical reason is that the experimental and theoretical understandings of the interaction and collision between plasma particle species in plasma physics have shown that they exchange their momentum and kinetic energy to maintain thermal equilibrium during their collisions. As it is well-known, for systems that are in thermodynamical equilibrium, the distribution function to describe these plasma particles is the prominent Maxwell–Boltzmann distribution function which depends exponentially on the velocities of the plasma particles. In addition, the inertia of the electron and negative ions is neglected because the phase velocity of IAWs is much higher than the thermal speed of the positive ions and in turn, much lower than the thermal speeds of the electrons and negative ion. The self-consistent electric field acting in a plasma retards the most mobile [50,101,102] charged particles, which usually leads to a Boltzmann distribution of electrons.

In the absence of the magnetic field, the model has been extensively used in one, two and three dimensions to study the emergence of rogue waves, solitons and their link to the MI phenomenon. Also, the dust plasma period is assumed to be much lower than the time scale of the IAWs, which makes the dust to be stationary. However, in the presence of a magnetic field, we consider the following fluid continuity and momentum equations for the positive ions:

$$\frac{\partial n_p}{\partial t} + \nabla \cdot (n_p \mathbf{u}_p) = 0, \quad (1a)$$

$$\frac{\partial \mathbf{u}_p}{\partial t} + (\mathbf{u}_p \cdot \nabla) \mathbf{u}_p = -\frac{q_p}{m_p} \nabla \Phi + \frac{q_p}{m_p} (\mathbf{u}_p \times \mathbf{B}), \quad (1b)$$

where \mathbf{u}_p , q_p , m_p , $\mathbf{E} = -\nabla \Phi$ and $\mathbf{B} = (0, 0, B)$ are the positive ion mean velocity, ion charges, ion mass, the electrostatic potential and external magnetic field, respectively. Variations of the electrostatic potential Φ are described by the Poisson's equation

$$\nabla^2 \Phi = -4\pi e(Z_p n_p - Z_n n_n - n_e), \quad (2)$$

where

$$n_e = n_{e0} e^{\frac{e\Phi}{k_B T_e}}, \quad n_n = n_{n0} e^{\frac{\sigma_n e\Phi}{k_B T_e}},$$

with the electron-to-negative ion temperature ratio $\sigma_n = T_e/T_n$, the positive ions charge $q_p = +Z_p e$ of mass m_p , the negative ions charge $q_n = -Z_n e$ of mass m_n and the electron charge $q_e = -e$, mass m_e . We consider for simplicity by introducing the Nabla (∇) operator as

$$\nabla = \frac{\partial}{\partial x} \mathbf{e}_x + \frac{\partial}{\partial z} \mathbf{e}_z,$$

indicating that the waves propagate in the (x, z) -plane and the normalised ion continuity, momentum and Poisson's equations take the form of the following system of scalar equations:

$$\frac{\partial n}{\partial t} + \frac{\partial(nu_x)}{\partial x} + \frac{\partial(nu_z)}{\partial z} = 0, \quad (3a)$$

$$\frac{\partial u_x}{\partial t} + \left(u_x \frac{\partial}{\partial x} + u_z \frac{\partial}{\partial z} \right) u_x = -\frac{\partial \phi}{\partial x} + \Omega u_y, \quad (3b)$$

$$\frac{\partial u_y}{\partial t} + \left(u_x \frac{\partial}{\partial x} + u_z \frac{\partial}{\partial z} \right) u_y = -\Omega u_x, \quad (3c)$$

$$\frac{\partial u_z}{\partial t} + \left(u_x \frac{\partial}{\partial x} + u_z \frac{\partial}{\partial z} \right) u_z = -\frac{\partial \phi}{\partial z}, \quad (3d)$$

$$\frac{\partial^2 \phi}{\partial x^2} + \frac{\partial^2 \phi}{\partial z^2} = 1 + a_1 \phi + a_2 \phi^2 + a_3 \phi^3 - n, \quad (3e)$$

where $n = n_p/n_{p0}$, with charge neutrality condition at equilibrium defined by $Z_p n_{p0} = Z_n n_{n0} + n_{e0}$, $\mathbf{u} = (u_x, u_y, u_z) = \mathbf{u}_p/C_s$ with

$$C_s = \sqrt{\frac{Z_p k_B T_e}{m_i}}$$

which is the characteristic speed scale used for velocity normalisation, $\phi = e\Phi/k_B T_e$. The space (x, z) and time (t) variables are normalised by the Debye length

$$\lambda_{De} = \sqrt{\frac{k_B T_e}{4\pi Z_p n_{p0} e^2}},$$

$\Omega = \Omega_i/w_{pi}$ is the normalised parameter of ion cyclotron and ion plasma frequency ratio, with

$$w_{pi} = \sqrt{\frac{4\pi n_{p0} Z_p^2 e^2}{m_i}}$$

and $\Omega_i = eB/m_i c$. The constants

$$a_1 = \mu_e + \mu_n \sigma_n, \quad a_2 = \frac{\mu_e + \mu_n \sigma_n^2}{2}$$

and

$$a_3 = \frac{\mu_e + \mu_n \sigma_n^3}{6}$$

are obtained after the power series expansion of the exponential factor around zero in n_p and n_e . Here,

$$\mu_e = \frac{n_{e0}}{Z_p n_{p0}} = \frac{1}{1 + \alpha}$$

and

$$\mu_n = \frac{Z_n n_{n0}}{Z_p n_{p0}} = \frac{\alpha}{1 + \alpha}$$

which assume the neutrality condition of the plasma $\mu_e + \mu_n = 1$, with $\alpha = Z_n n_{n0}/n_{e0}$ being the negative-ion concentration ratio.

The standard reductive perturbation expansion will be implemented to find the DS equations that govern the propagation of IAWs in the proposed plasma system. To start, we introduce the stretched variables $\xi = \varepsilon(x - v_{gx}t)$, $\eta = \varepsilon(z - v_{gz}t)$ and $\tau = \varepsilon^2 t$ in space and time, where v_{gx} and v_{gz} are the group velocities in x and z directions, respectively that will be found later using the solvability condition of eqs (3a)–(3d). ε is a small expansion parameter ($0 < \varepsilon \ll 1$) that measures the strength of nonlinearity. The dependent physical variables around their equilibrium values are expanded via the trial solutions

$$\begin{pmatrix} n(x, z, t) \\ u_x(x, z, t) \\ u_y(x, z, t) \\ u_z(x, z, t) \\ \phi(x, z, t) \end{pmatrix} = \begin{pmatrix} 1 \\ 0 \\ 0 \\ 0 \\ 0 \end{pmatrix} + \sum_{p=1}^{+\infty} \varepsilon^p \sum_{l=-\infty}^{+\infty} \begin{pmatrix} n_l^{(p)}(\xi, \eta, \tau) \\ u_{xl}^{(p)}(\xi, \eta, \tau) \\ u_{yl}^{(p)}(\xi, \eta, \tau) \\ u_{zl}^{(p)}(\xi, \eta, \tau) \\ \phi_l^{(p)}(\xi, \eta, \tau) \end{pmatrix} A^l(x, z, t), \quad (4)$$

which includes all overtones $A^l(x, z, t) = e^{il(k_x x + k_z z - \omega t)}$ up to order p and generated by the nonlinear terms. Here, ω is the wave frequency, k_x and k_z are the wave numbers in x and z directions, such that $k^2 = k_x^2 + k_z^2$. In other words, the corresponding coefficients of such overtones are of maximum order ε^p . Moreover, the relations

$$\begin{aligned} (n_l^{(p)})^* &= n_{-l}^{(p)}, & (u_{xl}^{(p)})^* &= u_{x-l}^{(p)}, \\ (u_{yl}^{(p)})^* &= u_{y-l}^{(p)}, & (u_{zl}^{(p)})^* &= u_{z-l}^{(p)}, & (\phi_l^{(p)})^* &= \phi_{-l}^{(p)} \end{aligned}$$

should be satisfied because of the reality condition of the physical variables, with the asterisk (*) denoting the complex conjugate. After substituting the trial solution (4) into eqs (3a)–(3e) and equating the quantities with equal power of ε , we obtain several coupled equations in different orders of ε that leads, after a few calculations, to the investigated DS equations. In doing so, the first

harmonic of perturbation (ε^1), we obtain

$$n_0^{(1)} = u_{x0}^{(1)} = u_{y0}^{(1)} = u_{z0}^{(1)} = \phi_0^{(1)} = 0$$

for $l = 0$ and

$$\begin{aligned} u_{x1}^{(1)} &= \frac{\beta}{k_x \omega (k^2 + a_1)} n_1^{(1)}, \\ u_{y1}^{(1)} &= -\frac{i \Omega \beta}{k_x \omega^2 (k^2 + a_1)} n_1^{(1)}, \\ u_{z1}^{(1)} &= \frac{k_z}{\omega (k^2 + a_1)}, \quad \phi_1^{(1)} = \frac{1}{k^2 + a_1} n_1^{(1)}, \end{aligned}$$

for $l = 1$, under the condition that the linear dispersion relation

$$\omega^4 - \left(\frac{k^2}{k^2 + a_1} + \Omega^2 \right) \omega^2 + \frac{\Omega^2 k_z^2}{k^2 + a_1} = 0, \quad (5)$$

be verified, leading to the first harmonic perturbation. The solution of the quadratic equation in ω^2 (eq. (5)) is given by

$$\omega^2 = \frac{1}{2} \left(\frac{k^2}{k^2 + a_1} + \Omega^2 \pm \sqrt{\left(\frac{k^2}{k^2 + a_1} + \Omega^2 \right)^2 - \frac{4k_z^2 \Omega^2}{k^2 + a_1}} \right). \quad (6)$$

We note that for pure perpendicular propagation and strong magnetic field, we obtain the following dispersion relation:

$$\omega^2 - \Omega^2 = \frac{k^2}{k^2 + a_1}. \quad (7)$$

Along the same line, the second harmonic of perturbation (ε^2) admit the relations

$$u_{x0}^{(2)} = -\frac{2\beta}{k_x \omega (k^2 + a_1)} |n_1^{(1)}|^2, \quad u_{y0}^{(2)} = 0$$

and

$$n_0^{(2)} = a_1 \phi_0^{(2)} + \frac{2a_2}{(k^2 + a_1)^2} |n_1^{(1)}|^2$$

for $l = 0$, while for $l = 1$, solutions are obtained as

$$n_1^{(2)} = (k^2 + a_1) \phi_1^{(2)} - \frac{2ik}{k^2 + a_1} \frac{\partial n_1^{(1)}}{\partial \xi} - \frac{2ik}{k^2 + a_1} \frac{\partial n_1^{(1)}}{\partial \eta},$$

$$u_{x1}^{(2)} = u_{x\phi} \phi_1^{(2)} + i u_{x\xi} \frac{\partial n_1^{(1)}}{\partial \xi} + i u_{x\eta} \frac{\partial n_1^{(1)}}{\partial \eta},$$

$$u_{y1}^{(2)} = i u_{y\phi} \phi_1^{(2)} + u_{y\xi} \frac{\partial n_1^{(1)}}{\partial \xi} + u_{y\eta} \frac{\partial n_1^{(1)}}{\partial \eta}$$

and

$$u_{z1}^{(2)} = u_{z\phi} \phi_1^{(2)} + i u_{z\xi} \frac{\partial n_1^{(1)}}{\partial \xi} + i u_{z\eta} \frac{\partial n_1^{(1)}}{\partial \eta},$$

under the solvability condition

$$\begin{aligned} v_{gx} &= \frac{k_x \omega \left(\frac{\beta_1(\omega^2 - \Omega^2)}{k_x^2} + \omega^2 - 2\omega^2(\omega^2 - \Omega^2) \right)}{2(\omega^4(k^2 + a_1) - k_z^2 \Omega^2)}, \\ v_{gz} &= \frac{k_z \omega (\omega^2 - \Omega^2 - \omega^2(\omega^2 - \Omega^2))}{(\omega^4(k^2 + a_1) - k_z^2 \Omega^2)}, \end{aligned} \quad (8)$$

that gives the group velocities, with $v_g^2 = v_{gx}^2 + v_{gz}^2$. Still at order ε^2 , the following solutions are obtained for $l = 2$:

$$\begin{aligned} n_2^{(2)} &= \alpha_n (n_1^{(1)})^2, \quad u_{x2}^{(2)} = \alpha_{u_x} (n_1^{(1)})^2, \\ u_{y2}^{(2)} &= i \alpha_{u_y} (n_1^{(1)})^2, \quad u_{z2}^{(2)} = \alpha_{u_z} (n_1^{(1)})^2, \\ \phi_2^{(2)} &= \alpha_\phi (n_1^{(1)})^2. \end{aligned}$$

For its part, the third-order (ε^3) reduced equations for $l = 0$ are obtained as a set of coupled equations in “Appendix B” (eq. (B.1)), which after some calculations lead to the following equation verified by the potential $\phi_0^{(2)}$:

$$\begin{aligned} \delta_1 \frac{\partial^2 \phi_0^{(2)}}{\partial \xi^2} + \delta_{\xi\eta} \frac{\partial^2 \phi_0^{(2)}}{\partial \xi \partial \eta} + \delta_\eta \frac{\partial^2 \phi_0^{(2)}}{\partial \eta^2} + \delta_2 \frac{\partial^2 |n_1^{(1)}|^2}{\partial \xi^2} \\ + \delta_{23} \frac{\partial^2 |n_1^{(1)}|^2}{\partial \xi \partial \eta} + \delta_3 \frac{\partial^2 |n_1^{(1)}|^2}{\partial \eta^2} = 0. \end{aligned} \quad (9)$$

Finally, various expressions derived in the above calculations are considered in the ($l = 1$)-component of the third-order part of the equations, leading to the amplitude equation

$$\begin{aligned} i \frac{\partial n_1^{(1)}}{\partial \tau} + \gamma_1 \frac{\partial^2 n_1^{(1)}}{\partial \xi^2} + \gamma_{12} \frac{\partial^2 n_1^{(1)}}{\partial \xi \partial \eta} + \gamma_2 \frac{\partial^2 n_1^{(1)}}{\partial \eta^2} \\ + \left(\gamma_3 |n_1^{(1)}|^2 + \gamma_4 \phi_0^{(2)} - k_z u_{z0}^{(2)} \right) n_1^{(1)} = 0. \end{aligned} \quad (10)$$

We recall that all the coefficients of various equations are given in Appendices A and B. Further, adopting the notation $\psi_1 = n_1^{(1)}$ and $\psi_2 = \phi_0^{(2)}$, $k_z = 0$, $v_{gz} = 0$ for case of pure perpendicular (i.e., when the wave in perpendicular to the magnetic field ($k_2 = 0$)), the set of eqs (9) and (10) reads as

$$\begin{aligned} i \frac{\partial \psi_1}{\partial \tau} + \gamma_1 \frac{\partial^2 \psi_1}{\partial \xi^2} + \gamma_2 \frac{\partial^2 \psi_1}{\partial \eta^2} \\ + (\gamma_3 |\psi_1|^2 + \gamma_4 \psi_2) \psi_1 = 0, \\ \delta_1 \frac{\partial^2 \psi_2}{\partial \xi^2} + \frac{\partial^2 \psi_2}{\partial \eta^2} + \delta_2 \frac{\partial^2 |\psi_1|^2}{\partial \xi^2} + \delta_3 \frac{\partial^2 |\psi_1|^2}{\partial \eta^2} = 0, \end{aligned} \quad (11)$$

which are known as the DS equations [59] that couple a complex field, for the wave amplitude ψ_1 and a

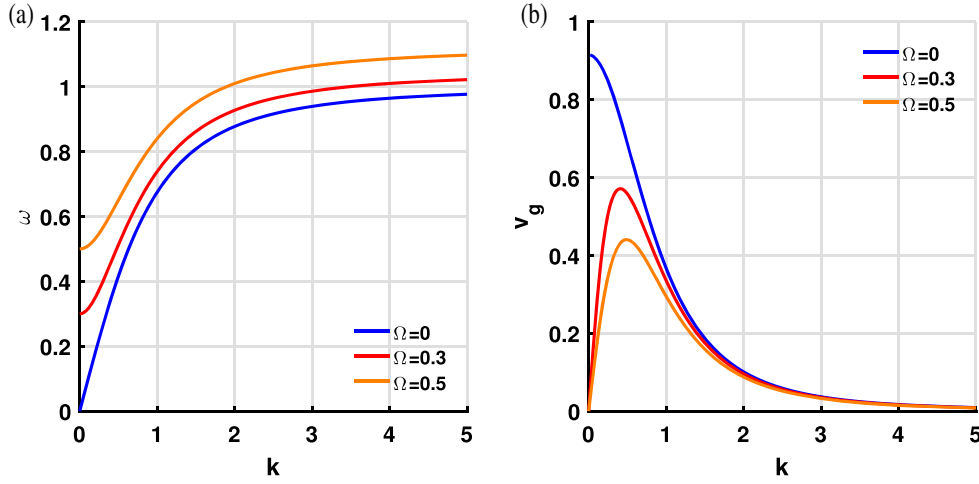


Figure 1. (a) The variation of the wave frequency ω with the wave number k and (b) the variation of the group velocity with wave number k , both under different magnetic fields. The electron-to-negative ion temperature ratio σ_n and the negative-ion concentration ratio α take the respective values $\sigma_n = 2.5$ and $\alpha = 0.01$.

real field, for a mean flow ψ_2 . Seminally, the DS equations were derived to describe nonlinear evolution of $(2 + 1)$ -dimensional waves packets in water of finite depth [59]. It has thereafter found applications in diverse areas of physics, including nonlinear-optics [60] as well as related fields, such as the study of matter waves in Bose–Einstein condensates [61] and the study of the propagation of electromagnetic waves in ferromagnets [62]. Moreover, in the context of nonlinear propagation of gravity-capillary surface waves under tension, a rigorous derivation of the DS equations was proposed in ref. [103]. Without being exhaustive, we may also point out various contributions devoted to multidimensional classical plasma systems in refs [104–107]. Specifically, DSEs were shown in ref. [104] to arise in multidimensional plasmas under the assumption that ion waves were parallel to the magnetic field. More recently, Panguetna *et al* [27,52] derived the DS equations both in two and three dimensions and used then to establish strong relationship between MI and dromion solitons, even during collision. In the context of the present paper, the reader should notice that different coefficients for eq. (11) depend on the system parameters. This renders easier the evolution of the contribution of both nonlinear and dispersive effects to the emergence of nonlinear waves and solitons. In the meantime, it should be noted that the wave frequency ω and the group velocity, respectively represented in figures 1a and 1b, are very sensitive to the changes in the magnetic field reflected by Ω . In general, the frequency ω is an increasing function of the magnetic field, while the group velocity shows a reverse behaviour. However, there has been little discussion on the effect of a magnetic field on the nonlinear evolution of IAWs governed by the DS equations.

3. Modulational instability analysis in the DS system

MI is one of the direct mechanisms responsible for the formation of solitons in nonlinear media. This occurs when a constant wave background becomes unstable and induces sinusoidal modulations under the competitive contribution of nonlinear and dispersive effects. Otherwise, under such effects, a plane-wave solution breaks up into trains of solitonic objects. In this section, we consider the DS system (11) with the trial plane-wave solutions [27,108,109]

$$\psi_1 = \psi_{10} e^{i(\alpha_1 \xi + \alpha_2 \eta - R\tau + \varphi)}, \quad \psi_2 = \psi_{20}, \quad (12)$$

where ψ_{10} , ψ_{20} , α_1 , α_2 and φ are real constants. Indubitably, such trial solutions will propagate in the system if the condition

$$R = \gamma_1 \alpha_1^2 + \gamma_2 \alpha_2^2 - \gamma_3 \psi_{10}^2 - \gamma_4 \psi_{20}, \quad (13)$$

is satisfied. Here, R obtained by substituting eq. (12) in the DS system, is the so-called linear dispersion relation or unperturbed dispersion relation. To further proceed, we study the stability of the plane-wave solution by introducing small perturbations so that

$$\begin{aligned} \psi_1 &= (\psi_{10} + \delta\psi_1) e^{i(\alpha_1 \xi + \alpha_2 \eta - R\tau + \varphi + \delta\varphi)}, \\ \psi_2 &= \psi_{20} + \delta\psi_2, \end{aligned} \quad (14)$$

where the small perturbations $\delta\psi_1$, $\delta\psi_2$ and $\delta\varphi$ are taken to be

$$\begin{pmatrix} \delta\psi_1 \\ \delta\psi_2 \\ \delta\varphi \end{pmatrix} = \begin{pmatrix} \Delta\psi_1 \\ \Delta\psi_2 \\ \Delta\varphi \end{pmatrix} Re \left(e^{i(\mu_1 \xi + \mu_2 \eta - \nu\tau)} \right), \quad (15)$$

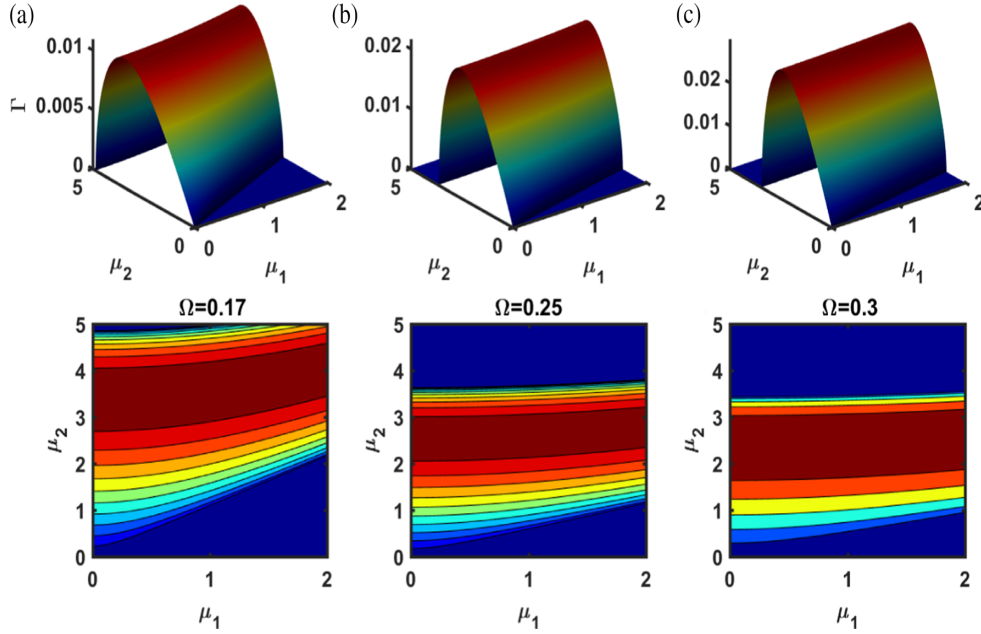


Figure 2. MI growth rate in the (μ_1, μ_2) -plane for $\alpha = 0.2$ and the ion cyclotron frequency taking the values: (a) $\Omega = 0.17$, (b) $\Omega = 0.25$ and (c) $\Omega = 0.3$. The other parameters are: $\sigma_n = 20.5$, $k = 2.4$, $\alpha_1 = 2.5$, $\alpha_2 = 2.5$, $\psi_{10} = 0.06$ and $\psi_{20} = 0.025$.

with $\Delta\psi_1$, $\Delta\psi_2$, $\Delta\varphi$, μ_1 , μ_2 being real constants. Inserting eqs (14) and (15) into (11) and using the dispersion relation (13), we obtain a homogeneous system in $\Delta\psi_1$, $\Delta\psi_2$ and $\Delta\varphi$, which admits non-trivial solutions if its determinant is non-zero. This leads to the following nonlinear dispersion relation:

$$(N_D)^2 = (\gamma_1\mu_1^2 + \gamma_2\mu_2^2) \times \left(\gamma_1\mu_1^2 + \gamma_2\mu_2^2 - 2\gamma_3\psi_{10}^2 + 2\gamma_4\psi_{10}^2 \frac{\delta_2\mu_1^2 + \delta_3\mu_2^2}{\delta_1\mu_1^2 + \mu_2^2} \right), \quad (16)$$

where $N_D = \nu - 2\gamma_1\alpha_1\mu_1 - 2\gamma_2\alpha_2\mu_2$. The plane-wave solutions (12) will be unstable if $N_D^2 < 0$, which amounts to the explicit condition

$$(\gamma_1\mu_1^2 + \gamma_2\mu_2^2)^2 \times \left(1 - 2\psi_{10}^2 \frac{\gamma_3(\delta_1\mu_1^2 + \mu_2^2) - \gamma_4(\delta_2\mu_1^2 + \delta_3\mu_2^2)}{(\gamma_1\mu_1^2 + \gamma_2\mu_2^2)(\delta_1\mu_1^2 + \mu_2^2)} \right) < 0. \quad (17)$$

Obviously, the stability/instability condition of the plane wave only depends on the terms

$$\left(1 - 2\psi_{10}^2 \frac{\gamma_3(\delta_1\mu_1^2 + \mu_2^2) - \gamma_4(\delta_2\mu_1^2 + \delta_3\mu_2^2)}{(\gamma_1\mu_1^2 + \gamma_2\mu_2^2)(\delta_1\mu_1^2 + \mu_2^2)} \right),$$

which also fixes the threshold amplitude above which the plane wave is expected to break up into solitary structures, i.e.,

$$\psi_{10,cr}^2 = \frac{(\gamma_1\mu_1^2 + \gamma_2\mu_2^2)(\delta_1\mu_1^2 + \mu_2^2)}{2\gamma_3(\delta_1\mu_1^2 + \mu_2^2) - 2\gamma_4(\delta_2\mu_1^2 + \delta_3\mu_2^2)}. \quad (18)$$

For the above, one can deduce the MI growth rate $\Gamma = \sqrt{-N_D^2}$ that will be used in this section to characterise the emergence of unstable wave patterns in the magnetised ENP under study. We precise that studies carried out recently showed the strong impact of parameters, such as the negative ion-electron concentration ratio and electron-to-negative ion temperature ratio [26–28]. It is, therefore, of high importance here to insist on the combined effects due to such parameters and the magnetic field. The panels of figure 2 show, for example, how changing the frequency Ω influences the instability domain. As it increases, one clearly notices a reduction of the zone of instability in the (μ_1, μ_2) -plane, with fixed values of the other control parameters $\sigma_n = 20.5$ and $\alpha = 0.01$. Recent contributions in 2D and 3D showed that the two latter parameters could control ENP plasma instability. Under relativistic effects, the negative ion-electron concentration ratio and electron-to-negative ion temperature ratio were found to contribute to a suitable balance between nonlinear and dispersive effects for rogue waves to appear. At this point, one question arises: what could be the behaviour of the MI growth rate under the influence of changing α and σ_n ? Comprehensive answers to the previous

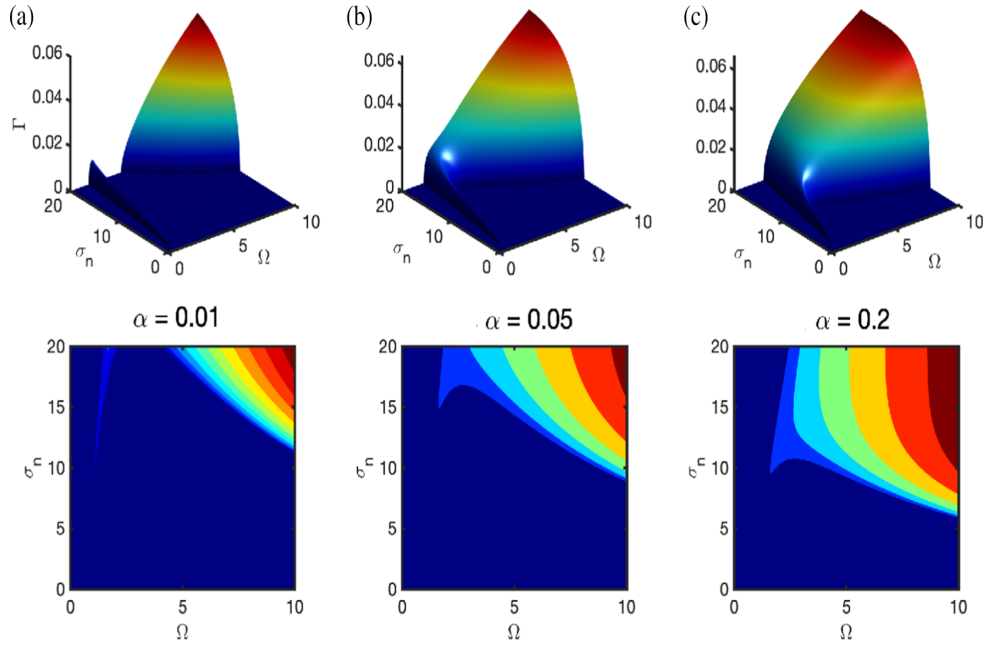


Figure 3. The growth rate of MI vs. the electron-to-negative ion temperature ratio σ_n and the frequency Ω when the negative-ion concentration ratio α takes the respective values (a) $\alpha = 0.01$, (b) $\alpha = 0.05$ and (c) $\alpha = 0.2$, with the other parameters being: $\sigma_n = 20.5$, $k = 2.4$, $\alpha_1 = 2.5$, $\alpha_2 = 2.5$, $\psi_{10} = 0.06$ and $\psi_{20} = 0.025$.

question are given in figures 3–5. Figure 3 shows the MI growth rate against the (Ω, σ_n) -plane with panels corresponding to different values of negative ion concentration ratio. For example, it is observed that for $\alpha = 0.01$, there are two regions of instability (see figure 3a) that merge with increasing α . Interestingly, most of the instability occurs for high values of σ_n , while instability is possible in a very restrained area of small magnetic field values. This is drastically modified for $\alpha = 0.05$ and 0.2 , where after merging, the common single region of instability expands. However, instability does not still occur for small values of electron-to-negative-ion temperature ratio σ_n . However, the growth rate maximum takes place for high values of both σ_n and the magnetic field. In figure 4, for two sets of wave numbers μ_1 and μ_2 , the effect of α on the MI growth rate appears clearly and concurs with the instability windows obtained in figure 3. Additional information on the appearance of instability due to the plasma parameters and the magnetic field is recorded in figure 5, this time in the (Ω, α) -plane by changing the electron-to-negative ion temperature ratio σ_n . Contrary to the features of figure 3, there is only one region of instability for all values of σ_n . However, increasing the σ_n value increasingly involves small values of α in the MI process. Nevertheless, the zone of instability gets reduced for high values of σ_n , even though the growth rate intensity increases. Indeed, such results confirm the existence of IAWs in the studied plasma system, especially in the presence of the magnetic field, which probably will contribute to the emergence of more complex patterns under the simulta-

neous effect of nonlinearity and dispersion. Therefore, when this is fulfilled, a random amplitude perturbation will grow, leading to the generation of IAWs. This is supported in the background by the physical information contained in the coefficients of the DS equations, which are functions of relevant plasma parameters as indicated by the above parametric analysis of MI. In such regions, exact solutions exist which can be obtained using different methods for different applications. In what follows, we propose solutions to the DS system (11) using Hirota's bilinear method.

4. One- and two-dromion solutions of the DS equations

Research on exact solutions of nonlinear evolution equations has attracted a lot of interest during the last decades. In this regard, many analytical methods for investigating exact solutions to nonlinear partial differential equations (PDEs) have been proposed, amongst which are the inverse scattering method [110], the Backlund and Darboux transformation method [111], the Hirota bilinear method [71,112], the pseudospectral method [113], the hyperbolic function method [114, 115], the homogeneous balance method and formal variable separation method [116–118], the generalised Riccati equation method [119], unified algebraic method and varied Jacobi elliptic function methods [120,121]. Interestingly, the Hirota bilinear method [71,112] has been used to construct dromions-like solutions to a

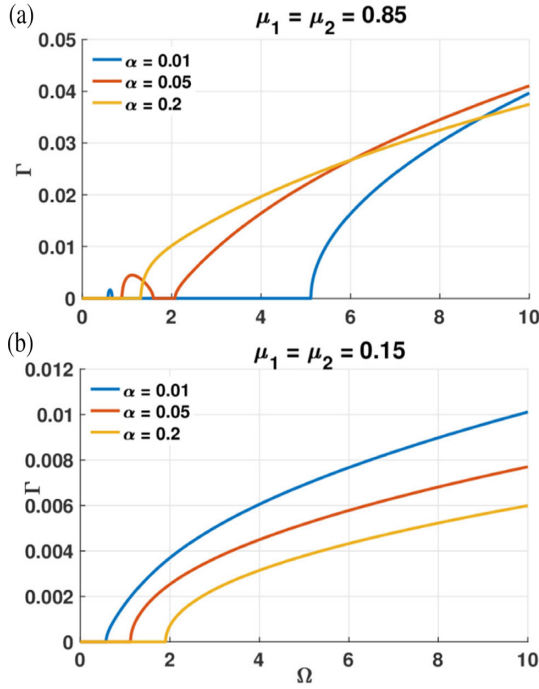


Figure 4. The growth rate of MI vs. the frequency Ω for two sets of wave numbers (a) $\mu_1 = \mu_2 = 0.85$ and (b) $\mu_1 = \mu_2 = 0.15$. In each panel, the negative-ion concentration ratio α takes increasing values, while the other parameters are fixed as: $\sigma_n = 20.5$, $k = 2.4$, $\alpha_1 = 2.5$, $\alpha_2 = 2.5$, $\psi_{10} = 0.06$ and $\psi_{20} = 0.025$.

system of equations similar to the DS system. More recently, Panguetna *et al* [27] used the Hirota bilinear method to obtain one- and two-dromion solutions for the DS system of equations. We should indicate that there exist types I and II DS equations depending on the sign of their coefficients [122,123]. However, from the results of §3, one may obtain the two types of systems. It has been shown that the system of eq. (11) may display DS-I behaviours if conditions $\gamma_1/\gamma_2 > 0$ and $\gamma_3 > 0$ are satisfied [124,125]. Figure 6 shows the parameters γ_1 , γ_2 and γ_3 vs. k . For $k > 0$, all the values of γ_1 and γ_2 are positive, $\gamma_3 > 0$ for DS-I, while $\gamma_3 < 0$ gives the DS-II equations.

The solutions of eq. (11) are exponentially localised and called dromions. Using the Hirota bilinear method, we will proceed to find the solutions of the system. Such solutions are investigated by first studying their domain of existence. Therefore, we first rescale dependent and independent variables as follows:

$$\begin{aligned} l\xi' &= \frac{1}{(\delta_1\gamma_3 - \delta_2\gamma_4)^{1/2}}\xi, \\ \eta' &= \frac{1}{(\delta_3\gamma_4 - \gamma_3)^{1/2}}\eta, \\ \psi &= \gamma_3|\psi_1|^2 + \gamma_4\psi_2. \end{aligned} \quad (19)$$

We also introduce the following new independent variables through a coordinate axis rotation by 45° :

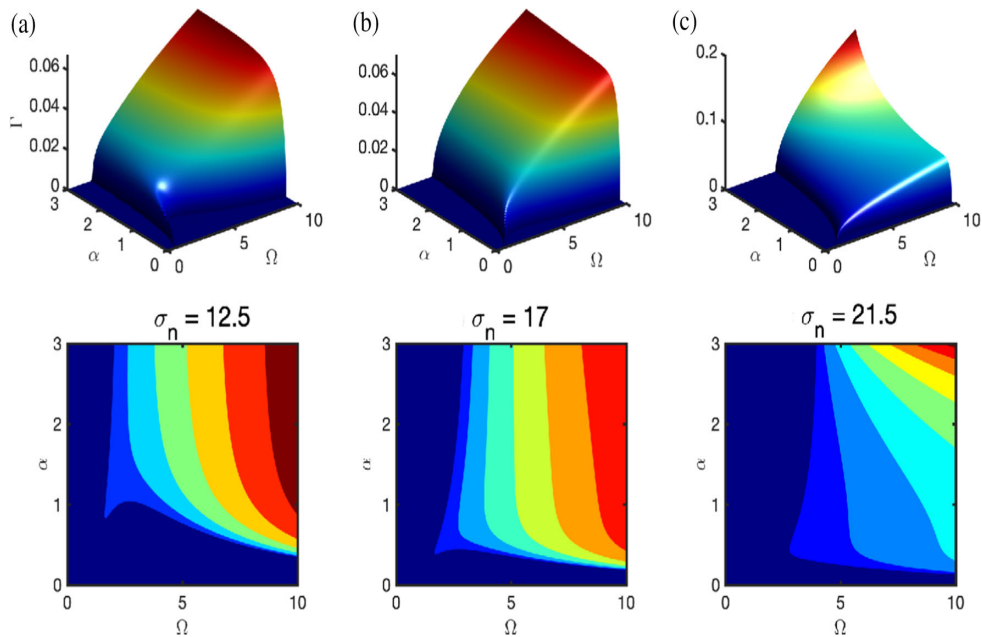


Figure 5. The MI growth rate vs. the negative-ion concentration ratio α and the frequency Ω when the electron-to-negative ion temperature ratio takes the respective values: (a) $\sigma_n = 12.5$, (b) $\sigma_n = 17$ and (c) $\sigma_n = 21.5$. The other parameters are: $k = 2.4$, $\alpha_1 = 2.5$, $\alpha_2 = 2.5$, $\psi_{10} = 0.06$ and $\psi_{20} = 0.025$.

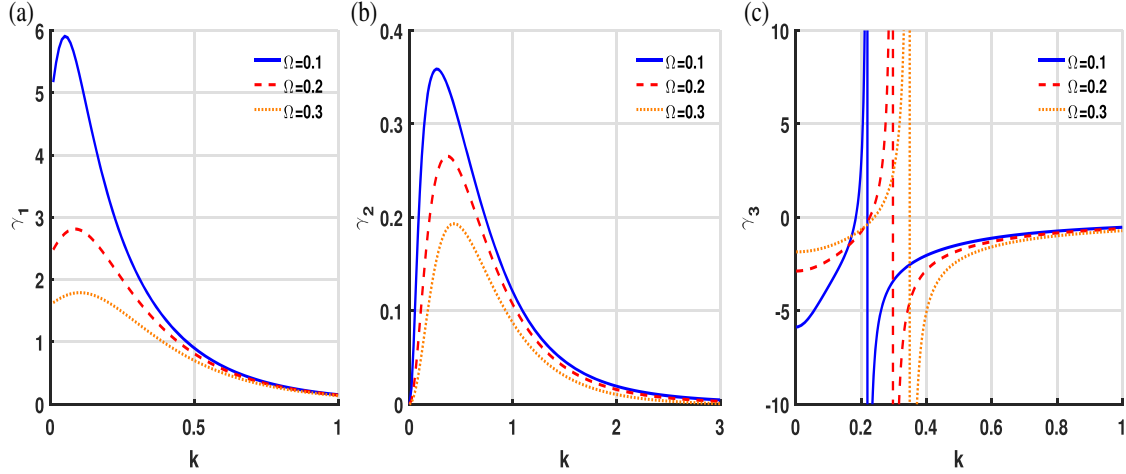


Figure 6. Plots of γ_1 , γ_2 and γ_3 vs. k (eqs (C.2), (C.4) and (C.5) for $\alpha = 0.01$ and $\sigma_n = 5.5$ and different values of Ω .

$$X = \frac{1}{\sqrt{2}}(\xi' + \eta'), \quad Y = \frac{1}{\sqrt{2}}(\xi' - \eta'). \quad (20)$$

Substituting relations (19) and (20) into eqs (11), we obtain the following set of equation:

$$i\psi_{1\tau} + a(\psi_{1XX} + \psi_{1YY}) + b\psi_{1XY} + \psi_1\psi = 0, \quad (21a)$$

$$c(\psi_{XX} + \psi_{YY}) + d\psi_{XY} = 2(|\psi_1|^2)_{XY}, \quad (21b)$$

where

$$a = \frac{1}{2} \left(\frac{\gamma_1}{\delta_1\gamma_3 - \delta_2\gamma_4} + \frac{\gamma_2}{\delta_3\gamma_4 - \gamma_3} \right),$$

$$b = \frac{1}{2} \left(\frac{\gamma_1}{\delta_1\gamma_3 - \delta_2\gamma_4} - \frac{\gamma_2}{\delta_3\gamma_4 - \gamma_3} \right),$$

$$c = \frac{1}{2} \left(\frac{\delta_1}{\delta_1\gamma_3 - \delta_2\gamma_4} - \frac{1}{\delta_3\gamma_4 - \gamma_3} \right),$$

$$d = \frac{1}{2} \left(\frac{\delta_1}{\delta_1\gamma_3 - \delta_2\gamma_4} + \frac{1}{\delta_3\gamma_4 - \gamma_3} \right).$$

We note that the above constants depend on the magnetised electronegative plasma parameters, such as Ω , σ_n and α . Solutions for system (21) are investigated by introducing the new dependent variables F (real) and G (complex) so that

$$\psi_1 = \sqrt{2bd} \left(\frac{G}{F} \right) \quad \text{and} \quad \psi = 2b(\ln f)_{XY}. \quad (22)$$

This leads to the bilinear form, with assumption

$$\frac{\gamma_1}{\delta_1\gamma_3 - \delta_2\gamma_4} = \frac{\gamma_2}{\gamma_3 - \delta_3\gamma_4}.$$

$$(iD_\tau + a(D_{XX} + D_{YY}))(G \cdot F) = 0, \quad (23a)$$

$$D_{XY}F \cdot F = 4G \cdot G^*, \quad (23b)$$

where D is an operator defined as

$$D_x^n G \cdot F = (\partial_{x_1} - \partial_{x_2})^n F(x_1)G(x_2)|_{x_2=x_1=x}, \quad (24)$$

which is also known as the Hirota bilinear operator. We further expand the new variables F and G in the power series of small parameter δ as $G = \delta G_1 + \delta^3 G_3 + \dots$ and $F = 1 + \delta^2 F_2 + \delta^4 F_4 + \dots$ to obtain the dromion-like solutions [27,124]. This is introduced in (23) to find G_1 , G_3 , F_2 and F_4 . Taking G_1 to be in the form

$$G_1 = \sum_{j=1}^N e^{\eta_j}, \quad (25)$$

$$\eta_j = p_j X + q_j Y + ia(p_j^2 + q_j^2)\tau + \eta_{0j},$$

with p_j , q_j and η_{0j} being the complex constants, the generalised form of the one-dromion solution is obtained as

$$\psi_{11D} = \frac{G_{1D}}{F_{1D}} = \frac{\rho \exp(\eta_1 + \eta_2)}{\left\{ 1 + J \exp(\eta_1 + \eta_1^*) + K \exp(\eta_2 + \eta_2^*) + L \exp(\eta_1 + \eta_1^* + \eta_2 + \eta_2^*) \right\}}, \quad (26)$$

$$\eta_1 = pX + iap^2\tau + \eta_{01}, \quad \eta_2 = qY + iaq^2\tau + \eta_{02}.$$

Moreover, in eq. (26), J , K and L are real constants, $p = p_1$, $q = q_1$ and $|\rho|^2 = 2L(p + p^*)(q + q^*) = 8Lp_Rq_R$.

These types of solutions have already been reported by Panguetna *et al* [27] as the excitation of IAWs in unmagnetised electronegative plasmas. It is interesting to see now if the presence of the magnetic field in the system impacts the structure and the propagation of the dromions in such a system. In figure 7, for example, the one-dromion solution is plotted vs. X , with figures 7a and 7b corresponding, respectively to $\alpha = 0.01$ and $\alpha = 0.08$. In each of these cases, the solution decreases by increasing the magnetic field, with the value $\Omega = 0$ corresponding to the non-magnetised plasma which agrees with the earlier findings [27].

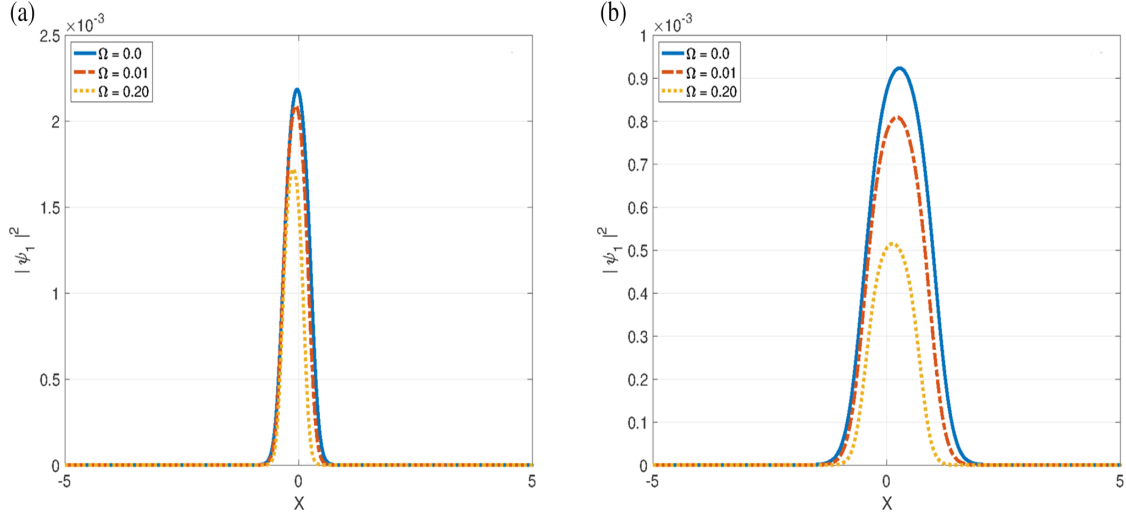


Figure 7. The behaviours of the one-dromion solution with increasing magnetic field. For (a), the negative ion concentration ratio is fixed as $\alpha = 0.01$, while (b) corresponds to $\alpha = 0.08$, with Ω taking values 0, 0.01 and 0.2 in each of the panels. The other parameters are $\sigma_n = 5.5$ and $J = K = L = 1$.

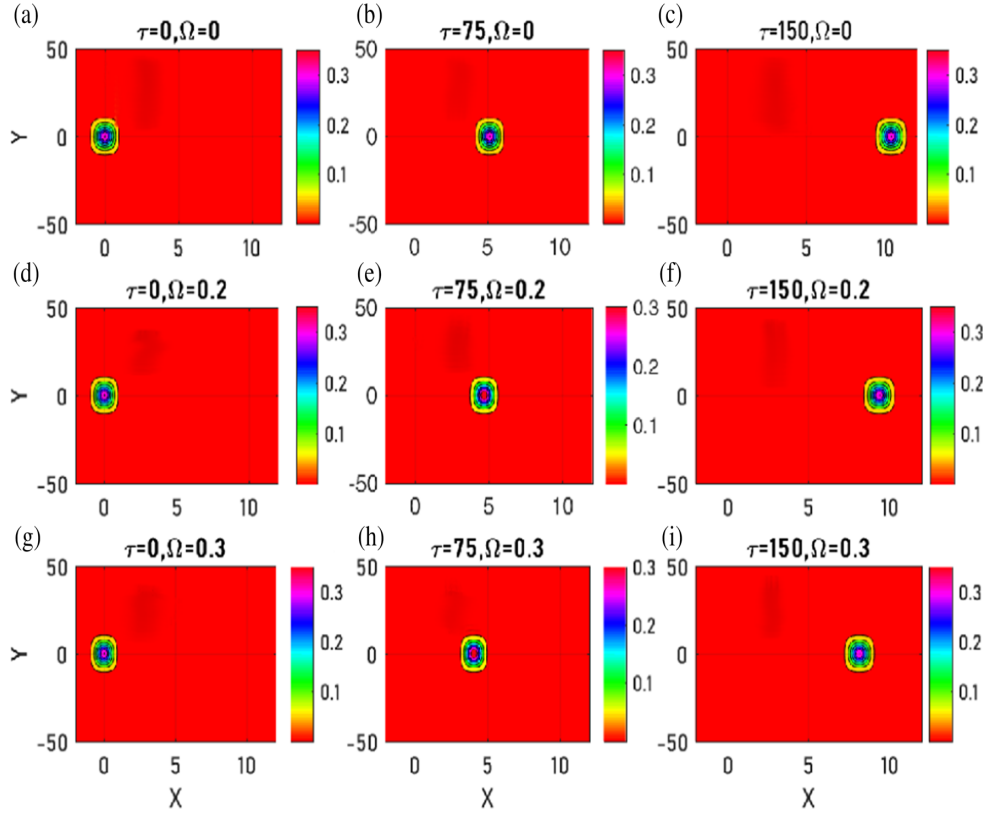


Figure 8. The propagation of one-dromion solutions (26) for increasing values of the magnetic field Ω at different instants τ when $\alpha = 0.01$, $\sigma_n = 5.5$ and $J = K = L = 1$.

On the one hand, a behaviour that was already seen is the increase of the base width of the solution with increasing negative-ion concentration ratio α . Additionally, the same base width gets decreased, together with the wave amplitude, when the strength of the magnetic field increases. In general, with increasing magnetic field, dispersive effects get dominated by the nonlinearity effects leading to more spiky dromions in the

studied plasma system. The panels of figure 8 show the propagation of the one-dromion solution of eq. (11) for different values of the magnetic field at different instants. We observe that in the absence of the magnetic field, the dromion can propagate with speed v_g . The speed of propagation decreases when the magnetic field increases. For example, at the instant $t = 150$, the peak of the dromion is at position $X = 9.4$ (see figure 8c) for

$\Omega = 0.2$, while at the same instant and for $\Omega = 0.3$, the peak of the dromion is at position $X = 8.2$. Therefore, it is clear that the presence of the magnetic field has a slowing effect on the propagation of the dromion solution.

Similarly, we can proceed and find the two-dromion solutions in the form

$$\psi_{12D} = \frac{G_{2D}}{F_{2D}} \frac{\left\{ \begin{array}{l} \rho_{11} \exp(\eta_1 + \eta_3) + \rho_{12} \exp(\eta_2 + \eta_3) \\ + \rho_{21} \exp(\eta_1 + \eta_1^* + \eta_2 + \eta_3) \\ + \rho_{22} \exp(\eta_1 + \eta_2 + \eta_2^* + \eta_3) \end{array} \right\}}{\left\{ \begin{array}{l} 1 + A \exp(\eta_1 + \eta_1^*) + B \exp(\eta_2 + \eta_2^*) \\ + C \exp(\eta_3 + \eta_3^*) \\ + D[\exp(\eta_1 + \eta_2^*) + \exp(\eta_2 + \eta_1^*)] \\ + E[\exp(\eta_1 + \eta_2^* + \eta_3 + \eta_3^*) \\ + \exp(\eta_2 + \eta_1^* + \eta_3 + \eta_3^*)] \\ + F \exp(\eta_1 + \eta_1^* + \eta_2 + \eta_2^*) \\ + G \exp(\eta_2 + \eta_2^* + \eta_3 + \eta_3^*) \\ + H \exp(\eta_1 + \eta_1^* + \eta_3 + \eta_3^*) \\ + I \exp(\eta_1 + \eta_1^* + \eta_2 + \eta_2^* + \eta_3 + \eta_3^*) \end{array} \right\}}, \quad (27)$$

$$\eta_1 = p_1 X + i a p_1^2 \tau + \eta_{01},$$

$$\eta_2 = p_2 X + i a p_2^2 \tau + \eta_{02},$$

$$\eta_3 = q_1 Y + i a q_1^2 \tau + \eta_{03},$$

where A, B, C, D, E, F, G, H and I are real, positive constants. The panels of figure 9 show the evolution of two dromion solutions and their elastic collision in the absence and presence of the magnetic field. Obviously, in the absence of the magnetic field, the collision happens with a delay (see figure 9(a)_{j=1,2,3,4}), while in the presence of the magnetic field, the collision process is accelerated (see figure 9(b)_{j=1,2,3,4}). However, in the two cases, the colliding objects keep their initial characteristics after the collision, implying no energy exchange. Nevertheless, it should be indicated that when two dromions interact, there might be an energy exchange which may affect their amplitude and some other characteristics [27,126]. This is for example the case in figure 10, where the two dromions of unequal amplitudes collide, share energies and end up displaying the same features. The dromion with the highest amplitude has shared its energy with the small dromion, which resulted in identical objects under elastic collision. We notice that even in this context, the impact of the magnetic field in the collision process is similar to what was already discussed in figure 9. Another possibility in the process of wave collision is that the colliding entities merge into one, a phenomenon that is also known as inelastic collision. This is depicted in figure 11, where initially, there are two dromions of different amplitudes that interact and form a single solitonic object. This particular case is typical in plasma systems where several components are involved, which is useful in producing

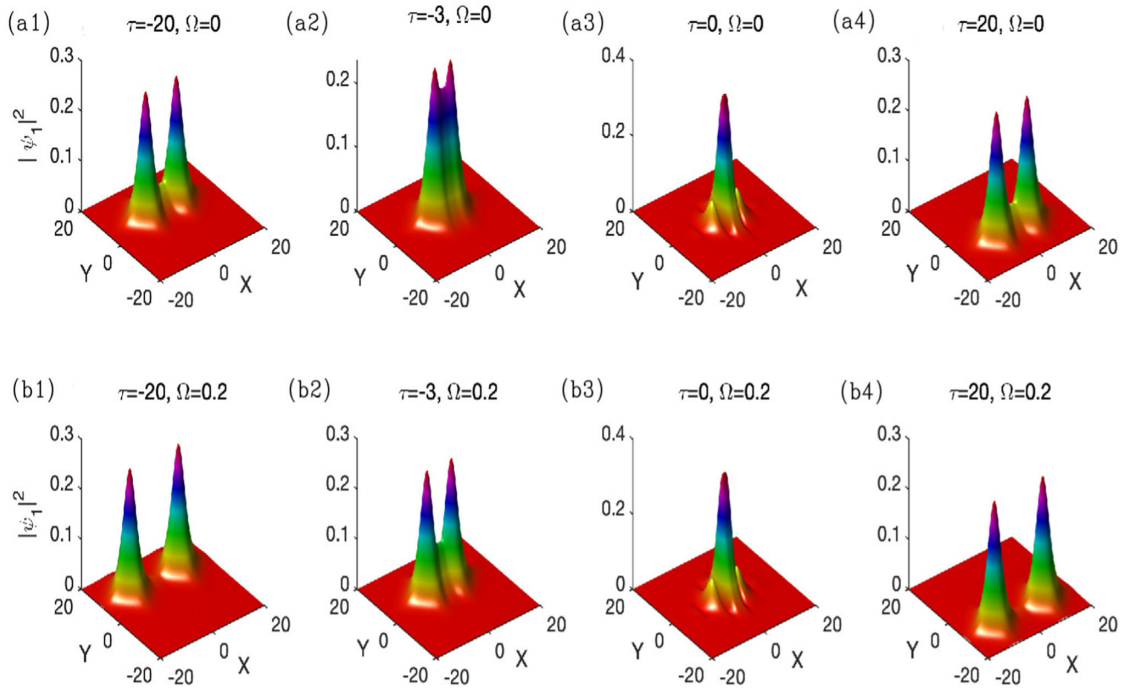


Figure 9. Elastic collision of the two-dromion solution (27) in a moving frame, where panels (a)_{j=1,2,3,4} display results in the absence of the magnetic field ($\Omega = 0$) and panels (b)_{j=1,2,3,4} show results in the presence of the magnetic field. In the process, two identical dromions interact and keep their shapes after collision. However, the presence of the magnetic field accelerates such a collision, with the other parameters being $\alpha = 0.01$, $\sigma_n = 20.5$ and $A = B = C = D = E = F = G = H = I = 1$.

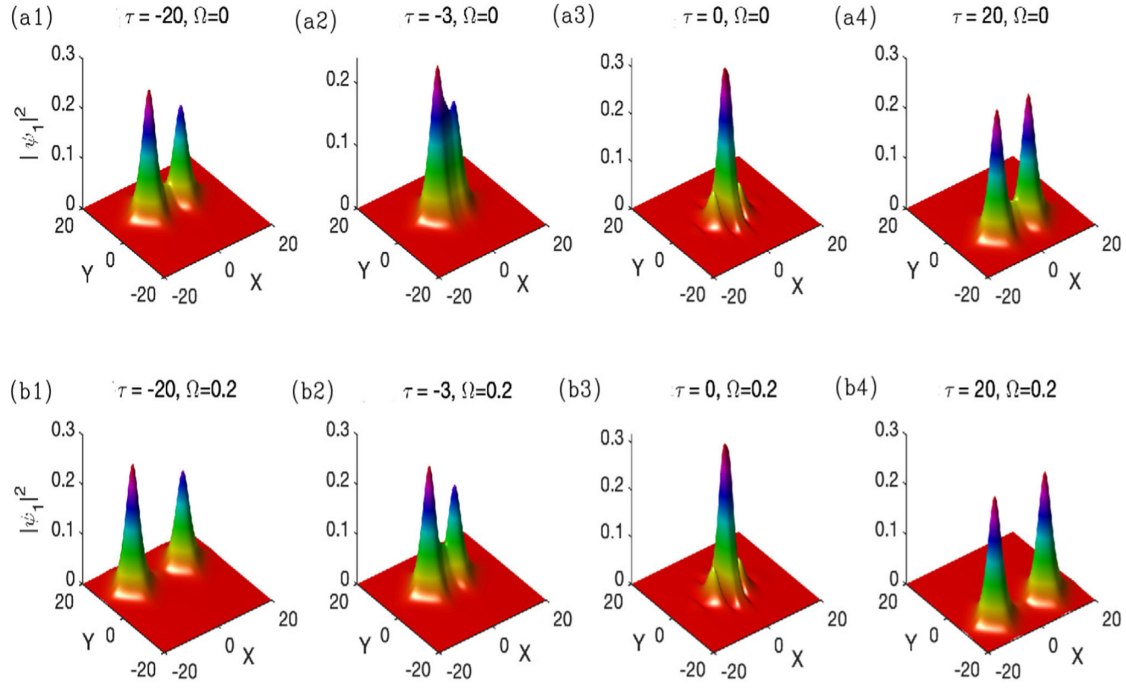


Figure 10. Elastic collision of two dromions with energy exchange both in the absence (panels (a)_{j=1,2,3,4}) and in the presence (panels (b)_{j=1,2,3,4}) of the magnetic field. The colliding objects involve two dromions of different amplitudes which, after collision, give rise to entities with equal amplitudes. The parameters are $\alpha = 0.01$, $\sigma_n = 20.5$ and $A = B = C = D = E = F = G = H = I = 1$.

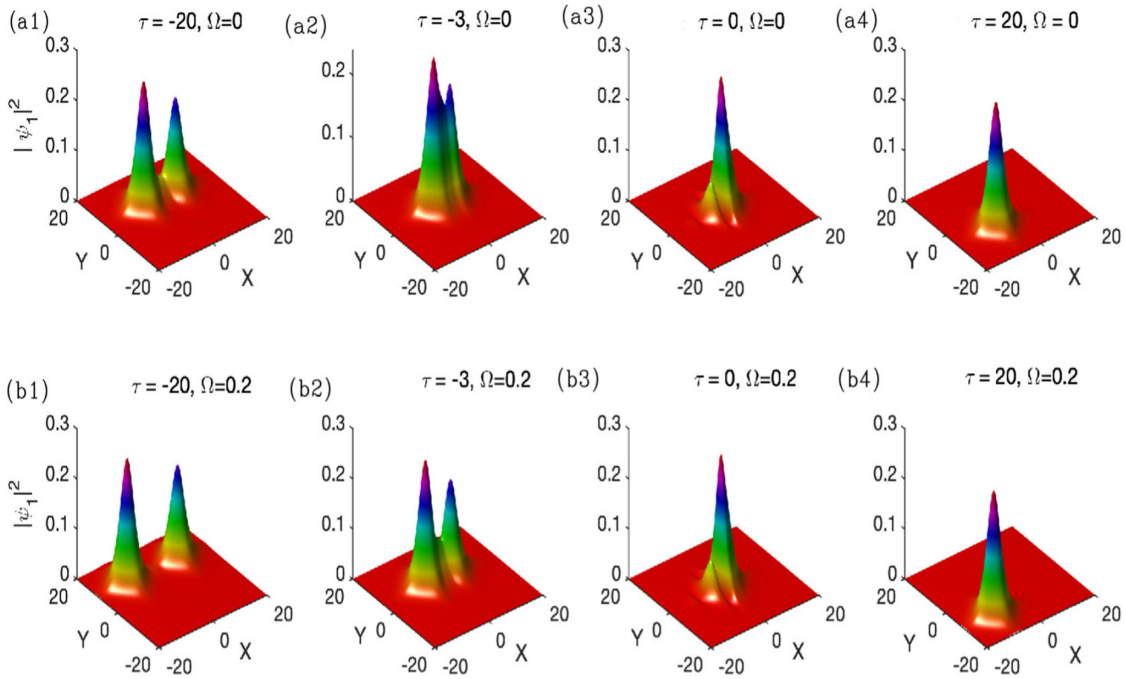


Figure 11. Inelastic collision of two dromions, both in the absence (panels (a)_{j=1,2,3,4}) and in the presence (panels (b)_{j=1,2,3,4}) of the magnetic field. In both cases, the dromions after collision combine and give rise to one soliton, but the presence of the magnetic field accelerates such a process. The parameters are $\alpha = 0.01$, $\sigma_n = 20.5$ and $A = B = C = D = E = F = G = H = I = 1$.

plasma particles in a process known as energy recombination. This is inherently facilitated by the presence of different dynamical modes [127,128]. However, the

results obtained here confirm that such a recombination process is accelerated by the magnetic field, which enhances the collision process. Many other scenarios

can be explored, especially when plasma parameters change, as was already reported by Panguetna *et al* [27] who showed that dromions and their interactions were very sensitive to changes in the electron-to-negative-ion temperature ratio and the negative-ion concentration ratio. Some other contributions also introduced the modulation angle, an important factor to be included when three-dimensional components are involved, a scenario that may enrich the features inherent to the presence of the magnetic field applied to two negative ion plasmas such as $\text{Xe}^+ - \text{F}^- - \text{SF}_6^-$ and $\text{Ar}^+ - \text{F}^- - \text{SF}_6^-$, for example.

5. Concluding remarks

To summarise, we have used the reductive perturbation method to study the propagation of IAWs in a magnetised ENP. After showing that the generic fluid-Maxwell equations can be reduced to a set of Davey–Stewartson (DS) equations, the linear stability analysis of MI has been adopted to discuss the existence of solitonic-like structures. The behaviour of MI growth rate has mainly been discussed based on the system parameters. Principally, the joined effects of the electron-to-negative ion temperature ratio σ_n and the negative-ion concentration ratio α have been compared to the change in the external magnetic field to show that MI can take place in some interval of such parameters under the suitable balance between nonlinear and dispersive effects. Under specific conditions, we have shown, using the bilinear Hirota method, that the solutions for the derived DS eq. (11) can be found as one- and two-dromion ion-acoustic solutions. The combined effects of various physical parameters, such as the electron-to-negative-ion temperature ratio, the negative-ion concentration ratio and the strength of magnetic field have been studied on the regions of existence and propagation properties of ion-acoustic dromions. We have noted that the shape of the obtained solutions depends both on the system parameters and the magnetic field. Increasing the magnetic field has generated solitonic profiles such as dromions-like shapes. The parametric analysis has been extended to two-dromion dynamics under different interaction scenarios. We have noticed the strong impact of the magnetic field on the energy exchange and recombination processes.

Data Availability Statement The datasets generated and analysed during the current study are available from the corresponding author on reasonable request.

Appendix A: Various coefficients

The coefficients appearing in various equations are defined as follows:

$$\begin{aligned}
 \beta_1 &= \omega^2(k^2 + a_1) - k_z^2, \\
 \beta_2 &= \omega^2(4k^2 + a_1) - k_z^2, \\
 u_{x\phi} &= \frac{\beta_1}{k_x \omega}, \\
 u_{z\phi} &= \frac{k_z}{\omega}, \\
 u_{y\phi} &= -\frac{i\beta_1 \Omega}{k_x \omega^2}, \\
 u_{x\xi} &= -\frac{2\omega}{k^2 + a_1} + \frac{\beta_1}{k_x^2 \omega(k^2 + a_1)} - \frac{\beta_2 v_{gx}}{k_x \omega^2(k^2 + a_1)}, \\
 u_{x\eta} &= -\frac{2k_z \omega}{k_x(k^2 + a_1)} + \frac{2k_z}{k_x \omega(k^2 + a_1)} \\
 &\quad - \frac{\beta_2 v_{gz}}{k_x \omega^2(k^2 + a_1)}, \\
 u_{y\xi} &= -\frac{2\Omega}{k^2 + a_1} + \frac{\beta_1 \Omega}{k_x^2 \omega^2(k^2 + a_1)} - \frac{2k_z^2 \Omega v_{gx}}{k_x \omega^3(k^2 + a_1)}, \\
 u_{z\xi} &= \frac{k_z v_{gx}}{\omega^2(k^2 + a_1)}, \\
 u_{z\eta} &= -\frac{1}{\omega(k^2 + a_1)} \left(v_{gz} \frac{k_z}{\omega} - 1 \right), \\
 \alpha_\phi &= \frac{\left\{ (4\omega^2 - \Omega^2)(2(k^2 + a_1)^2 \omega^2 + k_z^2(k^2 + a_1)) \right.}{2(k^2 + a_1)^2 (\beta_2(4\omega^2 - \Omega^2) - 4k_x^2 \omega^2)}, \\
 \alpha_n &= (4k^2 + a_1)\alpha_\phi + \frac{a_2}{(k^2 + a_1)^2}, \\
 \alpha_{u_x} &= \frac{\omega}{k_x}(\alpha_n - 1) - \frac{k_z}{k_x} \alpha_{u_z}, \\
 \alpha_{u_y} &= -\frac{\Omega}{2\omega} \left(\alpha_{u_x} - \frac{\beta_1}{k_x \omega(k^2 + a_1)} \right), \\
 \alpha_{u_z} &= \frac{k_z}{\omega} \alpha_\phi + \frac{k_z}{2\omega(k^2 + a_1)}. \tag{A.1}
 \end{aligned}$$

Appendix B: Equations and other coefficients

The third-order (ε^3) reduced equations for $l = 0$ are obtained as set of couple equations

$$\begin{aligned}
 &-v_{gx} \frac{\partial \phi_0^{(2)}}{\partial \xi} - v_{gz} \frac{\partial \phi_0^{(2)}}{\partial \eta} + \frac{\partial u_{z0}^{(2)}}{\partial \eta} \\
 &= A_\xi \frac{\partial |n_1^{(1)}|^2}{\partial \xi} + A_\eta \frac{\partial |n_1^{(1)}|^2}{\partial \eta}, \\
 &-v_{gx} \frac{\partial u_{z0}^{(2)}}{\partial \xi} - v_{gz} \frac{\partial u_{z0}^{(2)}}{\partial \eta} + \frac{\partial \phi_0^{(2)}}{\partial \eta} \\
 &= B_\xi \frac{\partial |n_1^{(1)}|^2}{\partial \xi} + B_\eta \frac{\partial |n_1^{(1)}|^2}{\partial \eta}, \tag{B.1}
 \end{aligned}$$

where

$$A_\xi = \frac{2v_{gx}a_2}{(k^2 + a_1)^2},$$

$$A_\eta = \frac{2v_{gz}a_2}{(k^2 + a_1)^2} - \frac{2k_z}{\omega(k^2 + a_1)},$$

$$B_\xi = \frac{2}{(k^2 + a_1)^2} \times \left[-\frac{k_z\beta_1}{k_x\omega^2} + k_xk_z + \frac{k_zv_{gz}}{2\omega^3(k^2 + a_1)^2}(\beta_1 + \beta_2) \right],$$

$$B_\eta = \frac{1}{(k^2 + a_1)^2} \left[\frac{\beta_1}{\omega^2} - \frac{3k_z^2}{\omega^2} + 2k_z^2 + \frac{k_zv_{gz}}{\omega^3}(\beta_2 - \beta_1) \right].$$

The coefficients of eq. (9) are as follows:

$$\begin{aligned} \delta_1 &= -v_{gx}^2a_1, \quad \delta_{\xi\eta} = -2v_{gx}v_{gz}a_1, \quad \delta_\eta = 1 - v_{gz}^2a_1, \\ \delta_2 &= -v_{gx}A_\xi, \quad \delta_{23} = -v_{gx}A_\eta - v_{gz}A_\xi - B_\xi, \quad (\text{B.2}) \\ \delta_3 &= -v_{gz}A_\eta + B_\eta, \end{aligned}$$

Appendix C Coefficients of DSEs

The set of both eqs. (10) and (9)

$$\gamma_\tau = \frac{2}{\omega}(\Omega^4(k^2 + a_1) + k_z^2\Omega^2), \quad (\text{C.1})$$

$$\gamma_1 = \frac{1}{\gamma_\tau} \left[\begin{array}{l} v_{gx} \left(-2k_x\omega(\omega^2 - \Omega^2) + k_x\omega^2(k^2 + a_1)u_{x\xi} + k_x\omega\Omega(k^2 + a_1)u_{y\xi} \right) \\ + k_z(\omega^2 - \Omega^2)(k^2 + a_1)u_{z\xi} \\ - \omega(\omega^2 - \Omega^2)(k^2 + a_1)u_{z\xi} - \omega^2(\omega^2 - \Omega^2) \end{array} \right], \quad (\text{C.2})$$

$$\gamma_{12} = \frac{1}{\gamma_\tau} \left[\begin{array}{l} -2\omega(\omega^2 - \Omega^2)(k^2 + a_1)(k_zv_{gx} + k_xv_{gz}) - \omega(\omega^2 - \Omega^2)(k^2 + a_1)(u_{x\eta} + u_{z\xi}) \\ + k_x\omega^2(k^2 + a_1)(v_{gx}u_{x\eta} + v_{gz}u_{x\xi}) + k_x\omega\Omega(k^2 + a_1)(v_{gx}u_{y\eta} + v_{gz}u_{y\xi}) \\ + k_z(\omega^2 - \Omega^2)(k^2 + a_1)(v_{gx}u_{z\eta} + v_{gz}u_{z\xi}) \end{array} \right], \quad (\text{C.3})$$

$$\gamma_2 = \frac{1}{\gamma_\tau} \left[\begin{array}{l} v_{gz}(-2k_z\omega(\omega^2 - \Omega^2) + k_x\omega^2(k^2 + a_1)u_{x\eta} + k_x\omega\Omega(k^2 + a_1)u_{y\eta} + k_z(\omega^2 - \Omega^2)(k^2 + a_1)u_{z\eta}) \\ - \omega(\omega^2 - \Omega^2)(k^2 + a_1)u_{z\eta} - \omega^2(\omega^2 - \Omega^2) \end{array} \right], \quad (\text{C.4})$$

$$\gamma_3 = \frac{1}{\gamma_\tau} \left[\begin{array}{l} -\omega(\omega^2 - \Omega^2) \left((k^2 + a_1)(k_x\alpha_{u_x} + k_z\alpha_{u_z}) + \frac{1}{\omega}(\alpha_n(\beta_1 + k_z^2) - 2\beta_1) \right) \\ + \frac{a_2}{\omega(k^2 + a_1)}(2\beta_1 + k_z^2) \\ + k_x\omega^2 \left(\alpha_{u_x} \left(\frac{2k_z^2\Omega}{\omega} - \frac{\beta_1}{\omega} \right) + \frac{\beta_1\alpha_{u_z}}{\omega} + \frac{2\beta_1^2}{k_x\omega^2(k^2 + a_1)} \right) \\ + k_x\omega\Omega \left(-2\alpha_{u_y} \left(\frac{\beta_1\Omega}{\omega} + \frac{k_z^2}{\omega} \right) + \frac{\beta_1\Omega\alpha_{u_x}}{\omega^2} + \frac{2\Omega\beta_1^2}{k_x\omega^3(k^2 + a_1)} + \frac{k_z\beta_1\Omega\alpha_{u_z}}{k_x\omega^2} \right) \\ + k_z(\omega^2 - \Omega^2) \left(-\alpha_{u_z} \left(\frac{2\beta_1}{\omega} + \frac{k_z^2}{\omega} \right) + \frac{2k_z\beta_1}{\omega^2(k^2 + a_1)} + \frac{k_xk_z\alpha_{u_x}}{\omega} \right) \\ + \omega^2(\omega^2 - \Omega^2) \left(2a_2\alpha_\phi - \frac{3a_3}{(k^2 + a_1)^2} \right) \end{array} \right], \quad (\text{C.5})$$

$$\gamma_4 = -\frac{(\omega^2 - \Omega^2)}{\gamma_\tau}(2k_z\omega v_{gz} - 1 + 2a_2\omega^2). \quad (\text{C.6})$$

References

- [1] D Mihalache, D Mazilu, F Lederer, Y V Kartashov, L-C Crasovan, L Torner and B A Malomed, *Phys. Rev. Lett.* **97**, 073904 (2006)
- [2] D D E Temgoua and T C Kofané, *Phys. Rev. E* **93**, 062223 (2016)
- [3] M Djoko and T C Kofané, *Opt. Commun.* **416**, 198 (2018)
- [4] A Djazet, S I Fewo, E B N Nkouankam and T C Kofané, *Eur. Phys. J. D* **74**, 67 (2020)
- [5] L T Megne, C B Tabi and T C Kofané, *Phys. Rev. E* **102**, 042207 (2020)
- [6] J A A Otsobo, L T Megne, C B Tabi and T C Kofané, *Chaos Solitons Fractals* **158**, 112034 (2022)
- [7] J B Okaly, A Mvogo, C B Tabi, H P E Fouda and T C Kofané, *Phys. Rev. E* **102**, 062402 (2020)
- [8] A S Etémé, C B Tabi and A Mohamadou, *Commun. Nonlin. Sci. Numer. Simulat.* **43**, 211 (2017)
- [9] C B Tabi, R Y Ondoua, H P Ekobena, A Mohamadou and T C Kofané, *Phys. Lett. A* **380**, 2374 (2016)
- [10] G R Y Mefire, C B Tabi, A Mohamadou, H P E Ekobena and T C Kofané, *Chaos* **23**, 033128 (2013)
- [11] A X Zhang and J K Xue, *Phys. Rev. A* **75**, 013624 (2007)
- [12] P Otladisa, C B Tabi and T C Kofané, *Phys. Rev. E* **103**, 052206 (2021)
- [13] P A Andreev and L S Kuzmenkov, *Phys. Rev. A* **78**, 053624 (2008)
- [14] E A Kuznetsov, A M Rubenchik and V E Zakharov, *Phys. Rep.* **142**, 103 (1986)
- [15] J Borhanian, I Kourakis and S Sobhanian, *Phys. Lett. A* **373**, 3667 (2009)
- [16] I Langmuir, *Proc. Natl. Acad. Sci.* **14**, 627 (1928)
- [17] S Ali, W M Moslem, P K Shukla and R Schlickeiser, *Phys. Plasmas* **14**, 082307 (2007)
- [18] I Paul, A Chatterjee and S N Paul, *Laser Part. Beams* **37**, 378 (2019)
- [19] X-W Cheng, Z-G Zhang and H-W Yang, *Chin. Phys. B* **29**, 124501 (2020)
- [20] K N Ostrikov, S Kumar and H Sugai, *Phys. Plasmas* **7**, 3490 (2001)
- [21] M Djebli, *Phys. Plasmas* **10**, 4910 (2003)
- [22] A A Mamun and P K Shukla, *Phys. Plasmas* **10**, 1518 (2003)
- [23] N Shahmohammadi and D Dorrani, *Contrib. Plasma Phys.* **55**, 643 (2015)
- [24] K Annou and R Annou, *Phys. Plasmas* **19**, 043705 (2012)
- [25] J-C Sun, Z-G Zhang, H-H Dong and H-W Yang, *Commun. Theor. Phys.* **72**, 125001 (2020)
- [26] Z X Wang, J Y Liu, X Zou, Y Liu and X G Wang, *Chin. Phys. Lett.* **20**, 1537 (2003)
- [27] C S Panguetna, C B Tabi and T C Kofané, *Phys. Plasmas* **24**, 092114 (2017)
- [28] C S Panguetna, C B Tabi and T C Kofané, *J. Theor. Appl. Phys.* **13**, 237 (2019)
- [29] X Zou, J Y Liu, Z X Wang, Y Gong, Y Liu and X G Wang, *Chin. Phys. Lett.* **21**, 1572 (2004)
- [30] X Zou, H-P Liu, M-H Qiu and X-H Sun, *Chin. Phys. Lett.* **28**, 125201 (2011)
- [31] M Aslaninejad and K Yasserian, *Phys. Plasmas* **19**, 033504 (2012)
- [32] J-J Li, J X Ma and Z-A Wei, *Phys. Plasmas* **20**, 063503 (2013)
- [33] A Aanesland, J Bredin and P Chabert, *Plasmas Sources Sci. Technol.* **23**, 044003 (2014)
- [34] K Yasserian and M Aslaninejad, *J. Theor. Appl. Phys.* **13**, 251 (2019)
- [35] S K El-Labany, E E Behery, H N A El-Razek and L A Abdelrazek, *Eur. Phys. J. D* **74**, 104 (2020)
- [36] R Paul, S Adhikari, R Moullick, S S Kausik and B K Saikia, *Phys. Plasmas* **27**, 063520 (2020)
- [37] L Wang, M Vass, Z Donko, P Hartmann, A Dersi, Y-H Song and J Schulze, *Plasmas Sources Sci. Technol.* **31**, 06LT01 (2022)
- [38] S Ganyou, S I Fewo, C S Panguetna and T C Kofané, *Results Phys.* **52**, 106821 (2023)
- [39] H Washimi and T Taniuti, *Phys. Rev. Lett.* **17**, 996 (1966)
- [40] T Kimura, K Imagaki and K Ohe, *J. Phys. D: Appl. Phys.* **31**, 2295 (1998)
- [41] O Rahman, A A Mamun and K S Ashrafi, *Astrophys. Space Sci.* **335**, 425 (2011)
- [42] V Berezhnoj, C B Shin, U Buddemeier and I Kaganovich, *Appl. Phys. Lett.* **77**, 800 (2000)
- [43] E N Kenkeu, A B T Motcheyo, T Kanaa and C Tchawoua, *Phys. Plasmas* **29**, 043702 (2022)
- [44] R Ichiki, S Yoshimura, T Watanabe, Y Nakamura and Y Kawai, *Phys. Plasmas* **9**, 4481 (2002)
- [45] R A Gottscho and C E Gaebe, *IEEE Trans. Plasma Sci.* **14**, 92 (1986)
- [46] J Jacquinet, B D McVey and J E Scharer, *Phys. Rev. Lett.* **39**, 88 (1977)
- [47] Y I Portnyagin, O F Klyuev, A A Shidlovsky, A N Evdokimov, T W Buzdigar, P G Matukhin, S G Pasynkov, K N Shamshev, V V Sokolov and N D Semkin, *Adv. Space Res.* **11**, 89 (2011)
- [48] R Sabry, W M Moslem and P K Shukla, *Phys. Plasmas* **16**, 032302 (2009)
- [49] A J Coates, F J Crary, G R Lewis, D T Young, J H Waite Jr and E C Sittler Jr, *Geophys. Res. Lett.* **34**, L22103 (2007)
- [50] A A Mamun, P K Shukla and B Eliasson, *Phys. Rev. E* **80**, 046406 (2009)
- [51] C S Panguetna, C B Tabi and T C Kofané, *Commun. Nonlin. Sci. Numer. Simulat.* **55**, 326 (2018)
- [52] C B Tabi, C S Panguetna and T C Kofané, *Physica B* **545**, 70 (2018)
- [53] M G Anowar, K S Ashrafi and A A Mamun, *J. Plasma Phys.* **77**, 133 (2011)
- [54] S Duha, M S Rahman, A A Mamun and G M Anowar, *J. Plasma Phys.* **78**, 279 (2012)
- [55] U M Abdelsalam, *Ain Shams Eng. J.* **12**, 4111 (2021)

- [56] A R Alharbi, *Comput. Model. Eng. Sci.* **134**(3), 2193 (2022)
- [57] A R Alharbi, *AIMS Math.* **8**(1), 1230 (2022)
- [58] S Frassu, T Li and G Viglialoro, *Math. Meth. Appl. Sci.* **45**(17), 11067 (2022)
- [59] A Davey and K Stewartson, *Proc. R. Soc. London-Ser. A* **338**, 101 (1974)
- [60] A C Newell and J V Moloney, *Nonlinear Optics* (Addison-Wesley, Redwood City, 1992)
- [61] G Huang, L Deng and C Hang, *Phys. Rev. E* **72**, 036621 (2005)
- [62] H Leblond, *J. Phys. A: Math. Gen.* **32**, 7907 (1999)
- [63] L Y Sung, *J. Math. Anal. Appl.* **183**, 121 (1994)
- [64] L Y Sung, *J. Nonlinear Sci.* **5**, 433 (1995)
- [65] Y Ohta and J Yang, *Phys. Rev. E* **86**, 036604 (2012)
- [66] Y Ohta and J Yang, *J. Phys. A: Math. Theor.* **46**, 105202 (2013)
- [67] H-X Jia, D-W Zuo, X-H Li and X-S Xiang, *Phys. Lett. A* **405**, 127426 (2021)
- [68] H G Abdelwahed, E K El-Shewy, S Alghanim and M A E Abdelrahman, *Fractal Fract.* **6**, 430 (2022)
- [69] H G Abdelwahed, A F Alsarhana, E K El-Shewy and M A E Abdelrahman, *Phys. Fluids* **35**, 037129 (2023)
- [70] E K El-Shewy, Y F Alharbi and M A E Abdelrahman, *Chaos Solitons Fractals* **170**, 113324 (2023)
- [71] J Hietarinta and R Hirota, *Phys. Lett. A* **145**, 5 (1990)
- [72] R H Heredero, L M Alonso and E M Reus, *Phys. Lett. A* **152**, 1 (1991)
- [73] M Boiti, J J-P Leon, L Martina and F Pempinelli, *Phys. Lett. A* **132**, 8 (1988)
- [74] T-C Xia and D-Y Chen, *Chaos Solitons Fractals* **22**, 577 (2004)
- [75] G Xu, *Chaos Solitons Fractals* **30**, 71 (2006)
- [76] N Prathap, S Arunprakash, M S M Rajan and K Subramanian, *Optik* **158**, 1179 (2018)
- [77] S Veni and M S M Rajan, *Opt. Quant. Electron.* **55**, 107 (2023)
- [78] R. Hirota, *Phys. Rev. Lett.* **27**, 1192 (1971)
- [79] L Li, C Duan and F Yu, *Phys. Lett. A* **383**, 1578 (2019)
- [80] W X Ma, *Opt. Quant. Electron.* **52**, 511 (2020)
- [81] W X Ma, *Math. Comput. Simulat.* **190**, 270 (2021)
- [82] S Kumar and B Mohan, *Part. Diff. Eq. Appl. Math.* **5**, 100274 (2022)
- [83] S Basnet, A Patel and R Khanal, *Plasma Phys. Control. Fusion* **62**, 115011 (2020)
- [84] M M Hatami, *Sci. Rep.* **11**, 9531 (2021)
- [85] M A Lieberman and A Lichtenberg, *Principle of plasma discharges and materials processing*, 2nd Edn (Wiley, New York, 2005)
- [86] D Vender, W W Stoffels, E Stoffels, G M W Kroesen and F J de Hoog, *Phys. Rev. E* **51**, 2436 (1995)
- [87] R N Franklin, *Plasma Sources Sci. Technol.* **11**, A31 (2002)
- [88] P Chabert, A J Lichtenberg and M A Lieberman, *Phys. Plasmas* **14**, 093502 (2007)
- [89] N Plihon, P Chabert and C S Corr, *Phys. Plasmas* **14**, 013506 (2007)
- [90] A Meige, N Plihon, G J M Hagelaar, J-P Boeuf, P Chabert and R W Boswell, *Phys. Plasmas* **14**, 053508 (2007)
- [91] T H Chung, *Phys. Plasmas* **16**, 063503 (2009)
- [92] P K Shukla and B Eliasson, *Rev. Mod. Phys.* **81**, 25 (2009)
- [93] N D'Angelo, *J. Phys. D* **37**, 860 (2004)
- [94] B M Annaratone, T Antonova, H M Thomas and G E Morfill, *Phys. Rev. Lett.* **93**, 185001 (2004)
- [95] B M Annaratone and J E Allen, *J. Phys. D* **38**, 26 (2005)
- [96] M Rosenberg and R L Merlino, *J. Plasma Phys.* **75**, 495 (2009)
- [97] A A Mamun, R A Cairns and P K Shukla, *Phys. Lett. A* **373**, 2355 (2009)
- [98] V M Vasyliunas, *J. Geophys. Res.* **73**, 2839 (1938)
- [99] R A Cairns, A A Mamun, R Bingham, R Bostrom, R O Dendy, C M C Nairn and P K Shukla, *Geophys. Res. Lett.* **22**, 2709 (1995)
- [100] C Tsallis, *J. Stat. Phys.* **52**, 479 (1988)
- [101] A Mannan, A A Mamun and P K Shukla, *Phys. Scr.* **85**, 065501 (2012)
- [102] S K El-Labany, W M Moslem, K A Shnishin, S A El-Tantawy and P K Shukla, *Phys. Plasma* **18**, 042306 (2011)
- [103] W Craig, U Schanz and C Sulem, *Ann. Inst. Henri Poincaré (C)* **14**, 615 (1977)
- [104] K Nishinari, K Abe and J Satsuma, *Phys. Plasmas* **1**, 2559 (1994)
- [105] J-K Xue, *Phys. Lett. A* **330**, 390 (2004)
- [106] C Bedi and T S Gill, *Phys. Plasmas* **19**, 062109 (2012)
- [107] P Carbonaro, *Chaos Solitons Fractals* **45**, 959 (2012)
- [108] K Nishinari, K Abe and J Satsuma, *J. Phys. Soc. Jpn* **6**, 2021 (1993)
- [109] K Nishinari, K Abe and J Satsuma, *Theor. Math. Phys.* **99**, 745 (1994)
- [110] M J Ablowitz and P A Clarkson, *Solitons, nonlinear evolution equations and inverse scattering* (Cambridge University Press, Cambridge, 1991)
- [111] V B Matveev and M A Salle, *Darboux transformations and solitons* (Springer-Verlag, Berlin, 1991)
- [112] J Hietarinta, *Introduction to the Hirota bilinear method* (Springer, Berlin, Heidelberg, 1997)
- [113] M Saravi, E Babolian, R England and M Bromilow, *Comput. Math. Appl.* **59**, 1524 (2010)
- [114] W Malfliet and W Hereman, *Phys. Scr.* **54**, 563 (1996)
- [115] Q Wang, Y Chen and H Zhang, *Appl. Math. Comput.* **181**, 247 (2006)
- [116] E Fan and H Zhang, *Phys. Lett. A* **246**, 403 (1998)
- [117] S Lou, *Phys. Scr.* **65**, 7 (2002)
- [118] S Lou and J Lu, *J. Phys. A* **29**, 4209 (1996)
- [119] Z Yan and H Q Zhang, *Phys. Lett. A* **285**, 355 (2001)
- [120] C B Tabi, A Mohamadou and T C Kofané, *Phys. Lett. A* **373**, 2476 (2009)
- [121] C B Tabi, A Mohamadou and T C Kofané, *Phys. Scr.* **77**, 045002 (2008)

- [122] M J Ablowitz and H Segur, *Solitons and the inverse scattering transform* (SIAM, Philadelphia, 1981)
- [123] R Radha and M Lakshmanan, *J. Phys. A: Math. Gen.* **30**, 3229 (1997)
- [124] S S Ghosh, A Sen and G S Lakhina, *Nonlin. Process Geophys.* **9**, 463 (2002)
- [125] N S Saini, Y Ghai and R Kohli, *J. Geophys. Res.* **121**, 5944 (2016)
- [126] M A-Moghanjoughi, *Phys. Plasmas* **17**, 092304 (2010)
- [127] H P Le and J-L Cambier, *Phys. Plasmas* **23**, 063505 (2016)
- [128] J Vranjes, M Kono, D Petrovic, S Poedts, A Okamoto, S Yoshimura and M Y Tanaka, *Plasma Sour. Sci. Technol.* **15**, S1 (2006)

Springer Nature or its licensor (e.g. a society or other partner) holds exclusive rights to this article under a publishing agreement with the author(s) or other rightsholder(s); author self-archiving of the accepted manuscript version of this article is solely governed by the terms of such publishing agreement and applicable law.



OPTICA Advancing Optics and Photonics Worldwide Formerly OSA


NASEY OPTICA CHAPTER

CERTIFICATE OF ATTENDANCE

This is to certify that

Mrs. GANYOU Stéphanie

has participated as an assistant trainer and organizer in the training seminar entitled: "**1st edition of Mastering MAPLE in a few weeks**",
from February 28 to April 13, 2024


Lucien MANDENG MANDENG
Seminar Supervisor

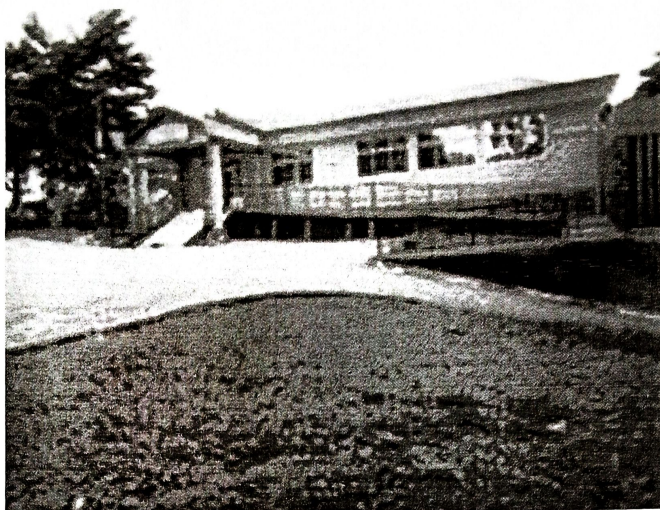


This certificate is not issued for any official institutional qualification awarded by the ENSPY / NASEY.



THE UNIVERSITY OF YAOUNDE I

P.O. Box : 337 Yaounde
Phone/Fax : +237 222 22 13 20
<https://uy1.uninet.cm>



This is to certify that

GANYOU Stéphanie

participated in and completed the

Doctoral Seminar 2022

Organized by the

Research and Postgraduate Training Unit for Physics and Applications

Postgraduate School of Science Technology and Geosciences

25 - 26 April 2023

Faculty of Science, The University of Yaounde I, Yaounde, Cameroon



A handwritten signature in black ink, appearing to read 'Luc C. Owono Owono'.

Research and Postgraduate Training Unit
for Physics and Applications
Luc C. OWONO OWONO, Coordinator



ATTESTATION DE PARTICIPATION

Cette attestation est délivrée à

GANYOU Stéphanie

Pour avoir participé au séminaire de formation portant sur l'**Intelligence
Artificielle pour les Sciences des Matériaux** du 09 au 10 Mai 2023
ENSPY / UY1

Coordonnateur PRICNAC

Elie Kamsen

Le Directeur de l'ENSPY

P. O. Directeur Adjoint

Marthe Boyomo



CPS

**UNIKASSEL
VERSITÄT**



Erasmus+



Certificate of Participation

This herewith certifies that

Stéphanie Ganyou

In recognition of her active and invaluable participation during the conduct of a Workshop on the “**Structural Control**” on March 22 to 23, 2022 in the Africa-Germany Scientific Cooperation Center of the University of Yaoundé I.

Prof. Dr. Blaise Romeo Nana Nbandjo
University of Yaoundé I, Cameroon
General Secretary of Cameroon Physical Society

Prof. Dr.-Ing Uwe Dorke
University of Kassel, Germany

March 23, 2022
Date





ACCEGID

AFRICAN CENTRE OF EXCELLENCE FOR GENOMICS OF INFECTIOUS DISEASES
Redeemer's University, Ede, Nigeria



African Center of Excellence

Centre d'Excellence Africain en
Technologies de l'Information
et de la Communication
Université de Yaoundé I

CERTIFICATE OF COMPLETION

Is hereby granted to:

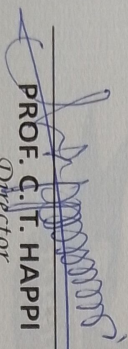
GANYOU Stéphanie

In recognition of the completion of the Genomics Foundation Training Workshop in

BIOINFORMATICS

May 6th to 10th, 2019

University of Yaounde I, Cameroon


PROF. C. T. HAPPI
Director
ACEGID



AFRICAN CENTRE OF EXCELLENCE FOR GENOMICS OF INFECTIOUS DISEASES
Redeemer's University, Nigeria


PROF. R. M. ETOUA
Coördinator,
CETIC

ORGANISATION OF WOMEN IN SCIENCE FOR THE DEVELOPING WORLD CAMEROON NATIONAL CHAPTER



Certificate of Participation

Presented to

Stéphanie Ganyou

at

OWSD-CAM National Chapter Official launching ceremony and workshop

Theme: Women in STEM contribution of research and innovative technology for the sustainable development of Cameroon

Amphi 700, University of Yaounde I, Yaounde , Cameroon
17th — 18th December, 2019


Prof. Biye Elvia Hortense
President OWSD-CAM



The Company of
Biologists




Prof. Jennifer A. Thomson
President OWSD

